

**The origin of pale and dark layers in Pliocene  
Jinsuo lignite basin from Yunnan Province,  
Southwestern China**

Dissertation

zur Erlangung des Doktorgrades  
der Naturwissenschaften

vorgelegt beim Fachbereich Geowissenschaften / Geographie  
der Johann Wolfgang Goethe -Universität  
in Frankfurt am Main

von

**Bangjun Liu**

aus Mianyang, Sichuan, China

Frankfurt am Main (2019)

(D 30)

vom Fachbereich Geowissenschaften / Geographie der

Johann Wolfgang Goethe - Universität als Dissertation angenommen.

Dekan: Prof. Dr. Georg Rumpker

Gutachter : Prof. Dr. Wilhelm Püttmann

Prof. Dr. Jens Fiebig

---

## Contents

<i>Acknowledgements</i> .....	V
<i>Abstract</i> .....	1
<i>Zusammenfassung (Summary)</i> .....	7
<i>List of Tables</i> .....	15
<i>List of Figures</i> .....	15
<i>Acronyms</i> .....	17
<b><i>Chapter 1 Introduction</i></b> .....	<b>19</b>
1.1 The pale and dark layers/lignites around the world.....	19
1.1.1 The pale and dark layers/lignites in China .....	21
1.1.2 The pale and dark layers/lignites in Germany .....	23
1.1.3 The pale and dark layers/lignites in Australia .....	27
1.1.4 The pale and dark layers/lignites in other countries .....	30
1.2 Focus of the research .....	32
<b><i>Chapter 2 Organic petrology and geochemical characteristics of pale and dark layers in Pliocene lignite deposits from Yunnan Province, Southwest China</i></b> .....	<b>33</b>
2.1 Abstract.....	33
2.2 Introduction.....	35
2.3 Geological setting .....	38
2.4 Samples and methods .....	40
2.4.1 Organic petrography .....	41
2.4.2 Biomarker analysis .....	41
2.4.4 Elemental analysis .....	42
2.5 Results and discussion .....	42
2.5.1 Macroscopic characteristics.....	42
2.5.2 Maceral composition .....	42
2.5.3 Maceral indices.....	47
2.5.4 Bulk geochemical parameters.....	50
2.5.5 Molecular composition of the EOM.....	53
2.6 Origin of pale and dark lignites in the Jinsuo opencast mine.....	62
2.7 Conclusions .....	65

<b><i>Chapter 3 Stable isotopic and elemental characteristics of pale and dark layers in Pliocene Jinsuo lignite deposit basin in Yunnan Province, southwestern China</i></b> .....	<b>67</b>
3.1 Abstract .....	67
3.2 Introduction .....	69
3.3. Geological setting.....	70
3.4. Samples and analytical methods .....	72
3.5. Results and discussion .....	72
3.5.1 Stable isotopic composition of lignites and fossil wood.....	<b>72</b>
3.5.2 Chemical composition of lignite samples and implications for paleoenvironment.....	78
3.5.3 Paleoenvironmental model for pale and dark layers .....	81
3.6 Conclusions .....	85
<b><i>Chapter 4 Reconstruction of paleobotanical and paleoenvironmental changes in the Pliocene Velenje Basin, Slovenia, by molecular and stable isotope analysis of lignites</i></b> .....	<b>87</b>
4.1 Abstract .....	87
4.2 Introduction .....	89
4.3 Geological setting.....	91
4.4 Samples and analytical procedures .....	93
4.4.1 Elemental analysis.....	93
4.4.2 Biomarker analysis.....	93
4.4.3 Stable isotopic analysis .....	94
4.5 Results and discussion .....	95
4.5.1 Bulk geochemical parameters .....	95
4.5.2 Saturated and aromatic hydrocarbons in the EOM .....	97
4.5.3 Isotopic composition of the lignites .....	110
4.6 Conclusions .....	115
<b><i>Chapter 5 Conclusions and outlook</i></b> .....	<b>118</b>
5.1 Conclusions .....	118
5.2 Outlook.....	123

*References* ..... 128  
*Appendix* ..... 142  
*Publications*..... 148  
*Curriculum Vitae* ..... 149



## **Acknowledgements**

I would like firstly give many thanks to my doctoral supervisor Prof. Dr. Wilhelm Püttmann for his help during my PhD study at Goethe-University Frankfurt am Main. His detailed guidance and many valuable suggestions helped me to finish my doctoral thesis successful. Prof. Dr. Wilhelm Püttmann provided an open working environment in his group, which allowed me to explore the topics of interest with freedom. Whenever I have met problems during my research, he always provided useful advices and assistance, and he discussed with me with patience to solve all the problems. I learned a lot from these discussions, which will encourage me to move forward in my academic career in the future.

Great thanks go also to my second supervisor Prof. Dr. Jens Fiebig from the Institute of Geoscience, Goethe-University Frankfurt am Main. He provided with his laboratory the opportunity to obtain valuable stable isotope data from my samples which greatly improved the quality of my PhD thesis. Thanks are also due to Dr. Miloš Markič from the Geological Survey of Slovenia and Prof. Dr. Marko Vrabc from the Department of Geology at University of Ljubljana for their support with samples from Velenje Basin in Slovenia. The data obtained from the analysis of these samples largely promoted my thesis. Special thanks are given to Prof. Dr. Dieter Uhl from Senckenberg Research Institute and Nature Museum, Frankfurt am Main, who guided me to analyze the charcoal and pollen in lignites and gave many suggestions for the paleobotanical analyses, which were significant for my study, although these data are not included in this thesis. PD. Dr. Achim Bechtel from Department of Applied Geosciences and Geophysics, Montanuniversity Leoben, Austria is gratefully acknowledged for his valuable discussions concerning the interpretation of stable isotopic data.

I also would like to thank Mr. Theodoros Potouridis very much for his profound help concerning by laboratorial works. He trained me the laboratory skills, the use of GC/MS system, and helped me whenever I got in trouble during the work vin in the organic geochemical laboratory. Special thanks to Dr. Lingli Zhou and Dr. Fangjie Li in our group, who provided helpful ideas and suggestions to improve this thesis. I learned a lot about the data analysis and data processing from them, and they also supported me with many life skills during my stay in Germany. Great thanks also go to Ursula Karges, Marco Hiltcher and Clara Löw for their help to let my life go easier in Germany. Tiantian Xu, Ting Liu and Yueling Ren were acknowledged for their help during their master study in the group.

Furthermore, I would like to acknowledge the support from some researchers of Hebei University of Engineering in Hebei, China. I greatly appreciate the help of Prof. Yuzhuang Sun for his tremendous support for my PhD project at Goethe-University Frankfurt am Main. Special thanks are given to Associate Prof. Cunliang Zhao and master student Jialiang Ma for their help to collect samples in Yunnan Province, and Dr. Yanheng Li and Dr. Zhixiang Shi for their help during the microscopical analyses and the inorganic geochemical analyses of the samples. Great thanks are going to the master students Jialiang Ma, Zheng Gao, Jiawei Zhang and other master students who helped me at Hebei University of Engineering.

The greatest thanks go to my family for their kind support and encouragement, only with their understanding I could successfully complete my thesis. My sincere appreciation goes to my wife for her support during my study in Germany and on my academic career. Her love kept me moving forward.

I acknowledge the financial support from Hebei University of Engineering for the first year of my study in Germany and the three-year financial support from China Scholarship Council for my PhD project.

Thanks to all the friends that I have met in Germany, they made my study and life interesting.

Thank you very much! Danke schön! 谢谢!

**Bangjun Liu**

Frankfurt am Main, 2020



## **Abstract**

Cenozoic lignite deposits are widespread across Europe, Asia, America, Australia, and Indonesia. These deposits were the subject of numerous studies on changes in regional/global paleoclimates, paleobotany, paleoenvironment, and basin evolutions, which led to the formation of these lignites. In some of these Cenozoic lignite deposit basins, a succession of pale and dark lignite layers has been described in the Miocene Lower Rhine Basin in Germany, the Oligo-Miocene Gippsland Basin in southeastern Australia, and several Mio-Pliocene basins in southwestern China. Furthermore, pale and dark lithotypes in lignite seams also have been found in some Pliocene lignite deposit basins from Slovenia, Serbia, and Poland. The widespread cyclic occurrence of pale and dark layers in lignite basins might represent alternating depositional conditions related to the changes in plant communities, the regional/global climate, the tectonic setting, the Asian monsoon, and orbital periodicity during peat formation.

The main objective of this doctoral thesis is to study the differences in geochemical characteristics (e.g., coal petrology, biomarkers, elements, mineralogy, and stable carbon and nitrogen isotopes of organic matter) of pale and dark layers from the Jinsuo Basin in Yunnan Province, Southwest China. In this project, a total of 49 samples (18 pale lignites, 19 dark lignites, 2 fusain samples, and 10 fossil wood pieces) were collected from the Pliocene No. 3 lignite seam in the Jinsuo Basin. Dark and pale samples were collected from the thick dark lignite layers (30 cm – 150 cm) and thin pale lignite layers (5 cm – 25 cm), fusain samples were collected from two independent charcoal layers, and wood pieces were picked out from both dark and pale layers. The thick, dark lignite layers usually contain large wood fragments, and sometimes even tree trunks have been found, but visible small fibrous plant residues are absent. Dark lignite samples have a density and hardness higher than that of pale lignites, and they show visible stratification. Pale lignite samples have low density and hardness, are usually yellowish-brown in fresh sections and become grayish-white after weathering. They are loose in structure and can be much more easily ground than dark lignites. Some small, fibrous plant residues can be seen under a magnifying glass in pale samples.

Based on the results from these investigations, the origin of pale and dark layers and the possible driving forces for the formation of cyclic pale and dark layers in lignite from the Jinsuo Basin can be reconstructed. This study not only focuses on the changes of plant community, regional climate, and depositional environment during the formation of pale and dark layers in the Jinsuo Basin, but it also compares its findings with the results obtained previously from pale and dark layers in lignite basins from other areas in the world to identify a possible global climate linkage for the occurrence of the Cenozoic pale and dark layers in lignite deposits.

In the first part of the thesis, the characteristics of coal petrology and the biomarker composition of pale and dark lignite layers in the Jinsuo Basin are described to explore whether changes in the depositional environment during peat formation and/or vegetation changes caused the color changes ultimately observed in the lignites. The results obtained from the 37 investigated lignite samples (excluding the 2 charcoal layers) showed that pale layers are characterized by a higher abundance of the macerals belonging to the liptinite group (av. 70.1%) compared with dark layers (av. 12.7%). The composition of liptinites is dominated by bituminite (including mineral-bituminous groundmass, av. 52.5%) and sporinite (av. 13.5%), along with a relatively low abundance of the macerals of the huminite group (18.6%). This indicates a higher degree of oxidation during deposition of pale layers due to deposition in drier peatland environments. The low values of the tissue preservation index (TPI, av. 0.9.), vegetation index (VI, av. 0.31), and gelification index (GI, av. 0.50) in pale layers suggest a relatively high decomposition rate of plant materials under dry/aerobic conditions. In contrast, the maceral composition of the dark layers is characterized as having a very high proportion of huminite (av. 79.2%) dominated by ulminite (av. 39%), along with a low content of liptinite (av. 12.7%) and inertinite (av. 8.1%) macerals, which suggests the prevalence of wet/anaerobic conditions in the peat-forming mire. The high values of TPI (av. 4.80), VI (av. 2.80), and GI (av. 2.19) in dark layers suggest better preservation of organic matter during deposition under anaerobic conditions and more wet/humid climatic conditions when compared with the pale lignite layers.

The concentrations of biomarkers in the saturated and aromatic hydrocarbon fractions of solvent extracts of the lignite samples also vary between pale and dark layers. The high concentrations of long-chain (C<sub>27</sub>-C<sub>31</sub>) *n*-alkanes in both pale and dark layers are typical characteristics of the predominance of higher terrestrial plants. Significant concentrations of mid-chain *n*-alkanes (*n*-C<sub>21</sub>-C<sub>25</sub>) (av. 18.6, wt. %) were detected preferentially in dark layers, suggesting that aquatic plants might also have contributed to the plant community during the formation of the dark layers. For the biomarkers of diterpenoids and triterpenoids, as the diterpenoid compounds are preferentially produced by gymnosperms, while angiosperms usually produce more triterpenoids. Therefore, the quantification of diterpenoids and triterpenoids in the saturated and aromatic hydrocarbon fractions of solvent extracts allows assessment of the relative proportion of gymnosperms and angiosperms in the former peat-forming vegetation. The content of diterpenoids and the average ratio of diterpenoids to the sum of diterpenoids and triterpenoids, Di/(Di+Tri-terpenoids), are higher in the pale layers (128 µg/g TOC and 0.3, respectively) than in dark layers (21.9 µg/g TOC and 0.07, respectively). This indicates that gymnosperms made a crucial contribution to the plant community during the formation of pale layers. In dark layers, triterpenoids are generally far more abundant than diterpenoids, which suggests that the dark layers were overwhelmingly formed by angiosperm plants. This is consistent with lower carbon/nitrogen ratios in the dark lignite

layers (av. 40.8) compared with the pale lignite layers (av. 60.6), as previous studies on modern plants suggested that gymnosperm trees have higher carbon/nitrogen ratios than angiosperm trees. Higher aerobic microbial activities in pale layers than in dark layers are reflected by the higher concentration of hopanoids and particularly of 17 $\alpha$ ,21 $\beta$ -homohopane (22R) in pale layers (553.2  $\mu$ g/g TOC), because homohopane is mostly produced by many prokaryotes as cell membrane components.

In the second part of the thesis, the compositions of stable carbon and nitrogen isotopes and elemental characteristics of Pliocene pale and dark layers in the Jinsuo Basin were investigated. Along with the paleobotanical data obtained from previous studies, paleoenvironmental models were suggested for the formation of pale and dark layers and possible geological driving forces for the formation of two kinds of layers are discussed. Stable isotopic data show that the  $\delta^{13}\text{C}$  values of fossil wood (av. -24.79‰) and fusain samples (av. -24.19‰) are generally higher than the values obtained from bulk pale (av. -27.01‰) and dark (av. -26.38‰) lignite samples. In contrast, the  $\delta^{15}\text{N}$  values of fossil wood (av. -0.63‰) and fusain samples (av. 1.29‰) are lower than the average values of bulk pale layers (av. 2.17‰) and dark layers (av. 1.79‰). The difference in the carbon isotopic values between pale and dark layers can be explained by the very high amount of liptinite and strong degradation of woody material by bacterial activity in pale layers, which resulted in depletion of  $^{13}\text{C}$  in pale layers relative to dark layers. The higher  $\delta^{13}\text{C}$  values in the fossil wood and fusain samples can be explained by the general enrichment of  $^{13}\text{C}$  in woody material in comparison with leaves. The weakly negative correlation between the  $\delta^{15}\text{N}$  and  $\delta^{13}\text{C}$  values indicates that, in addition to bacterial degradation, the liptinite content could also influence the carbon and nitrogen compositions of the organic matter in the layers. The influence of the original plant community (gymnosperms/angiosperms) on the carbon and nitrogen isotopic compositions of bulk lignites is probably insignificant in the Jinsuo Basin because of the limited variation from angiosperms to gymnosperms, as deduced from the variation in Di-/(Di+Tri-terpenoids) ratios.

The paleoenvironmental model for the Jinsuo Basin (Chapter 3) suggests that angiosperm trees (such as *Cyclobalanopsis* and *Castanopsis*) dominated the plant community, in association with some shrubby and herbaceous plants during the formation of the thick dark layers. This reconstruction is consistent with results from the previous biomarker analysis. The occurrence of gymnosperm trees of the Pinaceae family, such as *Pinus yunnanensis*, was restricted to the eastern and western mountains because of the higher altitude and lower ambient temperature. The high values of TPI, VI, and GI, along with the high proportion of macerals of the huminite group and relatively high abundance of mid-chain *n*-alkanes and authigenic minerals suggest deposition of the thick dark layers under stable conditions that were tropical to subtropical and wet to humid. However, pale layers were formed in relatively dry to

aerobic and cold conditions, as suggested by the low values of TPI, VI, and GI, as well as the extension of gymnosperms. The contribution of gymnosperms (*Pinus yunnanensis*) to the peat-forming vegetation increased, whereas the abundance of angiosperm plants (such as *Cyclobalanopsis* and *Castanopsis*) decreased during the cold and dry periods. This is confirmed by the high Di-/ (Di+Tri-terpenoids) values in pale layers. The high detrital/authigenic index (DAI) values, high content of TiO<sub>2</sub>, Zr, and detrital minerals (e.g., quartz) in pale layers further suggest unstable conditions during the peat formation in pale layers.

The possible driving forces for the formation of cyclic occurrence of pale and dark layers are suggested according to the results described in Chapter 2 and Chapter 3, along with the paleoenvironmental models. Between the thick dark layers, the thin pale layers are regularly intercalated, indicating that the conditions changed between the deposition of dark layers. One possible scenario is that the Asian monsoon intermittently strengthened as a result of the phased uplift of the Tibetan Plateau associated with global cooling. Changes in the plant composition and vegetation types were also suggested to be related to the altitude changes from north to south and associated global cooling. The combined influences of uplift of the Tibetan Plateau, intensity of the Asian monsoon, and global cooling on the local geological climate in the study area during the late Pliocene might ultimately have caused formation of the pale layers between the dark layers. The pale layers probably formed following periods of uplift of the Tibetan Plateau, which in turn led to increased monsoon intensity and a locally cold and dry climate in the Jinsuo Basin. The cold and dry climate that resulted in low precipitation and a low groundwater level in the basin, leading to the formation of thin pale layers. Considering the relatively warm, humid tropic to subtropical climate in Yunnan Province from the Miocene to late Pliocene and the long-term stability of the geological conditions, the dark layers formed gradually following the pale layers during periods in which the local climate became warmer and more humid between adjacent uplift steps of the Tibetan Plateau. Another hypothesis that can explain the appearance of cyclic pale and dark layers is related to the ~41-kyr cyclic fluctuations of ice-sheet extent relevant to cycles in insolation, which were influenced by changes of the Earth's axial tilt during the Pliocene. However, additional methods, such as age dating, paleobotany, and spectral analysis, are required in the future to provide more evidence for the hypothesis that the occurrence of cyclic pale and dark layers and their related vegetational and paleoenvironmental changes were related to orbital forcing. Probably, none of these suggested factors alone influenced the formation of cyclic dark and pale layers in the Jinsuo Basin lignites; interactions between different factors should also be considered.

In the third part of this thesis, investigation of three different lithotypes (xylic-pale, gelified-very dark, and matrix-dark) collected from a Pliocene lignite deposit in the Velenje Basin, Slovenia, is described along with comparison with the results from the

pale and dark layers in the Jinsuo Basin. From the biomarker results, the xylitic lithotype almost exclusively originates from gymnosperms (conifers such as Taxodiaceae), as indicated by the very high contents of sesquiterpenoids (av. 301.98  $\mu\text{g/g}$  TOC) and diterpenoids (av. 1,320.89  $\mu\text{g/g}$  TOC) but very low abundances of *n*-alkanes (5.08  $\mu\text{g/g}$  TOC) and non-hopanoid triterpenoids (av. 14.25  $\mu\text{g/g}$  TOC). The relative proportion of gymnosperms to angiosperms in the paleomire is reflected by the Di/(Di+Tri-terpenoids) values, which is close to 1 (av. 0.99) in the xylitic lithotype. The predominance of diterpenoids from conifers in the xylitic lithotype is associated with high carbon/nitrogen ratios (av. 86.5) and intermediate total sulfur (TS, av. 1.3). The very low abundance of hop-17(21)-ene (5.69,  $\mu\text{g/g}$  TOC) and the absence of further hopanoids in the xylitic lithotype indicate a restricted influence of bacterial degradation under relatively dry conditions in the paleomire. The matrix lithotype also originated preferentially from gymnosperms under dry depositional conditions, as indicated by the high Di/(Di+Tri-terpenoids) ratio (0.95), low amounts of hopanoids and low TS content. The gelified lithotype is characterized by a high content of *n*-alkanes and wide variation of the Di/(Di+Tri-terpenoids) ratio (0.13–0.88), indicating a fluctuating contribution of angiosperms to the plant community in the paleomire during formation of this lithotype. In addition, the high abundance of hop-17(21)-ene (av. 21.77,  $\mu\text{g/g}$  TOC) and TS (av. 1.91) in the gelified lithotype compared with the other two lithotypes suggests the effect of bacterial activity under relatively wet/humid conditions during formation of the gelified lithotype, which is also supported by the considerable amount of mid-chain *n*-alkanes (av. 23.26  $\mu\text{g/g}$  TOC).

The high correlation between the  $\delta^{13}\text{C}$  and  $\delta^{15}\text{N}$  values ( $R^2 = 0.68$ ) indicates that the stable carbon and nitrogen isotope composition of the organic matter in the Velenje lignites were probably influenced by the same factors (e.g., precursor plants and/or microbial activity). The stable carbon isotopic values (av.  $-25.44\text{‰}$ ) and nitrogen isotopic values (av.  $2.15\text{‰}$ ) of the xylitic lithotype are higher than those of the gelified lithotype (av.  $\delta^{13}\text{C} = -27.48\text{‰}$ ,  $\delta^{15}\text{N} = 1.37\text{‰}$ ) and the matrix lithotype (av.  $\delta^{13}\text{C} = -27.09\text{‰}$ ,  $\delta^{15}\text{N} = 1.10\text{‰}$ ). The relatively high correlation between the diterpenoid content and both  $\delta^{13}\text{C}$  ( $R^2 = 0.78$ ) and  $\delta^{15}\text{N}$  ( $R^2 = 0.46$ ) values suggests that the stable carbon and nitrogen isotopic composition of the three lithotypes might reflect the composition of the original plant material in the paleomire, which is indicated by the average  $2.5\text{‰}$  isotopically heavier of  $\delta^{13}\text{C}$  values for gymnosperms in comparison to angiosperms from previous studies and the high correlation between the  $\delta^{13}\text{C}$  and  $\delta^{15}\text{N}$  values in this case. The dominance of conifers as precursor plants in the xylitic lithotype might be the main reason for the higher  $\delta^{13}\text{C}$  values and probably also the higher  $\delta^{15}\text{N}$  values. The relatively higher  $\delta^{15}\text{N}$  values in the xylitic lithotype than in the other types could be explained by the high amount of decay-resistant xylem and low mineral (e.g., clay) content in the xylitic lithotype. The slightly lower  $\delta^{13}\text{C}$  but higher  $\delta^{15}\text{N}$  values in

the gelified lithotype than in the matrix lithotype can be explained by variation of parent plant materials and the influence of bacterial activity.

In conclusion, the results of this doctoral research provide new evidences for the mechanism behind the formation of pale and dark layers in Cenozoic lignite basins. These new results from the Pliocene lignites in the Jinsuo Basin and the comparison with results from previous studies on pale and dark layers from other Cenozoic basins all over the world highlight the specific knowledge gaps in changes in regional/global climate, the precursor plant community, and the depositional environment linked to the cyclic formation of pale and dark layers. The comprehensive study of pale and dark layering in this thesis using various geochemical methods improves the understanding of the formation of lignite-bearing strata and evolution of lignite basins, and provides new aspects for the reconstruction of paleoenvironmental changes from the Cenozoic lignite seams.

## **Zusammenfassung (Summary)**

Känozoische Braunkohlevorkommen sind in Europa, Asien, Amerika, Australien und Indonesien weit verbreitet. Diese Lagerstätten waren der Gegenstand umfangreicher Studien zur Rekonstruktion von Veränderungen des regionalen/globalen Paläoklimas, der Paläobotanik, der Paläoumwelt und der Beckenentwicklung, die zur Bildung dieser Braunkohle führten. Von einigen Känozoischen Lagerstätten von Braunkohlen wurde das Auftreten von Abfolgen mit hellen und dunklen Schichten beschrieben, z.B. aus den Miozänen Braunkohlen der Niederrheinischen Bucht in Deutschland, den Oligo-Miozänen Braunkohlen im Gippsland-Becken im Südosten Australiens und mehreren Mio-Pliozän-Braunkohlenbecken in Südwestchina. Darüber wurden helle und dunkle Lithotypen in Pliozänen Braunkohlen in Slowenien, Serbien und Polen gefunden. Das weite verbreitete zyklische Auftreten von hellen und dunklen Schichten in zahlreichen Braunkohlebecken könnte die Folge alternierender Depositionsbedingungen sein, die mit den Veränderungen der Pflanzengemeinschaft, des regionalen/globalen Klimas, der tektonischen Umgebung, der Intensität des asiatischen Monsuns und der Orbitalperiodizitäten während der Torfbildung zusammenhängen können.

Das Hauptziel der vorliegenden Doktorarbeit ist es, die Unterschiede der mikroskopischen und geochemischen Befunde durch Einsatz verschiedener Methoden (z.B. Kohlenpetrologie, Mineralogie und Analytik der Biomarker, der Haupt- und Spurenelemente und der stabilen Isotope von C und N in der organischen Substanz) an hellen und dunklen Schichten von Braunkohlen aus dem Jinsuo Basin in der Provinz Yunnan in Südwestchina zu untersuchen. In diesem Projekt wurden insgesamt 49 Proben (18 helle Braunkohlen, 19 dunkle Braunkohlen, 2 Fusinitproben und 10 fossile Holzstücke) aus dem Pliozänen Braunkohlenflöz Nr. 3 im Jinsuo-Becken entnommen. Aus den mächtigen dunklen Braunkohlschichten (30 cm - 150 cm) und den weniger mächtigen hellen Braunkohlschichten (5 cm - 25 cm) wurden dunkle und helle Proben entnommen. Fusinitproben wurden aus zwei unabhängigen Kohlschichten gesammelt und Holzstücke wurden sowohl aus dunklen und hellen Schichten ausgewählt. Die mächtigen dunklen Braunkohlschichten enthalten in der Regel große Holzfragmente und manchmal wurden sogar Baumstämme gefunden, aber sichtbare kleine faserige Pflanzenreste fehlen. Dunkle Braunkohleproben haben eine höhere Dichte und Härte als helle Proben und zeigen eine sichtbare Schichtung. Helle Braunkohlen haben eine geringe Dichte und geringere Härte, sind in frischen Anschnitten meist gelblich-braun und werden nach der Verwitterung gräulich-weiß. Sie sind locker in der Struktur und leichter zu schleifen als dunkle Braunkohlen. Einige kleine, faserige Pflanzenreste sind unter der Lupe in hellen Proben von Braunkohlen zu sehen.

Ausgehend von den Ergebnissen dieser Untersuchungen sollte die Entstehung von hellen und dunklen Schichten und die möglichen Triebkräfte für die Bildung von zyklisch

auf tretenden hellen und dunklen Schichten in Braunkohlen aus dem Jinsuo-Becken rekonstruiert werden. Die Studie konzentriert sich nicht nur auf die Untersuchung einer möglichen Veränderungen der Pflanzengemeinschaft, des regionalen Klimas und der Ablagerungsbedingungen bei der Bildung von hellen und dunklen Schichten im Jinsuo-Becken sondern vergleicht die Ergebnisse auch mit den Ergebnissen, die zuvor aus hellen und dunklen Schichten in Braunkohlebecken aus anderen Regionen der Welt gewonnen wurden, um dadurch eine mögliche globale Klimaveränderung für das Auftreten der Känozoischen hellen und dunklen Schichten in Braunkohlelagerstätten zu identifizieren.

Im ersten Teil der Arbeit wurden die Methoden der Kohlenpetrologie und die Biomarkeranalytik an hellen und dunklen Braunkohlschichten im Jinsuo-Becken zur Erkennung möglicher Veränderungen der Ablagerungsbedingungen während der Torfbildung und/oder Vegetationsänderungen als mögliche Ursache für die letztendlich in den Braunkohlen beobachteten Farbänderungen eingesetzt. Die Ergebnisse der 37 untersuchten Braunkohleproben (mit Ausnahme von 2 Holzkohleschichten) haben gezeigt, dass helle Schichten durch einen höheren Anteil an Mazeralen der Liptinitgruppe (Av. 70,1%) im Vergleich zu dunklen Schichten (Av. 12,7%) gekennzeichnet sind. Die Zusammensetzung der Liptinite wird dominiert von Bituminit (einschließlich mineralisch-bituminöser Grundmasse, Durchschnitt 52,5%) und Sporinit (Durchschnitt 13,5%), zusammen mit einem relativ geringen Gehalt an Mineralien der Huminitgruppe (18,6%). Dies deutet auf einen höheren Oxidationsgrad bei der Abscheidung von hellen Schichten durch Ablagerung in trockeneren Moorlandschaften hin. Die niedrigen Werte des Gewebeerhaltungsindex (TPI, av. 0,9.), des Vegetationsindex (VI, av. 0,31) und des Gelifikationsindex (GI, av. 0,50) in hellen Schichten deuten auf eine relativ hohe Zersetzungsrate von Pflanzenmaterial unter trockenen/aeroben Bedingungen hin. Im Gegensatz dazu weist die Mazeralzusammensetzung der dunklen Schichten einen sehr hohen Anteil an Huminit (Av. 79,2%) auf, der von Ulmininit (Av. 39%) dominiert wird. Zusammen mit einem niedrigen Gehalt an Liptinit (Av. 12,7%) und Inertinit (Av. 8,1%) deutet dies auf die Dominanz von nassen/anaeroben Bedingungen im früheren Torfmoor hin. Die hohen Werte von TPI (av. 4,80), VI (av. 2,80) und GI (av. 2,19) in dunklen Schichten zeigen eine bessere Erhaltung der organischen Substanz während der Deposition unter anaeroben Bedingungen und feuchtere/nassere klimatische Bedingungen im Vergleich zu den hellen Braunkohle-Schichten an.

Die Konzentrationen von Biomarkern in den Fraktionen der gesättigten und aromatischen Kohlenwasserstoffe aus den Extrakten der Braunkohleproben mit einem organischen Lösungsmittel variieren ebenfalls deutlich zwischen hellen und dunklen Schichten. Die hohen Konzentrationen von langkettigen ( $C_{27}$ - $C_{31}$ ) *n-Alkanen* sowohl in hellen als auch in dunklen Schichten sind typische Merkmale für die Vorherrschaft von höheren terrestrischen Pflanzen. Signifikante Konzentrationen von mittelkettigen *n-Alkanen* ( $n$ - $C_{21}$ - $C_{25}$ ) (Av. 18,6, Gew. %) wurden vorzugsweise in dunklen Schichten nachgewiesen, was darauf hindeutet, dass Wasserpflanzen auch während der Bildung der



dunklen Schichten zur Pflanzengemeinschaft beigetragen haben. Die Biomarker aus der Gruppe der Diterpenoide und Triterpenoide lassen Rückschlüsse auf die Vergesellschaftung der Pflanzen zu, da die Diterpenoide bevorzugt von Gymnospermen produziert werden, während Angiospermen in der Regel mehr Triterpenoide produzieren. Daher ermöglicht die Quantifizierung von Diterpenoiden und Triterpenoiden in der gesättigten und aromatischen Kohlenwasserstofffraktion von Lösungsmittelextrakten die Abschätzung des relativen Anteils von Gymnospermen und Angiospermen in der ehemaligen torfbildenden Vegetation. Der Gehalt an Diterpenoiden und das durchschnittliche Verhältnis von Diterpenoiden zur Summe von Diterpenoiden und Triterpenoiden ( $\text{Di-} / (\text{Di-} + \text{Tri-Terpenoide})$ ) sind in den hellen Schichten (Mittelwert 128,  $\mu\text{g/g TOC}$  bzw. 0,3) deutlich höher als in dunklen Schichten (Mittelwerte 21,9,  $\mu\text{g/g TOC}$  bzw. 0,07). Dies deutet darauf hin, dass die Gymnospermen bei der Bildung heller Schichten einen entscheidenden Beitrag zur Pflanzengemeinschaft geleistet haben. In dunklen Schichten sind Triterpenoide im Durchschnitt viel stärker vertreten als Diterpenoide, was darauf hindeutet, dass die dunklen Schichten überwiegend von Angiospermen gebildet wurden. Dies steht im Einklang mit niedrigeren C/N-Verhältnissen in den dunklen Braunkohlschichten (Mittelwert 40,8) im Vergleich zu den hellen Braunkohlschichten (Mittelwert 60,6), da frühere Studien an rezenten Pflanzen darauf hindeuteten, dass Gymnospermen höhere C/N-Verhältnisse aufweisen als Angiospermen. Höhere aerobe mikrobielle Aktivitäten bei der Bildung der hellen Schichten im Vergleich zu den dunklen Schichten spiegeln sich in der höheren Konzentration von Hopanoiden und insbesondere von  $17\alpha,21\beta$ -Homohopan (22R) in hellen Schichten wider (553,2,  $\mu\text{g/g TOC}$ ), da die Ausgangssubstanz von  $17\alpha,21\beta$ -Homohopan (22R) überwiegend von vielen Prokaryoten als Zellmembranbestandteile produziert wird.

Im zweiten Teil der Arbeit wurden die stabile Isotopenzusammensetzungen von Kohlenstoff- und Stickstoff sowie einige Haupt- und Spurenelemente in Proben aus den Pliozänen hellen und dunklen Schichten im Jinsuo-Becken untersucht. Neben den paläobotanischen Daten aus früheren Studien wurden Modelle für die Paleoumweltbedingungen während der Bildung von hellen und dunklen Schichten vorgeschlagen und mögliche geologische Triebkräfte für die Bildung der beiden Arten von Schichten diskutiert. Stabile Isotopendaten zeigen, dass die  $\delta^{13}\text{C}$ -Werte von fossilem Holz (Mittelwert  $-24,79\text{‰}$ ) und Fusiniten (Mittelwert  $-24,19\text{‰}$ ) im Allgemeinen höher sind als die Werte von hellen (Mittelwert  $-27,01\text{‰}$ ) und dunklen (Mittelwert  $-26,38\text{‰}$ ) Braunkohleproben. Im Gegensatz dazu sind die  $\delta^{15}\text{N}$ -Werte von fossilem Holz (Mittelwert  $-0,63\text{‰}$ ) und Fusiniten (Mittelwert  $1,29\text{‰}$ ) niedriger als die Werte von Proben aus den hellen Schichten (Mittelwert  $2,17\text{‰}$ ) und den dunklen Schichten (Mittelwert  $1,79\text{‰}$ ). Der Unterschied in den Kohlenstoffisotopenwerten zwischen hellen und dunklen Schichten erklärt sich durch den sehr hohen Anteil an Liptinit und den starken Abbau von holzigem Material durch bakterielle Aktivität in hellen Schichten,

was zu einem bevorzugten Abbau von  $^{13}\text{C}$  in hellen Schichten im Vergleich zu dunklen Schichten führte. Die höheren  $\delta^{13}\text{C}$ -Werte in den fossilen Holz- und Fusainproben lassen sich durch die allgemeine Anreicherung von  $^{13}\text{C}$  in holzigem Material im Vergleich zu Blättern erklären. Die schwach negative Korrelation zwischen den Werten  $\delta^{15}\text{N}$  und  $\delta^{13}\text{C}$  deutet darauf hin, dass neben dem bakteriellen Abbau auch der Liptinitgehalt die Kohlenstoff- und Stickstoffzusammensetzung der organischen Substanz in den Schichten beeinflussen könnte. Der Einfluss der ursprünglichen Pflanzengemeinschaft (Gymnospermen/Angiospermen) auf die Zusammensetzung der stabilen Kohlenstoff- und Stickstoffisotopie von Braunkohlen ist im Jinsuo-Becken wahrscheinlich unbedeutend, da die Variation von Angiospermen zu Gymnospermen begrenzt ist, die sich aus der Variation des Di- / (Di- + Tri-Terpenoide)-Verhältnisses ergibt.

Das paläoökologische Modell für das Jinsuo-Becken (Kapitel 3) deutet darauf hin, dass während der Bildung der mächtigen dunklen Schichten Angiospermen (wie *Cyclobalanopsis* und *Castanopsis*) in Verbindung mit einigen strauchigen und krautigen Pflanze die Pflanzengemeinschaft dominierten. Diese Rekonstruktion steht im Einklang mit den Ergebnissen der vorherigen Biomarker-Analyse. Das Vorkommen von Gymnospermen der Familie der Kieferngewächse, wie *Pinus yunnanensis*, war aufgrund der höheren Lage und niedrigeren Umgebungstemperatur auf das östliche und westliche Gebirge beschränkt. Die hohen Werte von TPI, VI und GI, zusammen mit dem hohen Anteil an Mazerale der Huminitgruppe und dem relativ hohen Anteil an mittelkettigen *n-Alkanen*, deuten auf eine Ablagerung der mächtigen dunklen Schichten unter stabilen, tropisch/subtropischen und entsprechend feuchten Klimabedingungen hin. Dies wird unterstützt durch den hohen Gehalt an authigene Mineralen. Allerdings werden bei relativ trockenen, aeroben und kalten Bedingungen die Schichten heller, wie die niedrigen Werte von TPI, VI und GI sowie die Ausdehnung von Gymnospermen vermuten lassen. Der Beitrag der Gymnospermen (*Pinus yunnanensis*) zur torfbildenden Vegetation nahm zu, während die Dominanz an Angiospermen (wie *Cyclobalanopsis* und *Castanopsis*) während der Kälte- und Trockenzeit abnahm. Dies wird durch die hohen Di- / (Di- + Tri-Terpenoide) Werte in hellen Schichten bestätigt. Die hohen DAI-Werte, der hohe Gehalt an  $\text{TiO}_2$ , Zr und Detritusmineralien (z.B. Quarz) in hellen Schichten deuten zudem auf instabile Bedingungen bei der Torfbildung in hellen Schichten hin.

Die möglichen Triebkräfte für die Bildung des zyklischen Auftretens von hellen und dunklen Schichten wurden gemäß diesen in Kapitel 2 und Kapitel 3 beschriebenen Ergebnissen sowie auf der Basis der paläoökologischen Modelle diskutiert. Zwischen den mächtigen dunklen Schichten werden die dünnen hellen Schichten regelmäßig eingelagert, was darauf hindeutet, dass sich die Bedingungen zwischen der Ablagerung der dunklen Schichten geändert haben. Ein mögliches Szenario ist, dass es zu einer intermittierenden Verstärkung des asiatischen Monsuns infolge der schrittweisen Hebung des tibetischen Plateaus im Zusammenhang mit einer globalen Abkühlung kam. Es wurde auch vorgeschlagen, dass Änderungen in der Pflanzenzusammensetzung und

den Vegetationstypen mit den Höhenunterschieden von Nord nach Süd und der damit verbundenen globalen Abkühlung zusammenhängen. Die kombinierten Einflüsse der Hebung des tibetischen Plateaus, der Intensität des asiatischen Monsuns und der globalen Abkühlung auf das lokale geologische Klima des Untersuchungsgebietes im späten Pliozän könnten letztendlich zur Bildung der hellen Schichten zwischen den dunklen Schichten geführt haben. Die hellen Schichten bildeten sich wahrscheinlich nach den Hebungsphasen des tibetischen Plateaus, was zu einer zunehmenden Monsunintensität und einem lokal kalten und trockenen Klima im Jinsuo-Becken geführt haben könnte. Das kältere und trockenere Klima, das zu geringeren Niederschlägen und einem niedrigeren Grundwasserspiegel im Becken führte, führte danach auch zur Bildung der dünnen hellen Schichten. In Anbetracht des relativ warmen, feuchten tropischen/subtropischen Klimas in der Provinz Yunnan vom Miozän bis zum späten Pliozän und der langfristigen Stabilität der geologischen Bedingungen bildeten sich die dunklen Schichten allmählich nach den hellen Schichten während der Perioden, in denen das lokale Klima zwischen zwei Hebungsschritten des tibetischen Plateaus wärmer und feuchter wurde. Eine weitere Hypothese, die das Auftreten zyklischer heller und dunkler Schichten erklären kann, bezieht sich auf die ~41 kyr zyklischen Schwankungen des Eisschildumfangs, die für Zyklen der Sonneneinstrahlung relevant sind und die durch Veränderungen der Axialneigung der Erde während des Pliozäns beeinflusst wurden. Allerdings sind in Zukunft zusätzliche Methoden wie Altersdatierung, Paläobotanik und Spektralanalyse erforderlich, um mehr Beweise für die Hypothese zu liefern, dass das Auftreten zyklischer heller und dunkler Schichten und die damit verbundenen vegetativen und paläoökologischen Veränderungen mit dem Orbitalantrieb zusammenhängen. Wahrscheinlich hat nicht nur einer der vorgeschlagenen Faktoren die Bildung zyklischer dunkler und heller Schichten in den Braunkohleflözen des Jinsuo-Beckens beeinflusst; auch Wechselwirkungen zwischen verschiedenen Faktoren sollten berücksichtigt werden.

Im dritten Teil der Doktorarbeit wurden drei verschiedene Lithotypen (xylitisch-hell, gelifiziert-sehr dunkel und matrixdominiert-dunkel) aus einer Pliozänen Braunkohlelagerstätte im Velenje Becken, Slowenien, untersucht, um sie mit den Ergebnissen von den hellen und dunklen Schichten im Jinsuo Becken zu vergleichen. Nach den Ergebnissen der Biomarkeranalytik resultiert der xylitische Lithotyp fast ausschließlich aus Gymnospermen (Koniferen wie Taxodiaceae), wie der sehr hohe Gehalt an Sesquiterpenoiden (Mittelwert 301.98, µg/g TOC) und Diterpenoiden (Mittelwert 1320.89, µg/g TOC), aber sehr geringe Gehalte an *n-Alkanen* (Mittelwert 5.08, µg/g TOC) und den nicht-Hopanoiden Triterpenoiden (Mittelwert 14.25, µg/g TOC) zeigt. Das relative Verhältnis von Gymnospermen zu Angiospermen im Paläomoor spiegelt sich in den Di-/(Di++Tri-Terpenoiden) Werten wider, die im xylitischen Lithotyp nahe 1 (Mittelwert 0,99) liegen. Die Dominanz von Diterpenoiden von Koniferen im xylitischen Lithotyp ist mit hohen C/N-Verhältnissen (Mittelwert 86,5) und

intermediären TS (Mittelwert 1,3) verbunden. Der sehr geringe Gehalt an Hop-17(21)-en (Mittelwert 5,69,  $\mu\text{g/g TOC}$ ) und das Fehlen weiterer Hopanoide im xylitischen Lithotyp deuten auf einen eingeschränkten Einfluss des bakteriellen Abbaus unter relativ trockenen Bedingungen im Paläomoor hin. Der matrixdominierte Lithotyp stammt ebenfalls bevorzugt aus Gymnospermen ab und wurde unter trockenen Depositionsbedingungen gebildet, wie das hohe Di-/ (Di+Tri-Terpenoid)-Verhältnis (0,95), geringe Mengen an Hopanoiden und ein niedriger TS-Gehalt zeigen. Der gelifizierte Lithotyp zeichnet sich durch einen hohen Gehalt an *n-Alkanen* und eine große Variation des Di-/ (Di+Tri-Terpenoide)-Verhältnisses (0,13-0,88) aus, was auf einen schwankenden Anteil von Angiospermen an der Pflanzengemeinschaft im Paläomoor während der Bildung dieses Lithotyps hinweist. Darüber hinaus deutet der hohe Gehalt an Hop-17(21)-en (Mittelwert 21,77,  $\mu\text{g/g TOC}$ ) und TS (Mittelwert 1,91) im gelifizierten Lithotyp im Vergleich zu den beiden anderen Lithotypen auf die Wirkung bakterieller Aktivität unter relativ feuchten Bedingungen während der Bildung dieses Lithotyps hin. Dies wird auch durch den beträchtlichen Gehalt an mittelkettigen *n-Alkanen* (Mittelwert 23,26,  $\mu\text{g/g TOC}$ ) unterstützt.

Die hohe Korrelation zwischen den Werten von  $\delta^{13}\text{C}$  und  $\delta^{15}\text{N}$  ( $R^2 = 0,68$ ) zeigt, dass die Zusammensetzung der stabilen Kohlenstoff- und Stickstoffisotopie der organischen Substanz in den Velenje Braunkohlen wahrscheinlich von den gleichen Faktoren beeinflusst wurde (z.B. Vorläuferpflanzen und/oder mikrobielle Aktivität). Die stabilen Kohlenstoffisotopenwerte (Mittelwert  $-25,44\%$ ) und Stickstoffisotopenwerte (Mittelwert  $2,15\%$ ) des xylitischen Lithotyps sind höher als die des gelifizierten Lithotyps (Mittelwerte  $\delta^{13}\text{C} = -27,48\%$ ,  $\delta^{15}\text{N} = 1,37\%$ ) und des matrixdominierten Lithotyps (Mittelwerte  $\delta^{13}\text{C} = -27,09\%$ ,  $\delta^{15}\text{N} = 1,10\%$ ). Die relativ hohe Korrelation zwischen dem Diterpenoidgehalt und den Werten  $\delta^{13}\text{C}$  ( $R^2 = 0,78$ ) und  $\delta^{15}\text{N}$  ( $R^2 = 0,46$ ) deutet darauf hin, dass die Zusammensetzung der stabilen Kohlenstoff- und Stickstoffisotopie der drei Lithotypen die Zusammensetzung des ursprünglichen Pflanzenmaterials im Paläomoor widerspiegelt, was durch die durchschnittlich 2,5 isotopisch höheren  $\delta^{13}\text{C}$ -Werte für Gymnospermen im Vergleich zu Angiospermen aus früheren Studien und die hohe Korrelation zwischen den Werten  $\delta^{13}\text{C}$  und  $\delta^{15}\text{N}$  in diesem Fall angezeigt wird. Die Dominanz von Koniferen als Vorläuferpflanzen im xylitischen Lithotyp könnte der Hauptgrund für die höheren  $\delta^{13}\text{C}$ -Werte und wahrscheinlich auch die höheren  $\delta^{15}\text{N}$ -Werte sein. Die relativ höheren  $\delta^{15}\text{N}$ -Werte im xylitischen Lithotyp im Vergleich zu den anderen Lithotypen lassen sich durch den hohen Anteil an zerfallsresistentem Xylem und niedrigem Mineralgehalt (z.B. Ton) im xylitischen Lithotyp erklären. Die etwas niedrigeren  $\delta^{13}\text{C}$ -, aber höheren  $\delta^{15}\text{N}$ -Werte im gelifizierten Lithotyp als im Matrixlithotyp lassen sich durch die Variation der pflanzlichen Ausgangsmaterialien und den Einfluss der Bakterienaktivität erklären.

Zusammenfassend lässt sich sagen, dass die Ergebnisse dieser Doktorarbeit neue Erkenntnisse für die Bildung heller und dunkler Schichten in Känozoischen

Braunkohlebecken liefern. Diese neuen Ergebnisse aus der Pliozänen Braunkohle im Jinsuo-Becken und der Vergleich mit Ergebnissen aus früheren Studien zu hellen und dunklen Schichten aus anderen Känozoischen Becken auf der ganzen Welt verdeutlichen die spezifischen Wissenslücken bei den regionalen/globalen Klimaänderungen, die Veränderungen der Vorläuferpflanzengemeinschaft und die Veränderungen der Ablagerungsbedingungen im Paläomoor, die mit der zyklischen Bildung von hellen und dunklen Schichten verbunden sind. Die umfangreichen Untersuchungen von hellen und dunklen Schichten in dieser Dissertation unter Verwendung verschiedener mikroskopischer und geochemischer Methoden verbessern das Verständnis der Bildung von hellen und dunklen Schichtungen in Braunkohlenlagerstätten und der Evolution von Braunkohlebecken und liefern neue Aspekte für die Rekonstruktion von Paläoumweltbedingungen in den Känozoischen Braunkohleflözen.



## List of Tables

Table 2-1 Summary of the current knowledge and associated references regarding the formation of pale and dark lignites.....	37
Table 2-2 Maceral composition based on mineral matter-free basis (vol.%) of the examined samples from the Neogene Jinsuo opencast lignite mine, Yunnan Province.....	43
Table 2-3 Bulk geochemical data and parameters of lignite samples from Jinsuo opencast mine .....	52
Table 2-4 Biomarker concentrations of lignite samples from Jinsuo opencast mine .....	55
Table 2-5 Hopanoids ( $\mu\text{g/g}$ TOC) concentrations of lignite samples from Jinsuo opencast mine .....	60
Table 4-1 Bulk organic geochemistry data along with carbon and nitrogen isotopic composition of the lignite samples from Velenje Basin .....	97
Table 4-2 Biomarker compounds identified by GC-MS analysis in saturated and aromatic hydrocarbon fractions (Fig. 2), obtained from solvent extracts of lignites from the Velenje Basin, Slovenia ....	99
Table 4-3 Concentration of some compounds and biomarker parameters calculated from the distributions of n-alkanes, terpenoids and hopanoids in samples from the Velenje Basin, Slovenia.....	103
Table A1 Values of stable carbon isotopes ( $\delta^{13}\text{C}$ ) and stable nitrogen isotopes ( $\delta^{15}\text{N}$ ) of lignites and fossil woods from Jinsuo Basin, Yunnan Province. ....	142
Table A2 Major-element oxides (%), Zr (ppm) and related parameters of the lignites from Jinsuo Basin, Yunnan Province, on a whole coal basis.....	144
Table A 3 Major-element oxides (%) and related parameters of the lignites from Jinsuo Basin, Yunnan Province, on ash basis.....	146

## List of Figures

Figure 1-1 (a): Distribution of pale and dark layers in lignite basins in Yunnan Province southwest China; (b) stratigraphic column and profile of pale and dark layers in Jinsuo opencast lignite mine. $Q_P$ = Pleistocene, $E_2$ = Middle Cambrian .....	23
Figure 1-2 Cross section (north to south) through the Rhenish Hambach mine showing changes of lithotype through the main lignite seam (Holdgate et al., 2016). Bright layer-facies (HB-facies); Angiosperm-forest-facies (A-facies); Pinus-Myricaceen-Palm Tree-facies (P-facies); Marcoduria-facies (M-facies); Conifer-forest-facies (K-facies) and Glumifloren-facies (G-Facies).....	25
Figure 1-3 (a) The presumed depositional conditions for Miocene lignite types in the Lower Rhine basin, Germany (after Teichmüller, 1962); (b) Schematic facies profile of the peat-forming plant communities and presumed depositional conditions for the brown coal lithotypes in the Rhenish district, Germany (after Hiltmann, 1976). ....	27
Figure 1-4 Typical lithotypes in Latrobe Valley in Gippsland Basin (Holdgate et al., 2014).....	28
Figure 1-5 Facies model of the vegetation succession in the Early Miocene peatlands of the Latrobe Valley. Latrobe Valley, Gippsland Basin, Australia (Korasidis et al., 2016) .....	29
Figure 1-6 Charcoal data (i.e., number of charcoal fragments recorded per count of 200 palynomorphs) for each lithotype in the Morwell and Yallourn coal seams, Gippsland Basin. The central box represents the middle 50% of the data while the whiskers represent the extreme values that are not outliers. A thick black line represents the median while a black circle represents the mean (Korasidis et al., 2019).....	30
Figure 2-1 Location and stratigraphic column of Jinsuo opencast lignite mine. $Q_P$ = Pleistocene, $E_2$ = Middle Cambrian .....	39

Figure 2-2 Field observations of Jinsuo opencast lignite mine. (a) pale layers and wood fragment (brown color) in the thick dark lignites; (b) typical pale lignite (top) and dark lignite (bottom); (c) typical tree trunk in the dark lignite layers; (d) thin fusain as internal seam in the pale, yellowish brown color of fresh pale lignite and grayish white color of weathered pale lignite .....	40
Figure 2-3 Diagram (a) of the Gelification Index (GI) vs. Tissue Preservation Index (TPI) with data point of pale and dark lignites from Jinsuo Basin (after Diessel, 1986, modified), and diagram (b) of Vegetation Index (VI) vs. Ground Water Index (GWI) of pale and dark lignites from Jinsuo Basin (modified after Calder et al., 1991).....	50
Figure 2-4 Gas chromatograms (total ion current) of the saturated hydrocarbon fractions of: (a) sample Jinsuo-21 (pale lignite), and (b) sample Jinsuo-26 (dark lignite). n-Alkanes are labeled according to their carbon number. Std. = Standard (squalane). Traces (c) and (d) show mass chromatograms ( $m/z = 191$ ) of the hopanes of sample Jinsuo-21 (pale lignite), and sample Jinsuo-26 (dark lignite).....	54
Figure 2-5 Gas chromatograms (total ion current) of the aromatic hydrocarbon fractions of: (a) sample Jinsuo-19 (pale lignite), and (b) Jinsuo-24 (dark lignite). Std. = Standard (1,1'-binaphthyl).....	59
Figure 3-1 Geological map and location of Jinsuo Basin (a), modified from Zhu et al., (2008), along with the stratigraphic column and sample profile of Jinsuo opencast lignite mine (b). Q = Pleistocene, C <sub>2</sub> = Middle Cambrian. Sample JS-03 and JS-08 are fusain samples. Brown color: pale layers; gray color: dark layers.....	72
Figure 3-2 Stable carbon (a) and nitrogen (b) isotopic composition of samples (pale, dark, fossil wood and fusain samples) collected from the Pliocene lignite profile in the Jinsuo Basin, Yunnan Province, Southwestern China .....	73
Figure 3-3 Correlation between $\delta^{13}C$ , $\delta^{15}N$ values and TOC, along with $\delta^{15}N$ values versus TN and $\delta^{13}C$ values of lignites from Jinsuo Basin. Data of TOC and TN are from Liu et al. (2018).....	75
Figure 3-4 Mineral and elemental (Si, Al and O) distribution in pale (a, sample no. JS-02) and dark lignites (b, sample no. JS-26), areal scanning by SEM-EDS .....	79
Figure 3-5 Correlation diagrams of (a) SiO <sub>2</sub> versus Al <sub>2</sub> O <sub>3</sub> , (b) SiO <sub>2</sub> versus K <sub>2</sub> O in pale and dark lignites from Jinsuo Basin.....	81
Figure 3-6 Conceptual models of the depositional paleoenvironment for the formation of dark (a) and pale (b) layers in Jinsuo lignite deposit basin, Yunnan Province, China.....	83
Figure 4-1 (A): Geological map of the Velenje Basin, Slovenia (modified from Brezigar et al., 1987). (B): Stratigraphic column of the Velenje Basin and the sample location (modified from Brezigar 1986; Brezigar et al., 1987); (C): Photographs of gelified, matrix and xylitic lithotypes.....	92
Figure 4-2 Sections of TIC chromatograms obtained from GC-MS analysis of the saturated hydrocarbon fractions (A) and aromatic hydrocarbon fractions (B) in three different kinds of lithotypes from the Velenje Basin, Slovenia .....	99
Figure 4-3 n-Alkane distribution according to SIM $m/z$ 85 of representative lithotypes from Velenje Basin, Slovenia. Numbers correspond to carbon atoms in the n-alkane chain .....	101
Figure 4-4 Cross-correlation of carbon isotopic composition ( $\delta^{13}C$ ) versus (A): extractable organic matter (EOM), (B): total content of diterpenoids (Diterpenoids), (C): nitrogen isotopic composition ( $\delta^{15}N$ ), and correlation of $\delta^{15}N$ versus (D): extractable organic matter (EOM), (E): total content of diterpenoids (Diterpenoids), (F): hop-(17)21-ene .....	112
Figure 5-1 Summary results of different lithotypes from Jinsuo Basin, Lower Rhine Basin, Gippsland Basin and Velenje Basin .....	122



## **Acronyms**

---

TPI	Tissue preservation index
GI	Gelification index
VI	Vegetation index
GW	Groundwater Index
Di-/(Di++Tri-terpenoids)	Average concentration ratio of diterpenoids to the sum of diterpenoids and angiosperm triterpenoids
TOC	Total organic carbon
TN	Total nitrogen
TS	Total sulfur
GC-MS	Gas chromatography coupled to mass spectrometry
TIC	Total ion current
EOM	Extractable organic matter
DCM	dichloromethane
N.A.	Not analyzed
N.D.	Not detected
NHG	Northern Hemisphere glaciation
DAI	detrital/authigenic index

---



## Chapter 1 Introduction

Lignite is a kind of sedimentary rock and a younger coal characterized by low coalification; high contents of oxygen, inherent moisture, and volatiles; and a low calorific value (<https://www.britannica.com/science/lignite>). It was previously called brown coal or soft coal due to its brown to brownish-black color and typical softness. With these features, lignite is not as good as hard coal for most industrial processes, and most lignites are directly used for electricity production in power plants. So, on the one hand, most research on lignites in the last few decades has focused on the treatment of lignites (such as cleaning and drying technology) prior to its utilization in power plants (Ozbas et al., 2000; Aksoy et al., 2014; Sivrikaya, 2014; Zhao et al., 2015; Koca et al., 2017). Moreover, the pyrolysis, liquefaction, and gasification of lignite have been investigated in numerous studies (i.e., Ozbas et al., 2000; Chen and Bhattacharya, 2013; Li, 2013; Aksoy et al., 2014; Sivrikaya, 2014; Li et al., 2015; Zhao et al., 2015; Koca et al., 2017). On the other hand, lignite as a relatively young sediment, which was not subjected to high temperature, pressure, and compaction over geological time, has a high potential to be useful for research concerning changes of paleoenvironmental and paleoclimatic conditions, especially during the Paleogene and Neogene (Large et al., 2004; Stock et al., 2016; Valero et al., 2016; Singh et al., 2017; Naafs et al., 2018; Oskay et al., 2019). The information obtained from lignite seams and related strata in lignite basins also has great significance for determining the evolution of local basin and geology (Kalkreuth et al., 1991; Bechtel et al., 2007a; Kortenski et al., 2013; Singh et al., 2016, 2017). Lignites and the fossil wood materials in lignite seams were also extensively used for palynological investigations to investigate plant community changes over time (Harrington et al., 2005; Bechtel et al., 2008; Dutta et al., 2011; Oikonomopoulos et al., 2015; Korasidis et al., 2016). Over the last few decades, lignites have been increasingly used in biogeochemical research, such as the carbon and nitrogen cycle (Harrington et al., 2005; Briggs et al., 2007; Large, 2007; Holdgate et al., 2009; Kanduč et al., 2012; Huang et al., 2018; Naafs et al., 2018, 2019; Bechtel et al., 2019).

In the last few decades, abundant methods have been developed and applied to lignites as possible paleoenvironmental proxies. These methods involve organic petrological indices, such as tissue preservation index (TPI), gelification index (GI), vegetation index (VI), and groundwater index (GWI) (Kershaw et al., 1991; Kalaitzidis et al., 2000; Stock et al., 2016); biomarker composition indices, such as Di-/ (Di+Tri-terpenoids) (Bechtel et al., 2003, 2008),  $P_{aq}$ , and average chain length (Ficken et al., 2000; Eglinton and Eglinton, 2008; Bush and McInerney, 2015); and the stable carbon isotopic composition of bulk lignite materials (Bechtel et al., 2003, 2007, 2008; Holdgate et al., 2009; Kanduč et al., 2012; Erdenetsogt et al., 2017) and of individual compounds extracted from lignites (Bechtel et al., 2003, 2007b, 2019; Talbot et al., 2016; Naafs et al., 2017, 2019; Inglis et

al., 2019). Moreover, a color index and paleomagnetism has been applied to lignite seams and lignite-bearing strata (Large et al., 2004; Yue et al., 2005; Zhu et al., 2008a; Holdgate et al., 2009, 2016; Korasidis et al., 2016). All these parameters have been used to clarify the depositional conditions, plant composition, and regional/global climate changes during the formation of lignites.

China has a large amount of lignite deposits from Jurassic to Pliocene age, which are mostly distributed in the northeast and southwest of China with a known amount of about 130 billion tons of lignite in total (Wang et al., 2016). Both regions together contribute about 90% of all lignite deposits in China, with about 77% being located in the northeast region (mainly in the eastern part of Inner Mongolia) and about 13% in the southwest region (mainly in Yunnan Province) (Yin, 2004; Fu et al., 2012). Although many lignite deposits in China are available for scientific research, most studies have focused on the industrial utilization of lignite, and only a few studies have concentrated on usability of Chinese lignites as archives for reconstruction of paleodepositional and paleoclimatic conditions (Urabe et al., 2001; Xu et al., 2004, 2008; Kou et al., 2006; Xia et al., 2009; Xie et al., 2012; Xing et al., 2012; Zhang et al., 2012; S. F. Li et al., 2015).

The related paleoenvironmental information (such as regional/global climate change, evolution of ancient plant and geology of basins, and carbon cycle) that has been stored in these geological archives during their formation has great implications for reconstruction of changes in the earth terrestrial system. However, these aspects still need to be investigated in the Cenozoic lignite basins in China in more detail.

Yunnan Province in southwest China is an important research area due to its complicated topography, diverse climates, and high plant diversity (Xu et al., 2008). There are over 100 lignite basins of Tertiary age alone in Yunnan Province, most of which are located in intermountain basins, and the lignite seams often have great thickness (Ming et al., 1994). The huge number of lignite deposits in Yunnan Province could provide more detailed information not only with respect to the local geological evolution, plant diversity, and climate change, but also are good archives for the study of pre-Quaternary global climate changes such as the development of the Asian monsoon and Northern Hemisphere glaciation. Previous studies suggested that intermittent strengthening of the Asian monsoon occurred as a result of the phased uplift of the Tibetan Plateau associated with global cooling (An et al., 1999, 2001; Li et al., 2014). In a previous study of the Cenozoic plant diversity in Yunnan, changes in the plant composition and vegetation types were suggested to be related to the altitude changes from north to south and associated global cooling (Huang et al., 2016). On the basis of results obtained from the investigation of the late Pliocene paleoflora of the Longling lignite mine (western Yunnan), Xu et al. (2004) found five major cycles of warming and cooling during that time. Furthermore, the Cenozoic monsoon evolution (Clift et al., 2008, 2010) and the approximate co-occurrence of the phased uplift of the Tibetan Plateau with stepwise strengthening of the Asian monsoon from the late Miocene (An et

al., 2001) is well established, and the Southeast Asian and East Asian monsoons also co-occurred in Yunnan during the late Miocene (Jacques et al., 2011). In general, the interaction between monsoon intensity and global climate change is well known (Kutzbach and Street-Perrott, 1985; Licht et al., 2014; Sun et al., 2015). Previous studies also suggested that stepwise enhanced monsoon activity and drying of the Asian interior were associated with episodic tectonic uplift of the Tibetan Plateau during and after the Miocene (~8 Ma). Moreover, global cooling in the Pliocene at ~3.2 Ma (Li et al., 2014), and uplift of the Tibetan Plateau together with contemporaneous enhancement of the monsoon further accelerated the Miocene–Pliocene global cooling (Sun et al., 2008; Ruddiman, 2013; Li et al., 2014; An et al., 2015).

The occurrence of cyclic dark and pale layers in lignite deposits from the late Miocene to late Pliocene in Yunnan Province provides an opportunity to study recorded paleoenvironmental changes and related floral changes during this time. Previously, dark and pale layers in Cenozoic lignite seams have already been reported from Australia, Germany, and some other European countries (e.g., Slovenia, Serbia, and Poland) (Chaffee et al., 1984; Dehmer, 1989; Holdgate et al., 1995, 2009b, 2014; Kanduč et al., 2005; Doković et al., 2018). The worldwide prevalence of the pale and dark layers in Cenozoic lignite deposits might also be linked to the global climate system. Hence, the systematic and comparative study of the pale and dark layers in lignite deposits around the world could not only advance our understanding of the origin of these layers, but it might also provide new information about pre-Quaternary global climate changes.

## **1.1 Pale and dark layers in lignites around the world**

### **1.1.1 Pale and dark layers in lignites from China**

Pale and dark layers have been found in several lignite deposits from the late Miocene to late Pliocene in Yunnan Province, southwest China (Lu and Zhang, 1986, 1989; Fu et al., 1987; Ming et al., 1994; Yu et al., 1997). At first, only the relatively thin pale layers were attractive to coal geologists because it is a particular kind of lignite that was thought to originate from *Sphagnum* spp. and has consequently been described as “Sphagnum coal,” which was considered to be a new genetic type of lignite (Lu and Zhang, 1989). The pale layers were found for the first time in the Jinsuo Basin, Yunnan Province, and were later widely found in other opencast lignite deposits in Yunnan Province, such as Liaohu, Zhujie, Jiangchuan, and Shanxincun (Fig. 1-1) (Ming et al., 1994; Wang et al., 1997). This kind of pale lignite layer is locally described as “Baipao coal” (Lu and Zhang, 1989; Wang et al., 1997; Yu et al., 1997), which means white in color and light in weight.

The pale layers in the Jinsuo Basin, Yunnan Province are characterized by thin and poorly stratified sections varying in thickness (5-25 cm) intercalated with thick dark lignite layers (30-150 cm). Pale lignites have a low density and hardness, and are usually

yellowish-brown in fresh sections, becoming grayish-white after weathering (Fig. 1-1). They are loose in structure and can be much more easily ground than dark lignites. Some small, fibrous plant residues can be seen under a magnifying glass in pale lignites, and dried pale samples are flammable. The thick, dark lignite layers usually contain large wood fragments inside the layer, and sometimes even tree trunks have been found, but visible small fibrous plant residues are absent. Dark lignites have a higher density and hardness than pale lignites, and show visible stratification, which suggests stable depositional conditions. More than 20 pale layers were found as thin internal sections within the thick dark layers throughout the basin (Fig. 1-1). The dark layers have a thickness of 0.3-1.5 m and contain large, brown-colored stems and roots of trees. Fusain horizons with a thickness of 2-6 cm occasionally occur as internal seams within the pale layers, or on top of the pale layers, and provide evidence for the occurrence of wildfires during peat accumulation.

The origin of pale and dark layers in lignites from Yunnan Province has been debated since the first description of pale lithotypes by Lu and Zhang (1986). These pale lignites were thought to originate from Sphagnum peat, but the formation of the dark lignites was not discussed (Fu et al., 1987; Lu and Zhang, 1989). However, organic geochemical and petrological studies carried out on various lignite deposits in Yunnan Province revealed the occurrence of both pale and dark lignite layers with different compositions (Qi et al., 1994). Gymnosperms were considered to be the source materials of both pale and dark lignites, and the difference between the two types of lignites was attributed to their degree of decomposition, with the pale lignites being a product of more intensive bacterial decomposition than the dark lignites (Qi et al., 1994). However, other studies of plant residues in pale and dark lignites from Yunnan Province have shown that the pale lignites were dominated by herbaceous tissues, while ligneous tissues were more prevalent in the dark lignites (Yu et al., 1996; Wang et al., 1997). Unfortunately, the origin of the pale and dark layers in the Jinsuo Basin, Yunnan Province, has not been conclusively clarified, even after 30 years. Possible reasons for the different interpretations of the origin of the types of lignites are lack of comprehensive consideration of the depositional conditions, the source of plant materials in the paleomire, and the influence of paleoclimate changes. In addition, previous studies were based on only a few samples from each site, and thus they could be unrepresentative and prevent a meaningful statistical evaluation of the data.

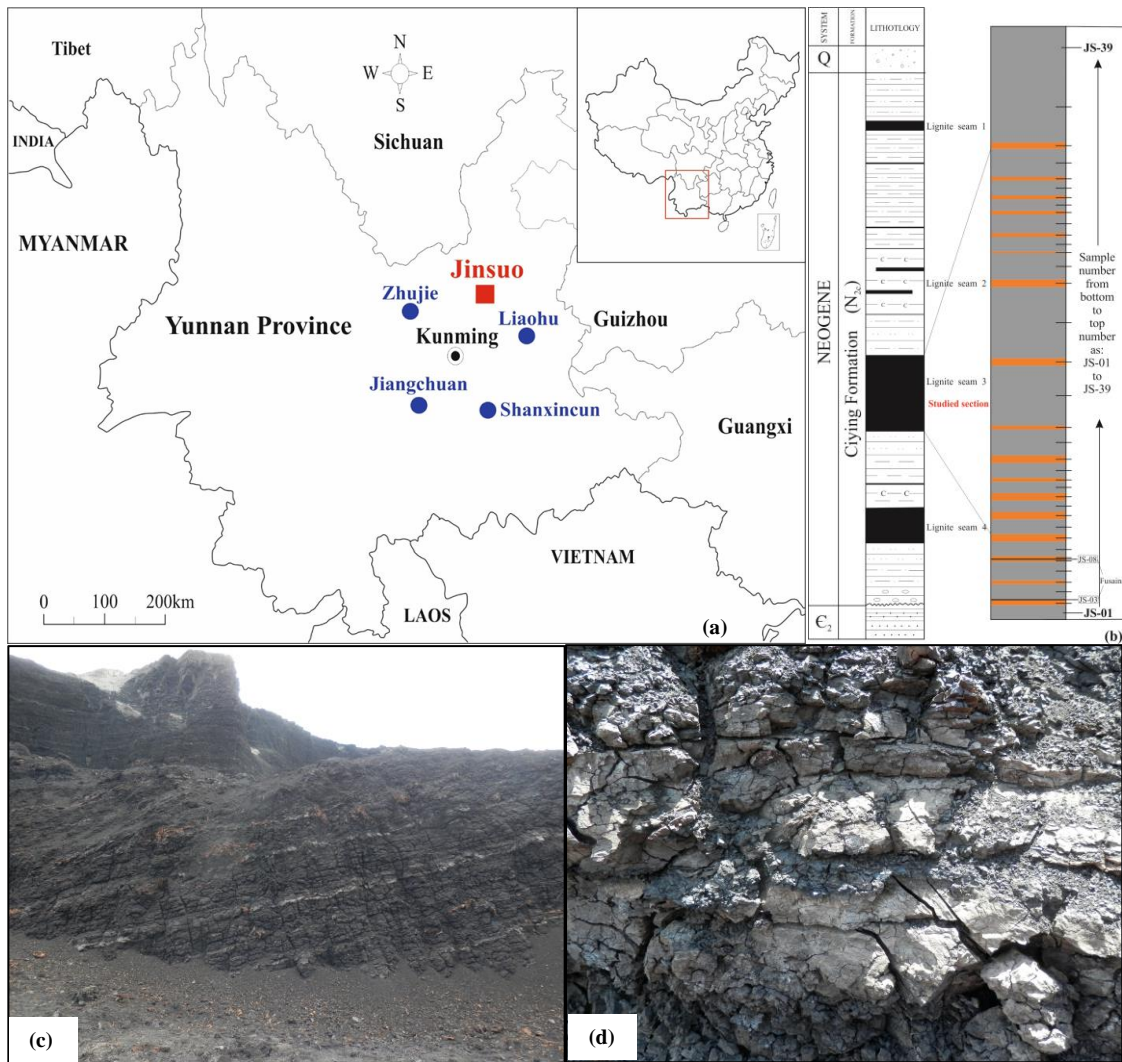


**Figure 1-1 (a): Distribution of pale and dark layers in lignite basins in Yunnan Province, Southwest China; (b) stratigraphic column and profile of pale and dark layers in Jinsuo opencast lignite mine.  $Q_P$  = Pleistocene,  $C_2$  = Middle Cambrian; (c): pale and dark layers in the Jinsuo Basin; (d): weathered pale layers and interbedded fusain layer.**

### 1.1.2 Pale and dark layers in lignites from Germany

In Germany, different brown coal classification systems have been evolved for different open cut areas (Hagemann and Wolf, 1987; Naeth et al., 2004; Holdgate et al., 2016). The economically significant Rhenish brown seams in Lower Rhine Basin occur within the Cologne Formation as the Ville Member, also known as the Main Seam. This unit was deposited during the Middle Miocene (15.9–11.6 Ma) and forms the thickest sequence of coal in the basin, coming to a total thickness of 100 m at the major coal depocenter (Lucke et al., 1999). To the north, the Main Seam splits into a series of thinner coal seams known as Morken, Frimmersdorf A and B, and Garzweiler II and I, in

ascending order (Fig. 1-2). Extensive peat accumulated until the Upper Miocene, forming a thick sequence of brown coal prograding to the north of the graben. In the Rhenish brown coals in Germany, lithotype color (from bright to dull) is generally regarded as being less important, and the relative degree of banding, diffuse reflectance, together with floral facies were considered to be more important than color (Hagemann and Hollerbach, 1980; Schneider, 1992; Naeth et al., 2004). Other coal aspects related to lithotype include the occurrence of charcoal, degree of gelification, and abundance of larger woody pieces (Holdgate et al., 2016). A more detailed grading is as follows (Naeth et al., 2004; Holdgate et al., 2016): (a) the dark G-facies is characterized by finely layered Glumiflores (Monocotyledons) without xylites, and the large number of leaves and the high level of gelification result in a dense coal, probably with low permeability in the facies; (b) P-facies (Pinus-Myricaceen-Palm Tree) contains a high quantity of perimotextite (Pinus bark) and phyllo-textite (Pinus leaves), formed in a mire not indicative of the water table status; (c) Sciadopitys-raised mire (M-facies) having a high quantity of marcoduria textite; (d) K-facies comprising unstratified or poorly stratified coals and containing xylitic tissues of various sizes from Taxodiaceae, bark, roots, and leaf fragments from Taxodium and Glyptostrobus; (e) A-facies (Angiosperm-forest), which is a nearly unstratified coal free of texture that fractures into shaley polygonal fragments, containing almost no xylites, and it is further characterized by Querus (oak) leaves, other smooth-edged leaves, and crushed Querus, Magnoliaesperumum geinitzi, and Magnolia burseraca seeds, implying standing water possibly more decomposed due to its angiosperm wood content; and (f) HB-facies described as a bright unit, with fusinite being the only macroscopically recognizable parts of this massive. Furthermore, the combined observations show a good correlation between the geophysical measurements and the A-, HB-, and G-facies on the one hand and P-, K-, and M- facies on the other. The P-, K-, and M-facies are characterized by similar depositional environments with a low groundwater table (Naeth et al., 2004).



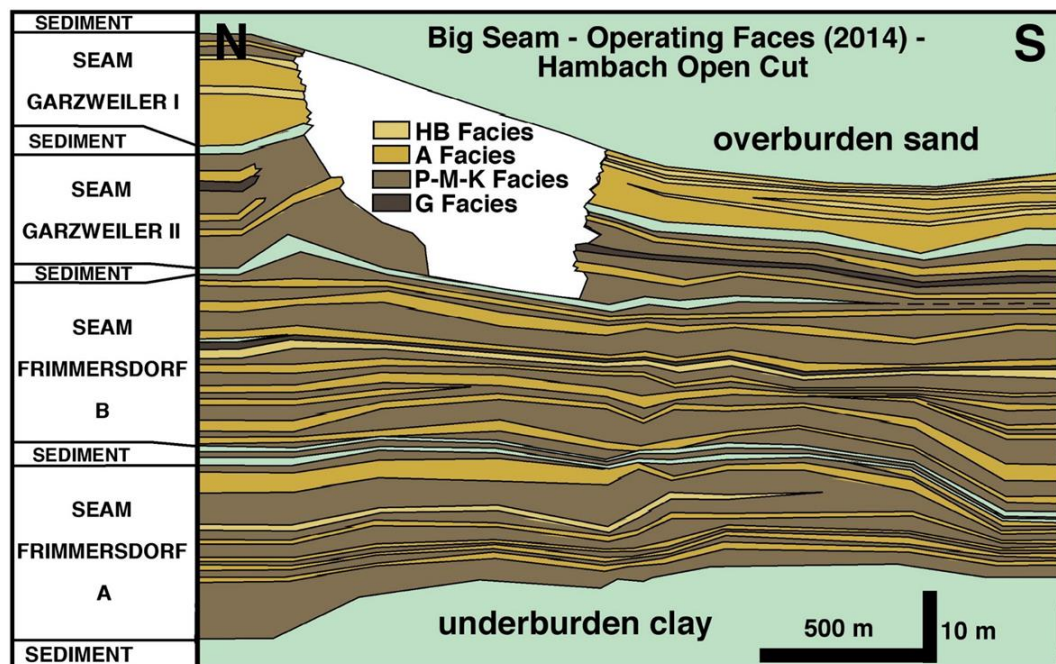


**Figure 1-2** Cross section (north to south) through the Rhenish Hambach mine showing changes of lithotype through the main lignite seam (Holdgate et al., 2016). Bright layer-facies (HB-facies); *Angiosperm*-forest-facies (A-facies); *Pinus-Myricaceen-Palm Tree*-facies (P-facies); *Marcoduria*-facies (M-facies); *Conifer*-forest-facies (K-facies) and *Glumifloren*-facies (G-facies)

With respect to the Miocene lignites in the Lower Rhine Basin in Germany, several explanations have been proposed for the formation of the pale and dark lithotypes. One explanation is that the change in color is caused by vegetation changes combined with changes in the depositional environment in the peat-forming mire. Pale lithotypes were suggested to result from reed marshes deposited in subaqueous environments, while dark lithotypes with tree stems resulted from deposition in relatively drier forest swamps above the water table and in open water areas (Fig. 1-3a) (Teichmüller, 1950, 1958, 1962). Accordingly, open-water brown coals are distinguished by a dark, black color (due to biochemical gelification) and high amounts of humodetrinite and liptinite. Reed marsh coals correspond to the “light layers” of the Rhenish brown coal and carry the highest amounts of humodetrinite and 10 times more pollen than that in forest coals. Forest coals are darker brown, carry stems and stumps from trees, and are microscopically distinguished by much more humotelinite, whose cell tissues are better preserved in coniferous rather than angiospermous forest coals. Sequoia coal is distinguished by thick stumps and especially well-preserved wood-cell structures.

However, this view has been countered by other explanations (Hiltmann, 1976; Hagemann and Wolf, 1987). According to Hiltmann (1976), the light/pale bands were deposited in relatively drier/aerobic conditions compared with the dark bands (Fig. 1-3b).

Light layers are rich in groundmass, and most likely represent conditions undergoing extensive frequent flooding. Further, the pollen in pale layers is suggested to come from surrounding swampy districts with shrubs and trees. Other coals, rich in humic groundmass, can be considered as genuine lacustrine formations, such as coals that have humic groundmass, contain tiny remnants of tissues, and are rich in pollen. These have been interpreted as reed marsh coals formed from dry peats. Lithotypes rich in tissues have been formally defined as formed from forest swamps. (Hiltmann, 1976). Hagemann and Wolf (1987) further pointed out that the influence of the peat-forming plant community played a subordinate role in the formation of light and dark bands in the lignites of the Lower Rhine Basin. According to Hagemann and Wolf (1987), the color difference is mainly the result of different degrees of plant decomposition, with light to pale lignites being generally formed by strong decay. However, in other studies, changes in the plant community were observed in the lignite layers from different facies types in the Lower Rhine Basin (Schneider, 1995; Naeth et al., 2004). More recently, comprehensive results obtained for dark and pale lignites from the Lower Rhine Basin by Holdgate et al. (2016) support the view that vegetation changes caused the color change and that dark lithotypes are characterized by a gymnosperm paleoflora, while light lithotypes are characterized by the dominance of angiosperms.

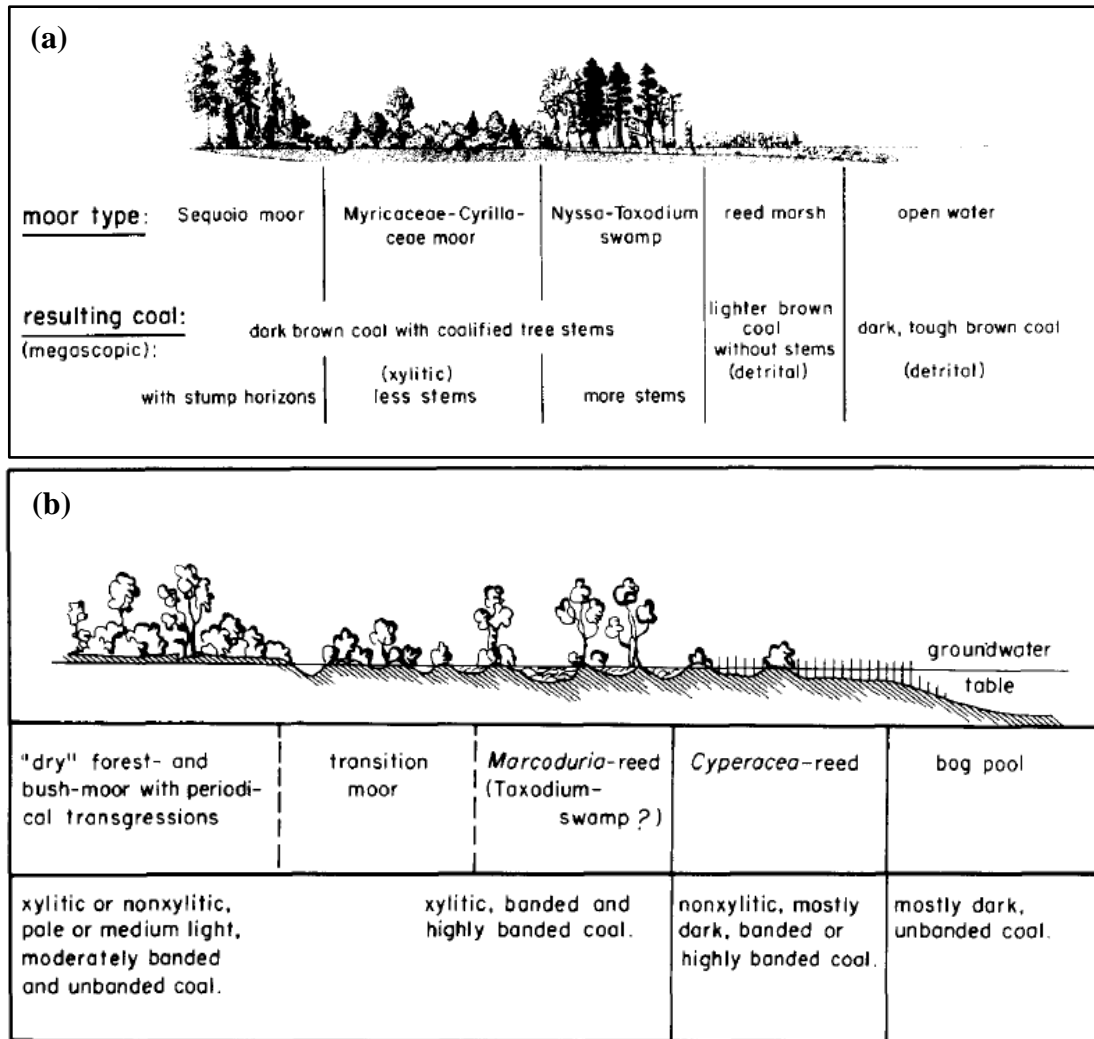


**Figure 1-3 (a) The presumed depositional conditions for Miocene lignite types in the Lower Rhine Basin, Germany (after Teichmüller, 1962); (b) Schematic facies profile of the peat-forming plant communities and presumed depositional conditions for the brown coal lithotypes in the Rhenish district, Germany (after Hiltmann, 1976).**

### 1.1.3 Pale and dark layers in lignites from Australia

The Gippsland Basin is located in southeastern Australia, and the Latrobe Valley Group represents the on-shore segment of the basin and comprises widespread terrestrial sediments including gravels, lignites, clays, and sands (Holdgate et al., 2014). Lignite seams (Olig-Miocene) were formed behind a barrier complex known as the Balook Formation, and lignite seams of the Latrobe Valley Group are separated into three main sequences of the Traralgon, Morwell, and Yallourn seams (Holdgate et al., 2016). In the lignites from the Latrobe Valley Group, lithotypes are characterized by variations in color, texture, gelification, shrinkage, weathering, amount of wood and other plant components, and the amount of charcoal (George, 1982). The pale and dark lithotypes of

the Latrobe Valley Group in the Gippsland Basin were deposited from the Oligocene to the Miocene, and were further divided into five types identified as light/pale, medium light, medium dark, dark, and laminated dark (Figs. 1-3, Holdgate et al., 2014, 2016).



**Figure 1-4 Typical lithotypes in Latrobe Valley in Gippsland Basin (Holdgate et al., 2014)**

The lignite seams in Gippsland Basin have been widely studied by use of organic geochemistry (Finotello and Johns, 1986), palynology (Luly et al., 1980; Kershaw et al., 1991; Blackburn and Sluiter, 1994), macrofossil analysis (Blackburn and Sluiter, 1994), and isotopic analysis (Holdgate et al., 2009). Previous results support a depositional model suggesting that pale/light layers originate from organic matter deposition under sub-aquatic conditions in open water environments, while dark layers were formed from organic matter deposited in relatively drier forest swamps above the water table. This model was termed recently as the dry-dark model (Holdgate et al., 2014, 2016). In contrast, previous geological studies of the lignites from the same basin in Australia came to the conclusion that the pale layers were deposited under drier conditions than the dark layers (Anderson and MacKay, 1990; Holdgate et al., 1995). This model was termed recently as the dry-light model (Figs. 1-4, Holdgate et al., 2014, 2016). According to the new results from Holdgate et al. (2014, 2016), the dry-light model is more suitable for the pale and dark layers that occur in the Gippsland Basin. Furthermore, new paleobotanical and palynological data on the cyclic, laminated, and dark to pale lithotypes in the Gippsland Basin suggested that the dark lithotypes originated from vegetation dominated by gymnosperms representing the transition from a meadow-marsh environment to a forested bog, while the light/pale lithotypes were generated from an angiosperm-dominated peat with intense weathering and aerobic degradation (Korasidis et al., 2016, 2017). These results also support the dry-light model for the pale and dark layers. The studies of the pale and dark layers from the Gippsland Basin did not focus only on the color change of the lignite, but also concentrated on the basin evolution and

related paleoenvironmental change during the formation of these lignite seams (Briggs et al., 2007; Holdgate et al., 2014; Korasidis et al., 2016, 2017).

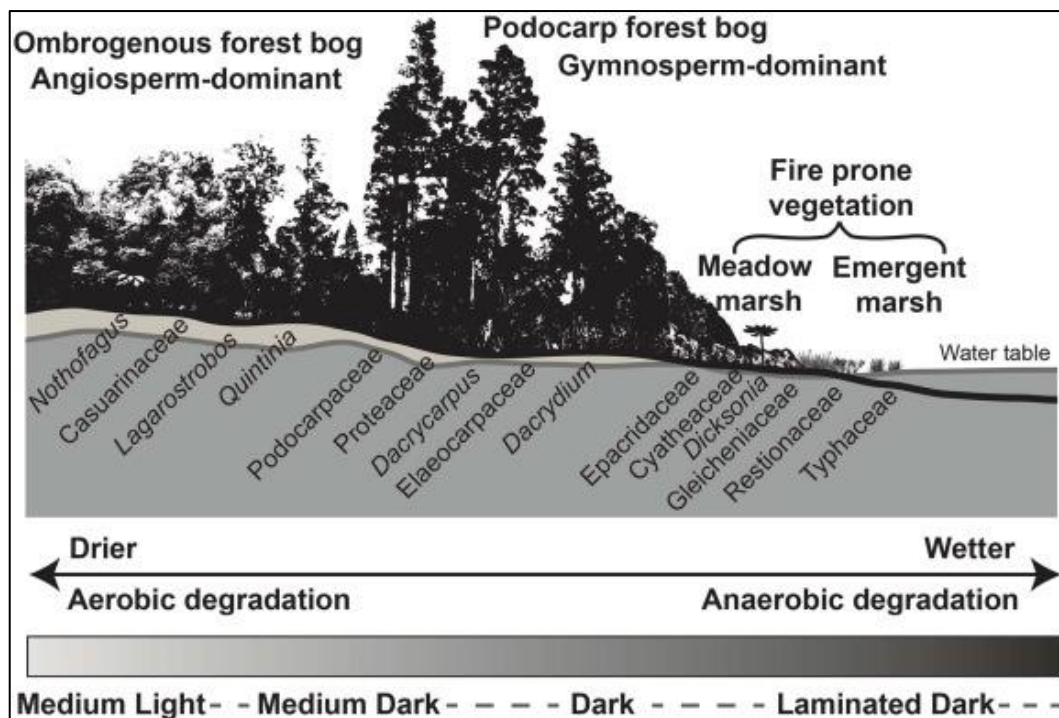


**Figure 1-5 Facies model of the vegetation succession in the Early Miocene peatlands of the Latrobe Valley. Latrobe Valley, Gippsland Basin, Australia (Korasidis et al., 2016)**

In addition, the evidence of wildfires in the Cenozoic Gippsland Basins has also been studied based on the results of charcoal and palynology (Holdgate et al., 2014; Korasidis et al., 2016, 2019). The new results suggested that the distribution of charcoal and fire-prone flora within lignite seams are entirely controlled by facies and the paleoenvironments within the peatland, but does not result from drier climates. Rather, they are associated with emergent and meadow marsh environments that produce darker coal lithotypes (Korasidis et al., 2019). The abundance of charcoal in dark lithotypes is explained by the fire-prone and highly flammable nature of herbaceous and reedy wetlands. Although the prevailing warm, wet climate conditions and the predominance of rainforests are suggested to be the characteristics of the Cenozoic formations in southern Australia, some swamp taxa were clearly already pre-adapted to tolerate fire (Holdgate et al., 2014). The quantification of charcoal in different lithotypes in the Morwell and Yallourn coal seams, Gippsland Basin (Figs. 1-6), show that laminated dark layers always have a very high abundance of charcoal. The emergent marsh or meadow/marsh environment was suggested by the paleobotanical data that the laminated dark lithotype is characterized by a relatively high abundance of fire-prone vegetation,

such as Gleicheniaceae, Cyatheaceae/Lindsaeaceae, Dicksonia, Gleicheniaceae, Restionaceae, and Ericaceae families, and in particular, the presence of the coral-fern family Gleicheniaceae indicates an open environment in which the facies was not forested (Korasidis et al., 2016).

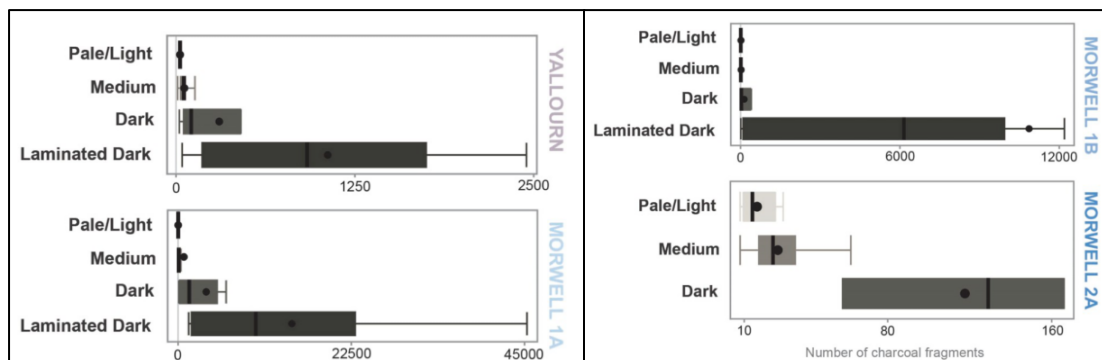


**Figure 1-6 Charcoal data (i.e., the number of charcoal fragments recorded per count of 200 palynomorphs) for each lithotype in the Morwell and Yallourn coal seams, Gippsland Basin (Korasidis et al., 2019).**

### 1.1.4 Pale and dark layers/lignites in other countries

In addition to the successive occurrence of pale and dark layers in Neogene lignite basins in China, Germany, and Australia, various pale and dark layers were also studied in lignite basins in other countries, such as Slovenia, Serbia, and Poland (Markic and Sachsenhofer, 1997; Markič and Sachsenhofer, 2010; Fabiańska and Kurkiewicz, 2013; Doković et al., 2018). However, these pale or dark lignites do not show a successions and cycles related to their basin.

The lithotypes within the Pliocene Velenje Basin lignite in Slovenia are defined by the lithotype components and form petrographically distinct stratified and/or non-stratified units, such as beds, bands, lenses, and irregular masses. Lithotype varieties are differentiated with regard to color and the degree of gelification, and they vary from xylite-rich (yellow/pale) to detrital (grey) and gelified (dark grey to black) (Markič and Sachsenhofer, 2010). These different lithotypes were found in different boreholes and in an underground mine in the Velenje Basin (Markic and Sachsenhofer, 1997). The lignite seams from the Velenje Basin have been studied previously according to geology, organic geochemistry, coal petrology, and stable carbon isotopes (Markic and Sachsenhofer, 1997; Bechtel et al., 2003; Kanduč et al., 2005, 2012; Markič, 2006). Xylite-rich lithotypes are mostly derived from trunks and bushes, which have high resistance to biogeochemical degradation, these lithotypes are characterized by  $\delta^{13}\text{C}$  values between -27.5‰ and -23.0‰. Detrital lithotypes are derived mostly from



herbaceous flora, which is biogeochemically less resistant than larger wooden pieces, having  $\delta^{13}\text{C}$  values between -28.7‰ and -26.3‰. Gelified lithotypes have strong gelification of its organic matter, with  $\delta^{13}\text{C}$  values between -28.7‰ and -27.2‰ (Kanduč et al., 2005). Both original plants and biogeochemical processes (e.g., gelification, degradation, and mineralization) were of great importance in the early diagenesis of the Velenje lignite (Kanduč et al., 2012). Organic geochemical data suggested that the gelification of plant tissue may be governed by the activity of anaerobic rather than aerobic bacteria. Although the variation in the proportions of gymnosperms versus angiosperms in the peat-forming vegetation is minor, the floral assemblage may influence the carbon isotopic composition of the coals (Bechtel et al., 2003). To compare the Velenje and Jinsuo lignites, the organic geochemistry and isotope composition of different lithotypes from Velenje Basin have been studied, and the results are discussed in detail in **Chapter 4**.

In Serbia, four types of xylite-rich coal (pale yellow, dark yellow, brown, and black) are found in the upper Miocene Kolubara and Kostolac lignite basins (Doković et al., 2018). Petrographic and biomarker analyses have been carried out by Doković et al. (2018). All four kinds of coal are dominated by diterpenoids from gymnosperms, followed by non-hopanoid triterpenoids and *n*-alkanes. The proportions of diterpenoids decrease in the following order: pale yellow > dark yellow > brown > black. Distributions of biomarkers indicate changes of the contribution of arboreal vegetation versus the impact of herbaceous peat-forming plants, which resulted in the reduction of tissue preservation. Conifers contributed significantly to the organic matter in all samples and predominated over angiosperms (Doković et al., 2018).

Lithotype changes in lignite seams have also been reported for brown coal from the Miocene Konin and Turoszów basins in Poland (Fabiańska and Kurkiewicz, 2013). Lithotypes in the two basins vary from xylitic and detro-xylitic to detritic and fusitic lignite. Xylitic lignites were from yellow or light brown to dark brown in color. Detritic lignites vary in color from gray to black humic lignites, but most of them are dark brown. They are softer than most xylites. Detro-xylitic lignites contain wood debris in detritic groundmass, often coarse-grained and differing in color but mostly grayish brown and dark brown. Fusitic lignites were black and brittle, with silky appearance. They occurred as numerous thin laminae within the main lignite bed. Detailed results from the analysis of biomarkers, aromatic hydrocarbons, and polar compounds have been published by Fabiańska and Kurkiewicz (2013). Results show that xylitic lignites originate from gymnosperms (Podocarpaceae, Pinaceae, Cupressaceae, and Taxodiaceae), while detritic lignites come from monocotyledonic material with some of them containing coniferous detritus-like needle leaves. Detro-xylitic lignites show geochemical features between those of detritic and xylitic lignites. Semifusinites and fusinites contribute to the maceral composition of fusitic lignites and originate rather from surface oxidation of wood

material during seasonal low water levels rather than from forest fires, because the anthracene concentration is low (Fabiańska and Kurkiewicz, 2013).

## 1.2 Focus of the research

The above-mentioned results from the investigated pale and dark layers in several Neogene lignite basins from all over the world revealed that controversy persists regarding the origin of pale and dark layers in these basins. Moreover, detailed petrological and geochemical investigations of the origin of pale and dark lignite layers in Yunnan Province were not available at the beginning of this research project, and the related paleoclimatic influence on the formation of pale and dark layers was likewise unclear. To fill these gaps, 49 samples (including bulk lignite samples, fusain samples, and fossil wood samples) from a lignite profile of Pliocene Jinsuo Basin in Yunnan Province were investigated by various geochemical methods. In addition, 11 samples from the Pliocene Velenje Basin in Slovenia were likewise analyzed for comparison with the results with those from the Jinsuo Basin.

The main objectives of this thesis were to:

- 1) Investigate the organic petrology and organic geochemistry of pale and dark layers from Jinsuo Basin lignites, study the difference of the characteristics between pale and dark layers, and clarify the depositional conditions and plant community changes between pale and dark layers.
- 2) Study the major and selected trace elements along with the minerals in pale and dark layers as markers for the geological and climatic influence on the deposition of pale and dark layers.
- 3) Study the elemental (C, N, and S) and stable isotopic composition (C and N) of pale and dark layers. The aim of the study is to determine the change of depositional condition and plant community influence on the stable isotopic composition of pale and dark layers.
- 4) Suggest paleoenvironmental models of pale and dark layers of Jinsuo Basin lignite from Yunnan Province using all of the results and discuss the forces behind of the formation of cyclic dark and pale layers.
- 5) Compare the results from Jinsuo Basin with the results of pale and dark layers in Neogene coal basins from other countries (specifically lignite lithotypes from Slovenia) and try to clarify the links (e.g., global climate, depositional environment, plant community) between lignite basins with respect to the world-wide formation of pale and dark layers in such deposits.



---

## **Chapter 2 Organic petrology and geochemical characteristics of pale and dark layers in Pliocene lignite deposits from Yunnan Province, Southwest China**

### **2.1 Abstract**

A set of 39 pale lignite and dark lignite samples, obtained from a profile of the Pliocene Jinsuo lignite basin, Yunnan Province, China, were analyzed using coal petrology and biomarkers to determine whether changes in the depositional environment and/or vegetation caused the color changes ultimately observed in the lignites. A comprehensive analysis of all the data obtained revealed significant differences in the petrological and geochemical composition of the two lignite types.

The pale lignites are characterized by a higher abundance of the liptinite group compared with the dark lignites. The composition of liptinites is dominated by bituminite (mineral-bituminous groundmass) and sporinite, along with a relatively low abundance of the huminite group. This indicates a higher degree of oxidation in the drier, more elevated peatland environments during deposition of the pale lignites. The low values of the TPI, VI, and GI in the pale lignites suggest a relatively high decomposition rate of plant materials under dry/aerobic conditions. In contrast, the dark lignites have a very high proportion of huminite dominated by ulminite, along with a low content of liptinite and inertinite macerals, which suggests the prevalence of wet/anaerobic conditions in the peat-forming mire. The high values of TPI, VI, and GI in the dark layers suggest better preservation of organic matter during deposition under anaerobic conditions, and more wet/humid climatic conditions, when compared with the pale lignites.

With respect to the biomarker composition, the high concentrations of long-chain ( $C_{27}$ - $C_{31}$ ) *n*-alkanes in both pale and dark lignites are typical characteristics for the predominance of higher terrestrial plants. Significant concentrations of mid-chain *n*-alkanes (*n*- $C_{21}$ - $C_{25}$ ) were detected preferentially in the dark lignites, suggesting that aquatic plants might also have contributed to the plant community during the formation of the dark layers. The content of diterpenoids and the average ratio of diterpenoids to the sum of diterpenoids and triterpenoids ( $Di- / (Di- + Tri-terpenoids)$ ) are higher in the pale lignites than in the dark lignites. This indicates that gymnosperms made a crucial contribution to the plant community during the formation of the pale lignites. In the dark lignites, triterpenoids are generally far more abundant than diterpenoids, which suggests that the dark layers were overwhelmingly formed by angiosperm plants. This is consistent with lower C/N ratios in the dark lignite layers (av. 40.8) compared with the pale lignite layers (av. 60.6). Higher microbial activities in the pale lignites than in the

dark lignites are reflected by the higher concentration of hopanoids and  $17\alpha,21\beta$ -homohopane (22R) in the pale lignites.

**Keywords:** *pale and dark lignites, petrology, Pliocene, diterpenoids, triterpenoids, Yunnan Province*

## 2.2 Introduction

The occurrence of successions of dark and pale lithotypes has previously been described for Tertiary age lignites in the Lower Rhine Basin in Germany, in the Gippsland Basin in southeastern Australia, and in several basins in southwestern China. With respect to the Miocene lignites in the Lower Rhine Basin in Germany, several explanations have been proposed for the formation of the pale and dark lithotypes. One explanation is that the change of color is caused by vegetation changes combined with changes of the depositional environment in the peat-forming mire. Pale lithotypes resulted from reed marshes deposited in subaqueous environments, while dark lithotypes with tree stems resulted from deposition in relatively drier forest swamps above the water table (Teichmüller, 1950, 1958, 1962). This view has been contested by other explanations. According to Hagemann and Wolf (1987), the light/pale bands were deposited in relatively drier/aerobic conditions compared with the dark bands. Hagemann and Wolf (1987) further pointed out that the influence of the peat-forming plant community played a subordinate role in the formation of light and dark bands in the lignites of the Lower Rhine Basin. According to Hagemann and Wolf (1987), the color difference is mainly the result of different degrees of plant decomposition, with light to pale lignites being generally formed by strong decay. However, changes in the plant community were observed in the lignite layers from different facies types in the Lower Rhine Basin (Schneider, 1995; Naeth et al., 2004). More recently, comprehensive results obtained for dark and pale lignites from the Lower Rhine Basin by Holdgate et al. (2016) support the view that vegetation changes caused the color change, and that darker lithotypes are characterized by a gymnosperm paleoflora, while lighter lithotypes are characterized by angiosperms.

Pale and dark lithotypes were also described from the Oligocene to the Miocene in the Gippsland Basin, Australia, and have been studied using organic geochemistry (Finotello and Johns, 1986), palynology (Luly et al., 1980; Kershaw et al., 1991; Blackburn and Sluiter, 1994), and macrofossil analysis (Blackburn and Sluiter, 1994). The results support a depositional model that suggests that pale/light layers originate from organic matter deposition under sub-aquatic conditions in open water environments, while dark layers were formed from organic matter deposited in relatively drier forest swamps above the water table. This model was termed the dry-dark model (Holdgate et al., 2014, 2016). In contrast, geological studies of the lignites from the same basin in Australia came to the conclusion that the pale layers were deposited under drier conditions than the dark layers (Anderson and Mackay, 1990; Holdgate et al., 1995). This model was later termed the dry-light model (Holdgate et al., 2014, 2016). More recently, new paleobotanical and palynological data on the cyclic, laminated, dark to pale lithotypes in the Gippsland Basin, Australia suggested that the dark lithotypes originated from vegetation dominated by gymnosperms representing the transition from a meadow marsh to a forested bog,

while the light/pale lithotypes were generated from an angiosperm-dominated peat with intense weathering and aerobic degradation (Korasidis et al., 2016, 2017).

Compared with the numerous studies on pale and dark lithotypes in lignites from Germany and Australia, investigations on similar pale and dark lignites from China are scarce. In the east and center of Yunnan Province, southwestern China, alternating layers of pale and dark lignites are mostly found in the late Miocene to late Pliocene (Qi et al., 1994). The origin of pale and dark layers in lignites from Yunnan Province has been contested since the first description of pale lithotypes by Lu and Zhang (1986). These pale lignites were thought to originate from sphagnum peat, but the formation of the dark lignites was not discussed (Fu et al., 1987; Lu and Zhang, 1989). However, organic geochemical and petrological studies carried out on various lignite deposits in the Yunnan Province revealed the occurrence of both pale and dark lignite layers, and with different compositions (Qi et al., 1994). Gymnosperms were considered to be the source materials of both pale and dark lignites, and the difference between the two types of lignites was attributed to their degree of decomposition with the pale lignites being a product of more intensive bacterial decomposition than the dark lignites (Qi et al., 1994). However, other studies of plant residues in pale and dark lignites from Yunnan Province have shown that the pale lignites were dominated by herbaceous tissues, while ligneous tissues were more prevalent in the dark lignites (Yu et al., 1996; Wang et al., 1997). Possible reasons for the different interpretations of the origin of the types of lignites are the lack of consideration given to depositional conditions, the source of plants materials in the paleomire, and the influence of paleoclimate changes. In addition, previous studies were based on only a small number of samples from each site and thus could be unrepresentative as well as preventing a meaningful statistical evaluation of the data.

Results obtained from previous studies on pale and dark lithotypes from the Miocene in the Lower Rhine Basin, Germany, the Oligocene-Miocene in the Gippsland Basin, Australia, and the Pliocene in Yunnan Province, China, are summarized and compared in Table 1. Based on the existing studies, the pale lithotypes in the Gippsland Basin are characterized by high H/C and low O/C ratios, low specific gravity, and high  $\delta^{13}\text{C}$  ratios, along with low levels of plant fragments and charcoal particles, while the dark lithotypes show the opposite features. Previous results obtained from the study of pale lignites in the Jinsuo Basin, Yunnan Province are partly consistent with some of the characteristics of pale lithotypes in the Gippsland Basin such as the high H/C and low O/C ratio. Disagreements over the origins of the dark and pale lithotypes in the Gippsland Basin and the Lower Rhine Basin are reflected by disagreements over the associated depositional conditions (wet/dry conditions, aerobic/anaerobic degradation, and subaqueous/subaerial deposition), and also by disputes over the source material of the plants (angiosperms/gymnosperms, and herbaceous/woody). Opposing results are usually generated for the same study areas by different analytical methods. Even for the

Gippsland Basin, which has been studied in great detail, no consensus has yet been reached on the origins of the pale and dark layers.

**Table 2-1 Summary of the current knowledge and associated references regarding the formation of pale and dark lignites**

Dark lithotypes	Pale lithotypes	Location Basin	References (cited therein)
lower H/C ratio	higher H/C ratio	Jinsuo Basin, Gippsland Basin	1, 5,
higher O/C ratio	lower O/C ratio	Gippsland Basin	5
higher specific gravity	lower specific gravity	Jinsuo Basin, Gippsland Basin	1, 2, 7, 9
wetter condition	drier condition	Jinsuo Basin, Gippsland Basin, Lower Rhine Basin	1, 2, 7, 8, 11, 16, 21, 22
drier condition	wetter condition	Jinsuo Basin, Gippsland Basin, Lower Rhine Basin	3, 4, 10, 12, 13, 14, 15, 17, 20, 23
subaqueous deposition	subaerial deposition	Gippsland Basin, Lower Rhine Basin	8, 21, 22
subaerial deposition	subaqueous deposition	Gippsland Basin, Lower Rhine Basin	10, 20
high amount of plant fragments	low amount of plant fragments	Gippsland Basin	7, 8, 9
high amount of charcoal particles	low amount of charcoal particles	Gippsland Basin	6, 8, 9, 16
more herbaceous residues	more ligneous residues	Jinsuo Basin	3, 4
	dominated by gymnosperms	various basin in Yunnan	2
	dominated by gymnosperm	Gippsland Basin, Lower Rhine Basin	9, 16
	semi/anaerobic degradation	Gippsland Basin, Lower Rhine Basin	6, 7, 9, 21, 24
lower $\delta^{13}\text{C}$	higher $\delta^{13}\text{C}$	Gippsland Basin	18, 19

Yunnan, China: 1. Lu and Zhang (1989), 2. Qi et al. (1994), 3. Yu et al. (1996), 4. Wang et al. (1997)

Victoria, Australia: 5. Allardice et al. (1977), 6. Mackay et al. (1985), 7. Anderson and Mackay (1990), 8. Holdgate et al. (2014), 9. Korasidis et al. (2017), 10. Luly et al. (1980), 11. Holdgate et al. (1995), 12. Kershaw and Sluiter (1982), 13. Sluiter and Kershaw (1982), 14. Blackburn and Sluiter (1994), 15. Finotello and Johns (1986), 16. Holdgate et al. (2016), 17. Kershaw et al. (1991), 18. Briggs et al. (2007), 19. Korasidis et al. (2016)

Rhenish, Germany: 20. Teichmüller (1950), 21. Hagemann and Wolf (1987), 22. Teichmüller (1962), 23. Thomson (1950), 24. Von der Brelie and Wolf (1981)

In the present study, 39 lignite samples from a continuous profile of Pliocene age in the Jinsuo Basin in Yunnan Province, southwestern China were investigated using a combination of coal petrology and organic geochemistry. The aim was to reconstruct variations in the depositional environment of peat deposition and to identify possible

variations in the plant community that ultimately contributed to the formation of pale and dark layers.

### **2.3 Geological setting**

The Jinsuo lignite Basin in southwestern China is located about 85 km northeast of Kunming City, Yunnan Province (Fig. 1). It is a Neogene intermountain Basin with a length of 9 km and a width of 1.5–4 km (Fu et al., 1987; Lu and Zhang, 1989).

The Ciyang formation ( $N_{2c}$ ) from the late Pliocene is the main lignite-bearing strata in the Jinsuo lignite basin and is mainly comprised of conglomerate, mudstone, sandstone, and lignite (Yunnan BGMR, 1990). There are four lignite seams (named no. 1–no. 4) in this basin (Fig. 1). Seams no. 1 and no. 2 are only locally minable, while seam no. 3 is the main minable lignite seam in the Jinsuo Basin, and has a thickness of approximately 14–26 m. The basement strata of the Jinsuo Basin are mainly composed of middle Cambrian calcareous shales of the Douposhi formation. The overlying strata of the Ciyang formation are composed of Quaternary sediments. The area has not been influenced by major tectonic activities since the late Pliocene and thus the peat in the Jinsuo Basin has been deposited under stable conditions for a long period of time (Yunnan BGMR, 1990).

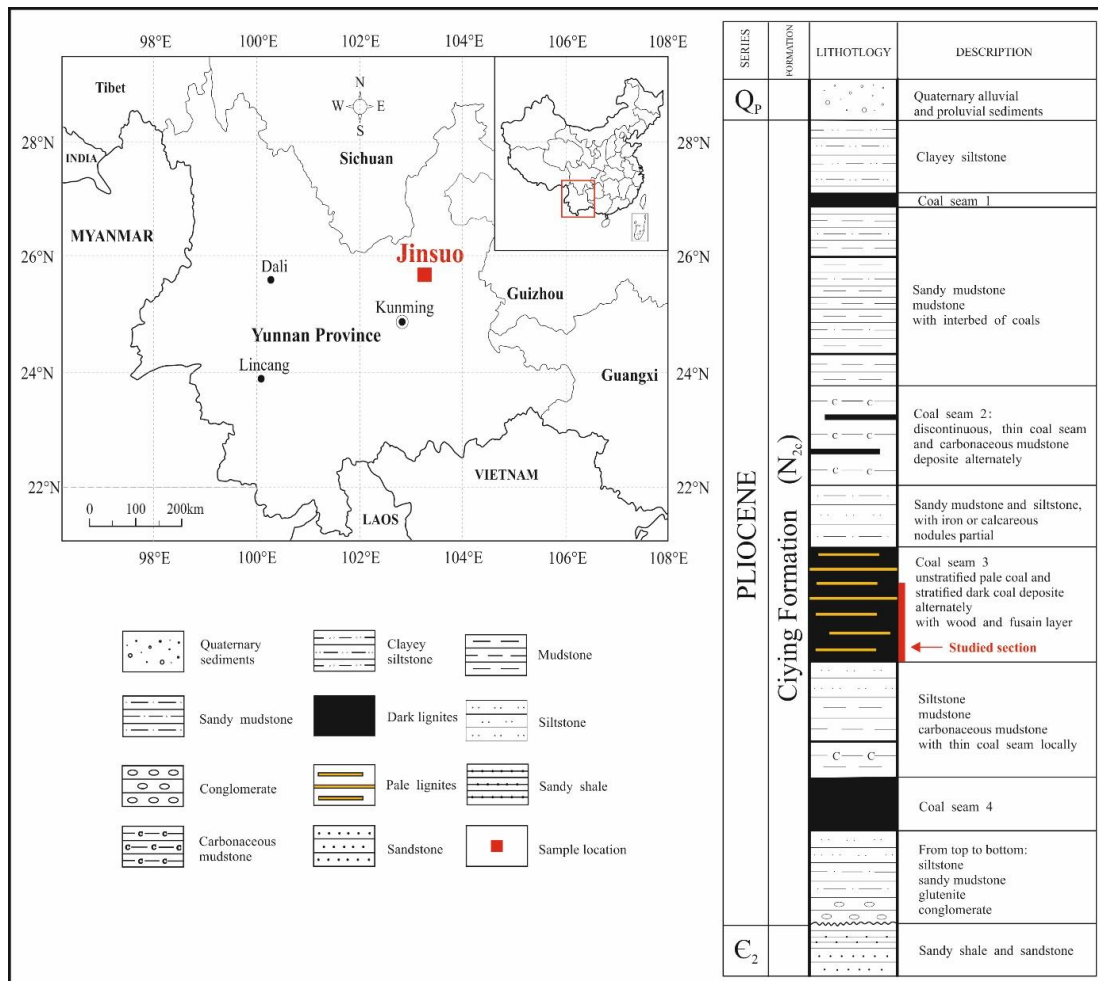


**Figure 2-1 Location and stratigraphic column of Jinsuo opencast lignite mine.**

**Q<sub>p</sub> = Pleistocene, E<sub>2</sub> = Middle Cambrian**

More than 20 pale layers, each having a thickness of 5–25 cm, were found as thin internal sections within the thick dark layers throughout the basin (Fig 2a). The dark layers have a thickness of 0.3 to 1.5 m. The pale and dark lignites show an obvious difference in color (Fig. 2b). Large, brown-colored stems (Fig. 2c) and roots of trees can be found in the dark layers. Fusain horizons with a thickness of 2–6 cm occasionally occur as internal seams (Fig. 2d) within the pale layers, or on top of the pale layers, and provide evidence for the occurrence of wild fires during peat accumulation. All these macroscopic characteristics are relevant for the interpretation of the origin and depositional environment of the pale and dark lignite layers in the Jinsuo Basin.

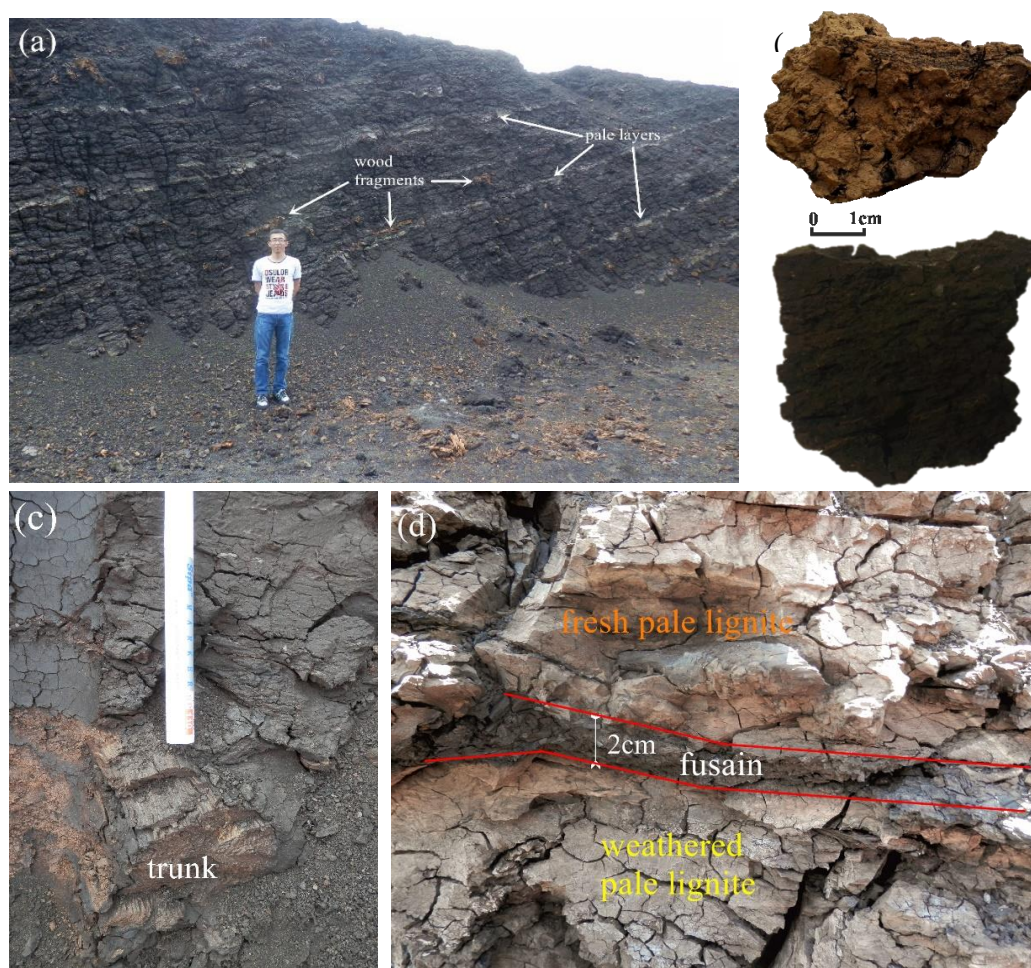


**Figure 2-2** Field observations of Jinsuo opencast lignite mine. (a) pale layers and wood fragment (brown color) in the thick dark lignites; (b) typical pale lignite (top) and dark lignite (bottom); (c) typical tree trunk in the dark lignite layers; (d) thin fusain as internal seam in the pale, yellowish brown color of fresh pale lignite and grayish white color of weathered pale lignite

## 2.4 Samples and methods

A total of 39 samples (including 18 pale lignites, 19 dark lignites, and 2 internal fusain samples) were collected vertically (from bottom to top, numbered JS-1 to JS-39) from lignite seam no. 3 in the Jinsuo opencast coal mine. Sampling followed the Chinese standard method (GB/T482-2008, 2008). All collected samples were immediately wrapped with aluminum foil, then sealed and stored in plastic bags to minimize contamination and oxidation. Samples were freeze dried and divided into two equal parts. One part was used for the analyses and the other part was stored as a reserve.



### 2.4.1 Organic petrography

For the organic petrological analyses, the samples were crushed to a maximum particle size of 1 mm, and then embedded in a silicone mold using epoxy resin as an embedding medium. Maceral analysis was conducted on polished sections with a Leica MPV microscope using reflected white light and blue-light excitation. The analysis used the approach described by Taylor et al. (1998). An oil immersion objective (50× magnification) was used. Every sample was subjected to 500 counts with fixed intervals between every count. In addition to normal incident light microscopy, fluorescence microscopy was applied for the identification of distinct liptinites. The maceral group determination for lignite followed the Stopes-Heerlen terminology (ICCP, 1998, 2001; Sýkorová et al., 2005).

### 2.4.2 Biomarker analysis

To carry out biomarker analyses, finely ground (<0.2 mm) samples were Soxhlet-extracted for 24 hours using dichloromethane as the solvent. On the basis of the different polarities of the components, the extracts were separated using flash column chromatography under a nitrogen pressure of less than 1.5 bars. The extracts were separated into four fractions by column chromatography over activated silica gel (particle size 40-63 µm). The saturated hydrocarbon fraction was eluted with *n*-hexane, the aromatic hydrocarbon fraction with *n*-hexane: dichloromethane (9:1 v:v), the ketones/esters fraction with dichloromethane, and the heterocompounds with methanol. The so-called “saturated hydrocarbon fraction” is not only composed of saturated hydrocarbons but also of mono-unsaturated hydrocarbons. Solvents were evaporated from each fraction under a stream of nitrogen.

In the present study, saturated and aromatic hydrocarbon fractions were analyzed by gas chromatography coupled to mass spectrometry (GC-MS) using a Thermo Scientific Ultra series gas chromatograph and a Thermo Scientific DSQ II mass spectrometer. Gas chromatography separation of the compounds was achieved using a Thermo Scientific TR-5MS fused silica capillary column (30 m × 0.25 mm ID × 0.25 µm film thickness). The oven temperature was programmed from 60 to 320 °C at a rate of 4 °C /min, with a 25 min isothermal period, and the injector and transfer temperature was 280 °C. Helium was used as carrier gas. The mass spectrometer was operated in the electron impact mode (EI) at 70 eV ionization energy. Mass spectra were obtained by scanning from *m/z* 50 to *m/z* 600 at 2 scans per second. Squalane and 1,1'-binaphthyl were used as internal standards for quantification of the saturated and aromatic hydrocarbons, respectively. For data processing, the Xcalibur Qual Browser software was used, and identification of individual compounds was accomplished using the retention time in the total ion current

(TIC) chromatogram and by comparison of the mass spectra with library and published data (Philp, 1985). The concentrations were normalized to the total organic carbon (TOC) content.

#### **2.4.4 Elemental analysis**

For all elemental analyses, samples were crushed and ground to less than 200  $\mu\text{m}$ . Measurements of total nitrogen were done using the Leco TruSpec Macro elemental analyzers. The TOC content was analyzed using the LECO RC-412 carbon analyzer. Samples were treated with diluted (10%) hydrochloric acid prior to the analysis to remove carbonates, and then rinsed with distilled water until neutral. The obtained values were then corrected to the original sample weight before calcite loss through acid treatment.

### **2.5 Results and discussion**

#### **2.5.1 Macroscopic characteristics**

Pale lignites have low density and hardness, are usually yellowish-brown in fresh sections, and become grayish-white after weathering (Fig. 2d). They are loose in structure and can be much more easily ground than dark lignites. Some small, fibrous, plant residues can be seen under magnifying glass in pale lignites, and dried pale samples are flammable. The thick, dark lignite layers usually contain large wood fragments inside the layer (Fig. 2a), and sometimes even tree trunks have been found (Fig. 2c), but visible small fibrous plant residues are absent. Dark lignites have a higher density and hardness than pale lignites, and show visible stratification, which suggests stable depositional conditions.

#### **2.5.2 Maceral composition**

The results of maceral analysis of the Jinsuo lignites (Table 2) are based on the mineral matter-free (mmf.) composition. The maceral compositions are significantly different for the pale and dark lignites. In the pale lignites, liptinite, with a volume ranging from 62.3%–89.8% (average of 70.2%) predominates over huminite (10.0%–28.0%, av. 18.6%) and inertinite (0.2%–17.7%, av. 11.2%) (Table 2). In the dark lignites, huminite predominates the whole maceral composition, ranging from 65.8% to 90.4% (av. 79.2%). The abundance of liptinite (4.7%–24.5%, av. 12.7%) is less than one fifth of that in pale lignites, and the abundance of inertinite (1.1%–17.5%, av. 8.1%) is slightly lower than in the pale lignites.

**Table 2-2 Maceral composition based on mineral matter-free basis (vol.%) of the examined samples from the Neogene Jinsuo opencast lignite mine, Yunnan Province**

Sample No.	Lithotypes	T	U	G	Co	A	D	TH	Sp	Cu	Sb	R	Al	Bi	Ld	TL	F+S F	Fg	Id	TI	TPI	GI	VI	GW
JS-39	dark	11.7	42	12.2	0.8	5.4	17.4	89.6	4.4	0	0	0	0	2.1	0	6.5	0	1	2.9	3.9	2.39	3.01	2.09	0.61
JS-38	dark	14.8	39.9	10.7	4.4	3.8	10.2	83.9	4.1	0	0.2	0	0	3.1	0	7.3	1.1	6.1	1.5	8.7	4.28	2.57	3.22	0.47
JS-37	pale	0	10.1	1.3	0	12.1	0	23.5	15.8	0	0	0.9	0	42.5	3.1	62.3	0	5.9	8.3	14.2	0.83	0.5	0.41	0.38
JS-36	dark	15.6	50.1	2.7	3.1	2.7	5.6	79.8	6.4	0	0	0.2	0	7.1	1	14.6	1	3.9	0.8	5.6	8.42	2.93	4.27	0.2
JS-35	pale	0	13.4	2.1	3.1	9.1	0.2	28	7.8	0	0	0	0	51.9	2.7	62.5	1	3.9	4.7	9.5	1.88	1.13	0.32	0.45
JS-34	dark	16.4	52.7	2.5	6.4	3.8	6.1	87.9	2.7	0	0.7	0	0	5.2	0.5	9.1	1.4	0.4	1.3	3	7.84	2.85	4.4	0.23
JS-33	pale	0	10.7	0	0	9	1.1	20.7	14.8	0	0	0	1.5	55.1	0	71.4	0.9	3.2	3.7	7.9	1.15	0.86	0.37	0.23
JS-32	dark	18.6	50.2	5.9	0.6	2	4.5	81.8	4.1	0	0	0	0	3.5	0.4	7.6	3.1	1.8	5.7	10.6	11.2	1.88	4.73	0.19
JS-31	pale	0	9.5	1.7	0.8	9.1	1.7	22.7	12.7	0	0	0	0.6	51.3	2.3	66.9	1.5	2.5	6.4	10.4	1.09	0.7	0.33	0.52
JS-30	dark	16.3	46.7	5.6	4.5	5.4	11.8	90.4	3.8	0	0.9	0	0	3.8	0	8.4	0.4	0.4	0.4	1.1	3.93	2.8	3.18	0.39
JS-29	pale	0	7.3	1.2	1.1	9.8	1.4	20.8	11.9	0	0.4	0	0.9	46.5	3.2	62.9	2	2.1	12.3	16.3	0.92	0.41	0.29	0.49
JS-28	dark	11.8	33.2	8.9	10.7	3.6	11.3	79.5	3.4	0	1.1	0	0	0.9	0	5.4	3.3	4.7	7.1	15.1	3.96	2.14	2.31	0.68
JS-27	pale	0	5.4	1.4	1.4	9	4.1	21.4	23.1	0	0	0	0.7	41.4	2.9	68.1	0.7	2.7	7	10.5	0.58	0.66	0.45	0.95
JS-26	dark	15.6	48.9	7.9	4	5.7	8.2	90.3	2.7	0	0	0	0	2	0	4.7	1.2	3.4	0.5	5	5.01	2.66	4.16	0.31
JS-25	pale	0	8.2	1.4	1.4	9.2	1	21.1	17.3	0	0	0	0.8	51.2	3	72.3	0.6	3.6	2.4	6.6	1	0.87	0.39	0.46
JS-24	dark	13.2	35.8	8.1	4.7	4.2	8.2	74.2	4.4	0	0.5	1.3	0.3	5.5	0.5	12.4	2.3	6.3	4.8	13.4	4.51	1.99	2.44	0.44
JS-23	pale	0	5.6	1	5.1	8.6	2.3	22.5	12.6	0	0.2	0.7	0.3	45.5	3.7	63	1.9	2.3	10.3	14.5	1.16	0.62	0.3	0.92
JS-22	dark	16.5	39.6	8.5	1.4	6.5	11.4	83.9	2.8	0	0.4	0	0	4.3	0.4	7.9	1	1.8	5.5	8.3	3.26	1.77	2.14	0.46
JS-21	pale	0	3.3	0.7	0	8.2	0.9	13.1	15.3	0.4	0	1.1	0.5	50.9	2.2	70.4	2.4	1.5	12.6	16.4	0.62	0.18	0.3	0.92
JS-20	dark	17.4	38.3	13.2	0.4	4.5	9.9	83.7	6.9	0	0	0.9	0	6.5	0.2	14.5	0.4	0.9	0.5	1.8	3.9	2.13	2.94	0.48
JS-19	pale	0.4	4.6	2	2.2	8.2	1.7	19.1	8.7	0	0.7	0.6	0	58.8	3.7	72.5	1.3	0	7.1	8.3	0.87	0.51	0.21	0.71
JS-18	dark	16	25.5	12.9	4.8	3.6	11.8	74.5	9.1	0	0.6	1.1	0.4	8.9	0.6	20.7	0.4	2.9	1.5	4.8	3.02	1.96	1.96	0.85
JS-17	pale	0.6	4.1	3.2	0	10.4	0.2	18.5	13.1	0	0.6	2.1	0.7	45	3	64.4	2.1	2.2	12.9	17.2	0.63	0.17	0.31	0.96
JS-16	dark	9.1	26.7	10.2	2.7	3.8	13.2	65.8	5.7	0	0	1.3	0	9.5	0.9	17.4	3.3	6	7.5	16.8	2.46	1.79	1.32	0.75
JS-15	pale	0	4.1	2	0.4	3.6	0	10	9.8	0	0	5.3	0	70.4	4.3	89.8	0	0.2	0	0.2	1.25	1.25	0.25	0.82
JS-14	dark	16.9	32.3	14.6	0.4	4.4	8.7	77.4	10.1	0.2	0.2	1.9	0	6.1	0.8	19.2	0.4	1.1	1.9	3.4	3.81	1.76	2.83	0.49
JS-13	pale	0	4.8	1.3	0.4	9.8	0.2	16.5	8.6	0	0	0	0.4	54.9	1.9	65.8	2.7	0.8	14.2	17.7	0.79	0.2	0.2	2.43
JS-12	dark	6.7	44.7	10.8	3.4	1.8	8.7	76.1	2	0	0.4	0	0	3.4	0.5	6.3	2.7	3.6	11.2	17.5	5.48	2.53	2.2	0.51
JS-11	pale	0	3.6	1.8	0.7	6.9	0	13	11.1	0	0	0	0.7	64.3	3.6	79.7	0.7	3.8	2.7	7.2	0.74	0.42	0.2	0.88
JS-10	dark	16.6	36.4	6	0.9	5.8	11.3	77	3.8	0.2	0.2	0	0.2	10.4	0.4	15.1	0.7	4	3.1	7.8	3.19	1.85	1.86	0.43
JS-9	pale	0	4	2.3	0	8.3	0	14.6	18.8	0.2	0	0	0.6	55.9	3	78.4	1.1	2.8	3	7	0.61	0.32	0.34	0.81
JS-7	pale	0	5	2.3	0.4	8.7	0	16.5	15.3	0.8	0.2	0	0.6	51.9	3.3	72.1	1.6	5.6	4.3	11.4	0.8	0.37	0.33	0.68
JS-6	dark	13.8	30	8.2	6	5.1	7.3	70.4	5.1	0.4	3.5	0	0	13.8	1.8	24.5	1.5	1.6	2	5.1	4.15	1.93	1.81	0.54
JS-5	pale	0	4.5	2	0.4	10.9	0.7	18.5	12	0.9	0	0.4	0	53.8	2.7	69.7	0.9	2.9	8	11.8	0.5	0.28	0.25	0.57
JS-4	dark	13.7	31.4	6.7	2.9	5.6	9.7	70	7.7	1	1.7	0	0	9.7	0.7	20.8	1.2	2	6	9.2	3.2	1.66	1.78	0.49
JS-3	fusain	0	6.2	0.4	2.6	3.8	0	13	4.2	0.2	1	0.4	0	0	0	5.8	55.8	0.8	24.6	81.2	17	0.1	2.39	0.76
JS-2	pale	0	5.6	0.5	1.2	7.1	0	14.4	15.3	0	0.2	0	0.3	52.5	2	70.3	1.2	1.7	12.4	15.3	1.12	0.33	0.3	0.67

JS-1	floor	11.9	30.2	12.1	9.7	6.6	11.5	82.1	5.3	0.4	1.8	0	0	0	0.5	8.1	0.4	3.3	6.2	9.9	2.88	2.05	2.01	0.74
	average of pale	0.1	6.3	1.6	1.0	8.8	0.9	18.6	13.5	0.1	0.1	0.6	0.5	52.5	2.8	70.1	1.3	2.6	7.3	11.2	0.90	0.50	0.31	0.77
	average of dark	14.7	39.0	8.4	3.6	4.3	9.3	79.2	5.0	0.1	0.6	0.4	0.1	6.1	0.5	12.7	1.5	3.0	3.6	8.1	4.80	2.19	2.80	0.47

T - Textinite; U - Ulminite; G - Gelinite; Co - Corpohuminite; ; A - Attrinite; D - Densinite TH - Total huminite; Sp - Sporinite; Cu - Cutinite; Su - Suberinite; R - Resinite; Al - Alginite; Bi - Bituminite; Ld - Liptodetrinite; TL - Total liptinite; F+SF - Fusinite + Semifusinite; Fg - Funginite; Id - Inertodetrinite; TI - Total inertinite;

TPI - Tissue Preservation Index = (Textinite+Ulminite+Corpohuminite+Fusinite+Semifusinite)/(Attrinite+Densinite) (Kalkreuth et al., 1991, Bechtel et al., 2003);

GI - Gelification Index = (Ulminite + Corpohuminite + Densinite)/(Textinite + Attrinite + Fusinite + Semifusinite+ Inertodetrinite) (Kalkreuth et al., 1991, Bechtel et al., 2003);

VI - Vegetation Index = (Textinite + Ulminite + Fusinite + Semifusinite + Cutinite + Sporinite + Suberinite + Resinite)/(Detrohuminite + Inertodetrinite + Alginite + Liptodetrinite + Other liptinites) (Kalkreuth et al., 1991, Bechtel et al., 2003);

GW - Groundwater Index = (Gelinite + Corpohuminite + Densinite + (Ash/2))/(Textinite + Ulminite + Attrinite) (Kalkreuth et al., 1991, Stock et al., 2016)

---

### 2.5.2.1 Huminite group

In pale lignites, huminite macerals are present in moderate proportions of the total maceral groups, and are mainly composed of attrinite (av. 9.1%) and ulminite (av. 6.5%). The other macerals of huminite contribute less than 2%, with a proportion (in decreasing order) of gelinite, corpohuminite, densinite, and textinite. Detrohuminite (av. 10%) is the maceral with the highest abundance in the total huminite group in pale lignites, and usually occurs with inertodetrinite distributed in the matrix of bituminite and minerals (Fig. 3). The high abundance of detrohuminite and the high ash content, along with the low proportion of telohuminite and gelinite (av. 1.6%), indicate that the pale lignites might have been deposited in a relatively high-energy environment with clastic input (Oikonomopoulos et al., 2015). An alternative explanation is that the occurrence of detrohuminite is the result of intense weathering and the prevalence of herbaceous vegetation, which is more susceptible to be degraded in the mire (Singh et al., 2017b).

However, in dark lignites, telohuminite dominates in comparison to the other subgroups of huminite, as would be expected, because of the high content of ulminite. The abundance of telohuminite in the dark lignites is about seven times higher than in the pale lignites and occurs as ulminite (av. 39.0%) and textinite (av. 14.7%). Telohuminite has an average concentration of 42.8% and reaches a maximum concentration of 69.1%. Among all the macerals, gelinite (8.4%), densinite (9.3%), and attrinite (4.3%) have a relatively high abundance in the dark lignite samples. The proportion of corpohuminite (av. 3.6%), present as both phlobaphinite and pseudophlobaphinite, is the lowest level of huminite in the dark lignites, but in some samples the proportion is higher than 5%. The abundance of the telohuminite fraction (textinite + ulminite) is higher compared with the detrohuminite (densinite + attrinite) fraction may be related to the fact that lignin-rich wood is structurally better preserved than the cellulose-rich tissues of herbaceous plants during coalification (Taylor et al., 1998). Phlobaphinite concentrated in peats is known to originate from plant communities rich in wood (Cohen et al., 1987; Taylor et al., 1998). The predominant presence of telohuminite in the dark samples together with the relatively low percentage of detrohuminite, and the relatively high percentage of gelohuminite (gelinite + corpohuminite), indicates the presence of vegetation in the dark lignites that consisted mainly of bushes or trees, which are more resistant to degradation in peat bogs (Diessel, 2012). In addition, the dark lignites are mainly composed of huminite, followed by liptinite, and have low contents of inertinite macerals, which suggests the prevalence of wet/anaerobic conditions in the peat-forming mire (Flores, 2002; Sýkorová et al., 2005; Erik, 2011).

### 2.5.2.2 Liptinite group

The pale and dark lignites also have large differences in the proportion of liptinite concentrations. In the pale lignites, liptinites have the highest concentration over all types of macerals, reaching a maximum concentration of up to 89.8%. This is mainly caused by the high content of bituminite (av. 52.5%), which is much higher than in the dark lignites (av. 6.1%) (Table 2). Bituminite, which has been referred to as the mineral-bituminous groundmass by Qi et al. (1994), often occurs as an amorphous groundmass associated with clay minerals and liptodetrinite (Fig. 3). Bituminite in pale lignites is characterized by an obvious red internal reflection under oil immersion, reflected light, and yellow fluorescence excited by blue light (Fig. 3). This type of bituminite has been observed in pale layers in Eocene brown coals from Germany (Teichmüller, 1989), and was interpreted as a product of strong bacterial decomposition (Pickel and Wolf, 1989).

Sporinite is the second most abundant maceral of the liptinite group in the pale lignites, and its abundance is higher than that of the dark lignites. High contents of sporinite have also been reported in other pale lignites from Liaohu in Yunnan Province (Qi et al., 1994; Yu et al., 1996). The composition of sporinite and pollen was shown to reflect the presence of a mixture of angiosperms and gymnosperms in the former mire (Yu et al., 1996; Wang et al., 1997). This is consistent with results from paleobotany suggesting that *Quercus* and *Pinaceae* were both common in the Tertiary in Yunnan Province (Yang, 1996). The low liptodetrinite content in the pale lignite may be caused by the presence of small liptodetrinite particles commonly distributed within the bituminite, making it difficult to separate them from the groundmass during statistical counting. Suberinite is enriched in some dark lignite samples, with a maximum content of 3.5%, but is almost absent in all pale lignites. Only small amounts of additional macerals, such as cutinite and resinite are observed (usually with values less than 1%) in most samples of pale and dark lignites. In some cases, these additional macerals are totally absent (Table 2). The big differences in the abundance of huminite and liptinite between the pale and dark lignites suggest either a variation in the plant community (gymnosperms vs. angiosperms) during peat accumulation in the basin, or a change in depositional environment during ancient peat formation. The high concentrations of liptinite (particularly sporinite) in pale lignites of the Gippsland Basin, Australia were previously considered to be indicative of larger degrees of oxidation in drier, more elevated, peatland environments (Anderson and Mackay, 1990).

### 2.5.2.3 Inertinite group

Inertinite has a relatively low abundance in both pale (av. 11.2%) and dark lignites (av. 8.1%) (Table 2). The inertodetrinite subgroup is more abundant in pale lignites (av. 7.3%) than in dark lignites (av. 3.6%). The relatively higher abundance of inertodetrinite in the pale samples may suggest relatively drier conditions during the accumulation of pale

lignites in the ancestral mire. Funginite is the second most abundant maceral in the inertinite group. The abundance of funginite is lower in the pale lignites (av. 2.6%) than in the dark lignites (av. 3.0%). This might indicate that the climate was more humid during the deposition of the dark lignites. Single- to multi-celled fungal spores are common. Figure 3c depicts a photomicrograph of one individual funginite under oil immersion, reflected white light. The morphological characteristics are typical for a multi-celled fungal spore and are similar to the morphology of fungal spores in Tertiary lignites from India (Singh and Singh, 2000; Singh et al., 2017b). The presence of funginite in considerable concentrations in the lignites indicates the presence of warm and humid/moist climatic conditions during peat formation (Singh et al., 2017b). In the area of the Jinsuo Basin, the climate during the Neogene was presumably warmer and more humid than today (Xu et al., 2008; Xie et al., 2012; Xing et al., 2012; Su et al., 2013). Such conditions are favorable for fungi, and for luxuriant growth of vegetation in a tropical to sub-tropical climate, as indicated by the relatively high abundance of funginite. Other macerals of the inertinite group, such as fusinite and semifusinite, are found in very low quantities (av. <2%) in both pale and dark lignites. Other macerals of the inertinite group (e.g. secretinite, macrinite, and micrinite) are absent in both pale and dark samples. The low content of inertinite in both pale and dark lignites is consistent with a warm and humid climate in the basin. However, the higher abundance of inertinite and inertodetrinite in the pale samples compared with the dark samples suggests relatively drier conditions during deposition of the pale lignites in the ancestral mire.

### 2.5.3 Maceral indices

Several models, based on quantitative maceral data or indices, have been developed for the reconstruction of paleomire conditions (Suárez-Ruiz et al., 2012; Sen et al., 2016). However, inaccurate conclusions might be drawn when the depositional conditions in the former peat mire are assessed only from petrographic data/indices (Crosdale, 1993; Dehmer, 1993; Wüst et al., 2001; Scott, 2002; Sen et al., 2016). Further proxies derived from palynology, geochemistry, etc. should be taken into account to support the interpretation from petrographic data/indices (Moore and Shearer, 2003; Sen et al., 2016).

The following maceral ratios, including TPI, the GI, GWI, and VI, were calculated in the present study to reconstruct the paleoenvironmental conditions during peat accumulation (Table 2).

The TPI and GI indexes were first introduced and applied by Diessel (1986) for high-rank coals, and were later modified for low-rank coals/lignites by Kershaw et al. (1991), Markic and Sachsenhofer (1997), Kalaitzidis et al. (2000), and Bechtel et al. (2003). The TPI is indicative of the degree of humification of the peat-forming materials, and focuses on the degree of tissue preservation and destruction. The TPI also provides information

on the amount of woody material that contributes to peat formation (Diessel, 1986; Amijaya and Littke, 2005; Singh et al., 2010). The GI reflects the degree of wetness in the former peatland. High GI values ( $>1$ ) indicate wet conditions, which are more likely to prevent oxidation of the organic matter and are suitable for the formation and preservation of huminite. High TPI and GI values ( $>1$ ) are, thus, indicators for low levels of aerobic decomposition, which may additionally result in a low inertinite content (Oikonomopoulos et al., 2015).

In the Jinsuo Basin, the dark lignites are characterized by very high TPI values (all samples  $>2$ ; Table 2) and high GI values ( $>1$ ; Table 2), and the maximum value is in the fusain layer because of the high content of fusinite. In contrast, the TPI values (av. = 0.9; Table 2) and GI values (av. = 0.5; Table 2) are low in the pale lignites. The very high TPI values (av. 4.8) in the dark lignites are reflected by the observed high telohuminite percentages, implying generally good organic matter preservation and the predominance of arboreal vegetation (Diessel, 1986; Teichmüller, 1989). The low TPI values in the pale lignites indicate either the predominance of herbaceous plants in the mire or intensive destruction of woody tissues as a result of advanced humification and bacterial/fungal activity (Gürdal and Bozcu, 2011; Oikonomopoulos et al., 2015). The differences in TPI values between dark and pale lignites suggest some alteration in the type of peat-forming plant community and in the paleoenvironmental conditions that are either favorable or unfavorable for tissue preservation (Oikonomopoulos et al., 2015).

In addition, in the TPI vs GI diagram (Fig. 4a) the data points obtained from pale and dark lignites are clearly separated from each other. All of the examined dark lignite samples have high TPI and GI values ( $>1$ ), indicating that the thick, dark layers formed in a wet swamp forest with a limited oxygen supply, low degradation, and increased bacterial activity (Dehmer, 1989). The high degree of gelification observed in the dark lignites from Jinsuo suggests a wet, warm, and humid climate during peat formation in the studied areas during the Neogene (Su et al., 2013; Zhu et al., 2015). In contrast, the low TPI and the variation of GI (0.2–1.3) values (Fig. 4a, Table 2) in the thin pale layers can be interpreted as the result of an unstable water table and more oxic conditions compared with the conditions during the deposition of the dark layers.

Calder et al. (1991) introduced the GWI and the vegetation index (VI) to characterize paleomires for hard coals. Kershaw et al. (1991), Kalaitzidis et al. (2000), and Bechtel et al. (2003) adopted, with some modifications, the GWI and VI for Tertiary low-rank coals/lignites. In the present study, the GWI was related to the ash content because ash content shows better and more quantitative information on the mineral matter content of coals than does counted mineral matter (Stock et al., 2016).

The plot of GWI versus VI allows the reconstruction of the type of the former paleomire (Fig. 4b). The data point plots from the pale and dark samples are clearly separated from each other in this diagram, and the difference is mostly related to the VI. The VI values are low (av. 0.31) for pale lignites and much higher (av. 2.8) for the dark



lignites. Both the pale and dark lignites plot within a field that is characteristic of a peat-bog environment with both mesotrophic and ombrotrophic hydrological conditions. The high huminite content associated with a low inertinite content (Table 2) is in agreement with a wet and relatively humid climate (Utescher et al., 2007) that was able to maintain water-saturated conditions and a stable water table in a nutrient-depleted environment (Stock et al., 2016). Such conditions enhance the preservation of tissues because of the lack of (or restricted) aeration and oxidation of the OM (Dehmer, 1995). High VI values ( $>2$ ) indicate that woody vegetation was the dominant source for the dark lignites, which is in agreement with the TPI values that indicate a high lignin content in plant materials accumulated in the peatland. The relatively low GWI values (av. = 0.47) in the dark layers result from the high telohuminite content, which was previously also observed in xylite-dominated Neogene lignite from Achlada, Greece (Oikonomopoulos et al., 2015). The variable GWI values, as well as the high TPI and GI values in the dark lignites, indicate paleoenvironmental conditions characterized by water table variation in the former mire combined with wet and humid conditions, which is consistent with the proposed climatic conditions in the Neogene of Yunnan Province (Xu et al., 2008; Xie et al., 2012; Su et al., 2013). However, the very low VI values are consistent with the low TPI values in the pale lignites and indicate either a relatively high decomposition rate of plant materials under aerobic conditions (low GI values), or the dominance of herbaceous plants during peat formation (Teichmüller, 1989; Singh et al., 2010; Diessel, 2012).

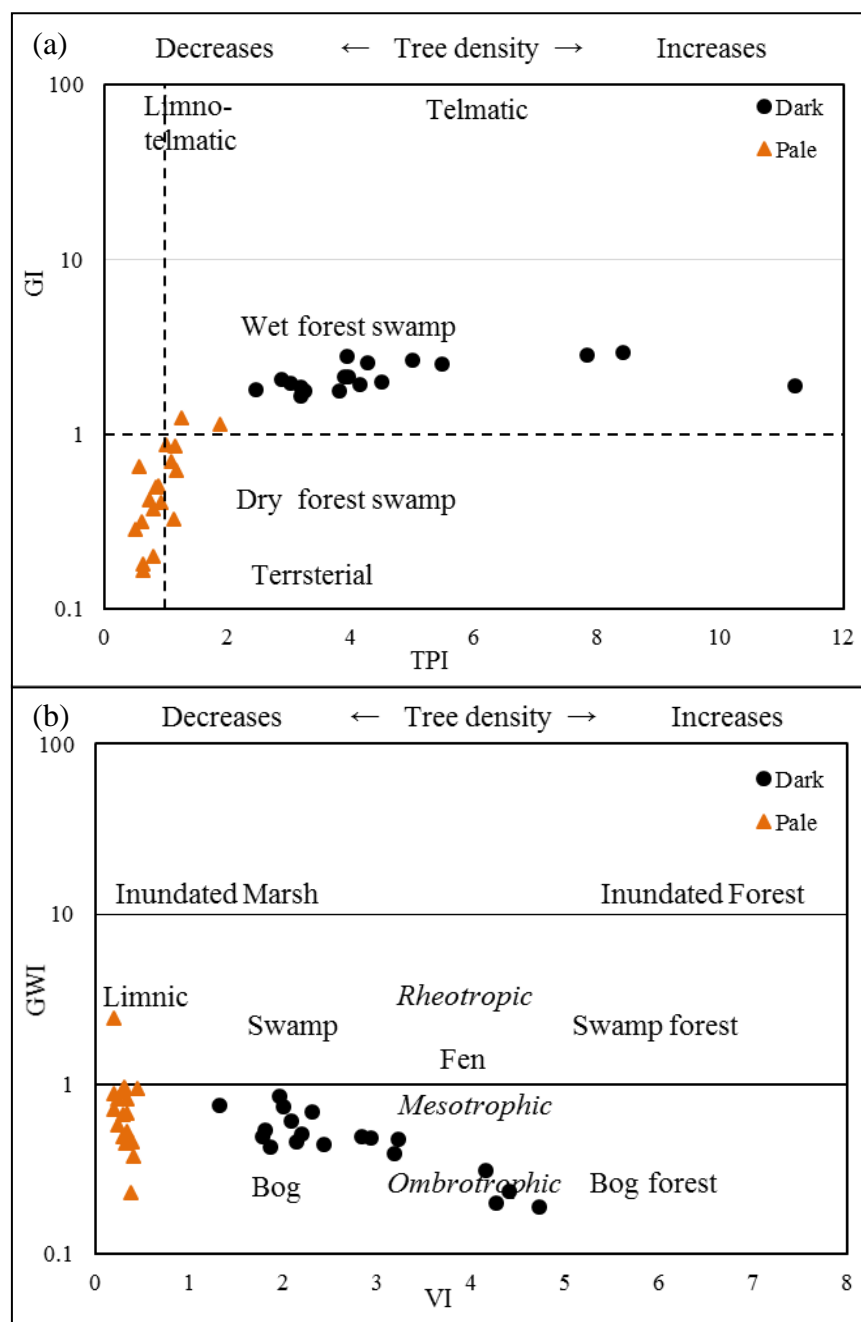


**Figure 2-3** Diagram (a) of the Gelification Index (GI) vs. Tissue Preservation Index (TPI) with data point of pale and dark lignites from Jinsuo Basin (after Diessel, 1986, modified), and diagram (b) of Vegetation Index (VI) vs. Ground Water Index (GWI) of pale and dark lignites from Jinsuo Basin (modified after Calder et al., 1991)

#### 2.5.4 Bulk geochemical parameters

The TOC on a dry basis varies between 42.0% and 62.4% (Table 3) in the pale lignite samples, and between 45.0% and 55.8% in the dark lignite samples. There is no obvious

difference in the average TOC values in pale (av. 52.5%) and dark lignite (av. 51.3%) samples; these TOC values are lower than the values reported from the Miocene lignite in the Lower Rhine Basin in Germany, which have an average higher than 54% (Stock et al., 2016), and from the Gippsland Basin in Australia with the average higher than 58% (Powell et al., 1991). The total nitrogen (TN) content ranges from 0.68% to 1.27% and from 1.00% to 1.38% (Table 3) in the pale and dark lignite samples, respectively. The average content of TN in the dark lignite samples (1.21%) is much higher than the value in the pale lignite samples (0.89%). Both the pale and dark lignite samples have higher TN content than the lignites from the Gippsland Basin in Australia, which had values of less than 0.7% (Chaffee et al., 1984; Russell, 1984). The extractable organic matter (EOM) yields of pale (30.6–179.9 mg/g TOC; Table 3), and dark lignite samples (14.3–75.0 mg/g TOC) vary within comparable ranges. The average EOM content in pale lignites (112.9 mg/g TOC) reaches nearly 3 times the EOM content of dark lignites (40.2 mg/g TOC). The high EOM content of the pale lignites is associated with a high bituminite content. Previous studies in Germany have also reported higher amounts of EOM from light lithotypes compared with dark lithotypes (Winkler, 1986; Hagemann and Wolf, 1987; Hagemann and Dehmer, 1991).

The average content of ash in the pale lignites (15.1%, Table 3) is higher than in the dark samples (8.4%). Higher ash content in the pale lithotypes was previously also observed in pale layers from Germany (Teichmüller, 1989), while the opposite results were found in lignites from the Gippsland Basin in Australia (Sluiter et al., 1995). However, other studies have shown no obvious systematic difference in ash content between pale and dark lithotypes (Winkler, 1986; Hagemann and Wolf, 1987; Holdgate et al., 2016).

The EOM was separated into four sub-fractions using column chromatography. The relative proportions of saturated hydrocarbons in the pale samples (av. 3.1%) are slightly higher than in the dark samples (av. 2.9%), while the dark lignite samples (av. 4.8%) have higher contents of aromatic hydrocarbons than the pale samples (av. 2.9%) in the Jinsuo Basin (Table 3). The low content of saturated and aromatic hydrocarbons is consistent with the low maturity of the lignites. The EOM is mainly represented by NSO compounds and asphaltenes.

The mean C/N ratio (Table 3) in pale lignites (av. 60.6) is higher than in dark lignites (av. 40.8) in the Jinsuo Basin. These values are much lower than the values reported from pale and dark layers from the Gippsland Basin in Australia (Chaffee et al., 1984). Cernusak et al. (2008) compared the C/N ratios of recent gymnosperm trees with recent angiosperm trees and found that gymnosperm trees have higher C/N ratios (64.7) than angiosperm trees (49.6). The obvious variation of C/N ratios in the pale and dark lignites might, therefore, reflect a change in plant species in the basin during peat formation. However, anaerobic decomposition could also result in decreasing C/N ratios in the

peatland (Kuhry and Vitt, 1996), which is consistent with the deposition of the dark lignites under more anaerobic conditions than the pale lignites.

**Table 2-3 Bulk geochemical data and parameters of lignite samples from Jinsuo opencast mine**

Sample No.	Lithotypes	Ash <sup>db</sup> (wt.%)	EOM (mg/g TOC)	Saturated HC	Aromatic HC	NSO-compounds + Asphaltenes	TO <sub>C<sup>db</sup></sub>	TN <sub>b</sub> <sup>d</sup>	C/N
				(wt.%, EOM)			(wt.%)		
JS-39	dark	10.9	32.3	4.2	3.5	92.3	51.3	1.32	38.9
JS-38	dark	4.6	42.4	3.3	8.8	87.9	55.2	1.22	45.2
JS-37	pale	14.3	179.9	2.1	2.3	95.6	52.5	0.76	68.6
JS-36	dark	4.6	60.3	2.2	4.1	93.8	55.8	1.26	44.1
JS-35	pale	9.4	98.9	2.5	2.3	95.2	54.3	1.02	53.0
JS-34	dark	4.0	41.4	4.3	7.8	87.8	55.2	1.09	50.5
JS-33	pale	6.8	128.6	2.1	2.5	95.4	55.2	0.92	59.9
JS-32	dark	5.1	75	2.6	0.5	96.9	55.8	1.09	51.2
JS-31	pale	11.1	146	2.6	2.3	95	53.7	0.81	66.5
JS-30	dark	9.6	34.8	3.7	5.4	90.9	47.7	1.11	43.0
JS-29	pale	9.3	95.5	2.5	3.8	93.7	57.0	0.9	63.1
JS-28	dark	4.9	14.3	4.5	6.0	89.5	52.8	1.07	49.5
JS-27	pale	13.3	90.7	2.3	3.2	94.5	53.4	0.78	68.7
JS-26	dark	3.6	35.5	5.2	4.9	90	48.6	1.01	48.1
JS-25	pale	8.3	154.3	3.0	3.9	93	62.4	0.68	91.4
JS-24	dark	5.2	55.9	4.3	4.4	91.3	54.6	1.28	42.6
JS-23	pale	9.2	174.4	2.8	2.7	94.4	54.6	1.07	51.1
JS-22	dark	15.2	29.3	4.6	6.2	89.2	46.2	1.36	33.9
JS-21	pale	18.0	128.1	3.0	1.9	95.1	52.2	0.73	71.3
JS-20	dark	11.0	23.3	4.0	5.9	90.1	51.0	1.16	43.9
JS-19	pale	6.9	30.6	5.2	6.2	88.6	55.8	1.27	43.9
JS-18	dark	17.7	38.0	4.6	4.4	90.9	49.2	1.35	36.5
JS-17	pale	22.2	82.3	3.0	2.0	94.9	43.8	0.94	46.3

JS-16	dark	7.4	50.4	3.8	2.7	93.5	51.6	1.16	44.4
JS-15	pale	7.9	153.9	1.7	1.5	96.8	56.4	0.71	79.5
JS-14	dark	5.2	35.5	3.5	1.6	94.9	53.4	1.36	39.3
JS-13	pale	67.0	81.3	6.2	2.6	91.1	42.0	0.77	54.9
JS-12	dark	8.4	22.6	5.7	4.3	90.0	51.6	1.29	39.9
JS-11	pale	13.5	65.2	3.7	2.9	93.4	52.8	1.03	51.1
JS-10	dark	14.0	34.9	3.6	3.6	92.8	50.4	1.38	36.6
JS-9	pale	15.5	105.6	2.1	1.8	96.1	45.6	0.84	54.4
JS-7	pale	13.3	34.4	4.3	2.3	93.3	49.8	0.95	52.5
JS-6	dark	10.0	48.8	4.1	4.6	91.2	45.0	1.19	37.9
JS-5	pale	11.5	138.3	2.5	2.4	95.0	51.0	0.93	54.9
JS-4	dark	11.6	40.6	3.7	3.4	92.9	48.6	1.18	41.0
JS-3	fusain	9.2	41.09	3.5	2.1	94.4	N.A.	N.A.	N.A.
JS-2	pale	13.6	143.7	3.3	5.5	91.2	52.2	0.87	59.7
JS-1	floor	5.3	69.7	2.2	8.5	89.2	54.3	1.0	54.3
Average of pale		15.1	112.9	3.1	2.9	94.0	52.5	0.89	60.6
Average of dark		8.4	40.2	3.9	4.8	91.3	51.3	1.21	42.8

db – dry basis.

HC – hydrocarbons.

NSO – Polar fraction, which contains nitrogen, sulphur and oxygen compounds.

N.A. – Not analyzed.

## 2.5.5 Molecular composition of the EOM

### 2.5.5.1 *n*-Alkanes and isoprenoids

In Figure 5, the TIC chromatograms of the saturated hydrocarbon fractions of sample JS-21 (Fig. 5a) and JS-26 (Fig. 5b) are shown as representative for the pale and dark lignites, respectively. The *n*-alkane patterns of all lignite samples are dominated by *n*-alkanes from *n*-C<sub>27</sub> to *n*-C<sub>31</sub> (Fig. 5 and Table 4), with a marked odd over even predominance. In the majority of pale lignites, the maximum abundance of *n*-alkanes is at *n*-C<sub>31</sub>, while in dark lignites the relative abundance of *n*-alkanes reaches a maximum from *n*-C<sub>27</sub> to *n*-C<sub>31</sub> in different samples.

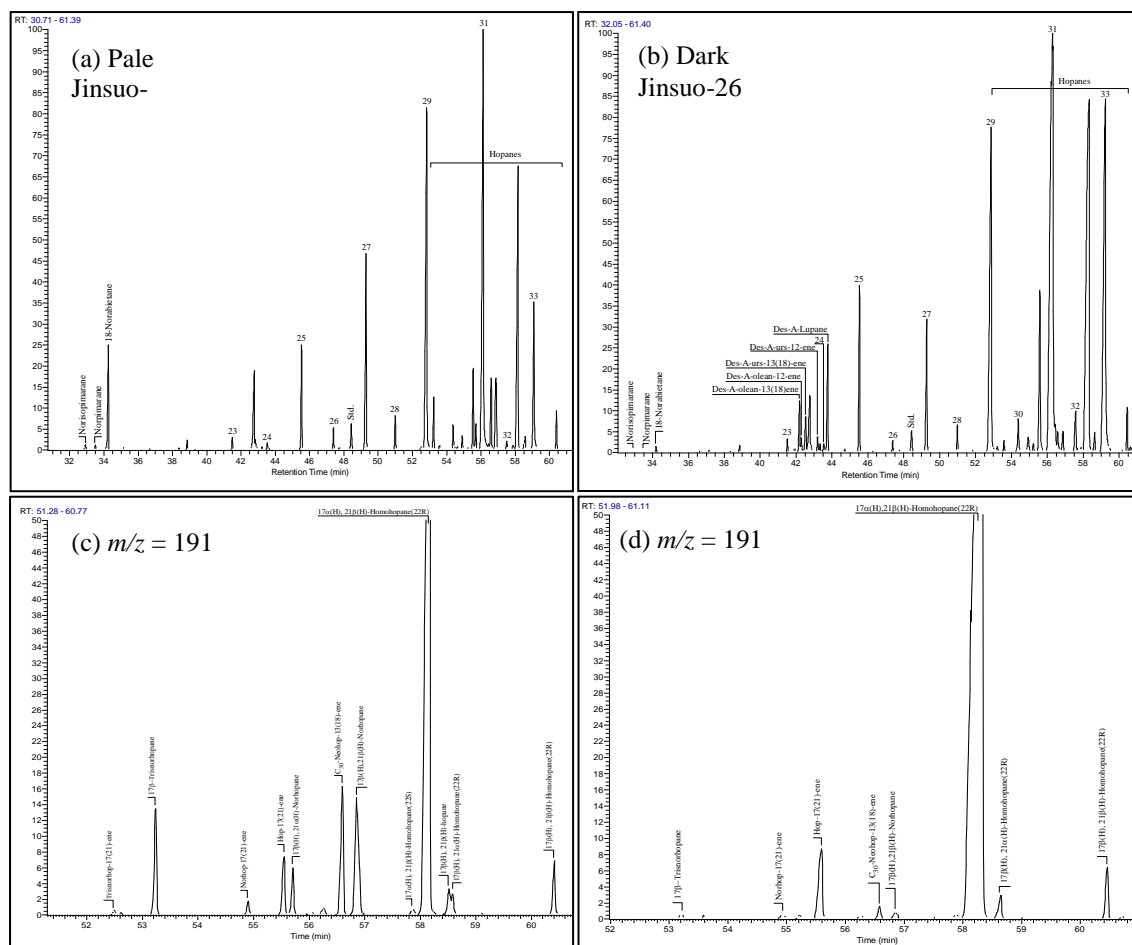


**Figure 2-4 Gas chromatograms (total ion current) of the saturated hydrocarbon fractions of: (a) sample Jinsuo-21 (pale lignite), and (b) sample Jinsuo-26 (dark lignite). *n*-Alkanes are labeled according to their carbon number. Std. = Standard (squalane). Traces (c) and (d) show mass chromatograms ( $m/z = 191$ ) of the hopanes of sample Jinsuo-21 (pale lignite), and sample Jinsuo-26 (dark lignite)**

The high concentrations of long-chain *n*-alkanes ( $C_{27}$ - $C_{31}$ ) relative to the sum of the *n*-alkanes in both the pale (av. 81.7%) and dark (av. 71.3%) lignites (Table 4; Fig. 5) are characteristic of the predominance of higher terrestrial plants, where they occur as the main components of plant waxes (Eglinton and Hamilton, 1967). The short-chain *n*-alkanes ( $<n$ - $C_{20}$ ) are reported to dominate mostly in algae and microorganisms (Cranwell, 1977). These compounds were detected in very low amounts in both the pale (av. 0.5%) and dark (av. 1.2%) lignites in nearly all samples, with the exception of samples JS-1, JS-32, and JS-36. It has been suggested that mid-chain *n*-alkanes ( $n$ - $C_{21-25}$ ) originate mainly from sphagnum or aquatic plants (Cranwell, 1977; Ficken et al., 2000; Nott et al., 2000), and are present in abundances of 10.6% and 18.6%, on average, relative to the sum of the *n*-alkanes in the pale and dark lignite samples, respectively.

**Table 2-4 Biomarker concentrations of lignite samples from Jinsuo opencast mine**

Sample No.	Lithotypes	<i>n</i> - Akane max.	<i>n</i> - C<20	<i>n</i> -	<i>n</i> -	Dit- Sat <sup>a</sup>	Tri- Sat <sup>b</sup>	Dit- Aro <sup>c</sup>	Tri- Aro <sup>d</sup>	Di- / (Di- + Tri- terpenoids)
				C <sub>21</sub> - <i>n</i> - C <sub>25</sub>	C <sub>27</sub> - <i>n</i> - C <sub>31</sub>					
JS-39	dark	C <sub>29</sub>	0.2	12.0	81.3	0.9	53.7	N.D. <sup>e</sup>	424.7	<0.01
JS-38	dark	C <sub>29</sub>	0.9	15.7	69.4	N.D.	5.7	N.D.	57.3	<0.01
JS-37	pale	C <sub>31</sub>	0.8	15.7	74.6	76.8	N.D.	1.2	113.9	0.41
JS-36	dark	C <sub>29</sub>	11.9	18.9	60.2	18.2	0.9	0.7	468.4	0.04
JS-35	pale	C <sub>31</sub>	1.1	15.3	74.3	13.5	0.0	0.8	470.2	0.03
JS-34	dark	C <sub>29</sub>	0.2	7.0	83.3	1.4	38.4	N.D.	40	0.02
JS-33	pale	C <sub>31</sub>	0.8	13.9	75.3	11.5	2.0	0.8	219	0.05
JS-32	dark	C <sub>25</sub>	3.3	29.4	60.2	5.6	8.3	0.3	568	0.01
JS-31	pale	C <sub>31</sub>	1.0	12.9	76.0	24.6	2.3	0.2	161.9	0.13
JS-30	dark	C <sub>29</sub>	0.5	22.3	72.5	0.9	18.6	3.5	1266.2	<0.01
JS-29	pale	C <sub>31</sub>	1.1	14.1	76.3	139.6	12.8	3.7	430.9	0.24
JS-28	dark	C <sub>31</sub>	0.3	11.5	77.8	5.1	13.4	N.D.	6.7	0.20
JS-27	pale	C <sub>27</sub>	0.4	8.1	84.3	211.5	2.8	1.5	639.2	0.25
JS-26	dark	C <sub>31</sub>	0.1	6.0	68.6	3.6	100.4	N.D.	266	0.01
JS-25	pale	C <sub>29</sub>	0.3	6.3	85.1	69.3	4.9	0.7	279.5	0.20
JS-24	dark	C <sub>31</sub>	0.1	3.1	84.4	195.4	9.5	1.3	617.4	0.24
JS-23	pale	C <sub>31</sub>	0.4	3.9	80.8	13.9	12.0	0.2	90	0.12
JS-22	dark	C <sub>27</sub>	0.1	19.0	78.4	3.4	237.4	9.5	467.3	0.02
JS-21	pale	C <sub>31</sub>	0.1	6.8	82.6	124.5	1.3	2.3	68.3	0.65
JS-20	dark	C <sub>27</sub>	0.2	30.9	64.6	42	8.6	14.2	845.9	0.06
JS-19	pale	C <sub>31</sub>	0.1	9.7	83.4	29.5	5.9	3.6	766.5	0.04
JS-18	dark	C <sub>27</sub>	0.1	24.3	72.0	6.6	89.5	5.9	912.7	0.01
JS-17	pale	C <sub>27</sub>	0.1	11.6	83.5	276.7	5.1	7.6	111.8	0.71
JS-16	dark	C <sub>31</sub>	0.1	3.2	81.9	133.5	4.7	0.7	235.5	0.36
JS-14	dark	C <sub>31</sub>	0.1	8.0	85.5	6.3	6.2	2.2	836.3	0.01
JS-13	pale	C <sub>31</sub>	<0.1	2.2	81.8	313.5	1.8	3	230	0.58
JS-12	dark	C <sub>31</sub>	0.1	6.9	74.5	18.8	8.0	1.3	831.9	0.02
JS-11	pale	C <sub>31</sub>	0.1	8.6	85.6	89.5	2.2	0.8	135.8	0.40
JS-10	dark	C <sub>31</sub>	0.1	7.8	83.4	4.4	4.1	0.9	234.2	0.02
JS-9	pale	C <sub>31</sub>	0.1	2.1	81.7	80.8	1.7	4.6	334.1	0.20
JS-7	pale	C <sub>31</sub>	0.1	5.3	87.3	71.6	1.1	4.2	558.9	0.12
JS-6	dark	C <sub>27</sub>	0.1	24.4	73.2	0.2	22.1	N.D.	655.6	<0.01
JS-5	pale	C <sub>31</sub>	1.0	11.3	84.0	13.8	N.D.	N.D.	108.8	0.11
JS-4	dark	C <sub>25</sub>	1.1	42.6	53.9	0.5	3.3	1.5	904.9	0.00
JS-3	fusin	C <sub>31</sub>	0.4	2.9	88.7	23.3	N.D.	2.4	63.3	0.29
JS-2	pale	C <sub>31</sub>	0.6	12.1	82.4	581.4	N.D.	N.D.	99.4	0.85
JS-1	floor	C <sub>19</sub>	21.5	43.1	29.2	35.3	N.D.	N.D.	127.3	0.22
	average of pale	--	0.5	10.6	81.7	126.0	3.3	2.0	267.7	0.30
	average of dark	--	1.2	18.6	73.3	19.5	35.9	2.4	526.8	0.07

<sup>a</sup> Dit-Sat = Total saturated diterpenoids.

<sup>b</sup> Tri-Sat = Total saturated triterpenoids.

<sup>c</sup> Dit-Aro = Total aromatic diterpenoids.

<sup>d</sup> Tri-Aro = Total aromatic triterpenoids.

<sup>e</sup> N.D. = Not detected.

Previous studies of *n*-alkane distributions in plants have been used for the chemotaxonomy of deciduous trees, grasses, and mosses. Deciduous trees are usually characterized by *n*-alkane distributions reaching a maximum at *n*-C<sub>27</sub> or *n*-C<sub>29</sub>, whereas grasses and mosses usually show a maximum at *n*-C<sub>31</sub> (Cranwell, 1973; Cranwell et al., 1987). However, new data from Bush and McInerney (2013) shows that the use of *n*-C<sub>27</sub>, *n*-C<sub>29</sub>, and *n*-C<sub>31</sub> for the separation of graminoids (grasses) and woody plants is not precise enough since both groups produce highly variable, but significant, amounts of all three chain lengths of *n*-alkanes. Hence, it is difficult to speculate from the *n*-alkane distribution which kind of vegetation was dominant in the biomass leading to the pale and dark lignites from the Jinsuo Basin. Nevertheless, *n*-C<sub>31</sub> represents *n*-alkane maximum in the majority of pale lignites, while in dark lignites the relative abundance of the most abundant *n*-alkane varies from *n*-C<sub>27</sub> to *n*-C<sub>31</sub> in different samples. The general agreement is that *Sphagnum* mosses are marked by the predominance of *n*-C<sub>23</sub> (Ficken et al., 2000; Nott et al., 2000; Nichols et al., 2006, 2010; Bush and McInerney, 2013). The very low abundance of the C<sub>23</sub> alkane in all of the analyzed lignites indicates that *Sphagnum* did not play a major role in the peat bog, and that the pale lignites, which were once defined as *Sphagnum* coal by Lu and Zhang (1986, 1989), could not originate from *Sphagnum*.

The concentrations of pristane and phytane in the majority of samples were below the limit of quantitation, and thus the pristane/phytane ratio could not be applied as an indicator for redox-conditions in the depositional environment of the lignites in the Jinsuo Basin.

### 2.5.5.2 Diterpenoids and triterpenoids with non-hopanoid skeletons

Diterpenoids are valuable biomarkers in crude oils and sedimentary organic matter for the identification of the type of precursor vegetation (Simoneit, 1986, 1998, 1999). They are mainly constituents of resins, wood, roots, and bark in gymnosperms (Karrer, 2013), but were detected in only a few angiosperms from contemporary plants (Otto and Wilde, 2001; Rowe, 1989). In the lignites from the Jinsuo Basin, only three individual diterpenoid hydrocarbons were identified in saturated hydrocarbon fractions from all the samples: 4β(H)-19-norisopimarane, 18-norpimarane, and 18-norabietane, which are common constituents of resins and lignites (Maxwell et al., 1971; Douglas and Grantham, 1974; Philp, 1985). Figure 5a shows a representative TIC chromatogram of a saturated hydrocarbon fraction with the peaks of the three compounds at retention times between 32 and 35 min. The concentrations of the three compounds are summarized in Table 4 as



Dit-Sat (Total saturated diterpenoids). Their content in pale and dark lignites shows significant differences. This suggests a major variation in the composition of vegetation during the formation of the pale and dark lithotypes. The pale lignites are characterized by a significantly higher abundance of the three diterpenoid biomarkers (av. 126.0  $\mu\text{g/g}$  TOC) compared with the dark lithotypes (av. 19.5  $\mu\text{g/g}$  TOC), suggesting that gymnosperms were more abundant in the vegetation during the formation of the pale lignites than during the formation of the dark layers. This observation is different to the results obtained previously from lignites in the Helmstedt deposit, northern Germany (Winkler, 1986) and Lower Rhine Basin, western Germany (Hagemann and Wolf, 1987). In both basins, light and dark lithotypes have low concentrations of diterpenoid compounds. All three diterpenoids detected in the extracts from the Jinsuo Basin are nor-diterpanes, indicating a loss of one methyl group from the originally-present diterpanes. Compared with saturated diterpenoids, the aromatic diterpenoids (Dit-aro) detected as 18-norabieta-8,11,13-triene, retene, and two mono-aromatic diterpenoids were either present at very low concentrations in both pale and dark lignites (av.  $<3$   $\mu\text{g/g}$  TOC, Table 4), or they were below the detection limit in some samples.

Non-hopanoid triterpenoids containing structures typical of the oleanane, ursane, or the lupane skeleton are biomarkers for angiosperms (Sukh, 1989; Karrer, 2013). However, since most angiosperm plants contain  $\beta$ -amyrin and  $\alpha$ -amyrin in considerable quantities (Gülz et al., 1992; Karrer, 2013), the use of the triterpenoid composition for chemotaxonomy of angiosperms has not been successful. The non-hopanoid triterpenoids identified in the saturated hydrocarbon fraction, which also contains mono-unsaturated hydrocarbons, are dominated by the following compounds:  $\text{C}_{30}$  neohop-13(18)-ene, des-A-olean-12-ene, des-A-urs-13(18)-ene, des-A-urs-12-ene and des-A-lupane (Fig. 5b) (identification according to retention time, following the methods of Philp, 1985; ten Haven et al., 1992; Logan and Eglinton, 1994). Although the contents of saturated triterpenoids are not very high in all samples, they are higher in the dark (av. 35.9  $\mu\text{g/g}$  TOC) than in the pale (av. 3.3  $\mu\text{g/g}$  TOC) lignites (Table 4).  $\text{C}_{30}$  neohop-13(18)-ene, des-A-olean-12-ene, des-A-urs-12-ene and des-A-lupane are usually detected in dark lignite samples (Fig. 5b) but are always absent in pale lignite samples (Fig. 5a). The different content of these compounds in dark and pale lignites indicates that angiosperms are the main source for dark lignites, whereas in the pale lignites the biomass originating from angiosperms was partly replaced by biomass from gymnosperms. This observation is supported by the results of the C/N ratios (Table 3). The ratios of diterpenoids over the sum of diterpenoids plus angiosperm-derived triterpenoids are listed in Table 4, and show that in the pale lignite samples the ratio is higher (av. 0.30) than in the dark lignites samples (av. 0.07). In some pale samples (JS-2, JS-12, JS-17 and JS-21), the ratios are higher than 0.5 and reached a maximum value of 0.85 in sample JS-2, indicating a high gymnosperm contribution to the peat-forming vegetation for the formation of pale layers relative to that from angiosperms. The Di- /

(Di- + Tri-terpenoids) ratio in the majority of dark lignite samples is lower than 0.1 (Table 4), indicating that angiosperms provided the principal contribution to the plant community during the formation of the dark layers.

The distribution profiles of individual non-hopanoid triterpenoids in aromatic hydrocarbon fractions of all samples are similar (Fig. 6). The profiles are represented by the following aromatic triterpenoids: tetramethyloctahydrochrysenes, trimethyltetrahydrochrysenes (Spyckerelle et al. (1977)), monoaromatic pentacyclic terpenoids (24,25-dinorursa-1,3,5(10),12-tetraene, 24,25-dinorolean-1,3,5(10),12-tetraene, 24,25-dinorlupa-1,3,5(10)-triene; Wolff et al. (1989), 24,25-dinorlupa-1,3,5(10),20(29)-tetraene; Simoneit et al. (2003)), tri- and tetra-aromatic pentacyclic terpenoids with oleanane and ursane structures (tetramethyloctahydronicenes, trimethyltetrahydronicenes; Laflamme and Hites (1979); Wakeham et al. (1980); Haberer et al. (2006)). The main compounds in most samples are 24,25-dinorursa-1,3,5(10),12-tetraene and 24,25-dinorlupa-1,3,5(10)-triene, while a few samples are dominated by trimethyltetrahydronicenes. In a similar manner to the content of saturated triterpenoids, the content of aromatic triterpenoids in the dark lignites (av. 526.8  $\mu\text{g/g}$  TOC) is extremely high (Table 4), indicating the predominance of angiosperms among the plants material in the whole peat profile. Aromatic triterpenoids are also present at considerable concentrations in the pale lignites (av. 267.7  $\mu\text{g/g}$  TOC), showing that angiosperms were always present in the peat bogs, but they were occasionally associated with varying proportions of gymnosperms. The much higher abundance of aromatized to non-aromatized angiosperm triterpenoids (Table 4) indicates intense aromatization of triterpenoids during early diagenesis. The same observation was also made in other investigations of lignites and fossils (Kalkreuth et al., 1998; Nakamura et al., 2010; Životić et al., 2014; Mitrović et al., 2016). According to the studies of Kalkreuth et al. (1998) and Nakamura et al. (2010), aliphatic angiosperm-derived triterpenoids are more easily altered to aromatic derivatives than gymnosperm-derived diterpenoids, resulting in the selective loss of analogous aliphatic compounds. Additionally, Mitrović et al. (2016) reported that pronounced aromatization of triterpenoids is consistent with intense microbial activity during peatification.

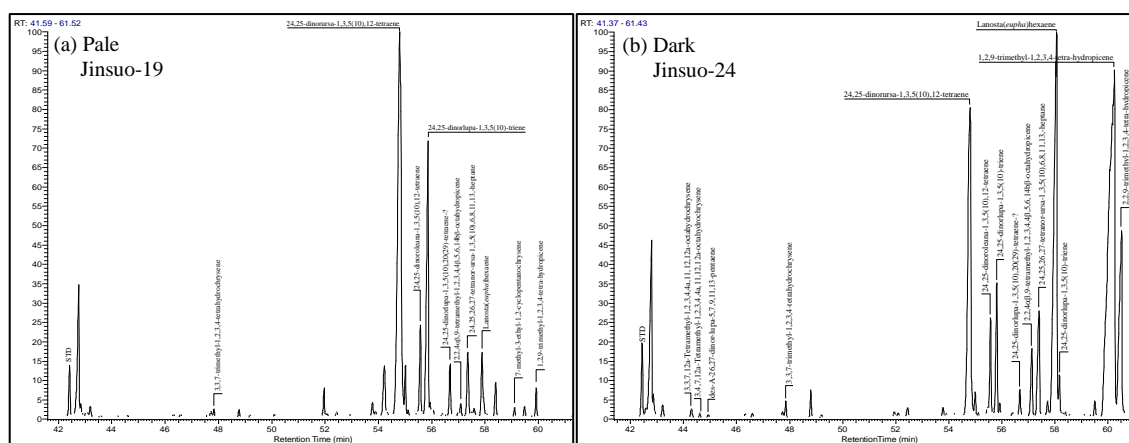


**Figure 2-5 Gas chromatograms (total ion current) of the aromatic hydrocarbon fractions of: (a) sample Jinsuo-19 (pale lignite), and (b) Jinsuo-24 (dark lignite). Std. = Standard (1,1'-binaphthyl)**

One of the most abundant compounds in the aromatic hydrocarbon fractions, particularly in some dark lignite samples, is a compound which has previously been tentatively identified as lanosta(*eupha*)hexaene (Hazai et al., 1986; Jacob et al., 2007). Although it was not detected in all samples, the average concentration of this compound is 142.7  $\mu\text{g/g}$  TOC in the dark lignites, and higher than 300  $\mu\text{g/g}$  TOC in samples JS-6, JS-22 and JS-39. The lanosta(*eupha*)hexaene compound has been proposed to be a ring A, B diaromatic derivative of lanostane-, euphane-, or tirucallane-type compounds (Jacob et al., 2007), but more research is necessary to clarify the exact structure and the biological origin of this compound.

### 2.5.5.3 Hopanoids

Hopanoids are important constituents of the non-aromatic cyclic triterpenoids, and are abundant in both pale (Fig. 5c) and dark lignite samples (Fig. 5d). The hopanoid patterns of all pale and dark samples are uniform and characterized by the occurrence of  $17\alpha(\text{H}),21\beta(\text{H})$ ,  $17\beta(\text{H}),21\alpha(\text{H})$ , and  $17\beta(\text{H}),21\beta(\text{H})$  compounds with 27–31 carbon atoms, with the exception of  $\text{C}_{28}$  homologues (Fig. 5c, d). The most abundant hopanoid in the saturated hydrocarbon fraction of almost all the studied samples is  $\text{C}_{31}$   $17\alpha(\text{H}),21\beta(\text{H})$ -homohopane(22R), whereas the  $\text{C}_{30}$  hop-17(21)-ene dominates the hopane distribution in a few samples. Usually, the total content of all hopanoids is higher in the pale lignite samples (av. 771.2  $\mu\text{g/g}$  TOC, Table 5) than in the dark lignite samples (av. 446.0  $\mu\text{g/g}$  TOC, Table 5).

**Table 2-5 Hopanoids ( $\mu\text{g/g}$  TOC) concentrations of lignite samples from Jinsuo opencast mine**

Sample No.	Lithotypes	17 $\alpha$ -Trisnorhopane	Hop-17(21)-ene	17 $\beta$ , 21 $\beta$ -Norhopane	17 $\alpha$ ,21 $\beta$ -Homohopane(2R)	17 $\beta$ ,21 $\beta$ -Homohopane(2R)	$\Sigma$ Hopanoids
		$\mu\text{g/g}$ TOC					
JS-39	dark	3.6	34.8	7.6	46.7	3.7	99.1
JS-38	dark	2.6	77.7	2.0	257.8	11.3	355.0
JS-37	pale	33.4	49.3	35.6	309.0	22.6	457.1
JS-36	dark	4.2	31.6	7.1	190.6	9.9	244.8
JS-35	pale	27.4	46.4	46.7	254.3	24.0	402.7
JS-34	dark	2.0	72.6	2.7	318.8	15.5	413.4
JS-33	pale	32.9	62.1	20.9	219.3	18.3	358.0
JS-32	dark	6.1	58.6	11.6	430.4	24.3	533.3
JS-31	pale	42.9	76.6	53.9	558.6	32.5	771.2
JS-30	dark	1.4	49.2	3.0	63.7	2.2	120.3
JS-29	pale	15.1	35.1	21.7	281.4	14.7	368.4
JS-28	dark	1.9	38.6	3.4	136.0	6.1	186.4
JS-27	pale	36.1	49.6	45.3	434.3	26.8	595.3
JS-26	dark	1.8	87.7	9.3	488.9	20.1	609.2
JS-25	pale	61.5	41.9	61.0	345.4	29.9	543.2
JS-24	dark	26.8	124.9	37.4	378.0	38.9	608.1
JS-23	pale	59.3	116.6	86.2	585.7	32.7	886.2
JS-22	dark	3.6	32.7	5.2	19.9	1.2	62.9
JS-21	pale	55.5	83.3	117.6	403.9	37.7	703.2
JS-20	dark	3.0	48.3	4.1	178.7	6.1	240.7
JS-19	pale	8.4	54.9	7.5	260.1	8.8	341.1
JS-18	dark	3.0	43.9	5.1	76.5	2.0	131.2
JS-17	pale	8.1	69.2	8.2	315.9	8.0	411.2
JS-16	dark	55.9	318.4	62.1	1117.7	55.2	1621.6
JS-14	dark	31.9	292.2	52.2	1149.4	43.7	1571.5
JS-13	pale	40.9	148.6	78.8	1477.4	80.3	1832.3
JS-12	dark	11.5	194.4	21.0	688.7	64.0	981.6
JS-11	pale	51.9	166.6	67.8	1186.9	53.3	1532.4
JS-10	dark	15.7	100.8	17.6	507.7	23.1	666.3
JS-9	pale	48.4	233.2	64.8	1183.3	70.4	1607.6
JS-7	pale	33.6	137.8	29.9	546.5	26.1	777.5
JS-6	dark	N.D <sup>a</sup>	103.8	N.D	15.7	1.2	122.6
JS-5	pale	41.2	161.8	20.7	730.5	21.1	994.1
JS-4	dark	2.5	196.2	3.7	82.8	4.0	289.3
JS-3	fusin	9.7	65.6	4.7	88.8	4.7	178.5
JS-2	pale	42.8	108.4	39.0	311.4	18.1	528.4
JS-1	floor	7.3	171.3	0.0	392.1	10.5	588.6
average of pale		37.6	96.6	47.4	553.2	30.9	771.2
average of dark		7.4	97.1	11.6	311.5	17.1	446.0

<sup>a</sup> N.D. = Not detected.

The hopanes are represented by very high amounts of 17 $\alpha$ (H),21 $\beta$ (H)-homohopane, with lower contents of 17 $\beta$ (H),21 $\beta$ (H)-homohopane (Table 5) occurring as 22R epimers. The prominence of 17 $\alpha$ (H),21 $\beta$ (H)-homohopane(22R) is a common feature of many other low-rank coals (Burhan et al., 2002; Stefanova et al., 2005; Vu et al., 2009; Mitrović et al., 2016), and is also found in the pale and dark layers in the Lower Rhine Basin (Hagemann and Hollerbach, 1980). Several possible sources of 17 $\alpha$ (H),21 $\beta$ (H)-homohopane(22R) have been proposed (Van Dorsselaer et al., 1975; Killops et al., 1998; Thiel et al., 2003). According to Van Dorsselaer et al. (1975), the formation of 17 $\alpha$ ,21 $\beta$ -homohopane (22R) in low-rank coals implies complex reactions in acidic environments under oxic conditions in the mire. This compound has been suggested to originate from decarboxylation of 31,32- bishomohopanoic acid in soils and peats (Killops et al., 1998). Thiel et al. (2003) has established the presence of homohopanoic acids with a “geological”  $\alpha\beta$  configuration in living microbial mats from the Black Sea, and thus the direct bacterial input to the organic matter should also be taken into consideration. The average content of 17 $\alpha$ (H),21 $\beta$ (H)-homohopane(22R) in the pale lignites (553.2  $\mu\text{g/g}$  TOC, Table 5) is much higher than in the dark lignites (311.5  $\mu\text{g/g}$  TOC, Table 5). This suggests that peatification of pale lignites took place under more oxic environmental conditions than dark lignites (Životić et al., 2014), and that both layers may have been influenced by bacterial activity.

The contents of hopanes in sediments are considered to reflect the level of degradation of organic matter by aerobic bacteria (Peters et al., 2005; Singh et al., 2017a), whereas anaerobic bacteria are considered as the precursor of hop-17(21)-ene (Wolff et al., 1992). Hop-17(21)-ene is found in significant amounts in both the pale and dark lignites, with only a small difference in average contents between the two lignite types (96.6  $\mu\text{g/g}$  TOC in the pale lignites and 97.1  $\mu\text{g/g}$  TOC in the dark lignites). High levels of hop-17(21)-ene were also found in the lignites from the Kostolac basin, Serbia (Životić et al., 2014). Its biological precursor has not been clarified so far, although the compound is present in many immature sediments, often together with its homologues. Bottari et al. (1972), Wakeham et al. (1980) and Volkman et al. (1986) argued that hop-17(21)-ene in sediments is introduced by bacteria, or, in some cases, by ferns and mosses, whereas Brassell et al. (1980) suggested a diagenetic origin through the transformation of hop-22(29)-ene. Sabel et al. (2005) studied the extracts of Eocene oil shale from Eckfeld Maar in Germany and considered diplopterol to be the most probable source of hop-17(21)-ene, whereas Bechtel et al. (2005) suggested that hop-17(21)-ene may reflect microbial activity under reducing conditions, based on the positive relationship between the concentration of hop-17(21)-ene and the ground water index. Wolff et al. (1992) suggested that hop-17(21)-ene is related to the activity of iron-reducing bacteria. Iron reduction is generally active in deeper sections of sedimentary environments (Lovley and Phillips, 1986; Thamdrup, 2000; Lipson et al., 2010). Although both pale and dark

lignites have considerable concentration of hop-17(21)-ene, the origin might be different depending on the depositional environment. The hop-17(21)-ene in the dark lignites could be more related to microbial activity under reducing conditions since the dark lignites were deposited under wet conditions with less oxidation during peat accumulation, whereas hop-17(21)-ene in pale lignites probably might have multiple origins.

## 2.6 Origin of pale and dark lignites in the Jinsuo opencast mine

Coal petrology and organic geochemical methods were used to study the pale and dark lignites of the Jinsuo opencast mine. The results show that the origin of the pale and dark lignites differs significantly in terms of the vegetation source material, the paleoenvironmental conditions of deposition, and the degree of decomposition of the organic matter during early diagenesis.

For the pale lignites, the low content of huminite (dominated by detrohuminite) along with the higher content of inertinite, indicates that they might have been deposited in the mire under relatively dry conditions associated with intense weathering. This is confirmed by field observations of abundant internal fusain layers preferentially occurring in the pale lignites, which indicates the temporal occurrence of former wildfires. The low content of huminite may result from the high abundance of herbaceous vegetation, which is more susceptible to degradation than woody vegetation (Singh et al., 2017b). The aerobic bacteria in the relatively dry bogs will also increase the decomposition of plant materials. The TPI-GI diagram (Fig. 4a) shows low GI and TPI values in the pale lignite samples, suggesting either the predominance of herbaceous plants, or intensive destruction of woody tissues as a result of advanced humification and bacterial activity (Gürdal and Bozcu, 2011; Oikonomopoulos et al., 2015). The high content of amorphous mineral-groundmass (bituminite) might also result from strong humification/degradation during the accumulation of pale lignite in peat bogs.

The very low abundance of the C<sub>23</sub> and C<sub>25</sub> alkanes in all of the analyzed lignites indicates that the pale lignites in the Jinsuo Basin could not originate from *Sphagnum* since these alkanes have previously been considered to be indicative for the occurrence of *Sphagnum* in peat mires (Ficken et al., 2000; Nott et al., 2000; Nichols et al., 2006, 2010; Bush and McInerney, 2013). However, higher concentrations of *n*-C<sub>25</sub> or *n*-C<sub>31</sub> alkane have been found in *Sphagnum* species from drier habitats (Bingham et al., 2010). Therefore, minor contributions of *Sphagnum* (from drier habitats) to precursor organic matter cannot be fully excluded in case of the pale lignite samples according to their relatively high abundance of *n*-C<sub>31</sub> and the presence of *n*-C<sub>25</sub>. The dominance of angiosperm plant materials in the pale lignites is confirmed by the relatively high content of triterpenoids in the aromatic hydrocarbon fraction (Table 4). However, the considerable concentrations of diterpenoids in the saturated hydrocarbon fractions of the

pale lignites (e.g. 4 $\beta$ (H)-19-norisopimarane, 18-norpimarane, and 18-norabietane) (Table 4) shows that gymnosperm (e.g. conifer) trees also made crucial contributions to the plant community, thus leading to the formation of the pale layers. The explanation for the formation of pale lignites in the Jinsuo opencast mine is generally consistent with the dry-light model proposed for the formation of the light lithotypes from the Gippsland Basin, Australia, and from the Lower Rhine Basin, Germany; in both cases the pale lignites were deposited under drier and more aerobic conditions compared with the dark lignites (Hagemann and Wolf, 1987; Holdgate et al., 2016; Korasidis et al., 2017).

With respect to vegetation changes, our results are not in agreement with results obtained from the Gippsland Basin in Australia where the darker lithotypes were characterized by gymnosperm paleoflora, while the lighter lithotypes were characterized by angiosperm paleoflora (Holdgate et al., 2016; Korasidis et al., 2016). One possibility for explaining this discrepancy is the different composition of the gymnosperms in the present study and in the Gippsland Basin. Based on palynological data, the gymnosperms in the Oligo-Miocene lignites of the Gippsland Basin were identified as being composed of *Dacrycarpus* and *Dacrydium* belonging to the family of Podocarpaceae (Korasidis et al., 2016). The palynological data were supported by previous biomarker data, which revealed the presence of 16 $\alpha$  (H)-phyllocladane and *ent*-16 $\alpha$  (H)-kaurane as the only diterpenoids (well-known tetracyclic diterpanes from extant and fossil Podocarpaceae) in the Miocene Yallourn coal from the Gippsland Basin, Australia (Noble et al., 1985). In the Tertiary, Podocarpaceae were part of the Antarctic flora and preferred the moist climate of Gondwana (Singh, 2006). However, in the late Pliocene in Yunnan Province, the gymnosperms were preferentially contributed by *Pinus* and *Tsuga* belonging to the family of Pinaceae (Xu et al., 2004; Kou et al., 2006). Diterpenoids with abietane, pimarane, and isopimarane skeletons were previously identified as the dominating diterpenoids in extant and fossil Pinaceae (Otto et al., 2007). Therefore, the identification of the related nor-diterpenoids, generated by demethylation from the parent compounds abietane, pimarane, and isopimarane during early diagenesis, supports the palynological results (Xu et al., 2004; Kou et al., 2006). This indicates the predominance of Pinaceae contributing occasionally as gymnosperm material to the generally angiosperm-dominated paleoflora in the studied basin. The different vegetation composition of the gymnosperms in the Pliocene in Yunnan Province and in the Oligo-Miocene Gippsland Basin can, thus, explain the differences described above and makes it reasonable to assume that gymnosperms contribute to the pale lignites from the Jinsuo Basin, while in the Gippsland basin the gymnosperms contribute more to the dark lignites. Flora changes in the Lower Rhine Basin in Germany are associated with changes in facies type during the deposition of lignites, and seven facies types were distinguished in the Lower Rhine Basin and Lausitz lignite mining area (Schneider, 1992, 1995; Naeth et al., 2004). These facies are the *Alnus-Liquidambar-alluvial forest-facies* (F-facies), *Conifer-forest-facies* (K-facies), *Angiosperm-forest-facies* (A-facies), *Glumifloren-facies* (G-Facies), *Pinus-*

Myricaceen-Palm Tree-facies (P-facies), Marcoduria-facies (M-facies), and bright layer-facies (HB-facies). The F-, A-, and G-facies were dominated by angiosperms while the K-, P-, and M-facies were dominated by gymnosperms. The origin of the HB-facies, with its high content of fusinite and liptinite, was explained by diminished bacterial activity in an acidic and oligotrophic environment, and did not appear to be represented within the paleobotanical data (Schneider, 1995; Naeth et al., 2004). However, there is no obvious correlation between the change of color and plant communities, and it is difficult to match the angiosperm- and gymnosperm-influenced pale layers in the Jinsuo Basin with the described facies types described from the Lower Rhine Basin according to the suggested vegetation. Previous organic geochemical results obtained from lignites from the Lower Rhine Basin show that both Pinus-related diterpenoids (norabietane, norpimarane, and norisopimarane with 19 carbon atoms) and triterpenoids (ursene and oleanene-types) are present in both the pale and dark layers (Hagemann and Hollerbach, 1980). However, in the study of Hagemann and Hollerbach (1980), no quantitative data were provided and it was not possible to identify in which facies type either diterpenoids or triterpenoids were enriched.

In addition, Korasidis et al. (2017) interpreted the thin light and pale layers on top of the dark to pale cycles in the Gippsland Basin, Australia, as residual layers of concentrated, oxidant-resistant, peat-forming elements that resulted from intense weathering and aerobic degradation of the peats. The weathering events were explained by a small fall in sea level, or a change to cooler and drier climates (Mackay et al., 1985; Anderson and Mackay, 1990; Holdgate et al., 2014). In the case of the Jinsuo Basin, some characteristics, such as thin thickness (<25cm) of pale layers, high concentration of extractable matter and liptinite (sporinite), poor preservation of plant fragments, are similar to the characteristics described in thin pale layers from the Gippsland Basin, reflecting intense oxidation and weathering in pale lignites. The results of our study confirm the high abundance of 17 $\alpha$ ,21 $\beta$ -homohopane(22R) in pale layers of the Jinsuo Basin, described previously by Qi et al. (1994). The high levels of this compound are consistent with the presence of oxic conditions, which are suitable for the growing of aerobic bacteria and fungal activities that would accelerate the weathering and decomposition of plant materials at a higher degree in the peat.

The petrographic and organic features of dark lignites in the Jinsuo Basin are very different from the pale lignites. The high concentration of huminite (telohuminite) and gelinite, along with the low concentrations of inertinite and liptinite, indicate a low-energy and more humid environment during peat accumulation. This is further supported by the warm and moist paleoclimate of the Neogene in Yunnan Province (Xu et al., 2008; Xie et al., 2012; Xing et al., 2012; Su et al., 2013). The TPI-GI and VI-GWI diagrams (Fig. 4) show that the dark lignites were deposited in a wet swamp forest with high tree density in an ombrotrophic to mesotrophic bog. The very low abundance of diterpenoids in both saturated and aromatic hydrocarbon fractions, as well as the extremely high



concentrations of triterpenoids in aromatic hydrocarbon fractions, suggests that the angiosperm plant community were dominant in the peat bog, resulting in the dark lignites. This is further supported by the low C/N values in the angiosperm-dominated dark lignites (Table 3) because recent gymnosperm trees have higher C/N values than angiosperm trees (Cernusak et al., 2008). This is largely consistent with the angiosperm-dominated, medium-dark lithotypes from the Gippsland Basin, Australia, but is different from the dark lithotypes that were characterized by abundant gymnosperm plants (Podocarps) in the layer (Korasidis et al., 2016; Korasidis et al., 2017). The observed color change from dark to pale lithotypes in the Jinsuo Basin is largely caused by environmental changes, evolving from an anaerobic to a more aerobic setting, and is in accord with results obtained from the Gippsland Basin, Australia (Korasidis et al., 2016; Korasidis et al., 2017) and the Lower Rhine Basin, Germany (Hagemann and Wolf, 1987). The gymnosperm plants (*Pinus* and *Tsuga*) in the pale lignites also partly contribute to the color change.

## 2.7 Conclusions

The coal petrology data show that the pale lignites from the Jinsuo Basin in Yunnan Province, southwestern China, are dominated by macerals of the liptinite group, followed by macerals of the huminite and then inertinite groups, while in the dark lignites the huminite group represents the most abundant macerals when compared with liptinite and inertinite. The predominance of bituminite (mineral-bituminous groundmass) in liptinite in the pale lignites is the reason for the high amount of EOM. Maceral parameters in the pale lignites are characterized by low TPI, VI, and GI values, and macroscopically visible fusain layers. These characteristics suggest that, compared with the dark lignites, the preservation of organic matter in the pale lignites (deposited under relatively dry and aerobic conditions with intensive weathering) was poor. In contrast, the high abundance of huminite and the strong gelification, along with the high TPI, VI, and GI values in the dark lignites indicate that the dark lignites in the Jinsuo Basin were deposited under wet and humid climate with less oxic conditions during peat accumulation.

With respect to the organic geochemical data, plant communities changed during the formation of the pale and dark lignites in the Jinsuo Basin. The low contents of *n*-C<sub>23</sub> and *n*-C<sub>25</sub> in both pale and dark lignites suggest that both kinds of layers do not originate from *Sphagnum*, which was proposed to be the main source material for the pale layers by Lu and Zhang (1986, 1989). In addition, the high concentration of triterpenoids in the dark lignites implies that angiosperms were the main component of the plant community in the basin during the formation of dark lignites. This is not consistent with the results from Qi et al. (1994) that indicated that gymnosperms were the only source materials for both the pale and dark layers in the peat. However, the higher content of diterpenoids and the

higher average ratio of Di-/(Di- + Tri-terpenoids) for the pale lignites compared with the dark lignites are indicative of the crucial contribution by gymnosperms to the plant community during peat accumulation, and the formation of pale lignites. The high abundance of hopanoids, and in particular of  $17\alpha,21\beta$ -homohopane (22R), in the pale lignites indicates intensive aerobic bacterial activity during or after the deposition.

Compared with the pale and dark layers from the Miocene Lower Rhine Basin in Germany and the Oligocene-Miocene Gippsland Basin in Australia, several similar trends were found in the Pliocene lignites from the Jinsuo Basin, Yunnan Province. In all three basins, the pale layers are generally characterized by higher proportions of liptinite macerals and stronger gelification in the dark layers than in the pale layers. The depositional model of lignites from the Jinsuo Basin is generally consistent with the dry-light model proposed by Holdgate et al. (2014, 2016) for the pale and dark layers from the Lower Rhine Basin in Germany and the Gippsland Basin in Australia. However, the plant community in the formation of the pale and dark lignites in the Jinsuo Basin is different from that of the other two basins. In the Jinsuo Basin, the source materials of pale lignites are mixed with both gymnosperm and angiosperm plants, while the dark lignites mostly originate from angiosperm plants. In the Gippsland Basin, gymnosperms are more abundant in the dark layers than in the pale layers.

## **Chapter 3 Stable isotopic and elemental characteristics of pale and dark layers in Pliocene Jinsuo lignite deposit basin in Yunnan Province, southwestern China**

### **3.1 Abstract**

The carbon and nitrogen stable isotopic compositions and elemental characteristics of Pliocene pale and dark lignites in the Jinsuo Basin, Yunnan Province, southwestern China, were investigated in this chapter. These data were used to develop paleoenvironmental models and to discuss possible geological driving forces for the formation of pale and dark layers.

The  $\delta^{13}\text{C}$  values of fossil wood (av.  $-24.79\text{‰}$ ) and fusain samples (av.  $-24.19\text{‰}$ ) are generally higher than the values obtained from bulk pale (av.  $-27.01\text{‰}$ ) and dark (av.  $-26.38\text{‰}$ ) lignite samples. In contrast, the  $\delta^{15}\text{N}$  values of fossil wood (av.  $-0.63\text{‰}$ ) and fusain samples (av.  $1.29\text{‰}$ ) are lower than the average values of bulk pale lignites (av.  $2.17\text{‰}$ ) and dark lignites (av.  $1.79\text{‰}$ ). The difference in the carbon isotopic values between pale and dark lignites can be explained by the very high amount of liptinite and strong degradation of woody material by bacterial activity in pale lignites, which resulted in depletion of  $^{13}\text{C}$  in pale lignites relative to dark lignites. The higher  $\delta^{13}\text{C}$  values in the fossil wood and fusain samples can be explained by the general enrichment of  $^{13}\text{C}$  in woody material compared to leaves. The weakly negative correlation between the  $\delta^{15}\text{N}$  and  $\delta^{13}\text{C}$  values indicates that, besides bacterial degradation, the liptinite content could also influence the carbon and nitrogen compositions of lignites. The influence of the original plant community (gymnosperms/angiosperms) on the carbon and nitrogen isotopic compositions of bulk lignites is insignificant in the Jinsuo Basin.

The paleoenvironmental model suggests deposition of the pale layers under relatively dry, cold conditions supporting the expansion of gymnosperms such as *Pinus yunnanensis*. The slight stepwise uplift of the Tibetan Plateau and the approximate co-occurrence of the more intense Asian monsoon might have supported short periods of a locally dry, cold climate that was favorable for the formation of pale layers. The relatively high  $\text{SiO}_2/\text{Al}_2\text{O}_3$  ratios, higher values of the average detrital/authigenic index, and high levels of  $\text{TiO}_2$  and Zr in pale layers further support this interpretation. The dark layers, however, formed in a tropical/subtropical warm, humid climate that favored angiosperm dominance of the vegetation. The long-term geologically stable conditions together with the regionally warm, humid climate were conducive to the formation of dark layers until the subsequent uplift of the Tibetan Plateau. This conclusion is also supported by the thickness differences between the pale (thin) and dark (thick) layers and the changes in major elements and minerals changes between the two types of layer. The orbital

periodicities and the development of Northern Hemisphere glaciation that resulted in the climate changes during the Pliocene could have been additional driving forces for the cyclic formation of pale and dark layers in the Jinsuo Basin.

*Keywords: Carbon isotopes; Nitrogen isotopes; Pale and dark layers; Paleoenvironment*

## 3.2 Introduction

The studies of stable carbon isotope on organic matter from lignites, in recent years, have been more and more used to improve reconstructions of floral assemblages in paleomires and paleoenvironmental changes during deposition of lignites all over the world (Bechtel et al., 2003, 2004, 2008; Harrington et al., 2005; Holdgate et al., 2009; Kanduč et al., 2012; Korasidis et al., 2016; Stock et al., 2016; Erdenetsogt et al., 2017; Radhwani et al., 2018). The  $\delta^{13}\text{C}$  variations of lignites are affected by several factors, such as the degree of degradation of plant tissues, differing lipids content in extractable organic matter, changes of vegetation in the peat, differences in the processes of carbon cycling and differences in the stable carbon isotopic value of atmospheric  $\text{CO}_2$  (Bechtel et al., 2007a, 2008; Diefendorf et al., 2015; Nordt et al., 2016; Radhwani et al., 2018). The stable carbon isotopic compositions of cellulose/fossil wood in lignites have been further linked to climatic changes (e.g. temperature and humidity) because the efficiency of water use by land plants is different (Lipp et al., 1991; Schleser et al., 1999; van Bergen and Poole, 2002; Bechtel et al., 2008; Jahren and Sternberg, 2008). Variations of the stable carbon isotope value of organic matter are, in addition, dependent on the abundance of decay-resistant macromolecules (Benner et al., 1987). The  $^{13}\text{C}$  depletion in lignites preferentially resulted from the progressive decay of cellulose by bacterial activity (Bechtel et al., 2008). Negative relationships between the  $\delta^{13}\text{C}$  values and liptinite contents of lignites (Bechtel et al., 2002, 2005, 2007a) indicate that the composition of carbon isotope in lignite is influenced by the content of lipids in organic matter. The influence of plant community changes (gymnosperms versus angiosperms) on  $\delta^{13}\text{C}$  is caused by the approximately 2.5‰ on average higher  $\delta^{13}\text{C}$  values of gymnosperms relative to angiosperms (Bechtel et al., 2008; Widodo et al., 2009; Chi et al., 2013) resulting from different leaf morphology as well as carbon assimilation efficiency of different plants (Murray et al., 1998).

In contrast to the large number of studies of the carbon isotopic composition of lignites, lignite nitrogen isotopic compositions have rarely been investigated. A previous study of Pliocene lignites from the Velenje Basin, Slovenia, demonstrated that the  $\delta^{15}\text{N}$  values of different lithotypes were influenced by a combination of compositional changes in the parent plant materials and biogeochemical processes during early diagenesis (Kanduč et al., 2005). In contrast, the nitrogen isotopic compositions of organic matter in mature sediments and coals have been studied in more detail. Variations of the nitrogen isotopic signatures have been explained by variations of several parameters, such as climate, source of organic materials, depositional environment, maturity, and degree of decomposition of organic matter (Rigby and Batts, 1986; Quan et al., 2008; Morford et al., 2011). Previous studies suggested that  $\delta^{15}\text{N}$  values do not change systematically with increasing maturity of coals/oil shales (Rigby and Batts, 1986; Whiticar, 1996; Ader et al., 1998). Ader et al. (1998) found a slight different  $\delta^{15}\text{N}$  values in anthracites from the

Pennsylvanian (U.S.A.) and the Bramsche Massif (Germany) and were interpreted to result from changes in the degree of decomposition of the organic matters, plant community, and paleoclimate. The nitrogen content of bedrock sediments and its weathering might also cause alterations in the nitrogen isotopic values in terrestrial ecosystems such as plants and soils (Morford et al., 2011). Furthermore, bacterial alteration of organic matter in woody tissues during early diagenesis and the peat-forming stage could also lead to preferential loss of  $^{14}\text{N}$  (Kanduč et al., 2005; Rimmer et al., 2006). Results from simulated experiments results suggested that the  $\delta^{15}\text{N}$  values of organic matter, which decayed under anoxic conditions, decrease to about 3‰ lower than the original value, but the  $\delta^{15}\text{N}$  values are increase first, and then decrease during the organic matter go through oxic decay (Lehmann et al., 2002). Residual organic matter in alkaline or aerobic environments yields heavier nitrogen isotope than their parent plants (Diessel, 1992; Taylor et al., 1998; Zhu et al., 2000). Moreover, less degradable stem xylem has higher  $\delta^{15}\text{N}$  values than the values obtained from the degradable leaves (Handley and Raven, 1992).

The Pliocene lignites of the Jinsuo Basin, Yunnan Province, have previously been studied to evaluate the origin of the pale and dark layers in these lignites (Ming et al., 1994; Wang et al., 1997; Yu et al., 1997; Liu et al., 2018). The most recent study suggested that the pale layers in the lignites are partly composed of gymnosperms and were deposited under dry/aerobic conditions; on the contrary, the dark lignites are dominated by organic matter from angiosperms and were deposited under prevailing wet/anaerobic conditions (Liu et al., 2018). In this paper, new data on stable carbon and nitrogen isotopes determined from the pale and dark lignites and fossil wood samples from the Jinsuo Basin are presented and potential reasons for the observed variations in the carbon and nitrogen isotope compositions are discussed. In addition, the major elements and trace elements in the lignites were measured, to identify the sedimentary sources of the two kinds of lignite. The combined application of stable isotopic and geochemical methods is expected to further improve understanding of the formation of pale and dark lignite layers in the Jinsuo Basin, Yunnan Province, southwestern China.

### **3.3 Geological setting**

Yunnan Province is geologically located at the junction of the East Asian Monsoon Zone, the Southern Asia–Qinghai/Tibet Plateau Zone, and the Southcentral Tropical Peninsula Monsoon geographical zone (Feng et al., 1998; Xu et al., 2004). Yunnan Province was influenced by the Himalayan movement from the late Eocene to the early Pleistocene (Yunnan BGMR, 1990). The Himalayan orogenic movement resulted in formation of a highly fragmented terrain in Yunnan Province, which was responsible for the variations in temperature and precipitation from the Neogene to the Quaternary (Xu

et al., 2004). During the Neogene, the main sedimentary facies in Yunnan Province was lacustrine and several intermountain coal-bearing basins were formed (Yunnan BGMR, 1990).

The Jinsuo Basin is located in the low hilly area of the karst plateau in eastern Yunnan. The basin is located between the East Xiaojiang Fault and the West Xiaojiang Fault (Fig. 1a), and is developed in a north–south direction with an area of about 18 km<sup>2</sup>. During the Himalayan movement, the strata in this area elevated slowly without any intense tectonic activities during the upper Pliocene (Yunnan BGMR, 1990). In Jinsuo Basin, The Ciyang Formation contains four lignite seams (Fig. 1b) and the strata underlying the Ciyang Formation consist mainly of a mixture of middle Cambrian calcareous shales of the Douposhi Formation and dolomites of the Shuanglongtan Formation, together with Lower Ordovician shales of the Tangchi Formation and sandstones of the Hongshiya Formation (Yunnan BGMR, 1990; Liu et al., 2018). The stratigraphic column of the Neogene succession in the Jinsuo Basin is shown together with the profile of the studied section in Fig. 1b. The profile of lignite seam No. 3, which was investigated in the present study, is enlarged in Fig. 1b. Further details of the lignite-bearing strata of the studied section were provided by Liu et al. (2018).

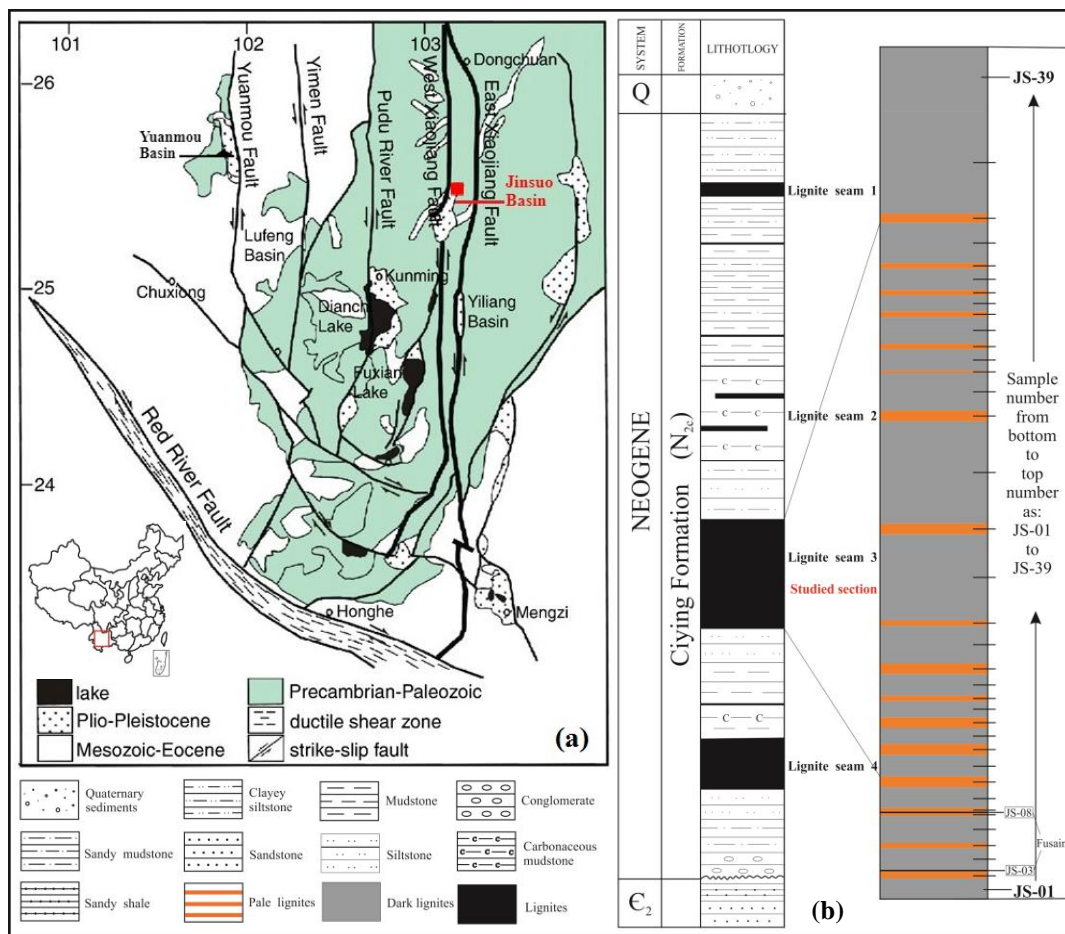


**Figure 3-1 Geological map and location of Jinsuo Basin (a), modified from Zhu et al., (2008), along with the stratigraphic column and sample profile of Jinsuo opencast lignite mine (b). Q = Pleistocene,  $\epsilon_2$  = Middle Cambrian. Sample JS-03 and JS-08 are fusain samples. Brown color: pale layers; gray color: dark layers**

### **3.4 Samples and analytical methods**

A total of 49 samples were collected from the lignite profile in the Jinsuo Basin. The lignite samples contain 18 pale lignites, 19 dark lignites, and 2 fusain samples, marked as JS-01 to JS-39 from bottom to top of the succession (Fig. 1b). A total of 10 fossil wood pieces were collected from both pale and dark layers. Each samples were wrapped in aluminum foil in the field, to minimize contamination and oxidation, and were stored in a plastic bag that were immediately sealed. Samples were crushed and ground to pass through a 200-mesh sieve for X-ray fluorescence (XRF) spectrometry, inductively coupled plasma mass spectrometry (ICP–MS), and stable isotopic composition analyses.

Ash yields of lignite samples were measured following American Society for Testing and Materials (ASTM) Standard D3174-11 (ASTM Standard D3174-11, 2011).

Proportions of major-element oxides in all lignite and fusain samples (on an ash basis; ashing at 815 °C) were analyzed by XRF spectrometry (OXAS, Version 2.2), and proportions of major-element oxides in the samples for a whole coal basis were calculated from the ash yields of each sample. The ICP–MS instrument (X series II) was operated in a pulse-counting mode to detect some interested trace elements (such as Zr) in the lignite samples. The detailed procedure and technical parameters of the XRF and ICP–MS analyses of the samples was described by Zhao et al. (2017).

The distribution characteristics of some interested minerals in lignite sample were performed on scanning electron microscope (HITACHI, SU8220) coupled with an energy-dispersive X-ray spectrometer (SEM-EDS).

The stable isotopic compositions of organic carbon ( $\delta^{13}\text{C}$ ) and nitrogen ( $\delta^{15}\text{N}$ ) in all lignite and fossil wood samples were carried out on a FlashEA™ 1112 Elemental Analyzer with a ConFlo III Interface from Thermo Fisher. The detailed procedures applied for the analyses were described previously by Liu et al. (2019).

### **3.5 Results and discussion**

#### **3.5.1 Stable isotopic composition of lignites and fossil wood**

##### **3.5.1.1 Stable carbon isotopic composition of lignite samples**

The stable carbon isotope values ( $\delta^{13}\text{C}$ ) and stable nitrogen isotope values ( $\delta^{15}\text{N}$ ) of pale and dark lignite samples and fossil wood and fusain samples from the studied profile



in the Jinsuo Basin are shown in Fig. 2 and the data are listed in Table A1. The  $\delta^{13}\text{C}$  values of all pale and dark bulk lignite samples are between  $-28.38\text{‰}$  and  $-25.36\text{‰}$ , with an average value of  $-26.69\text{‰}$  (Table A1). The two fusain samples yielded much higher values ( $-24.99\text{‰}$  for JS-03 and  $-23.38\text{‰}$  for JS-08) and were therefore excluded from the calculation of average values. Pale lignite samples have  $\delta^{13}\text{C}$  values ranging from  $-28.38\text{‰}$  to  $-25.96\text{‰}$ , average  $-27.01\text{‰}$ , and the  $\delta^{13}\text{C}$  values of dark lignite samples range from  $-27.91\text{‰}$  to  $-25.36\text{‰}$ , with an average value of  $-26.38\text{‰}$  (Table A1). On average, the  $\delta^{13}\text{C}$  values of the pale lignites are  $0.63\text{‰}$  lighter than the values obtained from the dark lignites. These  $\delta^{13}\text{C}$  values of lignites from the Jinsuo Basin exhibit a similar range of values to those of Miocene lignites from the Lower Rhine Basin ( $-24.5\text{‰}$  to  $-26.7\text{‰}$ ; Lücke et al., 1999), Pliocene lignites from the Velenje Basin ( $-25.3\text{‰}$  to  $-27.0\text{‰}$ ; Bechtel et al., 2003), and Cenozoic lignites from Central Europe ( $-27.4\text{‰}$  to  $-23.8\text{‰}$ ; Bechtel et al., 2008). Higher  $\delta^{13}\text{C}$  values (av.  $-25.25\text{‰}$ ) were reported from the laminated dark lithotypes in lignite seams in the Gippsland Basin, Australia (Holdgate et al., 2014; Korasidis et al., 2016).

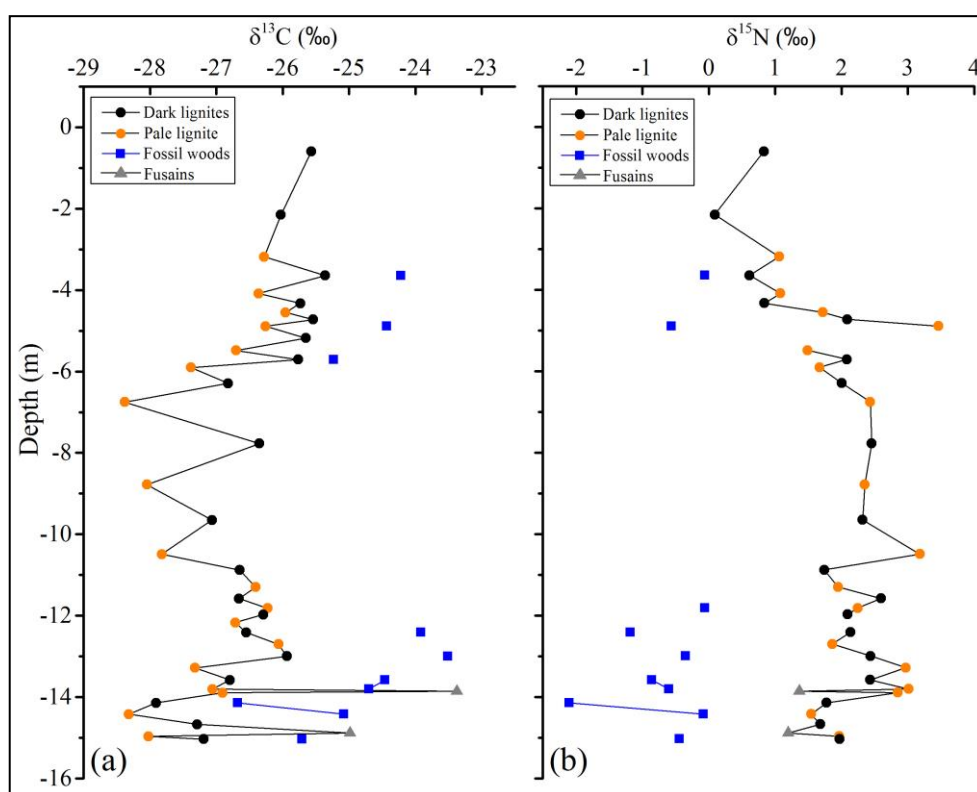


**Figure 3-2 Stable carbon (a) and nitrogen (b) isotopic composition of samples (pale, dark, fossil wood and fusain samples) collected from the Pliocene lignite profile in the Jinsuo Basin, Yunnan Province, Southwestern China**

The results are graphically presented in Fig. 2a along the investigated profile. The  $\delta^{13}\text{C}$  values of dark lignite samples are generally higher than those of adjacent pale lignite samples. Figure 2a also shows the outlying heavy  $\delta^{13}\text{C}$  values of the fusain samples

collected from the lower part of the section. From previous studies (Bechtel et al. 2008), one would expect that the increasing abundance of gymnosperms in the paleomire should result in increasing  $\delta^{13}\text{C}$  values of the resulting bulk organic matter, because gymnosperms are generally about 2.5‰ heavier than angiosperms growing in the same mire. However, in the present case of the Jinsuo lignites, the opposite trend is observed. The  $\delta^{13}\text{C}$  values of the dark lignites, which are dominated by angiosperms, are on average 0.63‰ heavier than those of the pale lignites, which are related to varying extents in being composed of additional gymnosperms, on the basis of the abundance of diterpenoids (Liu et al. 2018). However, no obvious correlation were found between the  $\delta^{13}\text{C}$  values and di-/(di- + triterpenoids) values (the concentration ratios of diterpenoids versus the sum of di- plus angiosperm-derived tri- terpenoid hydrocarbons) of lignites from the Jinsuo Basin (Liu et al., 2018). This is consistent with data from a previous study on the lower Miocene Oberdorf lignite seam of Austria, which also exhibited a lack of correlation between the two parameters (Bechtel et al., 2002). According to those authors, the influence of vegetation changes on the carbon isotopic composition of the lignites could be negligible when the variations of the peat-forming vegetation (gymnosperms vs. angiosperms) are not significant. In the case of the Jinsuo Basin, the strong bacterial degradation of organic matter in the pale layers might have influenced the  $\delta^{13}\text{C}$  values more than the vegetation change.

In the present study, the correlation between the  $\delta^{13}\text{C}$  values and total organic carbon (data from Liu et al. (2018)) is not obvious (Fig. 3a) for all lignite samples (excluding fossil wood and fusain) from the Jinsuo Basin. However, the correlation between the  $\delta^{13}\text{C}$  values and TOC in dark lignites ( $R^2 = 0.38$ ) is higher than that in pale lignites ( $R^2 = 0.11$ ). This finding can be explained by the better preservation of organic matter in the dark lignites whereas the organic matter in pale lignites was strongly reworked by microbial activity (Liu et al., 2018), because degradation by bacteria/fungi may result in changes in the stable carbon isotope of the original plant material resulting from differences in  $\delta^{13}\text{C}$  values between easily degradable polysaccharides and decay-resistant macromolecules such as lignin (Benner et al., 1987). Bechtel et al. (2008) reported that higher ratios of gymnosperms to angiosperms in the original peat-forming vegetation resulted in a  $\delta^{13}\text{C}$  shift to heavier values in Tertiary lignites and brown coals from Central Europe. In the present case of Pliocene lignites from the Jinsuo Basin, this shift is not observed, because the positive shift of  $\delta^{13}\text{C}$  values caused by floral changes was presumably overwhelmed by the negative shift caused by increased biodegradation of easily degradable organic matter.

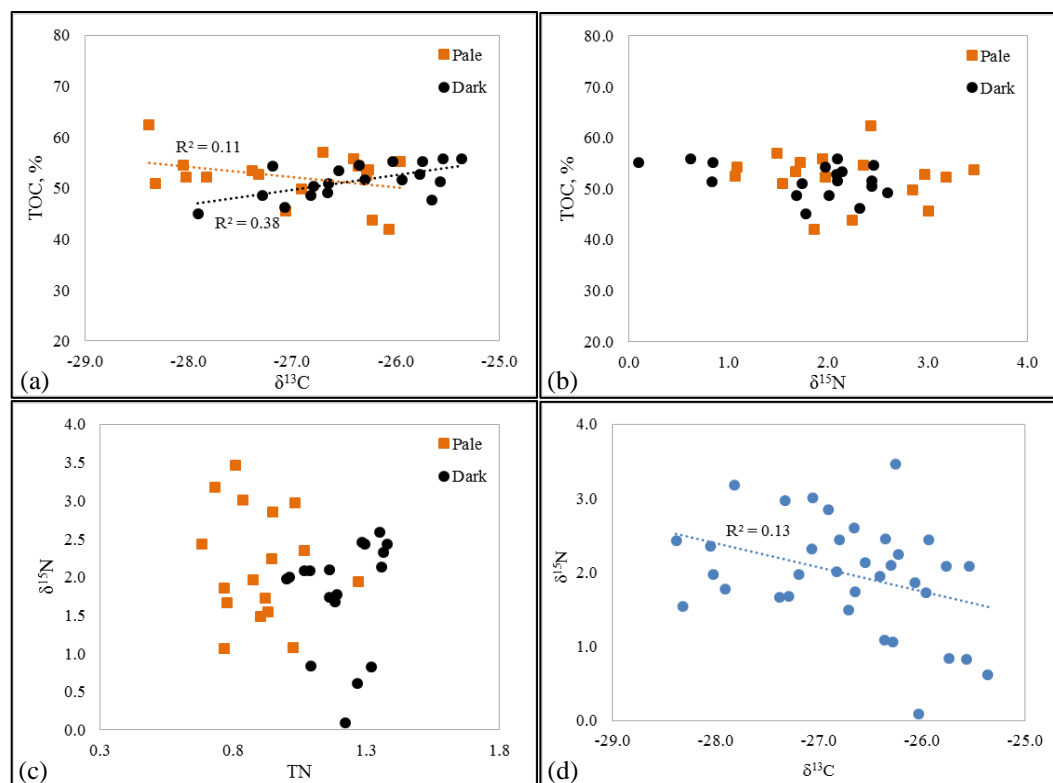


**Figure 3-3 Correlation between  $\delta^{13}\text{C}$ ,  $\delta^{15}\text{N}$  values and TOC, along with  $\delta^{15}\text{N}$  values versus TN and  $\delta^{13}\text{C}$  values of lignites from Jinsuo Basin. Data of TOC and TN are from Liu et al. (2018)**

Negative deviations of  $\delta^{13}\text{C}$  values generally occur in pale lignites (Fig. 2a). Bechtel et al. (2002) found a negative correlation between  $\delta^{13}\text{C}$  values and the contents of liptinite macerals in a lower Miocene lignite seam from the Styrian Basin, Austria, because the  $\delta^{13}\text{C}$  values of lipids from plants are 5–10 per mil depleted relative to whole plant materials/bulk organic matter (Park and Epstein, 1961; Degens, 1969). As there are very high amounts of liptinite macerals in pale lignites of the Jinsuo Basin (Liu et al., 2018), this could be one reason for the depletion in  $^{13}\text{C}$  in pale lignites relative to dark lignites. This explanation is also supported by results from previous studies of coal indicating that samples with high lipid contents (liptinites) showed the most depleted carbon isotopic values compared to macerals derived from cellulose and lignin (Rimmer et al., 2006). Furthermore, the poor preservation of fossil woody material and the low content of suberinite and textinite in pale lignites (Liu et al., 2018) might also explain the relatively lower  $\delta^{13}\text{C}$  values compared to the dark lignites, because resistant woody materials, including charcoal, are generally with higher  $^{13}\text{C}$  by 1‰–3‰ compared to the values for vulnerable leaves (Klumpp et al., 2005; Cernusak et al., 2009). This conclusion is further supported by the previously observed negative relationships between the  $\delta^{13}\text{C}$  values and the concentration of hopanes in lignites (Bechtel et al., 2005, 2007b), which has been explained by  $^{13}\text{C}$  depletion of lignites by bacterial activity caused by the progressive decay of cellulose (Bechtel et al., 2008). The higher content of hopanoids in pale lignites

compared to dark lignites indicates higher bacterial activity in the pale lignites (Liu et al., 2018). Apparently the higher bacterial activity in pale lignites lowered the  $\delta^{13}\text{C}$  values more than the contribution of gymnosperms could increase the values.

### 3.5.1.2 Stable carbon isotopic composition of fossil wood samples

The  $\delta^{13}\text{C}$  values of fossil wood pieces range from  $-26.68\text{‰}$  to  $-23.51\text{‰}$ , with a mean value of  $-24.79\text{‰}$  (Fig. 2, Table A1). Such values are consistent with previously published data for Neogene fossil wood in lignites from Central Europe (Lücke et al., 1999; Bechtel et al., 2007c, 2008) and modern plants (Smith and Epstein, 1971). The carbon isotopic composition of fossil wood remains in the Jinsuo Basin are on average higher by  $2.22\text{‰}$  compared to the corresponding bulk lignite material of pale lignites and by  $1.59\text{‰}$  compared to dark lignites (Table A1). Similar positive shifts in  $\delta^{13}\text{C}$  values between bulk material of lignites and brown coals and fossil wood collected from the same lignites have also been reported from the Miocene Lower Rhine Embayment in Germany (Lücke et al., 1999) and the Oligocene Trbovlje lignite in Slovenia (Bechtel et al., 2004). The isotopically lighter values of carbon in bulk lignites compared with values of fossil wood pieces is caused by the presence of organic matters which have light isotopic values in the coal matrix (e.g. leaves, resins and barks) (Park and Epstein, 1961) or result from higher microbial activity in the lignite matrix than in the wood fragments. The highest  $\delta^{13}\text{C}$  values in the studied section of the Jinsuo Basin were detected in the fusain samples, being  $2.83\text{‰}$  heavier than the average value for pale lignites and  $2.20\text{‰}$  heavier than the average value for dark lignites (Table A1). The average  $\delta^{13}\text{C}$  value of fusain samples is only  $0.6\text{‰}$  heavier than the value of fossil wood samples. This shift in  $\delta^{13}\text{C}$  values between fusain samples and bulk lignite samples (more than  $2\text{‰}$ ) is higher than the observed difference between fusain samples and fossil wood pieces ( $0.6\text{‰}$ ). Heavy carbon isotope compositions were also reported previously from the abundant macro- and micro-charcoal lithotypes in Cenozoic lignite seams from the Gippsland Basin, Australia (Holdgate et al., 2014; Korasidis et al., 2016) with a range of values from  $-25.50\text{‰}$  to  $-25.25\text{‰}$  (Korasidis et al., 2016). Similar relative  $\delta^{13}\text{C}$  enrichments have also been found in high-charcoal soils in Brazil (Gouveia et al., 2002; Pessenda et al., 2004), which was explained by the generally observed  $1\text{‰}$ – $3\text{‰}$  enrichment in  $^{13}\text{C}$  of woody materials, including charcoal, compared to leaves (Nordt et al., 2016, and references therein).

### 3.5.1.3 Stable nitrogen isotopic composition

The nitrogen isotope ( $\delta^{15}\text{N}$ ) values of all bulk lignite samples range from  $0.09\text{‰}$  to  $3.46\text{‰}$ , with a mean value of  $1.94\text{‰}$  (Table A1, Fig. 2b). These values are lower than the  $\delta^{15}\text{N}$  values ( $1.8\text{‰}$ – $4.6\text{‰}$ ; average  $2.99\text{‰}$ ) previously reported from Pliocene lignite lithotypes from the Velenje Basin, Slovenia (Kanduč et al., 2012). The  $\delta^{15}\text{N}$  values of pale lignites vary from  $1.06\text{‰}$  to  $3.46\text{‰}$  (av.  $2.17\text{‰}$ ) and the  $\delta^{15}\text{N}$  values of dark lignites

range from 0.09‰ to 2.59‰ (av. 1.79‰). Although the average  $\delta^{15}\text{N}$  value of pale lignites is slightly higher than the average value of dark lignite, the  $\delta^{15}\text{N}$  values in the whole profile are relatively consistent (Fig. 2b). The  $\delta^{15}\text{N}$  values of the fusain samples are slightly lower than the values obtained from the adjacent bulk material (Table A1, Fig. 2b).

In contrast to the plentiful studies of the nitrogen isotopic composition of modern materials (e.g. plants, soils, and sediments), research reports focusing on the stable nitrogen isotopes of lignites/coals and fossil woods are scarce (Rigby and Batts, 1986; Ader et al., 1998; Kanduč et al., 2005; Rimmer et al., 2006). Stiehl and Lehmann (1980) investigated 18 coal samples of different rank, ranging from brown coal to anthracite, to investigate the influence of the coalification process on  $\delta^{15}\text{N}$  values. In their study, the  $\delta^{15}\text{N}$  values ranged from 3.5‰ to 6.3‰ and no continuous trend with increasing coalification was observed. This finding is not surprising, as the coal samples originated from different basins and different geological ages. The nitrogen isotopic composition of organic matter can also be altered as a result of chemical exchange with transported nitrogen, which may tend to homogenize the isotopic composition and limit the range of organic and inorganic nitrogen isotopic composition (Schimmelmann and Lis, 2010).

Further studies of coals/anthracites confirmed that the nitrogen isotopic composition is not correlated with either the age or rank of the coal (Rigby and Batts, 1986; Whiticar, 1996; Ader et al., 1998), and the variation of  $\delta^{15}\text{N}$  values in coal could result from local variations in the  $^{15}\text{N}$  content of the nitrate ions available for the original vascular plant growth (Rigby and Batts, 1986). Moreover, studies on macerals isolated from coals showed that vitrinite (Whiticar, 1996; Rimmer et al., 2006) and liptinites (Rimmer et al., 2006) yielded higher  $\delta^{15}\text{N}$  values compared to inertinite, which may be because of the preferential loss of  $^{14}\text{N}$  of woody tissues, possibly caused by bacterial alternation during the peat formation/early diagenesis (Rimmer et al., 2006). In the present study, no significant correlations were found between  $\delta^{15}\text{N}$  values and TOC (Fig. 3b) which suggests that the nitrogen isotopic compositions of lignites from the Jinsuo Basin are not significantly related to changes in the amount of organic carbon. The correlation between  $\delta^{15}\text{N}$  values and total nitrogen (TN, data from Liu et al. (2018)) is also not significant ( $R^2 = 0.04$ ), but in the plot of  $\delta^{15}\text{N}$  values vs. TN (Fig. 3c), the relatively high  $\delta^{15}\text{N}$  values in pale lignites are associated with relatively low TN values, whereas the low  $\delta^{15}\text{N}$  values in dark lignites correspond to relatively high TN values. This observation is consistent with results from a previous study showing that a decrease in organic nitrogen during aerobic degradation of organic matter is accompanied by an increase in the  $\delta^{15}\text{N}$  values, and a decrease in the stable nitrogen isotope ratio of total nitrogen in anoxic sediments during early diagenesis (Freudenthal et al., 2001). This conclusion was further confirmed by results from petrological and organic geochemical investigations (Liu et al., 2018) indicating that pale layers were formed in a more aerobic condition while dark lignites were deposited under an anaerobic condition. Consequently, following the reasoning of

Holmes et al. (1999) and Freudenthal et al. (2001), the difference in  $\delta^{15}\text{N}$  values between pale and dark lignites could be explained by strong preferential degradation of organic matter containing amino acids as the major N-bearing component in pale lignites under oxic conditions. Amino acids, which are enriched in  $^{15}\text{N}$ , have been shown to be preferentially degraded in the water column under relatively anoxic conditions, from analysis of particles collected in sediment traps in the ocean (Nakatsuka et al., 1997). In the present study, relatively higher  $\delta^{15}\text{N}$  values correspond to relatively lower  $\delta^{13}\text{C}$  values, resulting in a weak negative correlation ( $R^2 = 0.13$ ) of the  $\delta^{15}\text{N}$  values with the  $\delta^{13}\text{C}$  values (Fig. 3d), which is different from the positive correlation ( $R^2 = 0.68$ ) of  $\delta^{15}\text{N}$  and  $\delta^{13}\text{C}$  values in lignite from the Pliocene Velenje Basin, Slovenia (Liu et al., 2019). These observations can be interpreted by a higher degree of organic-matter degradation by aerobic bacteria in the liptinite-rich pale lignites than in liptinite-poor dark lignites formed in anaerobic conditions.

The fossil wood samples have lower  $\delta^{15}\text{N}$  values of  $-2.10\text{‰}$  to  $-0.06\text{‰}$ , with a mean value of  $-0.63\text{‰}$  (Table A1, Fig. 2b) compared to bulk lignite samples (av.  $1.94\text{‰}$ ). No data on the nitrogen isotopic composition of fossil wood have previously been reported. Kanduč et al. (2005) determined the  $\delta^{15}\text{N}$  values of recent plant parts around the Velenje Basin and detected low values in the range  $-3.7\text{‰}$  to  $-2.3\text{‰}$ . These values are much lower than those determined in the bulk lignites in the basin ( $1.8\text{‰}$  to  $4.6\text{‰}$ ). The  $\delta^{15}\text{N}$  values in modern higher land plants have a broad variation with more than  $20\text{‰}$  (Peoples et al., 1991; Craine et al., 2015; Elena et al., 2016) and even in different parts, such as leaves, roots, and stems, of the same plants, the  $\delta^{15}\text{N}$  values are different (Kolb and Evans, 2002). This huge variations make it very complicated to compare the  $\delta^{15}\text{N}$  values of fossil wood pieces and lignites with of the values of modern plants. The lower  $\delta^{15}\text{N}$  values in recent plants compared with the lignites from the Velenje Basin are, to some extent, consistent with the fact that recent plants are almost always more depleted in  $^{15}\text{N}$  than the soils on which they grow (Craine et al., 2015). This is explained by the great isotopic fractionation during solubilization of N in soil and strong mycorrhizal transfer of N and fractionation from soil to plants leading to enrichment of  $^{15}\text{N}$  in soils (Craine et al., 2015).

### **3.5.2 Chemical composition of lignite samples and implications for paleoenvironment**

The levels of major-element oxides and some related parameters for lignites (on whole coal basis) in the Jinsuo Basin are given in Table A2. Some of the major-element oxides show differences in abundance between the pale and dark layers. The average percentages of  $\text{SiO}_2$  ( $7.22\%$ ) and  $\text{TiO}_2$  ( $0.42\%$ ) in the pale layers are much higher than the proportions determined for dark layers ( $2.30\%$   $\text{SiO}_2$  and  $0.14\%$   $\text{TiO}_2$ ; Table A2).  $\text{Al}_2\text{O}_3$  ( $3.31\%$ ) and  $\text{Fe}_2\text{O}_3$  ( $0.79\%$ ) on average in the pale layers are slightly higher than

the values of dark layers (2.16% for  $\text{Al}_2\text{O}_3$ , 0.59% for  $\text{Fe}_2\text{O}_3$ , Table A2). Other major element oxides show similar abundance in pale and dark layers. Furthermore, the average Zr content in pale layers (123.5 ppm) is more than 3 times higher than that in dark lignites (36.8 ppm, Table A2).

The  $\text{SiO}_2/\text{Al}_2\text{O}_3$  ratio varies in the Jinsuo lignite samples from 0.10 to 9.26 (av. 1.93). The average value is higher than the average value of Chinese coals (1.42; Dai et al., 2012), and is also much higher than the theoretical value of kaolinite (1.18). However, the ratio differs significantly between the pale and dark lignites. The average  $\text{SiO}_2/\text{Al}_2\text{O}_3$  ratio of pale lignite samples (2.98) is much higher than that of dark lignite samples (0.88). The higher  $\text{SiO}_2/\text{Al}_2\text{O}_3$  ratios in pale lignite samples result from the higher content of quartz observed under the scanning electron microscope (Fig. 4a) compared with dark lignites (Fig. 4b). Vassilev et al. (2010) suggested that high Si/Al ratios and increased ash yields of coals indicate either unstable conditions during deposition of the peat from which the coal was generated after diagenesis and/or that the coal originated from peat formed in an intermountain basin. In contrast, low Si/Al ratios and decreased ash yields generally indicate that the peat was formed in stable depositional conditions with a low degree of tectonic movement in a lowland peat-forming environment or was formed from highly weathered products (Vassilev et al., 2010). The higher  $\text{SiO}_2/\text{Al}_2\text{O}_3$  ratios and higher Zr contents, together with the high ash yield (Liu et al., 2018), in the pale lignites are in the present case most likely the result of peat accumulation in an intermountain basin associated with unstable conditions of deposition caused by the slight uplift of the Tibetan Plateau during the late Pliocene (Clark et al., 2005; Kou et al., 2006; Sun et al., 2011; Zhang et al., 2012; Su et al., 2013).

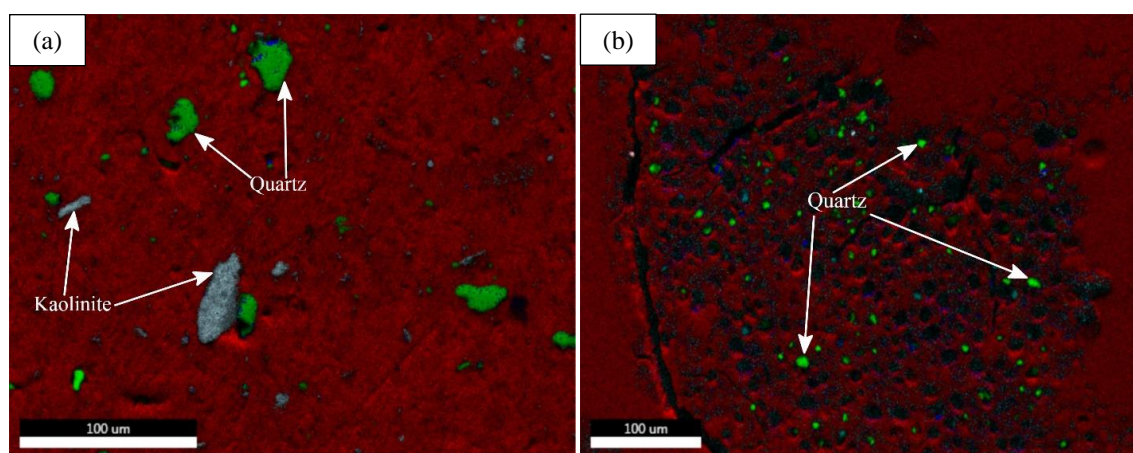


**Figure 3-4 Mineral and elemental (Si, Al and O) distribution in pale (a, sample no. JS-02) and dark lignites (b, sample no. JS-26), areal scanning by SEM-EDS**

The distribution and morphology of quartz (Fig. 4) can be attributed to different origins in pale and dark lignites. Large, angular to semi-rounded grains of quartz in pale lignites (Fig. 4a) imply an obvious detrital origin, whereas in dark lignites, small and fine quartz

particles fill the cells of organic matter (Fig. 4b). Similar quartz particles associated with organic matter have also been found previously in lignites and coals (Ruppert et al., 1991; Sykes and Lindqvist, 1993; Dai et al., 2014). According to Ward (2002, 2016), such quartz particles are clearly of authigenic origin and were incorporated into organic matter by syn-depositional or early diagenetic processes. Vassilev et al. (2010) suggested that high proportions of quartz and feldspars in coals strongly indicate a considerable influx of detrital materials. The occurrence of detrital and stable Ti-bearing accessory minerals may be used as indicators for previous geotectonic regimes in coal basins associated with washout of minerals from the source areas. The higher average detrital/authigenic index (DAI) value (3.01, Table A3) in pale lignites than in dark lignites further indicates an increased influx of detrital minerals during deposition or early diagenesis of the paleomire. The slight stepwise uplift of the Tibetan Plateau could have resulted in the high proportion of  $\text{TiO}_2$  and Zr content in pale lignites. According to Ward (2016), the origin of authigenic quartz in coal is not always clear because of the independent behavior of other minerals (e.g. clay minerals) during coal formation; similarly, Vassilev et al. (2010) proposed that quartz does not have any significant associations with other minerals in coal. Several hypotheses regarding the origin of authigenic quartz in coal have been made previously: quartz may be released from siliceous phytoliths (Andrejko et al., 1983; Wüst et al., 2008) or it may be leached from the basement rocks or be derived from volcanic ash during peat accumulation (Ward et al., 2001). Furthermore, authigenic quartz in coal seams may also precipitated from hydrothermal fluids (Dai et al., 2014). In the present study, the authigenic quartz (e.g. cell-filling) in dark lignites most likely originated from alteration of pre-existing detrital minerals in the peat mire caused by chemical weathering under wet/humid depositional conditions, or partly from silica phytoliths from peat-forming plants in the peat swamp. The different correlations of  $\text{SiO}_2$  versus  $\text{Al}_2\text{O}_3$  and  $\text{K}_2\text{O}$  (Fig. 5a and 5b) between the dark and pale lignites suggests that the silica in the two kinds of lignite had different origins. The low correlations of  $\text{SiO}_2$  versus  $\text{Al}_2\text{O}_3$  and  $\text{K}_2\text{O}$ , together with the high correlation between  $\text{Al}_2\text{O}_3$  and  $\text{K}_2\text{O}$  (Fig. 5c), indicate that the silica in the pale lignites occurs mostly as independent quartz, with small amounts in other silicates (e.g. feldspar and clay minerals). In contrast, the high correlation of  $\text{SiO}_2$  versus  $\text{Al}_2\text{O}_3$  and  $\text{K}_2\text{O}$  in dark lignites suggests that the silica is largely associated with Al and K minerals such as K-feldspar, illite, and/or kaolinite. This is further supported by the high correlation between  $\text{Al}_2\text{O}_3$  and  $\text{K}_2\text{O}$  in dark lignites (Fig. 5c).



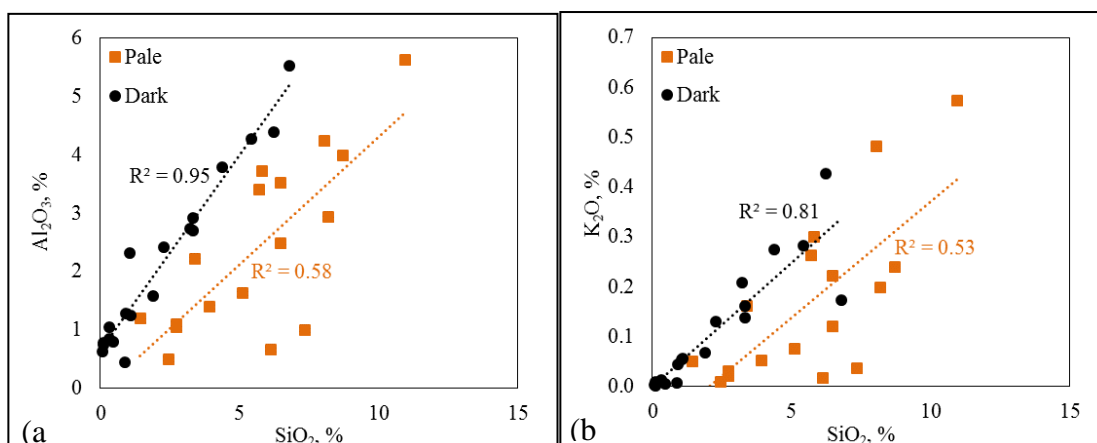


**Figure 3-5 Correlation diagrams of (a) SiO<sub>2</sub> versus Al<sub>2</sub>O<sub>3</sub>, (b) SiO<sub>2</sub> versus K<sub>2</sub>O in pale and dark lignites from Jinsuo Basin**

### 3.5.3 Paleoenvironmental model for pale and dark layers

The suggested model for the paleoenvironment during formation of pale and dark lignite layers in the Jinsuo Basin are shown in Fig. 6. The model is based on field observations, the petrographic and organic geochemical characteristics of the lignite samples (Liu et al., 2018), regional geological and climate changes (An et al., 2001; Xu et al., 2004; Kou et al., 2006; Dupont-Nivet et al., 2007; Chang et al., 2010; Xie et al., 2012; Sun et al., 2015), paleobotany (Wu et al., 1987; Xu et al., 2004), and stable isotopic and mineralogical data.

Previous coal petrological and organic geochemical data suggested that the thick dark layers in the Jinsuo Basin lignites were formed under wet, humid conditions with the paleomire containing almost entirely angiosperm plants (Liu et al., 2018). The regional paleoclimate reconstruction further supports warmer and more moist climatic conditions during the Pliocene in Yunnan Province compared to today (Xu et al., 2004; Sun et al., 2011; Yao et al., 2012; Su et al., 2013). The higher plant vegetation in central Yunnan Province during the late Pliocene was mainly composed of the angiosperms *Cyclobalanopsis glaucooides* and *Castanopsis orthacantha* and the gymnosperm *Pinus yunnanensis* (Wu et al., 1987; Xu et al., 2004), with variations in the vertical vegetation zonation depending on the altitude of the particular region (Kou et al., 2006; Xu et al., 2008; Sun et al., 2011; Huang et al., 2016).

Figure 7a shows the model for paleoenvironmental conditions and vegetation composition during formation of the dark layers in the Jinsuo Basin. Angiosperm trees (such as *Cyclobalanopsis* and *Castanopsis*) dominated the plant community, in association with some shrubby and herbaceous plants. This reconstruction is consistent with results from the previous biomarker analysis (Liu et al., 2018). The occurrence of gymnosperm trees of the Pinaceae family, such as *Pinus yunnanensis*, was restricted to the eastern and western mountains because of the higher altitude and lower ambient

temperature. During the warm periods, intensive rainfall events within this intermountain basin resulted in formation of a paleomire with a high degree of gelification of organic material and a high proportion of macerals of the huminite group (Liu et al., 2018). Moreover, during the formation of dark layers, thick peat horizons accumulated under stable conditions, and contained larger amounts of authigenic minerals (e.g. cell-filling quartz) compared to pale layers.

The model of the formation of thin pale layers in the Jinsuo Basin lignites is shown in Fig. 6b. The pale layers were generated under less wet and more oxic conditions compared to the dark layers (Liu et al., 2018). This difference can be explained by slight uplift of the Tibetan Plateau together with the co-occurrence of a more intensive Asian monsoon and/or global cooling. Compared to the warmer climate during the formation of dark layers, the thin pale layers were formed during cooling periods associated with less precipitation. As shown in Fig. 6b, during the dry and cooler periods, the abundance of angiosperm plants (such as *Cyclobalanopsis* and *Castanopsis*) decreased whereas gymnosperm and shrubby plants increased. The contribution of gymnosperms (*Pinus yunnanensis*) to peat-forming vegetation increased, forced by climate cooling and the increasing altitude resulting from uplift of the Tibetan Plateau. The contemporaneous enhancement of the Asian monsoon led to less rain in the basin and increasing activity of aerobic bacteria in the mire, which enhanced the decomposition of organic matter. The increased decomposition of organic matter might be the reason why the pale layers are very thin compared to the dark layers. Moreover, the stepwise slight uplift of the surrounding mountains and the increasing Asian monsoon also resulted in an increasing influx of detrital minerals (e.g. quartz),  $\text{TiO}_2$ , and Zr (Table A2) into the paleomire during formation of the pale layers. This conclusion is also supported by the high DAI values in the pale samples.

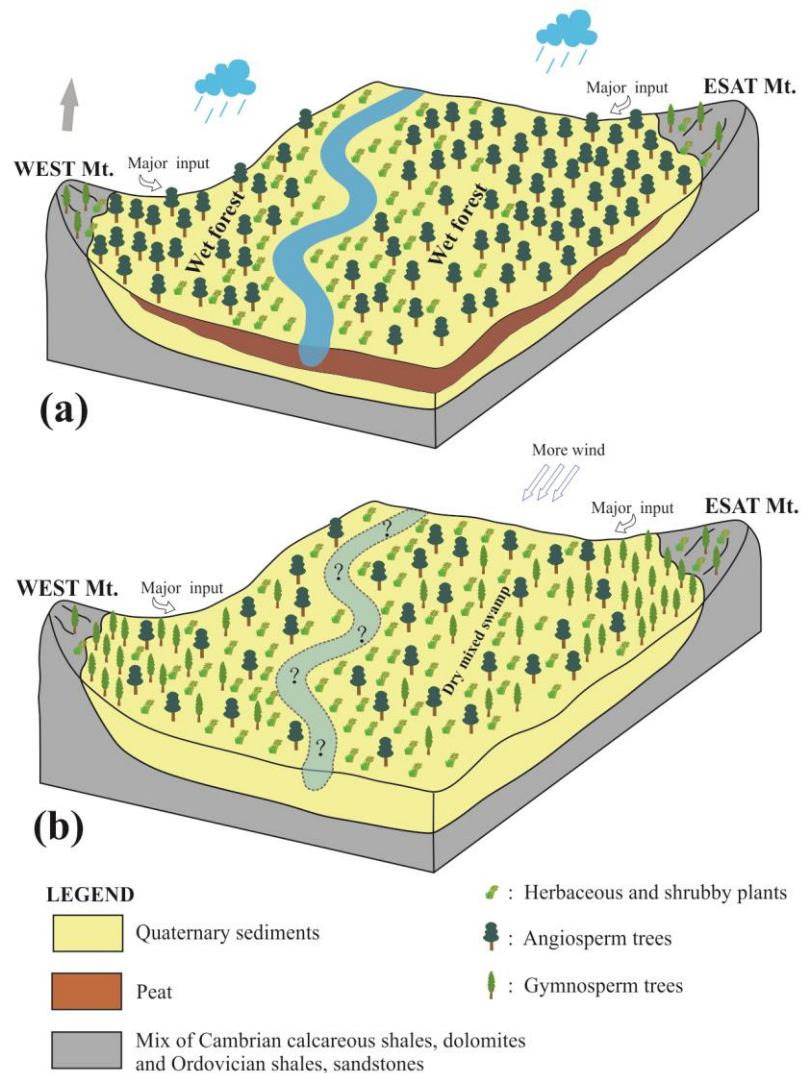


**Figure 3-6 Conceptual models of the depositional paleoenvironment for the formation of dark (a) and pale (b) layers in Jinsuo lignite deposit basin, Yunnan Province, China**

During formation of the pale layers (Fig. 6b), the conditions changed intermediate between dark layers. One possible scenario is that intermittent strengthening of the Asian monsoon occurred as a result of the phased uplift of the Tibetan Plateau associated with global cooling (An et al., 1999, 2001; Li et al., 2014). In a previous study of the Cenozoic plant diversity in Yunnan, changes in the plant composition and vegetation types were suggested to be related to the altitude changes from north to south and associated global cooling (Huang et al., 2016). On the basis of results obtained from the investigation of the late Pliocene paleoflora of the Longling lignite mine (western Yunnan), Xu et al. (2004) found five major cycles of warming and cooling during that time. Furthermore, the Cenozoic monsoon evolution (Clift et al., 2008, 2010) and the approximate co-occurrence of the phased uplift of the Tibetan Plateau with stepwise strengthening of the Asian monsoon from the late Miocene (An et al., 2001) is well established. In general, the interaction between monsoon intensity and global climate change is well known

(Kutzbach and Street-Perrott, 1985; Licht et al., 2014; Sun et al., 2015). Previous studies also suggested that stepwise enhanced monsoon activity and drying of the Asian interior were associated with episodic tectonic uplift of the Tibetan Plateau from the Miocene on (~8 Ma). Moreover, global cooling in the Pliocene at ~3.2 Ma (Li et al., 2014), and growth of the Tibetan Plateau together with contemporaneous enhancement of the monsoon further accelerated the Miocene–Pliocene global cooling (Sun et al., 2008; Ruddiman, 2013; Li et al., 2014; An et al., 2015). The combined influences of uplift of the Tibetan Plateau, intense Asian monsoon, and global cooling on the local geological climate of the studied area during the late Pliocene might ultimately have caused formation of the pale layers. However, the formation of periodic pale and dark layers cannot be directly related to uplift and fall of the Tibetan Plateau, because there is no evidence for a fall of the Tibetan Plateau during the late Pliocene. The pale layers probably formed following periods of uplift of the Tibetan Plateau that led to an intense monsoon and locally cold climate and a lower groundwater level in the basin. Considering the relatively warm, humid tropic/subtropical climate in Yunnan Province from the Miocene to the late Pliocene and the long-term stability of the geological conditions (YBGMR, 1990; Xiao et al., 2010; Xie et al., 2012; Zhang et al., 2012; Su et al., 2013), the dark layers formed gradually following the pale layers during periods in which the local climate became warmer and more humid between two uplift steps of the Tibetan Plateau. This interpretation is also supported by the thicknesses of the pale and dark layers. The thin pale layers (5–25 cm thick) were probably formed during periods of short-term cold, dry climate following each period of uplift of the Tibetan Plateau. In contrast, the thick dark layers (tens to hundreds of centimeters thick) most likely formed in long-term stable conditions with a warm, humid tropical/subtropical climate during periods of little/no uplift activity of the Tibetan Plateau.

Another hypothesis that can explain the appearance of cyclic pale and dark layers is related to the ~40-kyr cyclic fluctuations of ice-sheet extent relevant to cycles in insolation, which were influenced by changes of the Earth's axial tilt during the Pliocene. The geologically widespread ~40-kyr periodicity of Earth's climate system during the Pliocene is expressed in oxygen isotope ( $\delta^{18}\text{O}$ ) and temperature data from deep-sea sediments (Shackleton et al., 1984; Dwyer et al., 1995; Crundwell et al., 2008), ocean circulation (Hall et al., 2001), atmospheric circulation from continental dust deposits (Ding et al., 2002), global sea-level fluctuations (Naish, 1997), and ice-sheet changes (Naish et al., 2009). Furthermore, terrestrial climate and vegetation changes have been attributed to orbital forcing during the late Pliocene–early Pleistocene (Bonan et al., 1992; Willis et al., 1999a, 1999b; Sniderman et al., 2007). Willis et al. (1999b) provided high-resolution pollen data of lake sediments from Pula maar, Hungary, and suggested that the vegetation fluctuations (boreal vegetation vs. sub-tropical taxa) were responding to climate change associated with, in particular, the precession and obliquity causing from the development of the Northern Hemisphere glaciation (NHG). Meanwhile, the

Asian monsoon is also thought to be sensitive to orbital forcing (Clemens et al., 1996), and was influenced by northern summer insolation at the precession period and the change to the NHG in high latitudes (Tian et al., 2006). The increased albedo of the Tibetan Plateau could have resulted from vegetation feedback in increasingly glacial conditions (Clemens et al., 1996). However, the phases of East Asian monsoon changes compared with the global ice volume variations were not constant, but varied with the obliquity and precession periods in the Pliocene to Pleistocene (Tian et al., 2006). Furthermore, deposition of the 18.3-m-thick upper Paleocene subbituminous coal from the Powder River Basin, USA (Large et al., 2003), and the lower Miocene lignite from the Gippsland Basin, Australia (Large et al., 2004), have also been proved to be terrestrial records of orbital climate forcing. Stable carbon isotopic signals probably resulting from climatic or botanic responses to orbital forcing were also hypothesized by Jones et al. (1997) for Miocene lignites from the Lower Rhine Embayment in Germany. Recent study on geophysical logs also identified Milankovitch periodicities of eccentricity, obliquity, and precession in Late Permian coal seams from western Guizhou, China (Yan et al., 2019). Direct age dating of the sedimentary sequence of upper Pliocene cyclic pale and dark layers in the Jinsuo Basin that could demonstrate the presence of the 41-kyr periodic changes is missing so far. However, the observed characteristics (e.g. color, stable isotopes, and palynology) of the periodic pale and dark layers might result from the influence of orbital forcing by precession and/or obliquity on the vegetational and paleoenvironmental changes. Additional methods such as age dating, paleobotany, and spectral analysis are required in the future to provide more evidence for the hypothesis that the occurrence of cyclic pale and dark layers and their related vegetational and paleoenvironmental changes were related to orbital forcing.

Probably, not only one of the suggested factors (e.g. global and regional climate, tectonic activities, the Asian monsoon, orbital periodicities, and the NHG) influenced the formation of cyclic dark and pale layers in the Jinsuo Basin lignites; interactions between different factors should also be considered.

### 3.6 Conclusions

New data on the carbon and nitrogen stable isotopic compositions and the distribution of major elements in pale and dark lignites in the Jinsuo Basin, Yunnan Province, southwest China, were used to reconstruct the paleoenvironmental conditions in the paleomire and the driving forces for the formation of pale and dark layers.

Pale lignites generally have lower  $\delta^{13}\text{C}$  values (av.  $-27.01\text{‰}$ ) compared to dark lignites (av.  $-26.38\text{‰}$ ), and the  $\delta^{13}\text{C}$  values of fossil wood (av.  $-24.79\text{‰}$ ) are generally higher those of bulk lignite. Maximum  $\delta^{13}\text{C}$  values were detected in two fusain samples (av.  $-24.19\text{‰}$ ). The very high amount of liptinite together with the strong degradation of plant materials by bacterial activity in pale lignites (Liu et al., 2018) could have had a marked influence on  $\delta^{13}\text{C}$  values and resulted in lower  $^{13}\text{C}$  values in pale lignites compared to

dark lignites. Relatively high  $\delta^{15}\text{N}$  values in pale lignites (av. 2.17‰) are related to the low TN values (av. 0.89). In dark lignites,  $\delta^{15}\text{N}$  values are lower (av. 1.79‰) and correspond to higher TN values (av. 1.21). This difference might be caused by the greater loss of organic nitrogen during aerobic degradation of organic matter in pale lignites associated with preferential degradation of the  $^{14}\text{N}$  isotope. The weak negative correlation between the  $\delta^{15}\text{N}$  and  $\delta^{13}\text{C}$  values indicates that some factors (e.g. liptinite content and/or bacterial degradation) influenced both the stable carbon and the nitrogen compositions of lignites. The insignificant influence of the prevailing plant community on the carbon and nitrogen isotopic compositions of the lignites might have resulted from the strong degradation of organic matter by bacteria and the higher liptinite content of the pale layers.

The driving force for the formation of pale layers might have been the stepwise uplift of the Tibetan Plateau and the approximate co-occurrence of the intensive Asian monsoon, which resulted in a locally cold, dry climate in the study area. This is supported by the relatively high  $\text{SiO}_2/\text{Al}_2\text{O}_3$  ratios, DAI values, and high levels of  $\text{TiO}_2$  and Zr in the pale layers. Gymnosperms (such as *Pinus yunnanensis*) become more abundant in the basin during these short periods. In contrast, the dark layers formed during long-term stable geological conditions with a regionally tropical/subtropical warm, humid climate favoring the predominance of angiosperms in the vegetation. Changes in the composition of major elements and the variations in thickness of pale and dark layers further support this conclusion. Another hypothesis to explain the cyclic occurrence of pale and dark layers could be related to climate change (e.g. ice-sheet cyclic fluctuations, cycles in insolation) forced by orbital periodicities (e.g. obliquity [41 kyr]) and the development of the Northern Hemisphere glaciation during the Pliocene. Previous studies of upper Paleocene and lower Miocene coal and lignite deposits by Large et al. (2003, 2004) and Jones et al. (1997) previously demonstrated that the influence of orbital cycles can be recorded in subbituminous coal and lignite sequences. Further studies (e.g. exact age dating, determination of color index, and paleomagnetic and spectral analyses) need to be carried out to clarify whether this hypothesis is also valid for the alternating formation of pale and dark lignites in the Jinsuo Basin.

---

## **Chapter 4 Reconstruction of paleobotanical and paleoenvironmental changes in the Pliocene Velenje Basin, Slovenia, by molecular and stable isotope analysis of lignites**

### **4.1 Abstract**

Three different lithotypes (xylitic, gelified and matrix) of Pliocene lignite from the Velenje Basin, Slovenia, were investigated to establish the variations of biomarker compositions in solvent extracts and the stable isotope (carbon and nitrogen) compositions of bulk material. From the biomarker results, the xylitic lithotype almost exclusively originates from gymnosperms (conifers such as Taxodiaceae), as indicated by the very high contents of sesquiterpenoids and diterpenoids but very low abundances of *n*-alkanes and non-hopanoid triterpenoids. The relative proportion of gymnosperms to angiosperms in the paleomire is reflected by the ratio of diterpenoids to the sum of diterpenoids and non-hopanoid triterpenoids (Di/(Di+Tri-terpenoids)), which is close to 1 (av. 0.99) in the xylitic lithotype. The predominance of diterpenoids from conifers in the xylitic lithotype is associated with high C/N ratios and intermediate total sulfur (TS). The very low abundance of hop-17(21)-ene and the absence of further hopanoids in the xylitic lithotype indicate a restricted influence of bacterial degradation under relatively dry conditions in the paleomire. The matrix lithotype also originated preferentially from gymnosperms under dry depositional conditions, as indicated by the high Di/(Di+Tri-terpenoids) ratio (0.95), low amounts of hopanoids and low TS content. The gelified lithotype is characterized by a high content of *n*-alkanes and wide variation of the Di/(Di+Tri-terpenoids) ratio (0.13–0.88), indicating a fluctuating contribution of angiosperms to the plant community in the paleomire during formation of this lithotype. In addition, the high abundance of hop-17(21)-ene and TS in the gelified lithotype compared with the other two lithotypes suggests the effect of bacterial activity under relatively wet/humid conditions during formation of the gelified lithotype, which is also supported by the considerable content of mid-chain *n*-alkanes.

The high correlation between the  $\delta^{13}\text{C}$  and  $\delta^{15}\text{N}$  values ( $R^2 = 0.68$ ) indicates that the stable carbon and nitrogen isotope composition in the Velenje lignites were probably influenced by the same factors (e.g. precursor plants and/or microbial activity). The stable carbon isotopic values (av.  $-25.44\text{‰}$ ) and nitrogen isotopic values (av.  $2.15\text{‰}$ ) of the xylitic lithotype are higher than those of the gelified lithotype (av.  $\delta^{13}\text{C} = -27.48\text{‰}$ ,  $\delta^{15}\text{N} = 1.37\text{‰}$ ) and the matrix lithotype (av.  $\delta^{13}\text{C} = -27.09\text{‰}$ ,  $\delta^{15}\text{N} = 1.10\text{‰}$ ). The

relatively high correlation between the diterpenoid content and both  $\delta^{13}\text{C}$  and  $\delta^{15}\text{N}$  values suggests that the stable carbon and nitrogen isotopic composition of the three lithotypes might reflect the composition of the original plant material in the paleomire. The dominance of conifers as precursor plants in the xylitic lithotype might be the main reason for the higher  $\delta^{13}\text{C}$  values and probably also the higher  $\delta^{15}\text{N}$  values. The relatively higher  $\delta^{15}\text{N}$  values in the xylitic lithotype than in the other types could be explained by the high amount of decay-resistant xylem and low mineral (e.g. clay) content in the xylitic lithotype. The slightly lower  $\delta^{13}\text{C}$  but higher  $\delta^{15}\text{N}$  values in the gelified lithotype than in the matrix lithotype can be explained by variation of parent plant materials and the influence of bacterial activity.

*Keywords: lignite lithotypes, biomarkers, carbon isotopes, nitrogen isotopes, Velenje Basin.*



## 4.2 Introduction

During the last few decades, organic geochemical methods (e.g. analysis of the molecular composition of extractable organic matter) and stable isotope analyses of lignites have been widely applied to improve reconstruction of changes in paleoenvironment and paleovegetation during lignite deposition in paleomires under the influence of climate changes (Dehmer, 1995; Bechtel et al., 2003, 2008; Kanduč et al., 2012; Erdenetsogt et al., 2017; Bucha et al., 2018). The biomarkers present in the extractable organic matter of lignites have been shown, in addition, to reflect changes in the precursor vegetation and microbial degradation involved in lignite formation (Bechtel et al., 2005; Kenneth Eric Peters et al., 2005; Stefanova et al., 2008, 2016; Zdravkov et al., 2011; Marynowski et al., 2013). Furthermore, the stable isotopic composition of C and N in lignites is expected to provide valuable information for reconstruction of floral assemblages and paleoenvironmental changes (Lücke et al., 1999; Bechtel et al., 2008; Holdgate et al., 2009; Kanduč et al., 2012; Erdenetsogt et al., 2017).

The lithotypes of lignites from various basins have recently been intensively studied. The xylite-rich lithotypes found in the Neogene Konin and Turoszów lignite basins of Poland are characterized by the dominance of organic matter originating from gymnosperm plants (e.g. conifers), whereas the detrital (matrix) lignites originate from monocotyledonic material, with some detritus such as needle leaves (Fabiańska and Kurkiewicz, 2013). The xylite-rich lignites in the upper Miocene strata of the Pannonian Basin, Serbia, are also predominantly composed of plant materials derived from gymnosperms such as conifers (Đoković et al., 2018). In the Neogene Achlada lignite mine in Greece, the xylite-rich layers indicate the former presence of forests in a fluvial system, whereas the matrix layers suggest an environment in which tree coverage was restricted but herbaceous and bushy vegetation dominated (Oikonomopoulos et al., 2015). The xylite-rich lithotypes from several Miocene basins in the Czech Republic were formed from predominantly arborescent-gymnosperm vegetation associated with generally lower water table conditions, whereas the original vegetation leading to the formation of matrix coals in these basins combined arborescent and herbaceous plants as well as aquatic vegetation (Havelcová et al., 2012). Both xylite-rich and matrix lignites from the upper Miocene Kolubara Basin in Serbia are dominated by decay-resistant gymnosperms with considerable proportions of angiosperms deposited in a rather oxic environment with intense aerobic microbial activity (Životić et al., 2015). The xylite-rich and matrix lignites of the upper Miocene Kovin deposit, Serbia, are derived from prevalent woody vegetation and variable proportion of herbaceous peat-forming plants. These lignites are characterized by high proportions of decay-resistant gymnosperms (conifers) and low proportions of angiosperms (Mitrović et al., 2016). The variations in the  $\delta^{13}\text{C}$  values of the lignite matrix of the middle Miocene Garzweiler seam in the Lower

Rhine Embayment, Germany, were explained by varying proportions of gymnosperms within the peat-forming vegetation, whereas the high-frequency fluctuations were suggested to represent a signal of environmental changes (Lücke et al., 1999).

The  $\delta^{13}\text{C}$  values of the Pliocene lignites of the Velenje Basin, Slovenia, are lower for the detrital (matrix) lithotype than for the xylites, and the isotopic difference between the  $\delta^{13}\text{C}$  values of fossil woods and of the coal matrix is probably caused by the isotopically light organic matter from leaves, resins and bark in the coal matrix, and/or the extent of organic matter decomposition (Bechtel et al., 2007 and reference therein). Bechtel et al. (2008) further confirmed that depletion of  $^{13}\text{C}$  in whole lignites relative to gymnosperm-derived xylitic fragments is a general feature of investigated Miocene lignites in central Europe. If fossil wood is derived from angiosperms, xylitic fragments generally have carbon isotopic compositions similar to those of the whole lignites; the  $\delta^{13}\text{C}$  values of fossil gymnosperm wood are approximately 2.5‰ heavier than the angiosperm values (Bechtel et al., 2008). The carbon isotope  $\delta^{13}\text{C}$  values of brown coal matrix from the Eocene–Miocene Gippsland Basin of Australia follow gymnosperm/angiosperm fluctuations, with higher ratios coinciding with heavier  $\delta^{13}\text{C}$  values (Holdgate et al., 2009).

The Pliocene Velenje lignite of Slovenia has previously been investigated by means of coal petrology, organic geochemistry and stable isotope analysis. Based on pollen data, the xylitic lignite in Velenje originated mostly from *Sequoia–Taxodium–Metasequoia* (Šercelj, 1968). Markič and Sachsenhofer (1997) investigated the petrographic composition of the Velenje lignite seam to interpret the depositional environment during peat accumulation. The overall paleoenvironment changed through time from a fluvial forest swamp (unit I) to a relatively dry forest swamp (unit IIa), then to a slightly more wet bush moor (unit IIb/c) and subsequently to a bush moor that graded into a wet forest swamp (unit IIIa), which was finally superimposed by a lacustrine environment (Markič and Sachsenhofer, 1997). The stable carbon isotopic compositions (Pezdič et al., 1998; Kanduč et al., 2005) and the nitrogen isotopic compositions (Kanduč et al., 2005) of different lignite lithotypes from the Velenje Basin have been studied to explain their genesis. The  $\delta^{13}\text{C}$  and  $\delta^{15}\text{N}$  values of the different lithotypes appear to have been influenced by both the isotopic differences of the original plant materials and biogeochemical processes (such as gelification and mineralization of organic matter) during early diagenesis (Kanduč et al., 2005). Furthermore, biomarker and stable carbon isotope data have been applied to explain changes in the paleoenvironment and plant community during deposition of the Pliocene Velenje lignite (Bechtel et al., 2003). More recently, the carbon isotopes of different lithotypes, along with the  $\delta^{13}\text{C}$  values of  $\text{CO}_2$  and  $\text{CH}_4$  and the  $\delta^{13}\text{C}$  values of dissolved inorganic carbon were used to interpret carbon cycling in the Pliocene Velenje Basin (Kanduč et al., 2012). The majority of these studies focused on samples representing the whole lignite seam. In the present study, samples of individual lithotypes (gelified, matrix and xylitic lithotypes) were collected from the

Velenje Basin to investigate the molecular composition of solvent extracts and the C and N stable isotope compositions, with the aim of elucidating the conditions that determined the formation of distinct lithotypes.

In this paper, biomarkers in different lignite lithotypes from the Velenje Basin, Slovenia, are studied comparatively for the first time. This study is aimed to find out the factors controlling the variations of environmental conditions during deposition and the plant community variations that finally contributed to the formation of individual lithotypes.

### **4.3 Geological setting**

The Velenje Basin is about 10 km long and 4 km wide and is filled with Pliocene to Pleistocene clastic sediments. The sediments in the basin are bounded by the Smrekovec fault to the north and by the Šoštanj fault to the south (Fig. 1A). The Pliocene to Pleistocene clastic sedimentary fill is more than 1000 m thick in the central part of the basin and constitutes a typical continental fill-up succession (Brezigar, 1986). The lower part of the Pliocene coal-bearing sedimentary sequence consists of terrestrial coarse-grained basal beds with a fining-upward trend, fine-grained marshy sediments; above, the main Velenje lignite seam has developed. The strata of fresh-water lacustrine clayey, silty and sandy sediments with lenses of fluvial sandy gravels on the top of the lignite seam reach a thickness of up to 350 m. This succession is overlain by 90 m of Villafranchian sediments, which are marshy at the bottom with a locally developed thin lignite bed, and become terrestrial upward. The uppermost part of the basin fill consists of sands and gravels of Holocene age (Brezigar et al., 1985) (Fig. 1B). The stratigraphic sequence within the basin and vertical in-seam variations were mainly controlled by high subsidence rates. The majority of the basin succession is the result of a single-stage subsidence event, and was deposited in a transgressive setting during the transition from fluvial to lacustrine environments (Markič and Sachsenhofer, 2010).

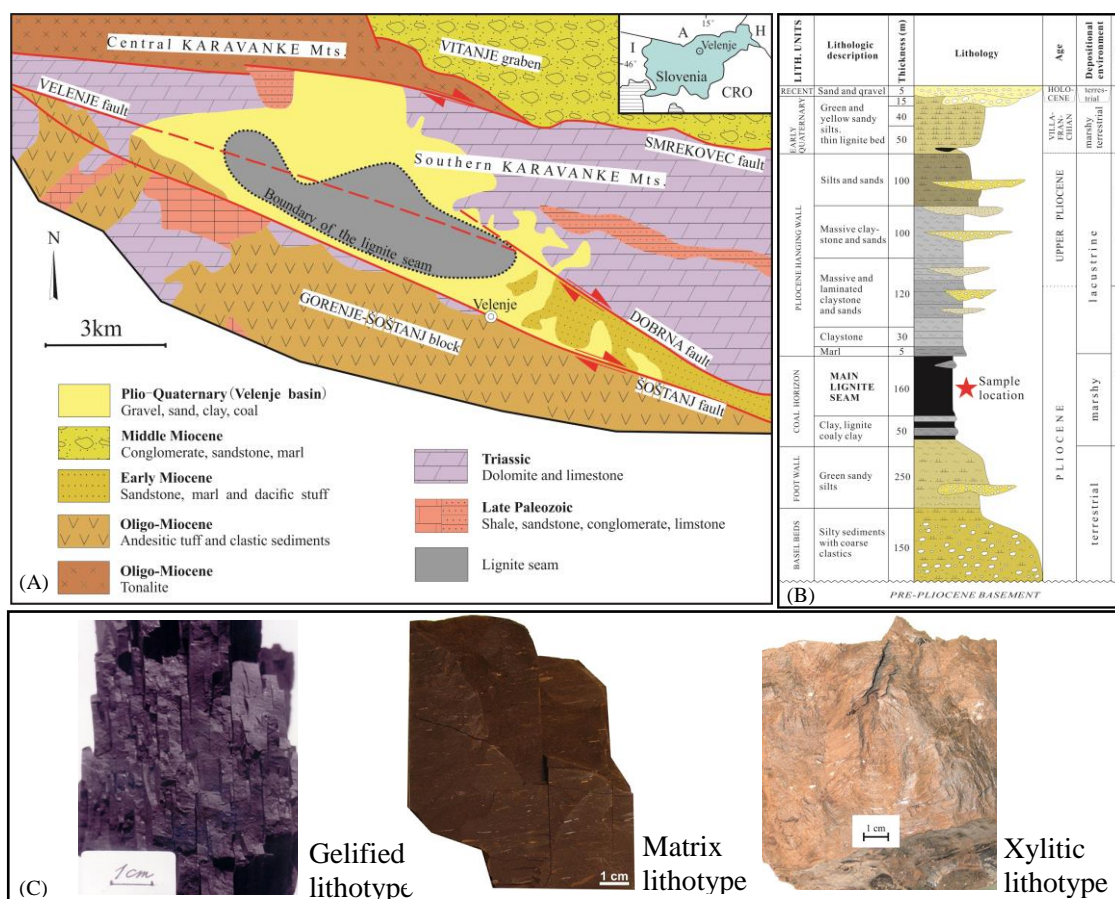


**Figure 4-1 (A): Geological map of the Velenje Basin, Slovenia (modified from Brezigar et al., 1987). (B): Stratigraphic column of the Velenje Basin and the sample location (modified from Brezigar 1986; Brezigar et al., 1987); (C): Photographs of gelified, matrix and xylitic lithotypes**

The main lignite seam in the Velenje Basin is located at about the middle of the Pliocene to Pleistocene succession. In the central part of the basin, the lignite seam is up to 165 m thick, and it gradually pinches out toward the margins. The nearly horizontal or slightly inclined lignite seam extends W–NW to E–SE for a length of 8.3 km, and is between 1.5 and 2.5 km wide (Brezigar, 1986). The main lithotypes of the main lignite seam in the Velenje Basin are matrix (detrital) lignite, gelified lignite, and xylitic lignite (Markič and Sachsenhofer, 2010). The matrix lignite is composed of fine-detrital homogeneous material with a dark brown color, and may contain thin (less than 1 mm thick) xylitic bands and/or lenses that did not undergo gelification. The gelified lignite experienced various degrees of gelification, and it also consists of fine-detrital homogeneous material but with no or very rare visible thin xylitic remains. It is brownish-black to black. The xylitic lignite consists of large pieces of wood (e.g. branches, stems, stumps and trunks). It is brown in color. In the xylitic lignite, xylitic fragments are often replaced by epigenetic calcite, commonly as separate layers, which are particularly frequent in the vicinity of faults and fractures. Fusain particles can be mostly found as

incrustations over xylitic lumps. In top view, fine-detrital lithotypes prevail in the inner part of the basin, whereas xylitic lignite is distributed along the periphery of the basin (Hamrla, 1952; Markič and Sachsenhofer, 2010). Vertically, the fine-detrital (matrix) lithotype especially occurs at the bottom, but predominates throughout the seam, and gelification increases toward the top of the seam. The xylite content decreases from the lower half of the seam to the upper quarter (Markič and Sachsenhofer, 1997; 2010).

#### 4.4 Samples and analytical procedures

Ten representative lignite samples were obtained from an underground longwall working face at a level of  $-50$  m. All samples were immediately wrapped with aluminum foil, then sealed and stored in plastic bags to minimize contamination and oxidation. These samples were represent three different lithotypes (Fig. 1C), which are classified according to ICCP (1993) as cited in Taylor et al. (1998): gelified lignites (five samples; G); matrix lignites (two samples, M); and xylitic lignites (three samples; X). Matrix lignites used to be termed “detrital lignites” in older literature, since they consist predominantly of fine-detrital vegetal material. The matrix lithotype samples can contain a high content of mineral matter, in this case especially calcite, on the basis of which they are classified as carbocalcite (analogous to carbominerite and carbopyrite). However, the matrix lignites are more gelified in some parts (bands) than in others. More gelified parts of the matrix lignites are often associated with calcite encrustations of plant remains.

##### 4.4.1 Elemental analysis

All lignite samples were crushed and ground to  $\leq 200$   $\mu\text{m}$  to do the elemental analysis. The analytical procedures for the determination of the TOC and TN have been described in detail previously (Liu et al., 2018). Total sulfur (TS) content was analyzed on a Leco TruSpec S analyzer. All data of elements are given in weight percentage at dry base. Analytical error of all data was less than 5%.

##### 4.4.2 Biomarker analysis

For biomarker analyses, all samples were finely ground ( $< 200$   $\mu\text{m}$ ) then Soxhlet-extracted for 24 hours using dichloromethane (DCM) as the solvent. The extracts were separated into four fractions based on the different polarities of the components using flash column chromatography filled with activated silica gel (particle size 40–63  $\mu\text{m}$ ) under a nitrogen pressure of  $\leq 1.5$  bars. The saturated hydrocarbon fraction was eluted with *n*-hexane, the aromatic hydrocarbon fraction with *n*-hexane: DCM (9:1 v:v), the

ketones/esters fraction with DCM, and the heterocompounds with methanol. The so-called “saturated hydrocarbon fraction” contains both saturated hydrocarbons and mono-unsaturated hydrocarbons. Solvents were evaporated from each fraction after the separation under a stream of nitrogen.

The saturated and aromatic hydrocarbon fractions were further analyzed using GC-MS using the same instruments and analytical parameters as described previously (Liu et al., 2018). *n*-Tetracosane-D50 and 1, 1'-binaphthyl were injected to the saturated and aromatic hydrocarbons, respectively, as internal standards for quantification of individual compounds. The Xcalibur Qual Browser software was used for data processing. Identification of individual compound was carried out through the retention time in the TIC chromatogram and by comparison of the mass spectra with library and published data. Relative percentages and absolute concentrations of different compounds in the saturated and aromatic hydrocarbon fractions were calculated using peak areas from the TIC compared with those of internal standards. The concentrations of different compounds were normalized to the TOC content.

#### 4.4.3 Stable isotopic analysis

The stable isotope compositions of organic carbon ( $\delta^{13}\text{C}$ ) and nitrogen ( $\delta^{15}\text{N}$ ) in all lignite samples was determined using a FlashEA<sup>TM</sup> 1112 Elemental Analyzer with a ConFlo III Interface from Thermo Fisher in the Stable Isotope Laboratory of the Institute of Earth Sciences, Goethe-University Frankfurt am Main, Germany. Lignite samples were first ground and homogenized, then 3–10 mg (depending on the carbon and nitrogen content) of each sample was weighed in a tin capsule and tightly sealed to remove the air in the capsule for carbon and nitrogen analysis. Samples for carbon analysis were pretreated with diluted hydrochloric acid (10%) to remove carbonates. The sample residues were washed with distilled water until neutral, then dried and homogenized for analysis. The isotopic compositions of carbon and nitrogen were determined after combustion of the samples in the capsules in a hot furnace (1020 °C). Generated products were transferred through a Cu tube (650 °C), where excess O<sub>2</sub> was absorbed. H<sub>2</sub>O was trapped on a drying column composed of Mg(ClO<sub>4</sub>)<sub>2</sub>. International Standards (IAEA-CH-7, USGS24, IAEA-N1 and IAEA-N2) were analyzed before, after and during sample analysis and were used for data correction. The resulting CO<sub>2</sub> was analyzed online either by a European Scientific or an Optima (Micromass Ltd.) isotope ratio mass spectrometer interfaced via a cryogenic trap. Carbon isotope values are reported relative to the international standard Vienna-Pee Dee Belemnite (V-PDB), which is defined in the International Atomic Energy Agency (IAEA) standard IAEA-NBS19 ( $\delta^{13}\text{C}$  of +1.95‰). Nitrogen isotope ratios are reported relative to an international atmospheric nitrogen (V-AIR) standard ( $\delta^{15}\text{N}$  of 0‰), with the AIR scale defined by IAEA standards IAEA-N1 (+0.4‰) and IAEA-N2 (+20.3‰). The analytical error is less than 0.2‰.

## 4.5 Results and discussion

### 4.5.1 Bulk geochemical parameters

Bulk geochemical data are presented in Table 1. Samples are grouped into gelified, matrix and xylitic lignite lithotypes. The gelified lithotype (G; samples 1a, 1b, 3, 4, 5, and 10) originated primarily from detrital materials or woody tissues prior to gelification. Sample 1a is a gelified fine-detrital lignite with rare <1 mm brown xylitic inclusions and very rare thin calcite. Sample 1b (Gc) is similar to 1a but contains more calcite (c) and fusinite. Sample 4 is a gelified lignite with calcite encrustations (1–5 mm wide, up to 10%) over plant remains. Sample 3 is gelified similarly to sample 4, but contains fewer calcite encrustations than sample 4. Sample 5 is a gelified wood. Samples 2 and 9 are matrix lignites (M), but sample 2 (Mc) contains a high amount of calcite. Samples 6, 7 and 8 are clearly xylites (X).

The average (av.) EOM content in the three lithotypes shows a decreasing trend from the gelified lignites (av. 15.6 mg/g TOC) to the matrix lignites (av. 12.2 mg/g TOC), and to the xylitic lignites (av. 10.2 mg/g TOC) (Table 1). These values are consistent with the results of previous studies of lignites from Slovenia (Bechtel et al., 2003, 2004). The maximum EOM value was from gelified lignite sample No. 3 (16.5 mg/g TOC); the minimum value of 9.1 mg/g TOC was obtained from a xylitic lithotype (sample No. 6). Higher EOM contents in gelified lignites have been explained by a higher degree of gelification under wet conditions in a paleomire, which resulted in better preservation of organic matter compared with its deposition under dry conditions (Dehmer, 1989; Oikonomopoulos et al., 2015).

The average TOC content is 50.9%, 21.3%, and 41.2% in the gelified, matrix, and xylitic lignites, respectively (Table 1). The high TOC content in the gelified lithotype is consistent with the high EOM. The lowest TOC value was detected in a sample of matrix lithotype (10.3%, sample No. 2). Low TOC values in matrix lignites have previously been explained by the higher content of inorganic matter (e.g. calcite) in the detrital matrix (ash = 8.16%, Markič and Sachsenhofer, 2010) and the poor preservation of organic matter compared with the gelified lithotype. The high TOC content of the gelified lignite is also consistent with previous results from lignites in Slovenia (Bechtel et al., 2003, 2004), and higher TOC values may be a result of increased bacterial organic matters since gelification is enhanced by humification of lignin through microbial activity.

The average TN content (Table 1) exhibit a similar tendency to EOM in the three lithotypes. The gelified lithotype has the highest TN content (av. 1.44%), with the

average TN values in the matrix and xylitic lithotypes being far lower, 0.72% and 0.51%, respectively. One of the lowest TN values (0.47%) was detected in the matrix lignite (sample No. 2), which might have resulted from the high content of calcite in this sample. TN contents have also been determined for pale (ungelified) and dark (gelified) lignites from the Pliocene lignite basin in Yunnan Province, China (Liu et al., 2018). In that study, the TN contents of gymnosperm-rich pale lignites (av. 0.89%) were much lower than those of gelified angiosperm-dominated dark lignites (av. 1.21%). The variations of TN contents in different lithotypes are, to some extent, a reflection of the proportions of gymnosperms to angiosperms in the plant community during lignite formation, because modern gymnosperm trees have higher C/N ratios (64.7) than angiosperm trees (49.6) (Cernusak et al., 2008). In the present study, the average C/N ratio in the xylitic lithotype is 86.5, with a maximum value of 118.2 in sample No. 7 (Table 1). These values are much higher than those of the gymnosperm-influenced pale lignite layers (av. 60.6) in Yunnan Province (Liu et al., 2018). The average C/N ratio of the gelified lithotype (35.5) is higher than that of the matrix lithotype (av. 27.7). The variations in the C/N ratio may have resulted from changing gymnosperm proportions in the palaeomire during the formation of the different lithotypes, with the xylitic lithotype having the highest proportion of gymnosperms.

The TS contents in Table 1 show that in the gelified lithotype, the TS (av. 1.91%) is higher than in the matrix (av. 0.92%) and xylitic lithotypes (av. 1.30%). Markič and Sachsenhofer (1997) suggested that variations in the sulfur content result from changes in the pH values in the paleomire. The relatively high sulfur contents in the Velenje lignites are a result of alkaline, calcium-rich surface waters. The pH values could control both reduction of sulfates by sulfate-reducing bacteria and bacterial decomposition of plant remains (Markič and Sachsenhofer, 1997). A positive correlation between the amount of TS and the degree of gelification was also described by Dehmer (1989) from the middle Miocene Oberpfalz brown coal deposit, Germany. A high degree of gelification in lignites is generally governed by the activity of anaerobic bacteria, which increase the availability of H<sub>2</sub>S under the wet depositional conditions required for sulfide formation, resulting in higher TS levels, particularly in gelified lithotypes (Bechtel et al., 2003).

The relative proportions of saturated and aromatic hydrocarbons, NSO compounds and asphaltenes of the EOM are listed in Table 1. In all lithotypes, NSO compounds + asphaltenes dominate the EOM, with proportions ranging from 70 wt.% to 93 wt.%. The xylitic lithotype generally contains higher proportions of saturated hydrocarbon fractions but similar proportions of aromatic hydrocarbon fractions compared with the gelified and matrix lithotypes (Table 1).



**Table 4-1 Bulk organic geochemistry data along with carbon and nitrogen isotopic composition of the lignite samples from Velenje Basin**

Sample	Lithotypes	EOM <sup>a</sup>	TOC <sup>b</sup>	TN <sup>c</sup>	TS <sup>d</sup>	Sa- HC <sup>e</sup>	Ar- HC <sup>f</sup>	NSO + Asphalt. <sup>g</sup>	C/N	$\delta^{13}\text{C}$	$\delta^{15}\text{N}$
		mg/g TOC	wt. %			(wt. %, EOM)				‰	
1a	G <sup>h</sup>	14.7	56.7	1.47	2.00	7	5	89	38.5	- 27.17	1.61
1b	Gc <sup>i</sup>	14.9	50.8	1.44	1.79	4	5	91	35.4	- 27.46	1.51
3	Gc	16.5	46.3	1.57	1.82	5	3	93	29.5	- 27.49	1.26
4	Gc	16.1	49.5	1.39	2.00	24	10	66	35.7	- 28.11	1.33
5	G	15.5	52.5	1.30	1.89	11	9	79	40.4	- 27.29	1.10
10	G	15.6	49.7	1.49	1.97	5	4	91	33.3	- 27.37	1.39
2	Mc <sup>j</sup>	13.7	10.3	0.47	0.52	12	7	81	22.0	- 27.58	0.79
9	M <sup>k</sup>	10.7	32.3	0.97	1.32	10	9	81	33.3	- 26.59	1.4
6	X <sup>l</sup>	9.1	29.6	0.65	1.51	19	8	73	45.5	- 25.78	2.27
7	X	9.8	45.6	0.39	1.02	20	10	70	118.2	- 25.34	2.21
8	X	11.6	48.3	0.50	1.37	16	6	78	95.7	- 25.19	1.96
Average of G		15.6	50.9	1.44	1.91	9	6	85	35.5	- 27.48	1.37
Average of M		12.2	21.3	0.72	0.92	11	8	81	27.7	- 27.09	1.10
Average of X		10.2	41.2	0.51	1.30	18	8	74	86.5	- 25.44	2.15

<sup>a</sup> Extractable organic matter; <sup>b</sup> Total organic carbon; <sup>c</sup> Total nitrogen; <sup>d</sup> Total sulfur; <sup>e</sup> Saturated hydrocarbons; <sup>f</sup> Aromatic hydrocarbons; <sup>g</sup> The sum of NSO compounds and asphaltenes. <sup>h</sup> G: gelified lithotypes; <sup>i</sup> Gc: gelified lithotypes contain calcite; <sup>j</sup> matrix lithotypes contain calcite; <sup>k</sup> matrix lithotypes; <sup>l</sup> xylitic lithotypes.

## 4.5.2 Saturated and aromatic hydrocarbons in the EOM

Investigations of the composition of saturated and aromatic hydrocarbon fractions were performed on all samples. Representative TIC chromatograms obtained by GC-MS analysis of both fractions of the three lithotypes are shown in Figure 2. The major biomarkers identified in these fractions are listed in Table 2.

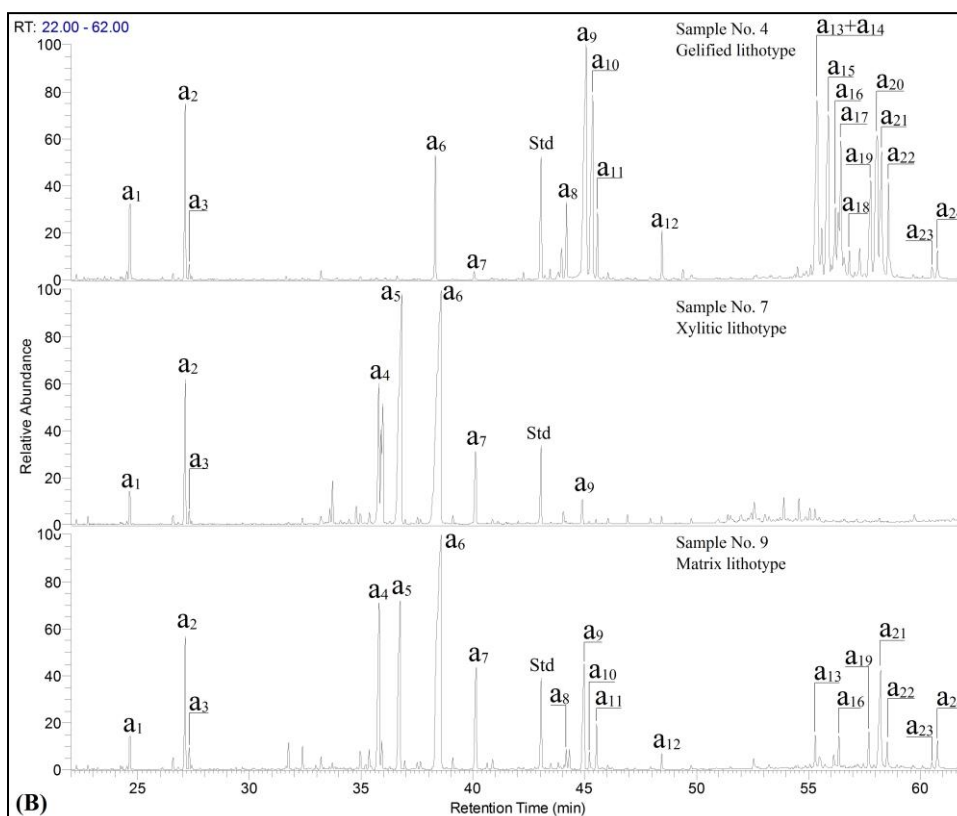
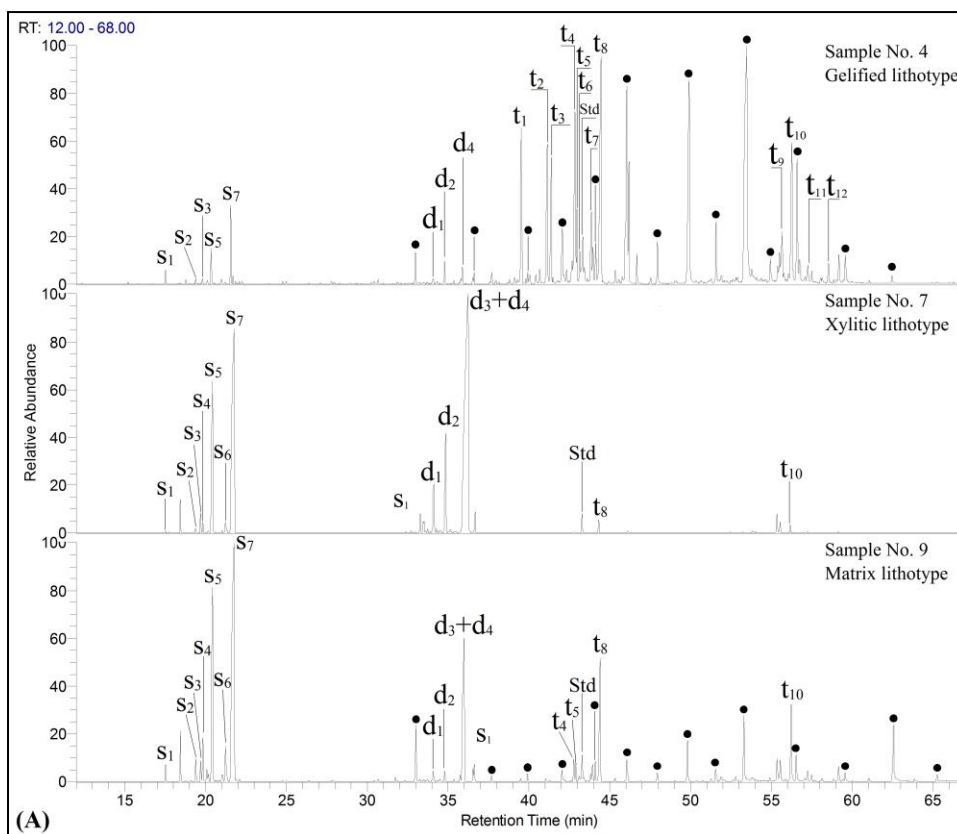


**Figure 4-2 Sections of TIC chromatograms obtained from GC-MS analysis of the saturated hydrocarbon fractions (A) and aromatic hydrocarbon fractions (B) in three different kinds of lithotypes from the Velenje Basin, Slovenia**

**Table 4-2 Biomarker compounds identified by GC-MS analysis in saturated and aromatic hydrocarbon fractions (Fig. 2), obtained from solvent extracts of lignites from the Velenje Basin, Slovenia**

Peak No.	Compounds	Formula	Key ions (m/z)	MW <sup>a</sup>	References
<b>Sesquiterpenoids</b>					
s1	Nordrimane	C <sub>14</sub> H <sub>26</sub>	81, 110, 179	194	A, B
s2	$\alpha$ -Cedrene*	C <sub>15</sub> H <sub>24</sub>	119, 161, 204	204	C
s3	Trans-cadinane*	C <sub>15</sub> H <sub>28</sub>	109, 165, 95	208	D
s4	$\beta$ -Patchoulane?	C <sub>15</sub> H <sub>26</sub>	191, 95, 121	206	
s5	4 $\beta$ (H)-Eudesmane	C <sub>15</sub> H <sub>28</sub>	109, 95, 193	208	D, E
s6	8 $\beta$ (H)-Drimane	C <sub>15</sub> H <sub>28</sub>	123, 95, 208	208	E
s7	4 $\alpha$ (H)-Eudesmane	C <sub>15</sub> H <sub>28</sub>	109, 95, 165	208	E
<b>Diterpenoids</b>					
d1	Norpimarane	C <sub>19</sub> H <sub>34</sub>	233, 123, 109	262	D
d2	18-Norabietane	C <sub>19</sub> H <sub>34</sub>	109, 95, 191	262	D
d3	Abietane	C <sub>20</sub> H <sub>36</sub>	163, 123, 191	276	D
d4	16 $\alpha$ (H)-phylocladane	C <sub>20</sub> H <sub>34</sub>	123, 95, 81	274	F
<b>Triterpenoids</b>					
t1	19 $\alpha$ (H) des-A-lup-13(18)-ene*	C <sub>24</sub> H <sub>40</sub>	285, 81, 161	328	
t2	19 $\beta$ (H) des-A-lup-13(18)-ene*	C <sub>24</sub> H <sub>40</sub>	285, 161, 313	328	
t3	Unknown	C <sub>24</sub> H <sub>40</sub>	313, 163, 189	328	
t4	10 $\alpha$ des-A-olean-13(18)-ene	C <sub>24</sub> H <sub>40</sub>	109, 95, 189	328	G, H
t5	10 $\alpha$ des-A-olean-12-ene	C <sub>24</sub> H <sub>40</sub>	218, 203, 189	328	G, H
t6	Des-A-urs-13(18)-ene	C <sub>24</sub> H <sub>40</sub>	95, 177, 313	328	G, H
t7	Des-A-urs-12-ene	C <sub>24</sub> H <sub>40</sub>	313, 218, 203	328	G, H
t8	Des-A-lupane	C <sub>24</sub> H <sub>42</sub>	123, 109, 163	330	I
t9	Olean-12-ene	C <sub>30</sub> H <sub>50</sub>	218, 203, 191	410	D, U
t10	Hop-17(21)-ene	C <sub>30</sub> H <sub>50</sub>	367, 231, 135	410	D, J
t11	2-Methylhop-17(21)-ene	C <sub>31</sub> H <sub>52</sub>	135, 245, 381	424	V
t12	D:A-Friedoolean-6-ene*	C <sub>30</sub> H <sub>50</sub>	95, 109, 218	410	
<b>Aromatic hydrocarbons</b>					
a1	5,6,7,8-Tetrahydrocadalene	C <sub>15</sub> H <sub>22</sub>	187, 159, 202	202	K
a2	Cadalene	C <sub>15</sub> H <sub>18</sub>	183, 198, 168	198	K
a3	Isocadalene	C <sub>15</sub> H <sub>18</sub>	183, 198, 168	198	L
a4	19-norabieta-8,11,13-triene	C <sub>19</sub> H <sub>28</sub>	159, 241, 185	256	D, M
a5	Dehydroabietane	C <sub>20</sub> H <sub>30</sub>	255, 173, 159	270	D, K
a6	Simonellite	C <sub>19</sub> H <sub>24</sub>	237, 252, 195	252	D, K

a <sub>7</sub>	Retene	C <sub>18</sub> H <sub>18</sub>	219, 204	234, 234	D, K
a <sub>8</sub>	Des-A-26-norlupa-5,7,9-triene	C <sub>23</sub> H <sub>34</sub>	157, 131	295, 310	N
a <sub>9</sub>	3,3,7,12a-Tetramethyl-1,2,3,4,4a,11,12,12a-octahydrochrysene	C <sub>22</sub> H <sub>28</sub>	292, 181	168, 292	O
a <sub>10</sub>	3,4,7,12a-Tetramethyl-1,2,3,4,4a,11,12,12a-octahydrochrysene	C <sub>22</sub> H <sub>28</sub>	207, 292, 193	292	O
a <sub>11</sub>	Des-A-26,17-dinor-lupa-5,7,9,11,13-pentaene	C <sub>22</sub> H <sub>28</sub>	292, 249,	207, 292	O
a <sub>12</sub>	3,3,7-Trimethyl-1,2,3,4-tetrahydrochrysene	C <sub>21</sub> H <sub>22</sub>	218, 202	274, 274	O
a <sub>13</sub>	24,25-Dinorursa-1,3,5(10),12-tetraene	C <sub>28</sub> H <sub>40</sub>	145, 172	158, 376	N
a <sub>14</sub>	24,25-Dinoroleana-1,3,5(10),12-tetraene	C <sub>28</sub> H <sub>40</sub>	158, 172	145, 376	N
a <sub>15</sub>	Unknown	C <sub>27</sub> H <sub>34</sub>	343, 195	358, 358	
a <sub>16</sub>	24,25-Dinorlupa-1,3,5(10),20(29)-tetraene*	C <sub>28</sub> H <sub>40</sub>	145, 376	158, 376	P
a <sub>17</sub>	24,25-Dinorlupa-1,3,5(10)-triene*	C <sub>28</sub> H <sub>42</sub>	145, 378	157, 378	N
a <sub>18</sub>	Triterpenoid aromatization	C <sub>26</sub> H <sub>28</sub>	255, 239	340, 340	Q
a <sub>19</sub>	2,2,4a,9-Tetramethyl-1,2,3,4,4a,5,6,14b-octahydronicene	C <sub>26</sub> H <sub>30</sub>	342, 205	218, 342	D, R
a <sub>20</sub>	24,25,26,27-tetranor-ursa-1,3,5(10),6,8,11,13-heptaene	C <sub>26</sub> H <sub>30</sub>	257, 243	342, 342	S
a <sub>21</sub>	Unknown (isomer of a <sub>20</sub> ?)	C <sub>26</sub> H <sub>30</sub>	342, 243	257, 342	
a <sub>22</sub>	Lanosta(eupha)hexaene*	C <sub>28</sub> H <sub>38</sub>	195, 211	207, 374	H
a <sub>23</sub>	3-Methyl-24-nor-friedela-1,2,5(10)-triene	C <sub>30</sub> H <sub>46</sub>	185, 171	391, 406	T
a <sub>24</sub>	2,2,9-trimethyl-1,2,3,4-tetra-hydronicene	C <sub>25</sub> H <sub>24</sub>	342, 252	268, 324	D

\*: Tentatively identified; a: Molecular weight; References: A: Weston et al. (1989); B: Papanicolaou et al. (2000); C: Otto and Simoneit, (2001); D: Philp, (1985); E: Alexander et al. (1983); F: Noble et al. (1985); G: Logan and Eglinton, (1994); H: Jacob et al. (2007); I: Boreham et al. (1994); J: Huang et al. (2010); K: Simoneit and Mazurek, (1982); L: Alexander et al. (1994); M: Simoneit, (1977); N: Wolff et al. (1989); O: Freeman et al. (1994); P: Simoneit et al. (2003); Q: Chaffee and Johns, (1983); R: Chaffee and Fookes, (1988); S: ten Haven et al., (1992); T: Schaeffer et al. (1995), U: Kashirtsev et al. (2008); V: Sessions et al. (2013).

#### 4.5.2.1 *n*-Alkanes and isoprenoids

The total *n*-alkane concentrations of the lignite samples from the Velenje Basin are listed in Table 3 and their distribution profiles in the different lithotypes are shown in Figure 3. The distributions and abundances of *n*-alkanes vary between different lithotypes. In all three lithotypes, *n*-alkanes ranging from C<sub>15</sub> to C<sub>35</sub> were found, with a marked odd over even predominance and maximum concentrations of the *n*-C<sub>29</sub> homologue. An exception is sample No. 6 (maximum at *n*-C<sub>35</sub>). Moreover, in some gelified lithotype samples *n*-alkanes extend to *n*-C<sub>37</sub> (Fig. 3). Although the *n*-alkane patterns of all samples are dominated by long-chain homologues, the *n*-C<sub>19</sub> alkane exhibits, in addition, a considerable concentration in some gelified samples.

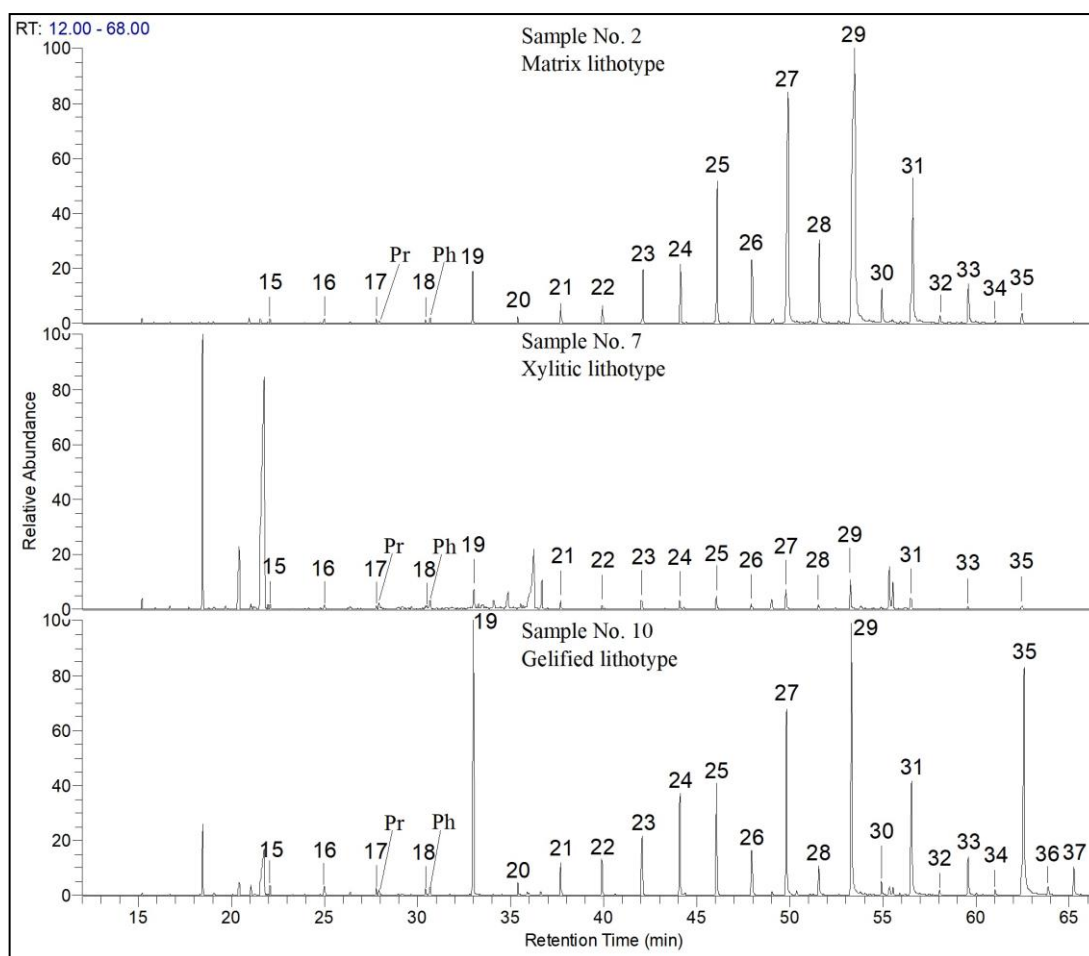


**Figure 4-3 *n*-Alkane distribution according to SIM  $m/z$  85 of representative lithotypes from Velenje Basin, Slovenia. Numbers correspond to carbon atoms in the *n*-alkane chain**

The average total *n*-alkane content (Table 3) is much higher in the gelified lithotype (125.17  $\mu\text{g/g}$  TOC) than in the matrix lithotype (51.58  $\mu\text{g/g}$  TOC), and decreases sharply in the xylitic lithotype (5.08  $\mu\text{g/g}$  TOC). This trend of decreasing levels of *n*-alkanes is consistent with the decreasing EOM content. This finding is different from results obtained from the lignite in Miocene Sokolov Basin, Czech Republic, where xylite-rich lithotypes contained a considerable concentration of *n*-alkanes (Havelcová et al., 2012). Investigations of both modern plants (Diefendorf et al., 2011; Bush and McInerney, 2013) and fossil plants (Lockheart et al., 2000; Otto et al., 2005) have shown that angiosperms consistently produce more *n*-alkanes than gymnosperms. *n*-Alkanes are present in leaf waxes of some individual gymnosperms (e.g. Pinaceae and Cupressaceae) in very low abundance (Herbin and Robins, 1968; Chikaraishi et al., 2004). The very low abundance of *n*-alkanes in the xylitic lithotype can thus be explained by the predominance of gymnosperms in the parent materials of this lithotype. The contribution

of angiosperms was much higher for the gelified and matrix lithotypes, which resulted in higher amounts of *n*-alkanes.

**Table 4-3 Concentration of some compounds and biomarker parameters calculated from the distributions of *n*-alkanes, terpenoids and hopanoids in samples from the Velenje Basin, Slovenia**

Sam- ple No.	Litho- ty- pes	<i>n</i> - Alka- ne max	<i>n</i> - Alka- nes ( $<C_{21}$ )	<i>n</i> - Alka- nes ( $C_{21}$ - $C_{25}$ )	<i>n</i> - Alka- nes ( $>C_{25}$ )	$\Sigma n$ - Alka- nes	4 $\beta$ - Eudesm- ane	4 $\alpha$ - Eudesm- ane	18- Norabiet- ane	Des- A- lupa- ne	Hop- 17(2 1)- ene	Simonel lite	Sesquiterpe- noids	Diterpen- oids	Non- hopanoid triterpen- oids	Di-/(Di- + Tri- terpenoi- ds)
$\mu\text{g/g TOC}$																
1a	G	29	16.22	20.55	59.30	99.84	19.7	44.03	0.17	0.36	25.6 0	25.57	143.14	127.13	19.67	0.87
1b	Gc	29	7.76	9.19	26.65	44.98	17.48	39.68	1.08	3.90	10.9 3	27.92	139.17	168.11	22.50	0.88
3	Gc	29	1.46	8.62	45.38	56.96	14.73	17.07	11.58	4.70	16.3 2	8.76	205.53	163.71	43.90	0.79
4	Gc	29	6.50	20.21	200.0 8	233.0 2	2.76	5.60	1.69	36.4 7	31.4 5	3.67	34.72	54.33	377.05	0.13
5	G	29	45.40	86.00	170.6 8	316.3	5.23	13.51	10.41	26.9 4	37.7 0	19.49	46.50	247.66	127.28	0.66
10	G	29	10.50	9.13	41.50	62.55	25.18	60.35	0.79	15	15.1 8	32.48	210.9	141.68	87.84	0.62
2	Mc	29	6.10	14.12	55.27	80.55	9.60	21.59	1.00	2.13	17.4 0	16.3	370.00	668.53	40.21	0.94
9	M	29	2.07	2.28	17.95	22.61	16.25	37.97	1.35	2.62	6.44	30.64	213.56	622.89	36.09	0.95
6	X	35	0.43	1.76	10.15	12.52	25.58	51.42	38.39	1.14	7.71	33.91	291.90	1510.02	10.20	0.99
7	X	29	0.31	0.50	1.16	2.06	48.30	134.62	35.52	2.61	3.56	40.42	444.59	1006.21	11.67	0.99
8	X	29	0.28	0.19	0.17	0.67	15.47	56.31	12.29	4.31	5.81	32.41	169.46	1446.45	20.88	0.99
	average of G		14.05	23.26	83.58	125.1 7	15.75	34.37	3.79	14.6 2	21.7 7	21.48	141.55	149.19	109.44	0.65
	average of M		4.09	8.20	36.61	51.58	12.93	29.78	1.18	2.38	11.9 2	23.47	291.78	645.71	38.15	0.95
	average of X		0.34	0.82	3.83	5.08	29.78	80.78	28.73	2.69	5.69	35.58	301.98	1320.89	14.25	0.99





In all samples, the concentrations of long-chain are greater than those of mid-chain *n*-alkanes, with short-chain *n*-alkanes being least abundant. In general, long-chain *n*-alkanes (>C<sub>25</sub>) are dominant in all samples, but *n*-C<sub>19</sub> and/or *n*-C<sub>35</sub> are present at considerable concentrations in some samples. The total concentration of total *n*-alkanes in the xylitic lithotype (av. 5.08 µg/g TOC, Table 3) is very low and will not be further discussed. The high concentrations of long-chain *n*-alkanes in the gelified lithotype (av. 83.58 µg/g TOC, Table 3) and the matrix lithotype (av. 36.61 µg/g TOC, Table 3) reflect the dominant contribution of higher terrestrial plants to organic matter, as these components are mainly present in epicuticular plant waxes (Eglinton and Hamilton, 1967; Cranwell, 1973; Rielley et al., 1991). The relatively low content of mid-chain *n*-alkanes (*n*-C<sub>21</sub>-*n*-C<sub>25</sub>) in the matrix lithotype (av. 8.20 µg/g TOC, Table 3) indicates low proportions of aquatic macrophytes (Ficken et al., 2000, 2002; Nott et al., 2000) in the plant community during formation of the lithotype. This is a different pattern from that of the matrix coals of the Miocene Sokolov Basin of the Czech Republic, which were dominated by mid-chain *n*-alkanes (Havelcová et al., 2012). Short-chain *n*-alkanes (<C<sub>21</sub>), which are predominantly found in algae and microorganisms (Han et al., 1968; Cranwell, 1977; Cranwell et al., 1987), were detected in the matrix lithotype samples, with an average amount of 4.09 µg/g TOC. However, the considerably higher levels of mid-chain (av. 23.26 µg/g TOC) and short-chain *n*-alkanes (14.05 µg/g TOC) (Table 3) in the gelified lithotype compared with the matrix lithotype suggest a higher input of *Sphagnum*/aquatic plants and algae/microorganisms to the organic matter, as well as wet conditions during the formation of the gelified lithotype. Wetter conditions in the peat swamp would have favored the occurrence of algae/anaerobic bacteria and aquatic plants, leading to formation of gelified rather than matrix lignites.

It is interesting to note that the C<sub>19</sub> *n*-alkane occurs at a relatively high concentration (0.62–41.5 µg/g TOC, data not shown) in some gelified lithotype samples (e.g. sample No. 10, Fig. 3), and *n*-C<sub>35</sub> is present at a relatively high concentration in some samples of all three lithotypes. The C<sub>19</sub> *n*-alkane was previously detected in green algae and anaerobic bacteria at very high concentrations (Han et al., 1968). This finding has recently been confirmed by determination of the hydrogen isotope composition of individual *n*-alkanes, which indicated that only short-chain (*n*-C<sub>18</sub> and *n*-C<sub>19</sub>) *n*-alkanes have a marked microbial component in sedimentary leaf wax under anaerobic conditions (Li et al., 2018). The relatively high *n*-C<sub>19</sub> content in the gelified lithotype could be explained by input of algae and/or anaerobic bacteria to the organic matter, because the gelified lithotype was deposited under wet conditions that were favorable for both algae/anaerobic bacteria and gelification. The C<sub>35</sub> *n*-alkane has been detected with a high abundance in the leaf wax of modern plants, such as *Bambusa* species (Li et al., 2012) and graminoids (Bush and McInerney, 2013). However, Bush and McInerney (2013) suggested that the predominance of *n*-alkanes with longer-chain-length (including *n*-C<sub>35</sub>) in graminoids could be a reflection of local climatic influences such as aridity rather than

an origin from particular plants. It is difficult to explain the origin of the high  $n$ -C<sub>35</sub> concentrations in some samples from the Velenje Basin, as there is no obvious pattern associated with the three lithotypes.

#### 4.5.2.2 Sesquiterpenoids

Sesquiterpenoids are frequently found in coal and lignite extracts. These compounds are widely used biomarkers for the maturity of organic matter (Weston et al., 1989) and the depositional environment because they are derived mostly from the essential oils, resins and ambers produced by higher plants (Simoneit, 1985; Wang and Simoneit, 1990; Wang et al., 1990). In the present study, the sesquiterpenoids in the saturated hydrocarbon fractions are characterized by high amounts of 4 $\beta$ (H)-eudesmane and 4 $\alpha$ (H)-eudesmane (up to 48.30  $\mu$ g/g TOC and 134.62  $\mu$ g/g TOC, respectively, Table 3), along with low amounts of drimane-, cadinane- and cedrane-type compounds (Fig. 2A, Table 2) in all three lithotypes. Relatively high contents of eudesmane-type sesquiterpenoids have been found previously in Tertiary coals and carbonaceous shales from Argentina (Villar et al., 1988), in coals from the Moschopotamos and Kalavryta basins of Greece (Papanicolaou et al., 2000) and in the South Sumatra Basin of Indonesia (Amijaya et al., 2006). In the aromatic hydrocarbon fractions, the sesquiterpenoids are dominated by cadalene-type compounds (e.g. cadalene, 5,6,7,8-tetrahydrocadalene and isocadalene) (Fig. 2A, Table 2). The same compounds were also detected in lignite samples from Slovenia (Bechtel et al., 2003, 2004). Although these compounds are present in all samples, the contents of total sesquiterpenoids (saturated and aromatic) vary between the three lithotypes. The xylitic lithotype has the highest total sesquiterpenoids content, with an average of 301.98  $\mu$ g/g TOC (Table 3), which is much higher than the values for the matrix lithotype (av. 291.78  $\mu$ g/g TOC) and the gelified lithotype (av. 141.55  $\mu$ g/g TOC). This is different from lignites from the Miocene Sokolov basin in the Czech Republic, where the matrix lithotypes have almost no sesquiterpenoids (Havelcová et al., 2012).

The main botanical sources of sesquiterpenoids are conifers, e.g. Pinaceae, Taxodiaceae, Podocarpaceae, Cupressaceae and Araucariaceae (Otto and Wilde, 2001), and the angiosperms such as Compositae and Dipterocarpaceae (Sukh Dev, 1989). The presence of sesquiterpenoids with an eudesmane skeleton is a non-specific indication of higher land plant sources of organic matter (Alexander et al., 1983). Previous studies have shown that eudesmanes are widely distributed in all conifer families except for Araucariaceae and Taxaceae (Otto and Wilde, 2001) and in some angiosperms (Havelcová et al., 2012, and references therein; Lu et al., 2013). The biological precursors of cadalene-type sesquiterpenoids (i.e. cadalene) are common constituents of the resins of conifers (i.e. Pinaceae, Taxodiaceae, Podocarpaceae, Cupressaceae and Araucariaceae) (Simoneit et al., 1986; Otto et al., 1997). In contrast, sesquiterpenoids such as cuparane are exclusively found in Cupressaceae s.str. (Otto and Wilde, 2001).

The very high content of eudesmane-type sesquiterpenoids suggests that conifers (except for Araucariaceae and Taxaceae) contributed to the plant community during the formation of all three lithotypes. Considering the absence of biomarkers such as cuparanes, which are restricted to species of Cupressaceae s.str (Otto and Wilde, 2001), Cupressaceae s.str might also have been absent from the plant community that provided the source material of the Velenje lignites. Furthermore, the average concentration of total sesquiterpenoids increases from the gelified lithotype to the matrix lithotype, and to the xylitic lithotype, which might suggest increasing proportions of conifers (e.g. Taxodiaceae) in the plant community of corresponding lithotypes. This finding is in agreement with a previous study of pollen assemblages, which concluded that the xylitic lignites in Slovenia originated mainly from a *Sequoia–Taxodium–Metasequoia* plant community (Šerclj, 1968).

#### 4.5.2.3 Diterpenoids and non-hopanoid triterpenoids

Diterpenoids are present in wood, roots, resins, and bark of gymnosperms (Collinson et al., 1994; Karrer, 2013) and are, therefore, valuable biomarkers for the identification of the type of precursor vegetation in lignites, sediments, and crude oils (Simoneit, 1986, 1998, 1999), whereas only a few recent angiosperms produce these compounds (Rowe, 1989; Otto and Wilde, 2001). The saturated diterpenoids in the Velenje lignite samples are represented by pimarane-, abietane-, and phyllocladane-type compounds with 19 and 20 carbon atoms (Fig. 2A, Table 2). 16 $\alpha$ (H)-Phyllocladane and abietane dominate among the diterpenoids in the saturated hydrocarbon fractions of all three lithotypes. Furthermore, 18-norabietane has a relatively high concentration in the xylitic lithotype (av. 28.74  $\mu\text{g/g}$  TOC, Table 3). These compounds were previously reported from xylitic lignites of the Miocene Sokolov basin of the Czech Republic (Havelcová et al., 2012). The diterpenoid 16 $\alpha$ (H)-phyllocladane, which is extremely abundant in xylitic lithotypes in the Velenje Basin, has also been found at high concentrations in peats (Dehmer, 1995), brown coal (Dehmer, 1988) and clay sediments (Otto et al., 1994, 1997), which all contain gymnosperm plant material from Taxodiaceae (e.g. *Taxodium*). This finding is in agreement with results from a previous study on pollen assemblages (Šerclj, 1968).

In the aromatic hydrocarbon fractions, diterpenoids are present mainly as abietane-type compounds: 19-norabieta-8,11,13-triene, dehydroabietane, simonellite and retene (Fig. 2B and Table 2) which is consistent with the observations in previous studies of lignites from Slovenia (Bechtel et al., 2003, 2004). Simonellite is the predominant compound among the aromatic diterpenoids in all analyzed samples, with a maximum concentration of 40.42  $\mu\text{g/g}$  TOC in xylitic sample No. 7 (Table 3); dehydroabietane, 19-norabieta-8,11,13-triene, and retene also exhibit relatively high abundances (Fig. 2B).

Phyllocladane-type diterpenoids are widespread in recent gymnosperms (e.g. Podocarpaceae, Araucariaceae, Cupressaceae and Taxodiaceae) (Otto et al., 1997, and references therein; Sukh Dev, 1989; Schulze and Michaelis, 1990). They should not be

used as biomarkers for individual families, but can be characteristic molecules for Pinales other than Pinaceae (with the exception of *Picea jezoensis*) (Otto et al., 1997; Otto and Wilde, 2001). The high abundance of abietane-type diterpenoids (mainly abietane, 18-norabietane, dehydroabietane, simonellite and retene) in hydrocarbon fractions (Table 3) can be generated from phyllocladane/kaurane and pimarane (Wakeham et al., 1980; Alexander et al., 1987) under acidic conditions catalyzed by clay minerals, but can also originate from labdane and abietic/pimaric acids by means of anaerobic or a combination of aerobic and anaerobic processes (Simoneit, 1986; Peters et al., 2005). There is marked variation in the total amount of gymnosperm-specific diterpenoids in both the saturated and aromatic hydrocarbon fractions in the three lithotypes (Table 3). The xylitic lithotype has the highest value of the sum of all diterpenoids, with an average value of 1320.89  $\mu\text{g/g}$  TOC (Table 3), compared with the matrix lithotype (av. 645.71  $\mu\text{g/g}$  TOC) and gelified lithotype (av. 149.19  $\mu\text{g/g}$  TOC). The variations in the total diterpenoids content suggest that gymnosperm plants made the dominant contribution to the xylitic lithotype, and that the proportion of gymnosperms in the plant community was greatest in the xylitic lithotype, less in the matrix lithotype, and less still in the gelified lithotype.

Non-hopanoid triterpenoids such as oleananes, ursanes and lupanes, which are formed by transformation of  $\beta$ -amyrin,  $\alpha$ -amyrin, lupeol, and tetrahymanol during diagenesis (Havelcová et al., 2012), are constituents of leaf waxes, bark, roots and wood (Karrer, 2013) and are significant biomarkers for angiosperm input to organic matter (Sukh Dev, 1989; Karrer, 2013). However, the use of triterpenoid composition for chemotaxonomy of angiosperms was unsuccessful yet, because many angiosperms contain  $\beta$ -amyrin and  $\alpha$ -amyrin in considerable quantities (Gülz et al., 1992; Karrer, 2013). In the lignite samples from the Velenje Basin, non-hopanoid triterpenoids are present at different concentrations in the three lithotypes. In the saturated hydrocarbon fractions of the gelified lithotype, the concentrations of these triterpenoid compounds (e.g. 19 $\alpha$  and 19 $\beta$  des-A-lupa-13(18)-ene, 10 $\alpha$  des-A-olean-13(18)-ene, 10 $\alpha$  des-A-olean-12-ene, des-A-urs-12-ene, Des-A-lupane, Fig. 2A, Table 2) are higher (109.44  $\mu\text{g/g}$  TOC, Table 3) than in the other two lithotypes. In the matrix lithotype, des-A-lupane has been detected at considerable concentrations (av. 13.74  $\mu\text{g/g}$  TOC), whereas 10 $\alpha$  des-A-olean-13(18)-ene and 10 $\alpha$  des-A-olean-12-ene are present at low levels (Fig. 2A). In the saturated hydrocarbon fractions of the xylitic lithotype, only des-A-lupane has been detected at very low abundance (av. 2.68  $\mu\text{g/g}$  TOC), whereas other triterpenoids are absent. The same trend has been found in the aromatic hydrocarbon fractions. The gelified lithotype has a relatively high concentration of aromatic triterpenoids, dominated by 24,25-dinorursa-1,3,5(10),12-tetraene, 24,25-dinoroleana-1,3,5(10),12-tetraene, 24,25-dinorlupa-1,3,5(10)-triene, 24,25,26,27-tetranor-ursa-1,3,5(10),6,8,11,13-heptaene, and lanosta(eupha)hexaene, along with low concentrations of 24,25-dinorlupa-1,3,5(10),20(29)-tetraene and 2,2,9-trimethyl-1,2,3,4-tetra-hydropicene. The triterpenoids in the aromatic hydrocarbon fractions of the matrix lithotype (24,25-

dinorursa-1,3,5(10),12-tetraene, 24,25-dinorlupa-1,3,5(10),20(29)-tetraene, 2,2,4a,9-tetramethyl-1,2,3,4,4a,5,6,14b-octahydronicene, lanosta(eupha)hexaene, and 2,2,9-trimethyl-1,2,3,4-tetra-hydronicene) are present at low levels (Fig. 2B). In the aromatic hydrocarbon fractions of the xylitic lithotype, aromatic non-hopanoid triterpenoids do not occur (Fig. 2A, Table 2). Comparing the amounts of total non-hopanoid triterpenoids in the three lithotypes, the gelified lithotype has the highest concentration, with an average of 109.44  $\mu\text{g/g}$  TOC (Table 3), followed by the matrix lithotype (av. 38.15  $\mu\text{g/g}$  TOC, Table 3) and the xylitic lithotype (av. 14.25  $\mu\text{g/g}$  TOC, Table 3). This variation of non-hopanoid triterpenoids confirms the decrease in the contribution of angiosperms to the plant community from the gelified lithotype to the matrix lithotype to the xylitic lithotype during peat accumulation.

To quantify the relative contributions of gymnosperms and angiosperms in the formation of different lithotypes in the Velenje Basin, the concentrations of diterpenoids and triterpenoids (organic-carbon normalized) were determined (Table 3), and the ratio of concentrations of the diterpenoids to the sum of diterpenoids plus non-hopanoid triterpenoids (Di-/ (Di+Tri-terpenoids)) was calculated. From the results, it is obvious that the xylitic lithotype, which has on average a Di-/ (Di+Tri-terpenoids) ratio of 0.99 (Table 3), almost exclusively originated from gymnosperm plants (e.g. conifers). This is consistent with a previous study of pollen assemblages, which indicated that the xylitic lignite in the Velenje Basin mainly originated from a gymnosperm (*Sequoia-Taxodium-Metasequoia*) plant community (Šercelj, 1968). The matrix lithotype yields slightly lower average values of the Di-/ (Di+Tri-terpenoids) ratio (0.95), suggesting predominance of gymnosperms during formation of this lithotype. The Di-/ (Di+Tri-terpenoids) ratio in the gelified lithotype ranges from 0.13 to 0.88, with an average of 0.65. Such large changes in this value indicate wide variation of the relative contributions of gymnosperm and angiosperm vegetation during formation of the gelified lithotype. The plant community of the gelified lithotype was generally dominated by gymnosperms, but angiosperm plants also made a considerable contribution and even sometimes dominated the plant community in the palaeomire.

#### 4.5.2.4 Hopanoids

Hop-17(21)-ene is the most abundant hopanoid presented in the three lithotypes in the Velenje Basin (Fig. 2A). The content of hop-17(21)-ene in the gelified and matrix lithotypes is relatively high, with average values of 21.77 and 11.92  $\mu\text{g/g}$  TOC, respectively (Table 3). In contrast, the concentration of this compound in the xylitic lithotype is only 5.69  $\mu\text{g/g}$  TOC (Table 3). Although hop-17(21)-ene, together with its homologues, are present in many immature sediments (Bottari et al., 1972; Wakeham et al., 1980; Volkman et al., 1986) and lignite samples (Bechtel et al., 2003, 2004; Zdravkov et al., 2011; Singh et al., 2016, 2017), the biological precursors of hop-17(21)-ene have not been clarified so far: it could originate from bacteria, or in some cases from ferns and

mosses in sediments (Wakeham et al., 1980; Volkman et al., 1986). Hop-17(21)-ene could also be related to the activity of iron-reducing bacteria (Wolff et al., 1992). Furthermore, Bechtel et al. (2005) found a positive correlation between the concentration of hop-17(21)-ene and GWI of Eocene Bourgas coals in Bulgaria and concluded that hop-17(21)-ene preferentially reflects microbial activity under reducing conditions. In the present study, the content of hop-17(21)-ene decreases from the gelified lithotype to the matrix lithotype, and to the xylitic lithotype. The compound might have had different origins in different lithotypes because the lignite types were formed in different depositional environments. The relatively high content of hop-17(21)-ene (21.77  $\mu\text{g/g}$  TOC) in the gelified lithotype could have originated either from iron-reducing bacteria (Wolff et al., 1992) or other anaerobic bacteria that prevailed under water/wet conditions in the mire. The xylitic lithotype was less affected by anaerobic bacteria, causing the lower abundance of hop-17(21)-ene (5.69  $\mu\text{g/g}$  TOC). Intermediate levels of this compound are present in the ungelified lithotype, and may have had a multiple origin. Although hop-17(21)-ene is present in all three lithotypes, the very low content of 17 $\beta$ ,21 $\beta$ (H)-homohopane (22R) (<0.1  $\mu\text{g/g}$  TOC), along with the absence of other kinds of hopanoids in all investigated sample, indicate a restricted influence of bacterial activity on most samples during early diagenesis resulting from the relatively high content of gymnosperms (conifers), which are highly decay-resistant plants (Zdravkov et al., 2011).

### 4.5.3 Isotopic composition of the lignites

#### 4.5.3.1 Carbon isotopes

The  $\delta^{13}\text{C}$  values of lignite samples from the Velenje Basin range from  $-25.19\text{‰}$  to  $-28.11\text{‰}$  (Table 1) and are consistent with the results of previous studies of lignites in Slovenia (Bechtel et al., 2003, 2004; Kanduč et al., 2005, 2012). However, there are variations between the three lithotypes. The  $\delta^{13}\text{C}$  values in the xylitic lithotype range from  $-25.19$  to  $-25.78\text{‰}$ , with an average of  $-25.44\text{‰}$ . These values are very similar to the  $\delta^{13}\text{C}$  values obtained from recent gymnosperm plants such as Taxodiaceae ( $-25.4\text{‰}$ ) and Araucariaceae ( $-25.9\text{‰}$ ) (Smith and Epstein, 1971). In the gelified lithotype, the  $\delta^{13}\text{C}$  values vary from  $-28.11$  to  $-27.17\text{‰}$  (av.  $-27.48\text{‰}$ , Table 1). These values are comparable to the stable carbon isotopic compositions of modern angiosperms (e.g. Iridaceae, Typhaceae and Gramineae,  $-27.7\text{‰}$  to  $-27.1\text{‰}$ ) (Smith and Epstein, 1971), but more negative compared to values obtained from fossil fragments of angiosperm wood (mean value about  $-26.0\text{‰}$ ) in lignite from the middle Miocene Lower Rhine Embayment (Lücke et al., 1999). The  $\delta^{13}\text{C}$  values of modern conifer species (Leonardi et al., 2012) and of fossil gymnosperm wood in lignites (Lücke et al., 1999; Bechtel et al., 2008) are generally higher than those of the corresponding angiosperms; for example, the  $\delta^{13}\text{C}$  values of fossil gymnosperm wood in lignite have been reported to be

approximately 2.5‰ heavier than fossil angiosperm wood from the same lignite layer (Bechtel et al., 2008). The average  $\delta^{13}\text{C}$  value of the matrix lithotype (−27.09‰) is between the values of the gelified and xylitic lithotypes.

The variations of the isotopic composition of lignites in Slovenia have previously been explained by a combination of several parameters, such as the proportions of angiosperms to gymnosperms within the peat-forming plant community, the contribution of algal or microbial biomass, biogeochemical processes, and climatic changes during the lifetime of the mire (Bechtel et al., 2003, 2004, and references therein; Kanduč et al., 2012). Gelification is the result of biochemical processes during early diagenesis, in which vegetal material is converted into peat and lignite (Diessel, 1992). The medium-term variations in  $\delta^{13}\text{C}$  values in the brown coal matrix of the middle Miocene Garzweiler seam in the Lower Rhine Embayment were explained by varying proportions of gymnosperms within the peat-forming vegetation, whereas the high-frequency oscillations were suggested to be a direct signal of environmental changes (Lücke et al., 1999). Bechtel et al. (2003) reported that the general tendency toward lower  $\delta^{13}\text{C}$  values in the lignite from Slovenia is accompanied by a generally increasing extent of gelification.

In the present study, the negative correlation ( $R^2 = 0.74$ ) between the EOM and  $\delta^{13}\text{C}$  values (Fig. 4A) shows that the low content of EOM (especially in the gymnosperm–xylitic lithotype) corresponds to high  $\delta^{13}\text{C}$  values (up to −25.19‰ in sample No. 8). This phenomenon was explained by Bechtel et al. (2002) by the facts that the low EOM is related to the low amount of free lipids present in the resins of conifers and that the  $\delta^{13}\text{C}$  values of plant lipids are 5‰–10‰ depleted relative to whole-plant tissue (Park and Epstein, 1961). Sample No. 4 (gelified lithotype) is dominated by angiosperms, as inferred from the low ratio of Di-/ (Di+Tri-terpenoids) (0.13, Table 3) and the lowest  $\delta^{13}\text{C}$  value (−28.11‰) of all the samples. Xylitic lithotype samples are dominated by gymnosperms with average ratios of Di-/ (Di+Tri-terpenoids) of 0.99 (Table 3). The difference between sample No. 4 and the xylitic lithotype is around 2.6‰. The difference is similar to that reported previously by Bechtel et al. (2008) for Cenozoic angiosperm and gymnosperm fossil wood (~2.5‰). Therefore, angiosperms did not obviously contribute to the plant community during the formation of the xylitic lithotype. Furthermore, the similarity of  $\delta^{13}\text{C}$  values in the xylitic lithotype and modern plants suggests that the precursors of the xylitic lithotype (gymnosperms) predominantly influenced the final carbon isotope composition, whereas the influence of bacterial activity in the mire on the  $\delta^{13}\text{C}$  values was obviously low. This interpretation is further supported by the positive correlation between the  $\delta^{13}\text{C}$  values and the diterpenoid contents (Fig. 4B), indicating that the variation of  $\delta^{13}\text{C}$  values was preferentially governed by the relative proportions of conifers and angiosperms in the peat-forming vegetation. The results are consistent with the suggestion of Meyers (1994) that the C/N

ratios and  $\delta^{13}\text{C}$  values of total organic matter in sediments appear to retain source information for multi-million year time periods.

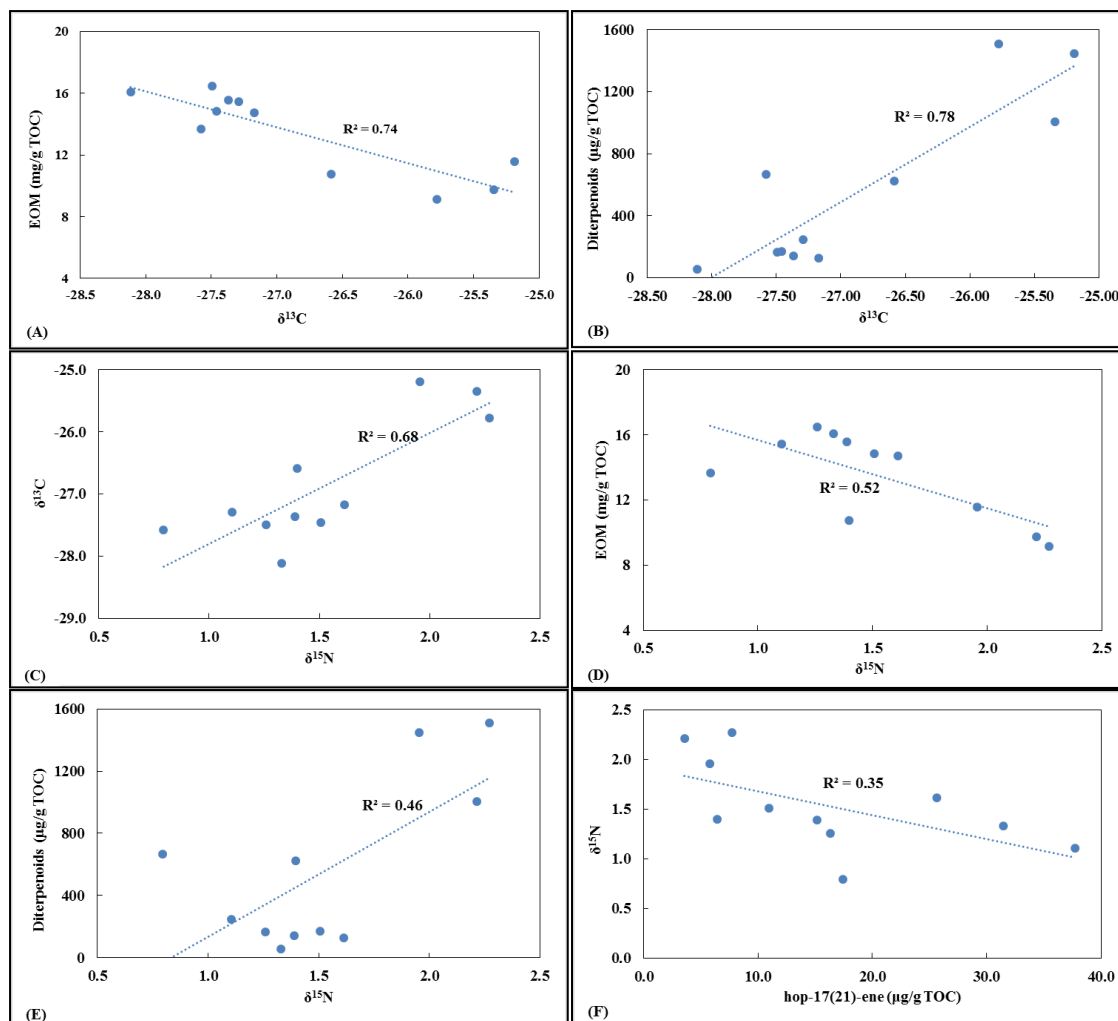


**Figure 4-4 Cross-correlation of carbon isotopic composition ( $\delta^{13}\text{C}$ ) versus (A): extractable organic matter (EOM), (B): total content of diterpenoids (Diterpenoids), (C): nitrogen isotopic composition ( $\delta^{15}\text{N}$ ), and correlation of  $\delta^{15}\text{N}$  versus (D): extractable organic matter (EOM), (E): total content of diterpenoids (Diterpenoids), (F): hop-(17)21-ene**

#### 4.5.3.2 Nitrogen isotopes

The  $\delta^{15}\text{N}$  values determined from all samples in different lithotypes range from 0.79‰ to 2.27‰ (Table 1) and the values are different in the three lithotypes. The xylitic lithotype samples have the highest values (1.96‰ to 2.27‰, average 2.15‰), which is consistent with the results from previous research on Velenje lignites (Kanduč et al., 2005, 2012). The matrix lithotype samples provide average  $\delta^{15}\text{N}$  values of 1.10‰ and the gelified lithotype shows an intermediate average value of 1.37‰, with a range of



1.10‰ to 1.61‰ (Table 1). The  $\delta^{15}\text{N}$  values of these lithotypes are higher than the values in recent plants (−3.7‰ to −2.3‰) around the Velenje Basin (Kanduč et al., 2005).

Considerable research has been carried out on the nitrogen isotopic compositions of modern plants, soils and sediments (Peters et al., 1978; Sweeney and Kaplan, 1980; Popp et al., 1997; Ader et al., 1998; Amundson et al., 2003; Meckler et al., 2007; Quan et al., 2008; Steiner et al., 2008), but data on stable nitrogen isotopes in coals/lignites are limited. The nitrogen isotopic signatures of soils and coals can be affected by many factors, such as the climate, parent materials, age/environment of deposition, maturity and degree of decomposition (Whiticar, 1996; Ader et al., 1998; Quan et al., 2008; Morford et al., 2011). The  $\delta^{15}\text{N}$  values in soils and plants have been suggested to systematically decrease with increasing mean annual precipitation (Amundson et al., 2003). Some previous studies showed that the  $\delta^{15}\text{N}$  values in soils increase with vertical depth (Natelhoffer and Fry, 1988; Shearer and Kohl, 1989; Gebauer and Schulze, 1991), which, however, was not confirmed in other soil profiles (Peoples et al., 1991; Amundson et al., 2003, and references therein). In Australian coals (age: 15 to 270 Ma), the nitrogen isotopic composition ranged from +0.8‰ to +3.7‰ and the values did not correlate with the age, rank or depositional environment of the coal; consequently, the possible use of nitrogen isotope data to characterize the deposition of coals was questioned (Rigby and Batts, 1986). Further studies suggested that the  $\delta^{15}\text{N}$  values did not change systematically with rank (vitrinite reflectance 0.4% to 7%) (Whiticar, 1996; Ader et al., 1998), but the slight differences in the  $\delta^{15}\text{N}$  values of Westphalian anthracites between the Pennsylvanian (U.S.A.) and the Bramsche Massif (Germany) suggested that nitrogen isotope data may be an indicator of the precursor flora, paleoclimate and type and degree of decomposition of the plant materials (Ader et al., 1998). In addition, bacterial alteration and mineralization of organic matter during the peat stage and early diagenesis will also influence the nitrogen isotopic composition of lignites (Kanduč et al., 2005; Rimmer et al., 2006).

In modern higher land plants, the  $\delta^{15}\text{N}$  values show a wide range of variation (Peoples et al., 1991; Handley and Raven, 1992; Craine et al., 2015; Elena et al., 2016). Different parts of individual plants (e.g. leaves, roots, and stems) can yield significant differences in  $\delta^{15}\text{N}$  values (Handley and Raven, 1992; Kolb and Evans, 2002). Even on a locally restricted scale, individual plants exhibit  $\delta^{15}\text{N}$  variation of more than 25‰ (Craine et al., 2012). This makes it difficult to compare the  $\delta^{15}\text{N}$  values in lignites with those of modern plants. In this study, correlations between  $\delta^{15}\text{N}$  values and other parameters have been conducted (Fig. 4C–F) to find out the possible factors influencing the nitrogen isotopic composition in the Velenje lignites. The relatively high correlation between the  $\delta^{13}\text{C}$  and  $\delta^{15}\text{N}$  values ( $R^2 = 0.68$  Fig. 4C) suggests that both the carbon and the nitrogen isotopic composition might have been largely influenced by the same factors, such as the abundance of the parent materials of the peat-forming vegetation and/or microbial activity.

A negative correlation between  $\delta^{15}\text{N}$  values and EOM (Fig. 4D) can be observed. The high  $\delta^{15}\text{N}$  values in the gymnosperm–xylic lithotype correspond to low EOM levels, which is very similar to the relationship between the  $\delta^{13}\text{C}$  values and EOM (Fig. 4A). As the  $\delta^{13}\text{C}$  values of plant lipids are depleted relative to whole-plant tissue (Bechtel et al., 2002, and references therein), and low EOM is related to the low amounts of free lipids present in conifer resins and/or thermally labile plant polymers (Tegelaar and Noble, 1994), the high  $\delta^{15}\text{N}$  values in the gymnosperm–xylic lithotype might also be explained by the low amounts of free lipids in conifer resin. The positive correlation between the diterpenoid concentrations and  $\delta^{15}\text{N}$  values (Fig. 4E), along with the very low content of hop-17(21)-ene (Table 3) in the gymnosperm–xylic lithotype, indicate that the precursor flora most likely influenced the nitrogen isotopic composition of the lithotype. Bacterial activity might have had a very limited effect on  $\delta^{15}\text{N}$  values in the xylic lithotype, which is further supported by the negative correlation of  $\delta^{15}\text{N}$  values and hop-17(21)-ene (Fig. 4F). In contrast, the relatively low  $\delta^{15}\text{N}$  values in the gelified and matrix lithotypes might be a result of multiple influences such as the precursor plants, gelification, and/or bacterial activity.

Previous studies have shown that the  $\delta^{15}\text{N}$  values of the less degradable stem xylem organic nitrogen are higher than those of the more degradable leaves (Handley and Raven, 1992). Moreover, residual organic matter (e.g. xylite) in alkaline/aerobic environments has higher  $\delta^{15}\text{N}$  values than their plant precursors (Diessel, 1992; Taylor et al., 1998; Zhu et al., 2000). Experimental results have further shown that the  $\delta^{15}\text{N}$  values in anoxic environments continuously decrease to about 3‰ below the initial value, whereas under oxic decay the  $\delta^{15}\text{N}$  values eventually have a value indistinguishable from the initial isotopic composition (Lehmann et al., 2002). Moreover, in clay-rich strata, fractionation of nitrogen isotopes resulting in lowered  $\delta^{15}\text{N}$  values has been reported (Delwiche and Steyn, 1970; Rau et al., 1987). These results from previous studies might explain the higher  $\delta^{15}\text{N}$  values present in the less degraded organic matter in the xylic lithotype relative to the values of the more degraded organic matter in the other two lithotypes. Assuming that microbial degradation of organic matter in peatlands results in preferential removal of the lighter organically bound nitrogen (Novák et al., 1999; Kalbitz et al., 2000; Kalbitz and Geyer, 2002), one would expect that the residual nitrogen would become heavier. The opposite is observed in the present case, i.e. the residual nitrogen is lighter in the gelified lithotype. This finding argues for a major influence of the original composition of the vegetation on the nitrogen isotopic composition of the ultimately generated peat. This view is supported by the previous suggestion that the nitrogen isotope composition of plants is largely preserved in peat (Skrzypek et al., 2008), and is further supported by the positive correlation between the  $\delta^{15}\text{N}$  values and the diterpenoid content (Fig. 4E) in this study. In addition, the relatively higher average  $\delta^{15}\text{N}$  values (1.37‰) in the gelified lithotype than the matrix lithotype (1.17‰) might be related to the higher gelification and bacterial decomposition of plant material in the

gelified lithotype. This gelification and decomposition would be expected to produce organic matter enriched in  $^{15}\text{N}$  as a result of preferential release of lighter N during the peat stage and early diagenesis (Rimmer et al., 2006).

## 4.6 Conclusions

The xylitic lithotype contains very low levels of *n*-alkanes and non-hopanoid triterpenoids compared with the other two lithotypes, but the highest contents of sesquiterpenoids (4 $\beta$ (H)-eudesmane and 4 $\alpha$ (H)-eudesmane) and extremely high levels of diterpenoids (e.g. abietane, 16 $\alpha$ (H)-phyllocladane, dehydroabietane, simonellite, and retene), indicating that conifers (preferentially Taxodiaceae) might have been the dominant precursor plants for this lithotype. This is further confirmed by the very high Di-/ (Di-+Tri-terpenoids) ratio and C/N ratio in the xylitic lithotype. The very low content of hop-17(21)-ene and the absence of hopanoids in the xylitic lithotype indicate a restricted influence of bacterial activity during lithotype formation under relatively dry/oxic conditions during early diagenesis. The low TS content in the xylitic lithotype is consistent with deposition of highly decay-resistant conifers in an oxic depositional environment. Compared with the matrix lithotype, the gelified lithotype has higher average C/N ratios and levels of total *n*-alkanes and non-hopanoid triterpenoids (e.g. des-A-lupenes, des-A-oleanenes, des-A-ursenes), but lower contents of sesquiterpenoids and diterpenoids. In addition, the range of Di-/ (Di-+Tri-terpenoids) ratio is wider for the gelified lithotype than for the matrix lithotype. These differences suggest that the gelified lithotype was affected by relatively high and varied proportions of angiosperms in the paleomire (angiosperms may even have dominated the plant community for short periods), whereas gymnosperms were the main contributors to the matrix lithotype. Furthermore, the macroscopical gelification, as well as the higher levels of TS and hop-17(21)-ene, in the gelified lithotype indicate higher activity of anaerobic bacteria under wet/humid conditions than for the matrix lithotype, which is further supported by the considerable abundance of mid-chain *n*-alkanes in the gelified lithotype.

Considering the stable isotope compositions of different lithotypes, the high correlation between the  $\delta^{13}\text{C}$  and  $\delta^{15}\text{N}$  values indicates that the carbon and nitrogen isotopic compositions might mostly have been influenced by the same factors (e.g. abundance of parent materials in the peat-forming vegetation and/or microbial activity). The negative correlations between EOM and both  $\delta^{13}\text{C}$  and  $\delta^{15}\text{N}$  values are consistent with this hypothesis. The stable carbon and nitrogen isotopic compositions of the three lithotypes apparently still reflect the composition of the original plant material in the paleomire, as is further supported by the relatively high correlation between the diterpenoid content and the  $\delta^{13}\text{C}$  and  $\delta^{15}\text{N}$  values. The dominance of gymnosperms in the precursor plant community could be the main reason for the high carbon and nitrogen isotope values in the xylitic lithotype because of the higher amount of less degradable

xylem and low mineral content in this lithotype than in the other two types. The slightly lower  $\delta^{13}\text{C}$  and higher  $\delta^{15}\text{N}$  values in the gelified lithotype than in the matrix lithotype can be explained by the higher degree of gelification and activity of anaerobic bacteria under wetter conditions in the gelified lithotype. This is further supported by the higher content of hop-17(21)-ene and TS in the gelified lithotype.



## **Chapter 5 Conclusions and outlook**

### **5.1 Conclusions**

The geochemical characteristics (e.g., petrological, organic/inorganic, elemental, mineralogical, and stable carbon and nitrogen isotopic features) of the pale and dark layers from Jinsuo Basin in Yunnan Province, Southwest China, were studied in detail for this doctoral thesis. Based on these results, a paleoenvironmental model of the formation of pale and dark layers in Jinsuo Basin is developed, and potential driving forces for the formation of these layers are discussed. The results from Jinsuo Basin were also compared with results from previous studies of pale and dark layers in lignites from other countries (e.g., Germany and Australia). Moreover, different lithotypes in the Pliocene lignites from the Velenje Basin in Slovenia were examined to discuss the similarities and differences of the formation of pale and dark layers in different locations of the world. The main conclusions in this doctoral thesis are summarized below.

#### **Characteristics of coal petrology of pale and dark layers in Jinsuo Basin**

The maceral compositions are significantly different for pale and dark layers. In pale layers, liptinite predominates with a very high volume (av. 70.2%, **Chapter 2**) over huminite (av. 18.6%) and inertinite (av. 11.2%). In dark layers, huminite (av. 79.2%) predominates the whole maceral composition. The abundance of liptinite (av. 12.7%) and inertinite (av. 8.1%) in dark layers is lower than in pale lignites (**Chapter 2**). The different maceral compositions between pale and dark layers might result from the different depositional conditions within the paleomire and/or from vegetation changes during the formation of these layers, which is reflected in the differences in maceral indices (e.g., TPI, VI, GI, and GWI). The high TPI values (>2), high GI values (>1), high VI values (>2), and variable GWI values in dark layers suggest a good preservation of organic matter from the mostly woody vegetation and a high degree of gelification of these organic materials, and also indicate that the dark layers were formed under wet/humid and less oxic conditions with variable influence of groundwater compared with the pale layers. In contrast, the low TPI value (av. 0.9), low GI value (av. 0.5), low VI value (av. 0.31), and the variable GWI values imply generally poor organic matter preservation in the pale layers, resulting either from the dominance of herbaceous plants or intensive destruction of woody tissues by bacterial/fungal activity under relatively oxic conditions.

### **Elemental and mineralogical characteristics of pale and dark layers in Jinsuo Basin**

The average TOC content in pale lignite layers (av. 52.5%) is slightly higher than the content in dark lignite layers (av. 51.3%) in the Jinsuo Basin (**Chapter 2**). The TOC content of the lignites in Jinsuo Basin is also generally higher than the values obtained from different lithotypes (av. 50.9%, 21.3%, and 41.2% for gelified/dark, matrix, and xylitic/pale lithotypes, respectively) from the Velenje Basin in Slovenia (**Chapter 4**). The mean carbon/nitrogen ratios in pale layers (av. 60.6) and dark layers (av. 40.8) show a large difference in the lignites from Jinsuo Basin (**Chapter 2**) as well as the lithotypes (xylitic lithotype, av. 86.5; gelified lithotype av. 35.5; and matrix lithotype, av. 27.7) from Velenje Basin in Slovenia (**Chapter 4**). The variation of the carbon/nitrogen ratios probably results from the change of proportions of gymnosperms and angiosperms in the peat-forming mires.

The pale layers are characterized by higher average contents of SiO<sub>2</sub> (7.22%), TiO<sub>2</sub> (0.42%), Al<sub>2</sub>O<sub>3</sub> (3.31%), Fe<sub>2</sub>O<sub>3</sub> (0.79%), and Zr (123.5 ppm) compared with dark layers (**Chapter 3**). Other major element oxides show similar abundances in pale and dark layers. The differences in these elements may be due to the different depositional conditions during the formation of pale and dark layers. Quartz of detrital origin dominates in pale layers, and its morphology is characterized by large, angular to semi-round grains, whereas small and fine quartz particles fill the cells of organic matter, showing an authigenic characteristic in dark layers. The authigenic quartz (e.g., cell-filling quartz) in dark layers most likely originates from alteration of pre-existing detrital minerals in the peat mire caused by chemical weathering under wet/humid depositional conditions. The low correlations of SiO<sub>2</sub> versus Al<sub>2</sub>O<sub>3</sub> and K<sub>2</sub>O, and the high correlation between Al<sub>2</sub>O<sub>3</sub> and K<sub>2</sub>O, imply that the silica in the pale lignites occurs mostly as independent quartz, whereas the high correlation of SiO<sub>2</sub> versus Al<sub>2</sub>O<sub>3</sub> and K<sub>2</sub>O indicates that the silica is largely associated with Al and K minerals in dark lignites.

### **Biomarkers of different lithotypes in Jinsuo Basin and Velenje Basin**

Both pale and dark layers in lignites from Jinsuo Basin have relatively high concentrations of long-chain *n*-alkanes, which are a characteristic feature of the predominance of the high terrestrial plants, but very low contents of *n*-C<sub>23</sub> and *n*-C<sub>25</sub> alkanes indicate that both kinds of layers do not originate from Sphagnum peat. The extremely high concentration of triterpenoids (av. 562.7 µg/g TOC, **Chapter 2**) and the very low Di/(Di+Tri-terpenoids) value (av. 0.07) in dark layers suggest that angiosperms were almost the only member of the plant community in the basin during the formation of dark layers. However, the relatively high diterpenoid content (av. 128.0 µg/g TOC) and the wide range of Di/(Di+Tri-terpenoids) values (0.03 to 0.85) in pale layers imply that gymnosperms contributed with various proportions to the plant community during the formation of pale layers. Furthermore, intensive aerobic bacterial

activity in pale layers is inferred from the high abundance of hopanoids (771.2  $\mu\text{g/g}$  TOC, **Chapter 2**) in pale layers.

Compared with pale and dark layers in Jinsuo Basin, the xylitic (pale) lithotype in Velenje Basin contains very low levels of *n*-alkanes and non-hopanoid triterpenoids, but very high levels of sesquiterpenoids and extremely high levels of diterpenoids, indicating that conifers were the dominant precursor plants for this lithotype (**Chapter 4**). In addition, gymnosperms were also the main contributors to the matrix lithotype. The very low content of hop-17(21)-ene and the absence of hopanoids in the xylitic (pale) lithotype indicate a restricted influence of bacterial activity under dry/cold conditions during peat formation in the Velenje Basin. The variation of the Di-/(Di+Tri-terpenoids) ratio of the gelified (dark) lithotype suggests variation in the contribution of angiosperms in the paleomire. The macroscopical gelification, as well as the high levels of TS and hop-17(21)-ene in the gelified (dark) lithotype, indicate high activity of anaerobic bacteria under wet/humid conditions.

#### **Stable isotopic characteristics of different lithotypes in Jinsuo and Velenje basins**

Pale layers in Jinsuo Basin generally have lower  $\delta^{13}\text{C}$  values (av.  $-27.01\text{‰}$ , **Chapter 3**) compared with dark layers (av.  $-26.38\text{‰}$ ), and the  $\delta^{13}\text{C}$  values of fossil wood (av.  $-24.79\text{‰}$ ) are generally higher than those in the bulk layer. Fusain samples have maximum  $\delta^{13}\text{C}$  values (av.  $-24.19\text{‰}$ ). The average  $\delta^{13}\text{C}$  value in samples of the xylitic (pale) lithotype (av.  $-25.44\text{‰}$ , **Chapter 4**) in the Velenje Basin is higher than the value in both pale and dark layers in Jinsuo Basin, but the gelified (dark) lithotype and matrix lithotype in the Velenje Basin both have  $\delta^{13}\text{C}$  values (av.  $-27.48\text{‰}$  and  $-27.09\text{‰}$ , respectively) similar to those of pale and dark layers in the Jinsuo Basin.

The weak negative correlation between the  $\delta^{15}\text{N}$  and  $\delta^{13}\text{C}$  values indicates that the stable carbon and nitrogen compositions of pale and dark layers in the Jinsuo Basin might have been influenced by different factors. The very high amounts of liptinite macerals and high concentrations of *n*-alkanes and hopanoids resulted in a depletion of  $^{13}\text{C}$  in pale lignites, while the wet/subaqueous depositional environment could probably contribute to the heavy carbon isotope compositions of dark layers in the Jinsuo Basin. As there is no obvious tendency of  $\delta^{15}\text{N}$  values between pale and dark layers, as well as in the total profile, the stable nitrogen isotope compositions in the Jinsuo Basin are probably influenced by multiple factors (e.g., parent plants, depositional conditions, and bacterial activities). However, a high correlation between  $\delta^{13}\text{C}$  and  $\delta^{15}\text{N}$  values was found in different lithotypes in the Velenje Basin, indicating that the carbon and nitrogen isotopic compositions probably have been mostly influenced by the same factors, such as original plant composition in the mire, which is further supported by the relatively high correlation between the diterpenoid content and the  $\delta^{13}\text{C}$  and  $\delta^{15}\text{N}$  values. The slightly lower  $\delta^{13}\text{C}$  and higher  $\delta^{15}\text{N}$  values in the gelified lithotype than in the matrix lithotype



suggest that the degree of gelification and activity of anaerobic bacteria might also have influenced the  $\delta^{13}\text{C}$  and  $\delta^{15}\text{N}$  values.

### **Paleoenvironmental models for the formation of pale and dark layers in Jinsuo Basin**

The paleoenvironmental model for the formation of pale and dark layers in the Jinsuo Basin is proposed in **Chapter 3** based on all the data discussed in this thesis. The thin pale layers (5–25 cm thick) were probably formed during periods of short-term cold, dry climatic conditions following each period of uplift of the Tibetan Plateau, which produced a low water table in the basin. During these relatively dry and cooler periods, the abundance of angiosperm plants (such as *Cyclobalanopsis* and *Castanopsis*) became restricted, whereas gymnosperms and shrubby plants extended from the eastern and western mountains (**Chapter 3**). Under the less wet and more oxic conditions, plant materials underwent strong aerobic decomposition, and the slight stepped uplift of the surrounding mountains and the increasing Asian monsoon also resulted in an increasing influx of detrital minerals (e.g., quartz) and elements (e.g.,  $\text{TiO}_2$  and Zr) (**Chapter 3**) into the paleomire. Finally, a poorly preserved mineral groundmass of pale layers formed. In contrast, the thick dark layers (tens to hundreds of centimeters thick) most likely formed during long-term stable conditions with a warm, humid tropical/subtropical climate, which resulted in a relatively high water table in the basin during periods of little to no uplift activity of the Tibetan Plateau. Angiosperm trees (such as *Cyclobalanopsis* and *Castanopsis*) dominated the plant community, in association with some angiosperm shrubs and herbaceous plants during the formation of dark layers. The gymnosperm trees were confined to the eastern and western mountains. During the warm periods, intensive rainfall events within the basin resulted in formation of a paleomire with a relatively higher water table and greater degree of gelification of organic material (**Chapter 2**), which finally resulted in the formation of well-preserved, gelified dark layers.

### **Driving forces for formation of pale and dark layers in Jinsuo Basin**

Two potential driving forces are suggested for the formation of pale and dark layers in the Jinsuo Basin. One could be the co-influence of stepwise uplift of the Tibetan Plateau and the approximate co-occurrence of intensive Asian monsoons. During the formation of thin pale layers, the Asian monsoon intermittently strengthened as a result of the phased uplift of the Tibetan Plateau, which is associated with global cooling, resulting in a locally cold, dry climate and low/fluctuating water table in the study area. Gymnosperms (such as *Pinus yunnanensis*) extended from the mountains into the basin during these short periods. In contrast, the long-term stable geological conditions with a regionally tropical/subtropical warmer and more humid climate compared with the modern climate contributed to the formation of thick angiosperm-dominated dark layers. Another hypothesis to explain the occurrence of pale and dark layers could be related to

climate change (e.g., ice-sheet cyclic fluctuations and insolation cycles) forced by orbital periodicities [e.g., obliquity (41 kyr)] during the Pliocene. Although previous studies suggested that the influence of orbital cycles can be recorded in coal and lignite sequences (Large et al., 2003, 2004; Jones et al., 1997; Yan et al., 2019), additional studies (e.g., exact age dating, determination of color index, and paleomagnetic and spectral analyses) need to be carried out to clarify whether this hypothesis is also valid to explain the alternating formation of pale and dark layers in the Jinsuo Basin. Probably, interactions between different factors might have contributed to the formation of pale and dark layers in the Jinsuo Basin lignites.

### **Similarities and differences of pale and dark layers in Cenozoic lignite basins all over the world**

Comparison of the pale and dark layers in the Miocene Lower Rhine Basin in Germany, the Oligocene-Miocene Gippsland Basin in Australia, the Pliocene lignites from the Jinsuo Basin in China, and the Pliocene Velenje lignite basin in Slovenia reveals some similarities and differences (Fig. 5-1). The depositional model of lignites from the Jinsuo Basin and Velenje Basin are generally consistent with the “dry-light model” (pale layers were formed under dry conditions, whereas dark layers were formed under wet conditions) proposed by Holdgate et al. (2014, 2016) for the pale and dark layers from the Lower Rhine Basin in Germany and the Gippsland Basin in Australia. The gelification degree increases from pale to dark layers for all four basins, showing the increase of anaerobic conditions from pale to dark lithotypes. However, the plant community in the formation of different lithotypes is not the same in different basins. In all basins, the source materials of dark layers are mostly composed of angiosperm plants, particularly in the Jinsuo Basin, in which the plant community was almost only composed of angiosperm plants during the formation of dark layers, whereas some dark layers from Gippsland Basin were also dominated by gymnosperms. The pale lithotype in the Gippsland Basin mostly originated from angiosperms, whereas the pale lithotype in the Jinsuo and Lower Rhine basins originated from both gymnosperms and angiosperms. In the Jinsuo Basin, gymnosperm plants even dominate in some pale layers, while the pale lithotype in the Velenje Basin exclusively originates from gymnosperms. According to these results, the depositional conditions (dry/aerobic for pale/light lithotypes, wet/anaerobic for dark lithotypes) can apparently be regarded as the main factor for the color changes of different lithotypes in different places, which also resulted in the local change of the plant community during the formation of different lithotypes. The different ages and locations (latitudes) of the four basins must also be considered as important factors for the plant composition in the different basin. The subtropic and tropic climate in the Gippsland and Jinsuo basins, respectively, could have contributed to the spread of angiosperms in most lithotypes, whereas a temperate climate might have favored the contribution of gymnosperms to the lithotypes in the Lower Rhine and Velenje basins.

However, it is hard to explain the nearly opposite plant composition (gymnosperms vs. angiosperms) of the pale and dark lithotypes in the Jinsuo and Gippsland basins, and there might be no single reason for this difference, and the different locations and regional climate and plants around individual basins may contribute to the difference.

Depositional conditions	Gippsland lignites, Australian		Lower Rhine lignites, Germany			Jinsuo lignites, Yunnan Province, China		Velenje lignites, Slovenia		
	Lithotypes Quantitative Colourimetry	Palynology	Colour	Facies	Palynology	Lithotypes Colour	Palynology	Lithotypes Colour	Palynology	
DRY ↑ Gelification ↓ WET	Pale	Angiosperms dominated with small parts of gymnosperms	Bright	HB	No preserved plant	Pale layers	Gymnosperms and angiosperms, some layers gymnosperms dominated	Xylitic (Pale) lithotypes	Exclusive gymnosperms	
	Light		Light brown	A	Bush swamp			Angiosperms and gymnosperms		
	Medium-Light		Light-dark brown	M	Sciadopitys bog			Gymnosperms dominated		
	Medium-Dark		Black-dark brown	P	Pinus bog	Gymnosperms dominated				
	Dark	Gymnosperm dominated	Dark brown	K	Conifer	Gymnosperms dominated	Dark layers	Almost only angiosperms	Matrix lithotypes	Gymnosperms dominated
	Laminated Dark	Polypodiopsida and angiosperms	Dark	G	Reed marsh	Gymnosperms and angiosperms	Dark layers	Almost only angiosperms	Gelified (Dark) lithotypes	Gymnosperms and angiosperms
			Dark	F	alluvial forests	Angiosperms dominated				

Figure 5-1 Summary results of different lithotypes from Jinsuo Basin, Lower Rhine Basin, Gippsland Basin and Velenje Basin

## 5.2 Outlook

This thesis describes a comprehensive investigation to clarify the occurrence of pale and dark lignite layers in the Pliocene Jinsuo Basin in Yunnan Province, southwestern China, using coal petrology, organic and inorganic geochemistry, and stable isotopic analysis. Different lithotypes from the Pliocene Velenje Basin in Slovenia have also been studied by organic geochemistry and stable isotopic methods in this project for comparison with the results from the Jinsuo Basin. The aim of the project was to identify the driving force for the formation of successive pale and dark layers and their possible relationship with depositional conditions and local/global paleoenvironmental changes. Finally, a depositional model for the formation of pale and dark lignite was developed in this thesis.

There are still some open questions that need to be solved and some further work has to be done to provide additional evidence, not only for the formation of the pale and dark layers in lignite from the Jinsuo Basin, but also for the pale and dark layers in other lignite basins in Yunnan Province as well as in other lignites all over the world.

- 1) For the pale and dark layers in lignite from the Jinsuo Basin, the results from coal petrology, biomarker proxies, elements, mineral composition, and stable carbon and nitrogen isotopes have been comprehensively used to establish a paleoenvironmental model of the formation of pale and dark layers and to provide evidence for the influence of climate changes on the paleovegetation in the basin. In the future, paleobotanical studies should be carried out to quantify pollen and

identify fossil wood pieces collected from the pale and dark layers. The fusain particles should be investigated by various microscopic methods, including SEM to provide possible evidence for an origin of the fusain layers and fusain particles from wildfires in the basin during the Pliocene. With these data, more evidence will be provided to identify changes in the ecosystem in the Jinsuo Basin during the Pliocene, such as the evolution of the plant community and the frequency of wildfires in the basin. The study of fusain bands in the lignites from Jinsuo Basin might also provide information on local climate change during the Pliocene.

- 2) Pale and dark layers in other lignite basins from Yunnan Province should be sampled in the future for comparative studies to establish evidence for possible regional links of the formation of pale and dark layers in Yunnan Province. The occurrence of pale and dark layers has previously been reported from the late Miocene to late Pliocene in several lignite basins in Yunnan Province (Lu and Zhang, 1986, 1989; Fu et al., 1987; Ming et al., 1994; Yu et al., 1997). Although some research has been carried out on the lignite from these basins, systematic studies of all these pale and dark layers in different basins and of different geological ages have not yet been carried out. The links between the occurrence of pale and dark layers in Yunnan Province and the local plant community, regional climate, or geological evolution need to be investigated in more detail for a better understanding of the formation of these pale and dark layers in the Pliocene lignite basin in Yunnan Province.
- 3) Investigations to identify the forces driving the formation of the Pliocene pale and dark layers in Yunnan Province have to be intensified and additional methods have to be applied. Some possible reasons for the development of pale and dark layers have been discussed in **Chapter 2** and **Chapter 3**, such as changes in the plant community, the movement of the Tibetan Plateau, the intensity of the Asian monsoon, the orbital periodicities, and global climate change. However, it is not yet clear which of these factors is dominant and how they interact with each other. It is difficult to quantify the influence of individual factors on the formation of the pale and dark layers, but some interactions have already been established. For example, the intensity of the Asian monsoon is related to the movement of the Tibetan Plateau (An et al., 2001; Sun et al., 2015), which will also influence the change of vegetation (Clemens et al., 1996). Furthermore, the orbital forcing at the obliquity and precession periods also influences the strength of the Asian monsoon and Northern Hemisphere glaciation (Clemens et al., 1996; Willis et al., 1999b), which finally results in the vegetation and climate changes during and after the Miocene. Large et al. (2003, 2004) has shown that the influence of orbital cycles is recorded in subbituminous and lignite coals (Miocene) and further studies (e.g., color index, paleomagnetic, and spectral analysis) are required in

our case for the pale and dark layers from Yunnan Province to clarify this hypothesis in the future.

- 4) Dating the ages of samples from the Jinsuo Basin is required to identify the time span between development of consecutive pale layers. If orbital cycles were the driving force, one would expect similar age differences between the pale layers of 41 kyr years. The precise age of lignite seams is difficult to determine, but paleomagnetic analysis might help for identifying the time scale of coal/lignite basin strata. Alternatively, time scales of coal deposition may be calculated using either total carbon content in conjunction with estimated long-term rates of carbon accumulation or thickness in conjunction with estimated rates of peat accumulation. The influence of orbital cycles recorded from lignite/coal seams might also be identified from the oscillation of the color index, the vitrinite/inertinite quotient, power spectrum analysis, and geophysical logs. These data could be used to exam whether the fluctuation of these parameters in lignite basins were consistent with the oscillation of orbital cycles during the same time scale.
- 5) On a global scale, the pale and dark layers in lignites from China, Germany, and Australia (Hagemann and Wolf, 1987; Ming et al., 1994; Holdgate et al., 2016; Korasidis et al., 2016; Liu et al., 2018) were formed during the Cenozoic period (mostly from Miocene to Pliocene). The paleoenvironmental information recorded in the pale and dark layers from these lignite basins probably has great significance for reconstruction of the global climate change, and the evolution of the terrestrial ecosystems during the Cenozoic. Systematic and comparative studies of the pale and dark layers in lignite basins around the world could provide more useful information on these topics, such as reconstruction of the concentration of greenhouse gas, interaction of the intensity of Asian monsoon with carbon cycles, history of the formation of the Tibetan Plateau, and the variation of ice sheets.
- 6) China has many lignite basins, but most previous studies focused on the utilization of lignite for industry and combustion in power plants, whereas the geological information stored in lignite seams for the reconstruction of paleoenvironment conditions has not been explored sufficiently. The well-preserved lignite seams in China (especially the large lignite basins of Inner Mongolia) not only provide a record of former changes of the regional vegetation, hydrology, carbon accumulation, and depositional environment, but they can also be used for long-term and high-resolution studies of the carbon cycle and global climate changes during peat formation over periods of more than several million years. The identification of an internal astronomical time scale in lignite is an important step toward realizing the potential of lignites to extend our knowledge of the earth's terrestrial system (Large et al., 2004). In the future, comprehensive

studies of these lignite seams in various basins in China will help us to better understand the evolution of Earth's terrestrial climate during the Cenozoic Era.



## References

- Ader, M., Boudou, J.P., Javoy, M., Goffé, B., Daniels, E., 1998. Isotope study on organic nitrogen of Westphalian anthracites from the Western middle field of Pennsylvania (U.S.A.) and from the Bramsche Massif (Germany). *Organic Geochemistry* 29, 315–323.
- Alexander, R., Kagi, R., Noble, R., 1983. Identification of the bicyclic sesquiterpenes drimane and eudesmane in petroleum. *Journal of the Chemical Society, Chemical Communications* 226–228.
- Alexander, R., Kagi, R.I., Singh, R.K., Sosrowidjojo, I.B., 1994. The effect of maturity on the relative abundances of cadalene and isocadalene in sediments from the Gippsland Basin, Australia. *Organic Geochemistry* 21, 115–120.
- Allardice, D., George, A., Hausser, D., Neubert, K., Smith, G., 1977. The variation of Latrobe valley brown coal properties and utilisation parameters with lithotype. State Electricity Commission of Victoria, Research and Development Department Report, Rep No. 342, 30 pp.
- Amijaya, H., Littke, R., 2005. Microfacies and depositional environment of Tertiary Tanjung Enim low rank coal, South Sumatra Basin, Indonesia. *International Journal of Coal Geology* 61, 197–221.
- Amijaya, H., Schwarzbauer, J., Littke, R., 2006. Organic geochemistry of the Lower Suban coal seam, South Sumatra Basin, Indonesia: Palaeoecological and thermal metamorphism implications. *Organic Geochemistry* 37, 261–279.
- Amundson, R., Austin, A.T., Schuur, E.A.G., Yoo, K., Matzek, V., Kendall, C., Uebersax, A., Brenner, D., Baisden, W.T., 2003. Global patterns of the isotopic composition of soil and plant nitrogen. *Global Biogeochemical Cycles* 17. doi:10.1029/2002GB001903
- An, Z., Kutzbach, J.E., Prell, W.L., Porter, S.C., 2001. Evolution of Asian monsoons and phased uplift of the Himalaya - Tibetan plateau since Late Miocene times. *Nature* 411, 62–66.
- An, Z., Wang, S., Wu, X., Chen, M., Sun, D., Liu, X., Wang, F., Li, L., Sun, Y., Zhou, W., Zhou, J., Liu, X., Lu, H., Zhang, Y., Dong, G., Qiang, X., 1999. Eolian evidence from the Chinese Loess Plateau: the onset of the Late Cenozoic Great Glaciation in the Northern Hemisphere and Qinghai-Xizang Plateau uplift forcing. *Science in China Series D: Earth Sciences* 42, 258–271.
- An, Z., Wu, G., Li, J., Sun, Y., Liu, Y., Zhou, W., Cai, Y., Duan, A., Li, L., Jiangyu, M., Hai, C., Zhengguo, S., Liangcheng, T., Hong, Y., Hong, A., Hong, C., Juan, F., 2015. Global Monsoon Dynamics and Climate Change. *Annual Review of Earth and Planetary Sciences* 43, 29–77.
- Anderson, K.B., Mackay, G., 1990. A review and reinterpretation of evidence concerning the origin of Victorian brown coal. *International Journal of Coal Geology* 16, 327–347.
- Andrejko, M.J., Raymond, R., Cohen, A.D., 1983. Biogenic silica in peats: possible source for chertification in lignites, in: *Proceedings of Workshop on Minerals in Peat: Its Occurrence, Form and Distribution*. pp. 25–37.
- ASTM Standard D3174-11, 2011. *Annual Book of ASTM Standards*. Test Method for Ash in the Analysis Sample of Coal and Coke. ASTM International West Conshohocken, PA.
- Bechtel, A., Gratzner, R., Sachsenhofer, R.F., Gusterhuber, J., Lücke, A., Püttmann, W., 2008. Biomarker and carbon isotope variation in coal and fossil wood of Central Europe through the Cenozoic. *Palaeogeography, Palaeoclimatology, Palaeoecology* 262, 166–175.
- Bechtel, A., Hámor-Vidó, M., Sachsenhofer, R.F., Reischenbacher, D., Gratzner, R., Püttmann, W., 2007a. The middle Eocene Márkushegy subbituminous coal (Hungary): Palaeoenvironmental implications from petrographical and geochemical studies. *International Journal of Coal Geology* 72, 33–52.
- Bechtel, A., Markic, M., Sachsenhofer, R.F., Jelen, B., Gratzner, R., Lücke, A., Püttmann, W., 2004. Palaeoenvironment of the upper Oligocene Trbovlje coal seam (Slovenia). *International Journal of Coal Geology* 57, 23–48.
- Bechtel, A., Reischenbacher, D., Sachsenhofer, R.F., Gratzner, R., Lücke, A., 2007b. Paleogeography and paleoecology of the upper Miocene Zillingdorf lignite deposit (Austria). *International Journal of Coal Geology* 69, 119–143.
- Bechtel, A., Reischenbacher, D., Sachsenhofer, R.F., Gratzner, R., Lücke, A., Püttmann, W., 2007. Relations of petrographical and geochemical parameters in the middle Miocene Lavanttal lignite (Austria). *International Journal of Coal Geology* 70, 325–349.
- Bechtel, A., Sachsenhofer, R., Zdravkov, A., Kostova, I., Gratzner, R., 2005. Influence of floral assemblage, facies and diagenesis on petrography and organic geochemistry of the Eocene Bourgas coal and the Miocene Maritza-East lignite (Bulgaria). *Organic geochemistry* 36, 1498–1522.
- Bechtel, A., Sachsenhofer, R.F., Gratzner, R., Lücke, A., Püttmann, W., 2002. Parameters determining the carbon isotopic composition of coal and fossil wood in the Early Miocene Oberdorf lignite seam (Styrian Basin, Austria). *Organic Geochemistry* 33, 1001–1024.



- Bechtel, A., Sachsenhofer, R.F., Markic, M., Gratzner, R., Lücke, A., Püttmann, W., 2003. Paleoenvironmental implications from biomarker and stable isotope investigations on the Pliocene Velenje lignite seam (Slovenia). *Organic Geochemistry* 34, 1277–1298.
- Bechtel, A., Widera, M., Sachsenhofer, R.F., Gratzner, R., Lücke, A., Woszczyk, M., 2007c. Biomarker and stable carbon isotope systematics of fossil wood from the second Lusatian lignite seam of the Lubstów deposit (Poland). *Organic Geochemistry* 38, 1850–1864.
- Benner, R., Fogel, M.L., Sprague, E.K., Hodson, R.E., 1987. Depletion of  $^{13}\text{C}$  in lignin and its implications for stable carbon isotope studies. *Nature* 329, 708–710.
- Bingham, E.M., McClymont, E.L., Väiliranta, M., Mauquoy, D., Roberts, Z., Chambers, F.M., Pancost, R.D., Evershed, R.P., 2010. Conservative composition of n-alkane biomarkers in Sphagnum species: Implications for palaeoclimate reconstruction in ombrotrophic peat bogs. *Org. Geochem.* 41, 214–220.
- Blackburn, D., Sluiter, I., 1994. The Oligo–Miocene coal floras of south-eastern Australia. In: Hill, R.S. (Eds) 'History of the Australian vegetation: Cretaceous to Recent' Cambridge University Press: Cambridge, UK, pp. 328–367.
- Bonan, G.B., Pollard, D., Thompson, S.L., 1992. Effects of boreal forest vegetation on global climate. *Nature* 359, 716–718.
- Boreham, C.J., Summons, R.E., Roksandic, Z., Dowling, L.M., Hutton, A.C., 1994. Chemical, molecular and isotopic differentiation of organic facies in the Tertiary lacustrine Duaringa oil shale deposit, Queensland, Australia. *Organic Geochemistry* 21, 685–712.
- Bottari, F., Marsili, A., Morelli, I., Pacchiani, M., 1972. Aliphatic and triterpenoid hydrocarbons from ferns. *Phytochemistry* 11, 2519–2523.
- Brezigar, A., 1986. Coal seam of the Velenje coal mine. *Geologija* 28/29, 319–336.
- Brezigar, A., Kosi, G., Vrhovšek, D., Velkoverh, F., 1985. Paleontological investigations of the Plio-Quaternary beds of the Velenje depression. *Geologija* 28, 93–119.
- Briggs, J., Large, D.J., Snape, C., Drage, T., Whittles, D., Cooper, M., Macquaker, J.H., Spiro, B.F., 2007. Influence of climate and hydrology on carbon in an early Miocene peatland. *Earth and Planetary Science Letters* 253, 445–454.
- Bucha, M., Jędrysek, M.-O., Kufka, D., Pleśniak, Ł., Marynowski, L., Kubiak, K., Błaszczuk, M., 2018. Methanogenic fermentation of lignite with carbon-bearing additives, inferred from stable carbon and hydrogen isotopes. *International Journal of Coal Geology* 186, 65–79.
- Burhan, R., Trendel, J., Adam, P., Wehrung, P., Albrecht, P., Nissenbaum, A., 2002. Fossil bacterial ecosystem at methane seeps: origin of organic matter from Be'eri sulfur deposit, Israel. *Geochimica et Cosmochimica Acta* 66, 4085–4101.
- Bush, R.T., McInerney, F.A., 2013. Leaf wax n-alkane distributions in and across modern plants: implications for paleoecology and chemotaxonomy. *Geochimica et Cosmochimica Acta* 117, 161–179.
- Calder, J.H., Gibling, M.R., Mukhopadhyay, P.K., 1991. Peat formation in a Westphalian B piedmont setting, Cumberland Basin, Nova Scotia; implications for the maceral-based interpretation of rheotrophic and raised peatmires. *Bulletin de la Société Géologique de France* 162, 283–298.
- Cernusak, L.A., Tcherkez, G., Keitel, C., Cornwell, W.K., Santiago, L.S., Knohl, A., Barbour, M.M., Williams, D.G., Reich, P.B., Ellsworth, D.S., Dawson, T.E., Griffiths, H.G., Farquhar, G.D., Wright, I.J., 2009. Why are non-photosynthetic tissues generally  $^{13}\text{C}$  enriched compared with leaves in  $\text{C}_3$  plants? Review and synthesis of current hypotheses. *Functional Plant Biology* 36, 199–213.
- Cernusak, L.A., Winter, K., Aranda, J., Turner, B.L., 2008. Conifers, Angiosperm Trees, and Lianas: Growth, Whole-Plant Water and Nitrogen Use Efficiency, and Stable Isotope Composition ( $\delta^{13}\text{C}$  and  $\delta^{18}\text{O}$ ) of Seedlings Grown in a Tropical Environment. *Plant Physiology* 148, 642–659.
- Chaffee, A., Johns, R., Baerken, M., De Leeuw, J., Schenck, P., Boon, J., 1984. Chemical effects in gelification processes and lithotype formation in Victorian brown coal. *Organic Geochemistry* 6, 409–416.
- Chaffee, A.L., Fookes, C.J.R., 1988. Polycyclic aromatic hydrocarbons in Australian coals-III. Structural elucidation by proton nuclear magnetic resonance spectroscopy. *Organic Geochemistry* 12, 261–271.
- Chaffee, A.L., Johns, R.B., 1983. Polycyclic aromatic hydrocarbons in Australian coals. I. Angularly fused pentacyclic tri- and tetraaromatic components of Victorian brown coal. *Geochimica et Cosmochimica Acta* 47, 2141–2155.
- Chang, Z., Xiao, J., Lü, L., Yao, H., 2010. Abrupt shifts in the Indian monsoon during the Pliocene marked by high-resolution terrestrial records from the Yuanmou Basin in southwest China. *Journal of Asian Earth Sciences* 37, 166–175.
- Chi, Y., Fang, X., Song, C., Miao, Y., Teng, X., Han, W., Wu, F., Yang, J., 2013. Cenozoic organic carbon isotope and pollen records from the Xining Basin, NE Tibetan Plateau, and their palaeoenvironmental significance. *Palaeogeography, Palaeoclimatology, Palaeoecology* 386, 436–444.
- Chikaraishi, Y., Naraoka, H., Poulson, S.R., 2004. Carbon and hydrogen isotopic fractionation during lipid biosynthesis in a higher plant (*Cryptomeria japonica*). *Phytochemistry* 65, 323–330.

- Clark, M.K., House, M.A., Royden, L.H., Whipple, K., Burchfiel, B.C., Zhang, X., Tang, W., 2005. Late Cenozoic uplift of southeastern Tibet. *Geology* 33, 525.
- Clemens, S.C., Murray, D.W., Prell, W.L., 1996. Nonstationary phase of the plio-pleistocene Asian monsoon. *Science* 274, 943–948.
- Clift, P.D., Giosan, L., Carter, A., Garzanti, E., Galy, V., Tabrez, A.R., Pringle, M., Campbell, I.H., France-Lanord, C., Blusztajn, J., Allen, C., Alizai, A., Lückge, A., Danish, M., Rabbani, M.M., 2010. Monsoon control over erosion patterns in the Western Himalaya: possible feed-back into the tectonic evolution. Geological Society, London, Special Publications 342, 185–218.
- Clift, P.D., Hodges, K. V., Heslop, D., Hannigan, R., Van Long, H., Calves, G., 2008. Correlation of Himalayan exhumation rates and Asian monsoon intensity. *Nature Geoscience* 1, 875–880.
- Cohen, A.D., Spackman, W., Raymond, R., 1987. Interpreting the characteristics of coal seams from chemical, physical and petrographic studies of peat deposits. Geological Society, London, Special Publications 32, 107–125.
- Collinson, M.E., Van Bergen, P.F., Scott, A.C., De Leeuw, J.W., 1994. The oil-generating potential of plants from coal and coal-bearing strata through time: a review with new evidence from Carboniferous plants. Geological Society, London, Special Publications 77, 31–70.
- Craine, J.M., Brookshire, E.N.J., Cramer, M.D., Hasselquist, N.J., Koba, K., Marin-Spiotta, E., Wang, L., 2015. Ecological interpretations of nitrogen isotope ratios of terrestrial plants and soils. *Plant and Soil* 396, 1–26.
- Craine, J.M., Towne, E.G., Ocheltree, T.W., Nippert, J.B., 2012. Community traitscape of foliar nitrogen isotopes reveals N availability patterns in a tallgrass prairie. *Plant and Soil* 356, 395–403.
- Cranwell, P.A., 1973. Chain-length distribution of n-alkanes from lake sediments in relation to post-glacial environmental change. *Freshwater Biology* 3, 259–265.
- Cranwell, P.A., 1973. n-Alkane distributions in lake sediments in relation to post-glacial environmental change. *Freshwater Biology* 3, 259–265.
- Cranwell, P.A., 1977. Organic geochemistry of Cam Loch (Sutherland) sediments. *Chemical Geology* 20, 205–221.
- Cranwell, P.A., Eglinton, G., Robinson, N., 1987. Lipids of aquatic organisms as potential contributors to lacustrine sediments—II. *Organic Geochemistry* 11, 513–527.
- Crosdale, P.J., 1993. Coal maceral ratios as indicators of environment of deposition: do they work for ombrogenous mires? An example from the Miocene of New Zealand. *Organic Geochemistry* 20, 797–809.
- Crundwell, M., Scott, G., Naish, T.R., Carter, L., 2008. Glacial–interglacial oceanclimate variability spanning the Mid-Pleistocene transition in the temperate Southwest Pacific, ODP site 1123. *Palaeogeogr. Palaeoclimatol. Palaeoecol* 260, 202–229.
- Dai, S., Li, T., Seredin, V. V., Ward, C.R., Hower, J.C., Zhou, Y., Zhang, M., Song, X., Song, W., Zhao, C., 2014. Origin of minerals and elements in the Late Permian coals, tonsteins, and host rocks of the Xinde Mine, Xuanwei, eastern Yunnan, China. *International Journal of Coal Geology* 121, 53–78.
- Dai, S., Ren, D., Chou, C.L., Finkelman, R.B., Seredin, V. V., Zhou, Y., 2012a. Geochemistry of trace elements in Chinese coals: A review of abundances, genetic types, impacts on human health, and industrial utilization. *International Journal of Coal Geology*.
- Dai, S., Wang, X., Seredin, V. V., Hower, J.C., Ward, C.R., O’Keefe, J.M.K., Huang, W., Li, T., Li, X., Liu, H., Xue, W., Zhao, L., 2012b. Petrology, mineralogy, and geochemistry of the Ge-rich coal from the Wulantuga Ge ore deposit, Inner Mongolia, China: New data and genetic implications. *International Journal of Coal Geology* 90–91, 72–99.
- Degens, E.T., 1969. Biogeochemistry of Stable Carbon Isotopes, in: *Organic Geochemistry*. Springer Berlin Heidelberg, Berlin, Heidelberg, pp. 304–329.
- Dehmer, J., 1988. Petrographische und organisch-geochemische Untersuchungen an rezenten Torfen und tertiären Braunkohlen: ein Beitrag zur Fazies und Genese gebänderter Braunkohlen. na.
- Dehmer, J., 1989. Petrographical and organic geochemical investigation of the Oberpfalz brown coal deposit, West Germany. *International Journal of Coal Geology* 11, 273–290.
- Dehmer, J., 1993. Petrology and organic geochemistry of peat samples from a raised bog in Kalimantan (Borneo). *Organic Geochemistry* 20, 349–362.
- Dehmer, J., 1995. Petrological and organic geochemical investigation of recent peats with known environments of deposition. *International Journal of Coal Geology* 28, 111–138.
- Delwiche, C.C., Steyn, P.L., 1970. Nitrogen Isotope Fractionation in Soils and Microbial Reactions. *Environmental Science and Technology* 4, 929–935.
- Diefendorf, A.F., Freeman, K.H., Wing, S.L., Currano, E.D., Mueller, K.E., 2015. Paleogene plants fractionated carbon isotopes similar to modern plants. *Earth and Planetary Science Letters* 429, 33–44.
- Diefendorf, A.F., Freeman, K.H., Wing, S.L., Graham, H. V., 2011. Production of n-alkyl lipids in living plants and implications for the geologic past. *Geochimica et Cosmochimica Acta* 75, 7472–7485.

- Diessel, C.F.K., 1986. On the Correlation between Coal Facies and Depositional Environments. Proceeding of 20th Symposium, Department of Geology. University Newcastle, NSW, pp. 19-22.
- Diessel, C.F.K., 1992. Coal-Bearing Depositional Systems. Springer Science & Business Media, Berlin. doi:10.1017/CBO9781107415324.004
- Diessel, C.F.K., 2012. Coal-bearing depositional systems. Springer Science & Business Media.
- Ding, Z.L., Derbyshire, E., Yang, S.L., Yu, Z.W., Xiong, S.F., Liu, T.S., 2002. Stacked 2.6-Ma grain size record from the Chinese loess based on five sections and correlation with the deep-sea  $\delta^{18}\text{O}$  record. *Paleoceanography* 17, 5-1-5-21.
- Doković, N., Mitrović, D., Životić, D., Bechtel, A., Sachsenhofer, R.F., Stojanović, K., 2018. Petrographic and biomarker analysis of xylite-rich coal from the Kolubara and Kostolac lignite basins (Pannonian Basin, Serbia). *Geologica Carpathica* 69, 51-70.
- Douglas, A., Grantham, P., 1974. Fingerprint gas chromatography in the analysis of some native bitumens, asphalts and related substances. In: Tissot, B., Biennier, F. (Eds.), *Advances in Organic Geochemistry 1973*. Éditions Technip, Paris, pp. 261-276.
- Dupont-Nivet, G., Krijgsman, W., Langereis, C.G., Abels, H.A., Dai, S., Fang, X., 2007. Tibetan plateau aridification linked to global cooling at the Eocene-Oligocene transition. *Nature* 445, 635-638.
- Dwyer, G.S., Cronin, T.M., Baker, P.A., Raymo, M.E., Buzas, J.S., Corrège, T., 1995. North Atlantic deepwater temperature change during late Pliocene and late Quaternary climatic cycles. *Science* 270, 1347-1351.
- Eglinton, G., Hamilton, R.J., 1967. Leaf epicuticular waxes. *Science* 156, 1322-1335.
- Elena, H.E., Elena, A.F., Miola, A., Glujovsky, D., Sueldo, C.E., 2016. Tratamiento exitoso de un embarazo heterotópico cervical luego de un procedimiento de fecundación in vitro. *Medicina (Argentina)* 76, 30-32.
- Erdenetsogt, B.-O., Lee, I., Ko, Y.-J., 2017. Carbon isotope analysis and a solid state  $^{13}\text{C}$  NMR study of Mongolian lignite: Changes in stable carbon isotopic composition during diagenesis. *Organic Geochemistry* 113, 293-302.
- Erik, N.Y., 2011. Hydrocarbon generation potential and Miocene-Pliocene paleoenvironments of the Kangal Basin (Central Anatolia, Turkey). *Journal of Asian Earth Sciences* 42, 1146-1162.
- Fabiańska, M.J., Kurkiewicz, S., 2013. Biomarkers, aromatic hydrocarbons and polar compounds in the Neogene lignites and gangue sediments of the Konin and Turoszów Brown Coal Basins (Poland). *International Journal of Coal Geology* 107, 24-44.
- Feng, Z.Z., Yang, S.Z., Wang, D.M., 1998. Rare trees in Yunnan province. China Esperanto Press, Beijing.
- Ficken, K., Li, B., Swain, D., Eglinton, G., 2000. An n-alkane proxy for the sedimentary input of submerged/floating freshwater aquatic macrophytes. *Organic Geochemistry* 31, 745-749.
- Ficken, K., Wooller, M., Swain, D., Street-Perrott, F., Eglinton, G., 2002. Reconstruction of a subalpine grass-dominated ecosystem, Lake Rutundu, Mount Kenya: a novel multi-proxy approach. *Palaeogeography, Palaeoclimatology, Palaeoecology* 177, 137-149.
- Ficken, K.J., Li, B., Swain, D.L., Eglinton, G., 2000. An n-alkane proxy for the sedimentary input of submerged /floating freshwater aquatic macrophytes. *Organic Geochemistry* 31, 745-749.
- Finotello, F., Johns, R., 1986. Some inter-relationships of kerogen and humic acid fractions in the Victorian brown coal pale lithotype. *Organic Geochemistry* 9, 265-273.
- Flores, D., 2002. Organic facies and depositional palaeoenvironment of lignites from Rio Maior Basin (Portugal). *International Journal of Coal Geology* 48, 181-195.
- Fodor, L., Jelen, B., Márton, E., Skaberne, D., Čar, J., Vrabec, M., 1998. Miocene-Pliocene tectonic evolution of the Slovenian Periadriatic fault: Implications for Alpine-Carpathian extrusion models. *Tectonics* 17, 690-709.
- Freeman, K.H., Boreham, C.J., Summons, R.E., Hayes, J.M., 1994. The effect of aromatization on the isotopic compositions of hydrocarbons during early diagenesis. *Organic Geochemistry* 21, 1037-1049.
- Freudenthal, T., Wagner, T., Wenzhöfer, F., Zabel, M., Wefer, G., 2001. Early diagenesis of organic matter from sediments of the Eastern subtropical Atlantic: Evidence from stable nitrogen and carbon isotopes. *Geochimica et Cosmochimica Acta* 65, 1795-1808.
- Fu, J., Sheng, G., Chen, D., Liu, D., Brassell, S.C., Gowar, A., Eglinton, G., 1987. Geochemical characteristics of sphagnum brown coal — A possible oil-generating precursor. *Chinese Journal of Geochemistry* 6, 289-296.
- GB/T482-2008, 2008. Sampling of Coal Seams. Chinese Management Committee of Standard Specifications, Beijing, pp. 9 (in Chinese).
- Gebauer, G., Schulze, E.D., 1991. Carbon and nitrogen isotope ratios in different compartments of a healthy and a declining *Picea abies* forest in the Fichtelgebirge, NE Bavaria. *Oecologia* 87, 198-207.
- Gouveia, S.E., Pessenda, L.C., Aravena, R., Boulet, R., Scheel-Ybert, R., Bendassoli, J., Ribeiro, A., Freitas, H., 2002. Carbon isotopes in charcoal and soils in studies of paleovegetation and climate changes during

- the late Pleistocene and the Holocene in the southeast and centerwest regions of Brazil. *Global and Planetary Change* 33, 95–106.
- Gülz, P.G., Müller, E., Herrmann, T., 1992. Chemical composition and surface structures of epicuticular leaf waxes from *Castanea Sativa* and *Aesculus Hippocastanum*. *Zeitschrift für Naturforschung - Section C Journal of Biosciences* 47, 661–666.
- Gürdal, G., Bozcu, M., 2011. Petrographic characteristics and depositional environment of Miocene Çan coals, Çanakkale-Turkey. *International Journal of Coal Geology* 85, 143-160.
- Haberer, R.M., Mangelsdorf, K., Wilkes, H., Horsfield, B., 2006. Occurrence and palaeoenvironmental significance of aromatic hydrocarbon biomarkers in Oligocene sediments from the Mallik 5L-38 Gas Hydrate Production Research Well (Canada). *Organic Geochemistry* 37, 519-538.
- Hagemann, H., Hollerbach, A., 1980. Relationship between the macropetrographic and organic geochemical composition of lignites. *Physics and Chemistry of the Earth* 12, 631-638.
- Hagemann, H.W., Dehmer, J., 1991. Spectrophotometric lightness and chromaticity measurements on absorbing peat and brown coal surfaces: Part I—method and evaluation. *International Journal of Coal Geology* 19, 163-183.
- Hagemann, H.W., Wolf, M., 1987. New interpretations of the facies of the Rhenish brown coal of West Germany. *International Journal of Coal Geology* 7, 335-348.
- Hall, I.R., McCave, I.N., Shackleton, N.J., Weedon, G.P., Harris, S.E., 2001. Intensified deep Pacific inflow and ventilation in Pleistocene glacial times. *Nature* 412, 809–812.
- Hamrla, M., 1952. Porocilo o Petrografski Preiskavi Velenjskega Lignita. Unpubl. Rep., Geoloski Zavod, Ljubljana.
- Han, J., McCarthy, E.D., Hoeven, W. V., Calvin, M., Bradley, W.H., 1968. Organic geochemical studies, II. A preliminary report on the distribution of aliphatic hydrocarbons in algae, in bacteria, and in a recent lake sediment. *Proceedings of the National Academy of Sciences of the United States of America* 59(1), 29-33.
- Handley, L.L., Raven, J.A., 1992. The use of natural abundance of nitrogen isotopes in plant physiology and ecology. *Plant, Cell & Environment* 15, 965–985.
- Harrington, G.J., Clechenko, E.R., Clay Kelly, D., 2005. Palynology and organic-carbon isotope ratios across a terrestrial Palaeocene/Eocene boundary section in the Williston Basin, North Dakota, USA. *Palaeogeography, Palaeoclimatology, Palaeoecology* 226, 214–232.
- Havelcová, M., Sýkorová, I., Trejtnarová, H., Šulc, A., 2012. Identification of organic matter in lignite samples from basins in the Czech Republic: Geochemical and petrographic properties in relation to lithotype. *Fuel* 99, 129–142.
- Hazai, I., Alexander, G., Szekely, T., Essiger, B., Radek, D., 1986. Investigation of hydrocarbon constituents of a young sub-bituminous coal by gas chromatography-mass spectrometry. *Journal of Chromatography A* 367, 117-133.
- Herbin, G.A., Robins, P.A., 1968. Studies on plant cuticular waxes—III. The leaf wax alkanes and  $\omega$ -hydroxy acids of some members of the cupressaceae and pinaceae. *Phytochemistry* 7, 1325–1337.
- Holdgate, G.R., Kershaw, A., Sluiter, I., 1995. Sequence stratigraphic analysis and the origins of Tertiary brown coal lithotypes, Latrobe Valley, Gippsland Basin, Australia. *International Journal of Coal Geology* 28, 249-275.
- Holdgate, G.R., McGowran, B., Fromhold, T., Wagstaff, B.E., Gallagher, S.J., Wallace, M.W., Sluiter, I.R.K., Whitelaw, M., 2009. Eocene-Miocene carbon-isotope and floral record from brown coal seams in the Gippsland Basin of southeast Australia. *Global and Planetary Change* 65, 89–103.
- Holdgate, G.R., Wallace, M., O'Connor, M., Korasidis, V., Lieven, U., 2016. The origin of lithotype cycles in Oligo-Miocene brown coals from Australia and Germany. *International Journal of Coal Geology* 166, 47-61.
- Holdgate, G.R., Wallace, M.W., Sluiter, I.R., Marcuccio, D., Fromhold, T.A., Wagstaff, B.E., 2014. Was the Oligocene–Miocene a time of fire and rain? Insights from brown coals of the southeastern Australia Gippsland Basin. *Palaeogeography, Palaeoclimatology, Palaeoecology* 411, 65-78.
- Holmes, M.E., Eichner, C., Struck, U., Wefer, G., 1999. Reconstruction of Surface Ocean Nitrate Utilization Using Stable Nitrogen Isotopes in Sinking Particles and Sediments, in: *Use of Proxies in Paleooceanography*. Springer Berlin Heidelberg, Berlin, Heidelberg, pp. 447–468.
- Huang, X., Wang, C., Xue, J., Meyers, P.A., Zhang, Z., Tan, K., Zhang, Z., Xie, S., 2010. Occurrence of diploptene in moss species from the Dajihuh Peatland in southern China. *Organic Geochemistry* 41, 321–324.
- Huang, Y., Jia, L., Wang, Q., Mosbrugger, V., Utescher, T., Su, T., Zhou, Z., 2016. Cenozoic plant diversity of Yunnan: A review. *Plant Diversity* 38, 271–282.
- ICCP, 1998. The new vitrinite classification (ICCP System 1994). *Fuel* 77, 349-358.
- ICCP, 2001. The new inertinite classification (ICCP System 1994). *Fuel* 80, 459-471.

- Jacob, J., Disnar, J.-R., Boussafir, M., Spadano Albuquerque, A.L., Sifeddine, A., Turcq, B., 2007. Contrasted distributions of triterpene derivatives in the sediments of Lake Caçó reflect paleoenvironmental changes during the last 20,000 yrs in NE Brazil. *Organic Geochemistry* 38, 180-197.
- Jahren, A.H., Sternberg, L.S.L., 2008. Annual patterns within tree rings of the Arctic middle Eocene (ca. 45 Ma): Isotopic signatures of precipitation, relative humidity, and deciduousness. *Geology* 36, 99-102.
- Jones, T.P., Fortier, S.M., Mosbrugger, V., Roessler, J., Utescher, T., Ashraf, A.R., 1997.  $^{13}\text{C}/^{12}\text{C}$  ratio double cyclicity in a Miocene browncoal: Isotopic signals and orbital forcing. *Terra Nova* 9, 19-23.
- Kalaitzidis, S., Bouzinos, A., Christanis, K., 2000. The lignite-forming palaeoenvironment before and after the volcanic tephra deposition in the Ptolemais basin, Hellas. *Mineral Wealth* 115, 29-42.
- Kalbitz, K., Geyer, S., 2002. Different effects of peat degradation on dissolved organic carbon and nitrogen. *Organic Geochemistry* 33, 319-326.
- Kalbitz, K., Geyer, S., Gehre, M., 2000. Land use impacts on the isotopic signature ( $^{13}\text{C}$ ,  $^{14}\text{C}$ ,  $^{15}\text{N}$ ) of dissolved humic substances in a German fen area. *Soil Science* 156, 728-736.
- Kalkreuth, W., Keuser, C., Fowler, M., Li, M., McIntyre, D., Püttmann, W., Richardson, R., 1998. The petrology, organic geochemistry and palynology of Tertiary age Eureka Sound Group coals, Arctic Canada. *Organic Geochemistry* 29, 799-809.
- Kalkreuth, W., Kotis, T., Papanicolaou, C., Kokkinakis, P., 1991. The geology and coal petrology of a Miocene lignite profile at Meliadi Mine, Katerini, Greece. *International Journal of Coal Geology* 17, 51-67.
- Kanduč, T., Markič, M., Pezdič, J., 2005. Stable isotope geochemistry of different lithotypes of the Velenje lignite (Slovenia). *Geologija* 48, 83-95.
- Kanduč, T., Markič, M., Zavšek, S., McIntosh, J., 2012. Carbon cycling in the Pliocene Velenje Coal Basin, Slovenia, inferred from stable carbon isotopes. *International Journal of Coal Geology* 89, 70-83.
- Karrer, W., 2013. *Konstitution und Vorkommen der organischen Pflanzenstoffe: exclusive Alkaloide*, 12. Springer-Verlag.
- Kashirtsev, V.A., Kontorovich, A.E., Moskvina, V.I., Kuchkina, A.Y., Kim, V.E., 2008. Biomarker hydrocarbons in the organic matter of Paleogene sediments in southern West Siberia. *Petroleum Chemistry* 48, 269-276.
- Kershaw, A., Sluiter, I., 1982. The application of pollen analysis to the elucidation of Latrobe Valley brown coal depositional environments and stratigraphy. *Australian Coal Geology* 4, 169-86.
- Kershaw, A.P., Bolger, P.F., Sluiter, I.R.K., Baird, J.G., Whitelaw, M., 1991. The nature and evolution of lithotypes in the tertiary brown coals of the Latrobe Valley, southeastern Australia. *International Journal of Coal Geology* 18, 233-249.
- Killops, S.D., Funnell, R.H., Suggate, R.P., Sykes, R., Peters, K.E., Walters, C., Woolhouse, A.D., Weston, R.J., Boudou, J.P., 1998. Predicting generation and expulsion of paraffinic oil from vitrinite-rich coals. *Organic Geochemistry* 29, 1-21.
- Klump, K., Schäufele, R., Lötscher, M., Lattanzi, F.A., Feneis, W., Schnyder, H., 2005. C-isotope composition of  $\text{CO}_2$  respired by shoots and roots: Fractionation during dark respiration? *Plant, Cell and Environment* 28, 241-250.
- Kolb, K.J., Evans, R.D., 2002. Implications of leaf nitrogen recycling on the nitrogen isotope composition of deciduous plant tissues. *New Phytologist* 156, 57-64.
- Korasidis, V.A., Wallace, M.W., Wagstaff, B.E., Holdgate, G.R., 2017. Oligo-Miocene peatland ecosystems of the Gippsland Basin and modern analogues. *Global and Planetary Change* 149, 91-104.
- Korasidis, V.A., Wallace, M.W., Wagstaff, B.E., Holdgate, G.R., Tosolini, A.-M.P., Jansen, B., 2016. Cyclic floral succession and fire in a Cenozoic wetland/peatland system. *Palaeogeography, Palaeoclimatology, Palaeoecology* 461, 237-252.
- Kou, X.Y., Ferguson, D.K., Xu, J.X., Wang, Y.F., Li, C. Sen, 2006. The reconstruction of paleovegetation and paleoclimate in the Late Pliocene of west Yunnan, China. *Climatic Change* 77, 431-448.
- Koukouzas, N., Ward, C.R., Li, Z., 2010. Mineralogy of lignites and associated strata in the Mavropigi field of the Ptolemais Basin, northern Greece. *International Journal of Coal Geology* 81, 182-190.
- Kuhry, P., Vitt, D.H., 1996. Fossil carbon/nitrogen ratios as a measure of peat decomposition. *Ecology* 77, 271-275.
- Kutzbach, J.E., Street-Perrott, F.A., 1985. Milankovitch forcing of fluctuations in the level of tropical lakes from 18 to 0 kyr BP. *Nature* 317, 130-134.
- Laflamme, R.E., Hites, R.A., 1979. Tetra- and pentacyclic, naturally-occurring, aromatic hydrocarbons in recent sediments. *Geochimica et Cosmochimica Acta* 43, 1687-1691.
- Large, D.J., Jones, T.F., Briggs, J., Macquaker, J.H.S., Spiro, B.F., 2004. Orbital tuning and correlation of 1.7 m.y. of continuous carbon storage in an early Miocene peatland. *Geology* 32, 873.
- Large, D.J., Jones, T.F., Somerfield, C., Goringe, M.C., Spiro, B., Macquaker, J.H.S., Atkin, B.P., 2003. High-resolution terrestrial record of orbital climate forcing in coal. *Geology* 31, 303-306.

- Lehmann, M.F., Bernasconi, S.M., Barbieri, A., McKenzie, J.A., 2002. Preservation of organic matter and alteration of its carbon and nitrogen isotope composition during simulated and in situ early sedimentary diagenesis. *Geochimica et Cosmochimica Acta* 66, 3573–3584.
- Leonardi, S., Gentilesca, T., Guerrieri, R., Ripullone, F., Magnani, F., Mencuccini, M., Noije, T. V., Borghetti, M., 2012. Assessing the effects of nitrogen deposition and climate on carbon isotope discrimination and intrinsic water-use efficiency of angiosperm and conifer trees under rising CO<sub>2</sub> conditions. *Global Change Biology* 18, 2925–2944.
- Li, G., Li, L., Tarozo, R., Longo, W.M., Wang, K.J., Dong, H., Huang, Y., 2018. Microbial production of long-chain n-alkanes: Implication for interpreting sedimentary leaf wax signals. *Organic Geochemistry* 115, 24–31.
- Li, J., Fang, X., Song, C., Pan, B., Ma, Y., Yan, M., 2014. Late Miocene–Quaternary rapid stepwise uplift of the NE Tibetan Plateau and its effects on climatic and environmental changes. *Quaternary Research* 81, 400–423.
- Li, R., Luo, G., Meyers, P.A., Gu, Y., Wang, H., Xie, S., 2012. Leaf wax n-alkane chemotaxonomy of bamboo from a tropical rain forest in Southwest China. *Plant Systematics and Evolution* 298, 731–738.
- Licht, A., van Cappelle, M., Abels, H.A., Ladant, J.-B., Trabuco-Alexandre, J., France-Lanord, C., Donnadieu, Y., Vandenberghe, J., Rigaudier, T., Lécuyer, C., Terry Jr, D., Adriaens, R., Boura, A., Guo, Z., Soe, A.N., Quade, J., Dupont-Nivet, G., Jaeger, J.-J., 2014. Asian monsoons in a late Eocene greenhouse world. *Nature* 513, 501–506.
- Lipp, J., Trimborn, P., Fritz, P., Moser, H., Becker, B., Frenzel, B., 1991. Stable isotopes in tree ring cellulose and climatic change. *Tellus B* 43, 322–330.
- Lipson, D.A., Jha, M., Raab, T.K., Oechel, W.C., 2010. Reduction of iron (III) and humic substances plays a major role in anaerobic respiration in an Arctic peat soil. *Journal of Geophysical Research: Biogeosciences* 115, G00I06.
- Liu, B., Vrabec, M., Markič, M., Püttmann, W., 2019. Reconstruction of paleobotanical and paleoenvironmental changes in the Pliocene Velenje Basin, Slovenia, by molecular and stable isotope analysis of lignites. *International Journal of Coal Geology* 206, 31–45.
- Liu, B., Zhao, C., Ma, J., Sun, Y., Püttmann, W., 2018. The origin of pale and dark layers in Pliocene lignite deposits from Yunnan Province, Southwest China, based on coal petrological and organic geochemical analyses. *International Journal of Coal Geology* 195, 172–188.
- Lockheart, M.J., van Bergen, P.F., Evershed, R.P., 2000. Chemotaxonomic classification of fossil leaves from the Miocene Clarkia lake deposit, Idaho, USA based on n-alkyl lipid distributions and principal component analyses. *Organic Geochemistry* 31, 1223–1246.
- Logan, G.A., Eglinton, G., 1994. Biogeochemistry of the Miocene lacustrine deposit, at Clarkia, northern Idaho, U.S.A. *Organic Geochemistry* 21, 857–870.
- Lovley, D.R., Phillips, E.J., 1986. Organic matter mineralization with reduction of ferric iron in anaerobic sediments. *Applied and Environmental Microbiology* 51, 683–689.
- Lu, J., Zhang, X., 1986. Discovery of Tertiary sphagnum coal in Jinsuo Basin Yunnan Province, and its significance. *Chinese Science Bulletin* 31(22), 1556–1559. (in Chinese), ISSN: 0023-074X.
- Lu, J., Zhang, X., 1989. Characteristics of sphagnum coal considered as a new genetic type of coal. *International Journal of Coal Geology* 11, 191–203.
- Lu, Y., Hautevelle, Y., Michels, R., 2013. Determination of the molecular signature of fossil conifers by experimental palaeochemotaxonomy-Part 1: The Araucariaceae family. *Biogeosciences* 10, 1943–1962.
- Lücke, A., Helle, G., Schleser, G.H., Figueiral, I., Mosbrugger, V., Jones, T.P., Rowe, N.P., 1999. Environmental history of the German Lower Rhine Embayment during the Middle Miocene as reflected by carbon isotopes in brown coal. *Palaeogeography, Palaeoclimatology, Palaeoecology* 154, 339–352.
- Luly, J., Sluiter, I.R.K., Kershaw, A.P., 1980. Pollen studies of Tertiary brown coals: Preliminary analysis of lithotypes within the Latrobe Valley, Victoria. *Monash Publications in Geography* 23, 1–78.
- Mackay, G.H., Attwood, D.H., Gaulton, R.J., George, A.M., 1985. The Cyclic Occurrence of Brown Coal Lithotypes. State Electricity Commission of Victoria Research and Development Department Report No. SO/85/93.
- Markic, M., Sachsenhofer, R., 1997. Petrographic composition and depositional environments of the Pliocene Velenje lignite seam (Slovenia). *International Journal of Coal Geology* 33, 229–254.
- Markič, M., Sachsenhofer, R.F., 2010. The Velenje lignite: its petrology and genesis. *Geološki Zavod Slovenije, Ljubljana*.
- Marynowski, L., Smolarek, J., Bechtel, A., Philippe, M., Kurkiewicz, S., Simoneit, B.R.T., 2013. Perylene as an indicator of conifer fossil wood degradation by wood-degrading fungi. *Organic Geochemistry* 59, 143–151.
- Maxwell, J.R., Pillinger, C.T., Eglinton, G., 1971. Organic Geochemistry, *Quart. Rev.* 25, in: Chem. Soc., London. 571–628.

- Meckler, A.N., Haug, G.H., Sigman, D.M., Plessen, B., Peterson, L.C., Thierstein, H.R., 2007. Detailed sedimentary N isotope records from Cariaco Basin for terminations I and V: Local and global implications. *Global Biogeochemical Cycles* 21, 1–13.
- Meyers, P.A., 1994. Preservation of elemental and isotopic source identification of sedimentary organic matter. *Chemical Geology* 114, 289–302.
- Ming, Q., Xilin, R., Dazhong, T., Jian, X., Wolf, M., 1994. Petrographic and geochemical characterization of pale and dark brown coal from Yunnan province, China. *International Journal of Coal Geology* 25, 65–92.
- Mitrović, D., Đoković, N., Životić, D., Bechtel, A., Šajnović, A., Stojanović, K., 2016. Petrographical and organic geochemical study of the Kovin lignite deposit, Serbia. *International Journal of Coal Geology* 168, 80–107.
- Moore, T.A., Shearer, J.C., 2003. Peat/coal type and depositional environment—are they related? *International Journal of Coal Geology* 56, 233–252.
- Morford, S.L., Houlton, B.Z., Dahlgren, R.A., 2011. Increased forest ecosystem carbon and nitrogen storage from nitrogen rich bedrock. *Nature* 477, 78–84.
- Murray, A.P., Edwards, D., Hope, J.M., Boreham, C.J., Booth, W.E., Alexander, R.A., Summons, R.E., 1998. Carbon isotope biogeochemistry of plant resins and derived hydrocarbons. *Organic Geochemistry* 29, 1199–1214.
- Naeth, J., Asmus, S., Littke, R., 2004. Petrographic and geophysical assessment of coal quality as related to briquetting: the Miocene lignite of the Lower Rhine Basin, Germany. *International Journal of Coal Geology* 60, 17–41.
- Naish, T., 1997. Constraints on the amplitude of late Pliocene eustatic sea-level fluctuations: New evidence from the New Zealand shallow-marine sediment record. *Geology* 25, 1139.
- Naish, T., Powell, R., Levy, R., Wilson, G., Scherer, R., Talarico, F., Krissek, L., Niessen, F., Pompilio, M., Wilson, T., Carter, L., DeConto, R., Huybers, P., McKay, R., Pollard, D., Ross, J., Winter, D., Barrett, P., Browne, G., Cody, R., Cowan, E., Crampton, J., Dunbar, G., Dunbar, N., Florindo, F., Gebhardt, C., Graham, I., Hannah, M., Hansaraj, D., Harwood, D., Helling, D., Henrys, S., Hinnov, L., Kuhn, G., Kyle, P., Läufer, A., Maffioli, P., Magens, D., Mandernack, K., McIntosh, W., Millan, C., Morin, R., Ohneiser, C., Paulsen, T., Persico, D., Raine, I., Reed, J., Riesselman, C., Sagnotti, L., Schmitt, D., Sjunneskog, C., Strong, P., Taviani, M., Vogel, S., Wilch, T., Williams, T., 2009. Obliquity-paced Pliocene West Antarctic ice sheet oscillations. *Nature* 458, 322–328.
- Nakamura, H., Sawada, K., Takahashi, M., 2010. Aliphatic and aromatic terpenoid biomarkers in Cretaceous and Paleogene angiosperm fossils from Japan. *Organic Geochemistry* 41, 975–980.
- Nakatsuka, T., Handa, N., Harada, N., Sugimoto, T., Imaizumi, S., 1997. Origin and decomposition of sinking particulate organic matter in the deep water column inferred from the vertical distributions of its  $\delta^{15}\text{N}$ ,  $\delta^{13}\text{C}$  and  $\delta^{14}\text{C}$ . *Deep Sea Research Part I: Oceanographic Research Papers* 44, 1957–1979.
- Natelhofer, K.J., Fry, B., 1988. Controls on natural nitrogen-15 and carbon-13 abundances in forest soil organic matter. *Soil Science Society of America Journal* 52, 1633.
- Nichols, J., Booth, R.K., Jackson, S.T., Pendall, E.G., Huang, Y., 2010. Differential hydrogen isotopic ratios of Sphagnum and vascular plant biomarkers in ombrotrophic peatlands as a quantitative proxy for precipitation—evaporation balance. *Geochimica et Cosmochimica Acta* 74, 1407–1416.
- Nichols, J.E., Booth, R.K., Jackson, S.T., Pendall, E.G., Huang, Y., 2006. Paleohydrologic reconstruction based on n-alkane distributions in ombrotrophic peat. *Organic Geochemistry* 37, 1505–1513.
- Noble, R.A., Alexander, R., Kagi, R.I., Knox, J., 1985. Tetracyclic diterpenoid hydrocarbons in some Australian coals, sediments and crude oils. *Geochimica et Cosmochimica Acta* 49, 2141–2147.
- Nordt, L., Tubbs, J., Dworkin, S., 2016. Stable carbon isotope record of terrestrial organic materials for the last 450 Ma yr. *Earth-Science Reviews* 159, 103–117.
- Nott, C.J., Xie, S., Avsejs, L.A., Maddy, D., Chambers, F.M., Evershed, R.P., 2000. n-Alkane distributions in ombrotrophic mires as indicators of vegetation change related to climatic variation. *Organic Geochemistry* 31, 231–235.
- Novák, M., Buzek, F., Adamová, M., 1999. Vertical trends in  $\delta^{13}\text{C}$ ,  $\delta^{15}\text{N}$  and  $\delta^{34}\text{S}$  ratios in bulk Sphagnum peat. *Soil Biology and Biochemistry* 31, 1343–1346.
- Oikonomopoulos, I.K., Kaouras, G., Tougiannidis, N., Ricken, W., Gurk, M., Antoniadis, P., 2015. The depositional conditions and the palaeoenvironment of the Achlada xylite-dominated lignite in western Macedonia, Greece. *Palaeogeography, Palaeoclimatology, Palaeoecology* 440, 777–792.
- Otto, A., Simoneit, B.R., Wilde, V., 2007. Terpenoids as chemosystematic markers in selected fossil and extant species of pine (*Pinus*, Pinaceae). *Botanical Journal of the Linnean Society* 154, 129–140.
- Otto, A., Simoneit, B.R.T., 2001. Chemosystematics and diagenesis of terpenoids in fossil conifer species and sediment from the Eocene Zeitz formation, Saxony, Germany. *Geochimica et Cosmochimica Acta* 65, 3505–3527.

- Otto, A., Simoneit, B.R.T., Rember, W.C., 2005. Conifer and angiosperm biomarkers in clay sediments and fossil plants from the Miocene Clarkia Formation, Idaho, USA. *Organic Geochemistry* 36, 907–922.
- Otto, A., Walther, H., Püttmann, W., 1994. Molecular composition of a leaf- and root-bearing Oligocene Oxbow Lake Clay in the Weissenlocher Basin, Germany. *Organic Geochemistry* 22, 275–286.
- Otto, A., Walther, H., Püttmann, W., 1997. Sesqui- and diterpenoid biomarkers preserved in Taxodium-rich oligocene oxbow lake clays, Weissenlocher basin, Germany. *Organic Geochemistry* 26, 105–115.
- Otto, A., Wilde, V., 2001. Sesqui-, di-, and triterpenoids as chemosystematic markers in extant conifers—a review. *The Botanical Review* 67, 141–238.
- Papanicolaou, C., Dehmer, J., Fowler, M., 2000. Petrological and organic geochemical characteristics of coal samples from Florina, Lava, Moschopotamos and Kalavryta coal fields, Greece. *International Journal of Coal Geology* 44, 267–292.
- Park, R., Epstein, S., 1961. Metabolic fractionation of C13 & C12 in plants. *Plant physiology* 36, 133–8.
- Peoples, M.B., Bergersen, F.J., Turner, G.L., Sampet, C., Rerkasem, B., Bhromsiri, A., Nuhayati, Faiseh, A.W., Sudin, M.N., Norhayati, M., Herridge, D.F., 1991. Use of the natural enrichment of 15N in plant available soil N for the measurement of symbiotic N2 fixation. Stable isotopes in plant nutrition, soil fertility and environmental studies. *Proceeding*, 117–129.
- Pessenda, L.C.R., Gouveia, S.E.M., Aravena, R., Boulet, R., Valencia, E.P.E., 2004. Holocene fire and vegetation changes in southeastern Brazil as deduced from fossil charcoal and soil carbon isotopes. *Quaternary International* 114, 35–43.
- Peters, K.E., Sweeney, R.E., Kaplan, I.R., 1978. Correlation of carbon and nitrogen stable isotope ratios in sedimentary organic matter. *Limnology and Oceanography* 23, 598–604.
- Peters, K.E., Walters, C.C., Moldowan, J.M., 2005. *The Biomarker Guide*, Vol. 1. Cambridge University Press.
- Pezdic, J., Markić, M., Lojen, S., Cermelj, B., Ulrich, M., Zavsek, S., 1998. Carbon isotope composition in the Velenje lignite mine - its role in soft brown coal genesis. *RMZ - Materials and Geoenvironment* 45, 149–153.
- Philp, R.P., 1985. *Fossil fuel biomarkers, Methods in Geochemistry and Geophysics*. Elsevier, New York.
- Pickel, W., Wolf, M., 1989. Kohlenpetrologische und geochemische Charakterisierung von Braunkohlen aus dem Geiseltal (DDR). *Erdol Kohle* 42, 481–484.
- Popp, B.N., Parekh, P., Tilbrook, B., Bidigare, R.R., Laws, E.A., 1997. Organic carbon  $\delta^{13}\text{C}$  variations in sedimentary rocks as chemostratigraphic and paleoenvironmental tools. *Palaeogeography, Palaeoclimatology, Palaeoecology* 132, 119–132.
- Powell, T.G., Boreham, C.J., Smyth, M., Russell, N., Cook, A.C., 1991. Petroleum source rock assessment in non-marine sequences: pyrolysis and petrographic analysis of Australian coals and carbonaceous shales. *Organic Geochemistry* 17, 375–394.
- Qi, M., Rong, X., Tang, D., Xia, J., Monika, W., 1994. Petrographic and geochemical characterization of pale and dark brown coal from Yunnan Province, China. *International Journal of Coal Geology* 25, 65–92.
- Quan, T.M., van de Schootbrugge, B., Field, M.P., Rosenthal, Y., Falkowski, P.G., 2008. Nitrogen isotope and trace metal analyses from the Mingolsheim core (Germany): Evidence for redox variations across the Triassic-Jurassic boundary. *Global Biogeochemical Cycles* 22, 1–14.
- Radhwani, M., Bechtel, A., Singh, V.P., Singh, B.D., Mannai-Tayech, B., 2018. Petrographic, palynofacies and geochemical characteristics of organic matter in the Saouef Formation (NE Tunisia): Origin, paleoenvironment, and economic significance. *International Journal of Coal Geology* 187, 114–130.
- Rau, G.H., Arthur, M.A., Dean, W.E., 1987. 15N/14N variations in Cretaceous Atlantic sedimentary sequences: implication for past changes in marine nitrogen biogeochemistry. *Earth and Planetary Science Letters* 82, 269–279.
- Rielley, G., Collier, R.J., Jones, D.M., Eglinton, G., 1991. The biogeochemistry of Ellesmere Lake, U.K.-I: source correlation of leaf wax inputs to the sedimentary lipid record. *Organic Geochemistry* 17, 901–912.
- Rigby, D., Batts, B.D., 1986. The isotopic composition of nitrogen in Australian coals and oil shales. *Chemical Geology: Isotope Geoscience Section* 58, 273–282.
- Rimmer, S.M., Rowe, H.D., Taulbee, D.N., Hower, J.C., 2006. Influence of maceral content on  $\delta^{13}\text{C}$  and  $\delta^{15}\text{N}$  in a Middle Pennsylvanian coal. *Chemical Geology* 225, 77–90.
- Rowe, J.W., 1989. *Natural products of woody plants: chemicals extraneous to the lignocellulosic cell wall*. Springer-Verlag Berlin Heidelberg, New York. DOI: <https://doi.org/10.1007/978-3-642-74075-6>. Print ISBN: 978-3-642-74077-0, Online ISBN: 978-3-642-74075-6.
- Rowe, J.W., 1989. *Natural products of woody plants: chemicals extraneous to the lignocellulosic cell wall*. Springer-Verlag, Berlin. doi:10.1007/978-3-642-74075-6
- Ruddiman, W.F., 2013. *Tectonic uplift and climate change*. Springer Science & Business Media.
- Ruppert, L.F., Stanton, R.W., Blaine Cecil, C., Eble, C.F., Dulong, F.T., 1991. Effects of detrital influx in the Pennsylvanian Upper Freeport peat swamp. *International Journal of Coal Geology* 17, 95–116.



- Russell, N.J., 1984. Gelification of Victorian tertiary soft brown coal wood. I. Relationship between chemical composition and microscopic appearance and variation in the degree of gelification. *International Journal of Coal Geology* 4, 99-118.
- Sabel, M., Bechtel, A., Püttmann, W., Hoernes, S., 2005. Palaeoenvironment of the Eocene Eckfeld Maar lake (Germany): implications from geochemical analysis of the oil shale sequence. *Organic Geochemistry* 36, 873-891.
- Schaeffer, P., Trendel, J.M., Albrecht, P., 1995. An unusual aromatization process of higher plant triterpenes in sediments. *Organic Geochemistry* 23, 273-275.
- Schimmelmann, A., Lis, G.P., 2010. Nitrogen isotopic exchange during maturation of organic matter. *Organic Geochemistry* 41, 63-70.
- Schleser, G.H., Frielingsdorf, J., Blair, A., 1999. Carbon isotope behaviour in wood and cellulose during artificial aging. *Chemical Geology* 158, 121-130.
- Schneider, W., 1992. Floral successions in Miocene swamps and bogs of Central Europe. *Zeitschrift für Geologische Wissenschaften* 20, 555-570.
- Schneider, W., 1995. Palaeohistological studies on Miocene brown coals of Central Europe. *International Journal of Coal Geology* 28, 229-248.
- Schulze, T., Michaelis, W., 1990. Structure and origin of terpenoid hydrocarbons in some German coals. *Organic Geochemistry* 16, 1051-1058.
- Scott, A.C., 2002. Coal petrology and the origin of coal macerals: a way ahead? *International Journal of Coal Geology* 50, 119-134.
- Sen, S., Naskar, S., Das, S., 2016. Discussion on the concepts in paleoenvironmental reconstruction from coal macerals and petrographic indices. *Marine and Petroleum Geology* 73, 371-391.
- Šercelj, A., 1968. Pelodna stratigrafija velenjske krovinske plasti z ostanki mastodontov.—Pollenstratigraphie des Hangenden von Velenje Schichten mit Funden von Mastodonten. *Acad. Sci. Art. Slovenica. Diss. Classis IV XI* 377-397.
- Sessions, A.L., Zhang, L., Welander, P. V., Doughty, D., Summons, R.E., Newman, D.K., 2013. Identification and quantification of polyfunctionalized hopanoids by high temperature gas chromatography-mass spectrometry. *Organic Geochemistry* 56, 120-130.
- Shackleton, N.J., Backman, J., Zimmerman, H., Kent, D. V., Hall, M.A., Roberts, D.G., Schnitker, D., Baldauf, J.G., Desprairies, A., Homrighausen, R., Huddleston, P., Keene, J.B., Kaltenback, A.J., Krumsiek, K.A.O., Morton, A.C., Murray, J.W., Westberg-Smith, J., 1984. Oxygen isotope calibration of the onset of ice-rafting and history of glaciation in the North Atlantic region. *Nature* 307, 620-623.
- Shearer, G., Kohl, D.H., 1989. Estimates of N<sub>2</sub> Fixation in Ecosystems: The Need for and Basis of the 15N Natural Abundance Method. Springer, New York, NY, pp. 342-374.
- Simoneit, B.R.T., 1977. Diterpenoid compounds and other lipids in deep-sea sediments and their geochemical significance. *Geochimica et Cosmochimica Acta* 41, 463-476.
- Simoneit, B.R.T., 1985. Cyclic terpenoids of the geosphere. *Methods in Geochemistry and Geophysics* 25, 43-99.
- Simoneit, B.R.T., 1998. Biomarker PAHs in the environment, PAHs and related compounds. Springer, pp. 175-221.
- Simoneit, B.R.T., 1999. A review of biomarker compounds as source indicators and tracers for air pollution. *Environmental Science and Pollution Research* 6, 159-169.
- Simoneit, B.R.T., Grimalt, J.O., Wang, T.G., Cox, R.E., Hatcher, P.G., Nissenbaum, A., 1986. Cyclic terpenoids of contemporary resinous plant detritus and of fossil woods, ambers and coals. *Organic Geochemistry* 10, 877-889.
- Simoneit, B.R.T., Mazurek, M.A., 1982. Organic matter of the troposphere—II. Natural background of biogenic lipid matter in aerosols over the rural western United States. *Atmospheric Environment* 16, 2139-2159.
- Simoneit, B.R.T., Otto, A., Wilde, V., 2003. Novel phenolic biomarker triterpenoids of fossil laticifers in Eocene brown coal from Geiseltal, Germany. *Organic Geochemistry* 34, 121-129.
- Singh, A., Shivanna, M., Mathews, R.P., Singh, B.D., Singh, H., Singh, V.P., Dutta, S., 2017. Palaeoenvironment of Eocene lignite bearing succession from Bikaner-Nagaur Basin, western India: Organic petrography, palynology, palynofacies and geochemistry. *International Journal of Coal Geology* 181, 87-102.
- Singh, M.P., Singh, A.K., 2000. Petrographic characteristics and depositional conditions of Eocene coals of platform basins, Meghalaya, India. *International Journal of Coal Geology* 42, 315-356.
- Singh, P.K., Rajak, P.K., Singh, M.P., Singh, V.K., Naik, A.S., Singh, A.K., 2016. Peat swamps at Giral lignite field of Barmer basin, Rajasthan, Western India: understanding the evolution through petrological modelling. *International Journal of Coal Science and Technology* 3, 148-164.

- Singh, P.K., Singh, M.P., Singh, A.K., Arora, M., 2010. Petrographic characteristics of coal from the Lati Formation, Tarakan basin, East Kalimantan, Indonesia. *International Journal of Coal Geology* 81, 109-116.
- Singh, V., 2006. Gymnosperm (naked seeds plant): structure and development. Sarup & Sons.
- Singh, V.P., Singh, B.D., Mathews, R.P., Singh, A., Mendhe, V.A., Singh, P.K., Mishra, S., Dutta, S., Shivanna, M., Singh, M.P., 2017a. Investigation on the lignite deposits of Surkha mine (Saurashtra Basin, Gujarat), western India: Their depositional history and hydrocarbon generation potential. *International Journal of Coal Geology* 183, 78-99.
- Singh, V.P., Singh, B.D., Singh, A., Singh, M.P., Mathews, R.P., Dutta, S., Mendhe, V.A., Mahesh, S., Mishra, S., 2017b. Depositional palaeoenvironment and economic potential of Khadsaliya lignite deposits (Saurashtra Basin), western India: Based on petrographic, palynofacies and geochemical characteristics. *International Journal of Coal Geology* 171, 223-242.
- Skrzypek, G., Paul, D., Wojtun, B., 2008. Stable isotope composition of plants and peat from Arctic mire and geothermal area in Iceland. *Polish Polar Research* 29, 365-376.
- Sluiter, I., Kershaw, A., 1982. The nature of Late Tertiary vegetation in Australia. *Alcheringa* 6, 211-222.
- Sluiter, I., Kershaw, A., Holdgate, G., Bulman, D., 1995. Biogeographic, ecological and stratigraphic relationships of the Miocene brown coal floras, Latrobe Valley, Victoria, Australia. *International Journal of Coal Geology* 28, 277-302.
- Smith, B.N., Epstein, S., 1971. Two Categories of  $^{13}\text{C}/^{12}\text{C}$  Ratios for Higher Plants. *Plant Physiology* 47, 380-384.
- Sniderman, J.M.K., Pillans, B., O'Sullivan, P.B., Kershaw, A.P., 2007. Climate and vegetation in southeastern Australia respond to Southern Hemisphere insolation forcing in the late Pliocene - Early Pleistocene. *Geology* 35, 41-44.
- Spyckerelle, C., Greiner, A., Albrecht, P., Ourisson, G., 1977. Aromatic hydrocarbons from geological sources. Part III. *Journal of Chemical Research* 3746-3777.
- Stefanova, M., Ivanov, D., Yaneva, N., Marinov, S., Grasset, L., Amblès, A., 2008. Palaeoenvironment assessment of Pliocene Lom lignite (Bulgaria) from bitumen analysis and preparative off line thermochemolysis. *Organic Geochemistry* 39, 1589-1605.
- Stefanova, M., Markova, K., Marinov, S., Simoneit, B.R.T., 2005. Molecular indicators for coal-forming vegetation of the Miocene Chukurovo lignite, Bulgaria. *Fuel* 84, 1830-1838.
- Stefanova, M., Simoneit, B.R.T., Marinov, S.P., Zdravkov, A., Kortenski, J., 2016. Novel polar biomarkers of the Miocene Maritza-East lignite, Bulgaria. *Organic Geochemistry* 96, 1-10.
- Steiner, C., Glaser, B., Teixeira, W.G., Lehmann, J., Blum, W.E.H., Zech, W., 2008. Nitrogen retention and plant uptake on a highly weathered central Amazonian Ferralsol amended with compost and charcoal. *Journal of Plant Nutrition and Soil Science* 171, 893-899.
- Stock, A.T., Lücke, A., Zieger, L., Thielemann, T., 2016. Miocene depositional environment and climate in western Europe: The lignite deposits of the Lower Rhine Basin, Germany. *International Journal of Coal Geology* 157, 2-18.
- Su, T., Jacques, F.M.B., Spicer, R.A., Liu, Y.S., Huang, Y.J., Xing, Y.W., Zhou, Z.K., 2013. Post-Pliocene establishment of the present monsoonal climate in SW China: evidence from the late Pliocene Longmen megafloora. *Climate of the Past* 9, 1911-1920.
- Suárez-Ruiz, I., Flores, D., Mendonça Filho, J.G., Hackley, P.C., 2012. Review and update of the applications of organic petrology: Part 1, geological applications. *International Journal of Coal Geology* 99, 54-112.
- Sukh Dev, 1989. Terpenoids, in: *Natural Products of Woody Plants*. Springer, Berlin, Heidelberg, pp. 691-807.
- Sun, B.N., Wu, J.Y., Liu, Y.S.C., Ding, S.T., Li, X.C., Xie, S.P., Yan, D.F., Lin, Z.C., 2011. Reconstructing Neogene vegetation and climates to infer tectonic uplift in western Yunnan, China. *Palaeogeography, Palaeoclimatology, Palaeoecology* 304, 328-336.
- Sun, D., Dong, G., Zhang, Y., Wu, X., Qiang, X., Chen, M., Li, L., Zhou, W., Lu, H., Wang, F., Zhou, J., Liu, X., Wang, S., An, Z., Sun, Y., Liu, X., 2008. Eolian evidence from the Chinese Loess Plateau: the onset of the Late Cenozoic Great Glaciation in the Northern Hemisphere and Qinghai-Xizang Plateau uplift forcing. *Science in China Series D: Earth Sciences* 42, 258-271.
- Sun, Y., Ma, L., Bloemendal, J., Clemens, S., Qiang, X., An, Z., 2015. Miocene climate change on the Chinese Loess Plateau: Possible links to the growth of the northern Tibetan Plateau and global cooling. *Geochemistry, Geophysics, Geosystems* 16, 2097-2108.
- Sweeney, R.E., Kaplan, I.R., 1980. Natural abundances of  $^{15}\text{N}$  as a source indicator for near-shore marine sedimentary and dissolved nitrogen. *Marine Chemistry* 9, 81-94.
- Sykes, R., Lindqvist, J.K., 1993. Diagenetic quartz and amorphous silica in New Zealand coals. *Organic Geochemistry* 20, 855-866.
- Sýkorová, I., Pickel, W., Christanis, K., Wolf, M., Taylor, G.H., Flores, D., 2005. Classification of huminite—ICCP System 1994. *International Journal of Coal Geology* 62, 85-106.

- Taylor, G.H., Teichmüller, M., Davis, A., Diessel, C.F.K., Littke, R., Robert, P., 1998. *Organic Petrology* 704. ISBN: 978-3-443-01036-2.
- Tegelaar, E.W., Noble, R.A., 1994. Kinetics of hydrocarbon generation as a function of the molecular structure of kerogen as revealed by pyrolysis-gas chromatography. *Organic Geochemistry* 22, 543–574.
- Teichmüller, M., 1950. Zum petrographischen Aufbau und Werdegang der Weichbraunkohle. *Geol. Jb* 64, 429–488.
- Teichmüller, M., 1958. Reconstruction of the various moor types in the main coal seam of the Lower Rhineland. *Fortschritte in der Geologie von Rheinland und Westfalen* 2, 599–612.
- Teichmüller, M., 1962. Die genese der Kohle, CR 4th Congress International Stratigraphie et Geologie Carbonifere (Heerlen, 1958), pp. 699–722.
- Teichmüller, M., 1989. The genesis of coal from the viewpoint of coal petrology. *International Journal of Coal Geology* 12, 1–87.
- ten Haven, H.L., Peakman, T.M., Rullkötter, J., 1992. Early diagenetic transformation of higher-plant triterpenoids in deep-sea sediments from Baffin Bay. *Geochimica et Cosmochimica Acta* 56, 2001–2024.
- Thamdrup, B., 2000. Bacterial manganese and iron reduction in aquatic sediments, *Advances in microbial ecology*. Springer, pp. 41–84.
- Thiel, V., Blumenberg, M., Pape, T., Seifert, R., Michaelis, W., 2003. Unexpected occurrence of hopanoids at gas seeps in the Black Sea. *Organic Geochemistry* 34, 81–87.
- Thomson, P.W., 1950. Grundsätzliches zur tertiären Pollen-und Sporenmikrostratigraphie auf Grund einer Untersuchung des Hauptflözes der rheinischen Braunkohle in Liblar, Neurath, Fortuna und Brühl. *Geol. Jb.* 65, 113–26.
- Tian, J., Pak, D.K., Wang, P., Lea, D., Cheng, X., Zhao, Q., 2006. Late Pliocene monsoon linkage in the tropical South China Sea. *Earth and Planetary Science Letters* 252, 72–81.
- Utescher, T., Djordjevic-Milutinovic, D., Bruch, A., Mosbrugger, V., 2007. Palaeoclimate and vegetation change in Serbia during the last 30 Ma. *Palaeogeography, Palaeoclimatology, Palaeoecology* 253, 141–152.
- van Bergen, P.F., Poole, I., 2002. Stable carbon isotopes of wood: a clue to palaeoclimate? *Palaeogeography, Palaeoclimatology, Palaeoecology* 182, 31–45.
- Van Dorsselaer, A., Albrecht, P., Connan, J., 1975. Changes in composition of polycyclic alkanes by thermal maturation (Yallourn Lignite, Australia). In: Campus, R., Goñi, J. (Eds.), *Advances in Organic Geochemistry*. Enadimsa, Madrid, pp. 53–59.
- Vassilev, S. V., Vassileva, C.G., Baxter, D., Andersen, L.K., 2010. Relationships between chemical and mineral composition of coal and their potential applications as genetic indicators. Part 1. Chemical characteristics. *Chemical characteristics. Geologica Balcanica* 39, 21–41.
- Villar, H.J., Püttmann, W., Wolf, M., 1988. Organic geochemistry and petrography of Tertiary coals and carbonaceous shales from Argentina. *Organic Geochemistry* 13, 1011–1021.
- Volkman, J.K., Allen, D.I., Stevenson, P.L., Burton, H., 1986. Bacterial and algal hydrocarbons in sediments from a saline Antarctic lake, Ace Lake. *Organic Geochemistry* 10, 671–681.
- Von der Brellie, G., Wolf, M., 1981. Zur Petrographie und Palynologie heller und dunkler Schichten im rheinischen Hauptbraunkohlenflöz. *Fortschr. Geol. Rheinl. Westfalen* 29, 95–163.
- Vu, T., Zink, K.-G., Mangelsdorf, K., Sykes, R., Wilkes, H., Horsfield, B., 2009. Changes in bulk properties and molecular compositions within New Zealand Coal Band solvent extracts from early diagenetic to catagenetic maturity levels. *Organic Geochemistry* 40, 963–977.
- Wakeham, S.G., Schaffner, C., Giger, W., 1980. Poly cyclic aromatic hydrocarbons in Recent lake sediments—II. Compounds derived from biogenic precursors during early diagenesis. *Geochimica et Cosmochimica Acta* 44, 415–429.
- Wang, S., Yu, B., Zhang, J., Tang, j., 1997. Coal Forming Plants of Tertiary Baipao Coal in Yunnan and its genesis. *Journal of China Coal Society* 22, 8–12.
- Wang, T.-G., Simoneit, B.R.T., 1990. Organic geochemistry and coal petrology of Tertiary brown coal in the Zhoujing mine, Baise Basin, South China: 2. Biomarker assemblage and significance. *Fuel* 69, 12–20.
- Wang, T.G., Simoneit, B.R.T., Philp, R.P., Yu, C.P., 1990. Extended 8.beta.(H)-drimane and 8,14-secohopane series in a Chinese boghead coal. *Energy & Fuels* 4, 177–183.
- Ward, C.R., 2002. Analysis and significance of mineral matter in coal seams. *International Journal of Coal Geology* 50, 135–168.
- Ward, C.R., 2016. Analysis, origin and significance of mineral matter in coal: An updated review. *International Journal of Coal Geology* 165, 1–27.
- Ward, C.R., Crouch, A., Cohen, D.R., 2001. Identification of potential for methane ignition by rock friction in Australian coal mines. *International Journal of Coal Geology* 45, 91–103.
- Weston, R.J., Philp, R.P., Sheppard, C.M., Woolhouse, A.D., 1989. Sesquiterpanes, diterpanes and other higher terpanes in oils from the Taranaki basin of New Zealand. *Organic Geochemistry* 14, 405–421.

- Whiticar, M.J., 1996. Stable isotope geochemistry of coals, humic kerogens and related natural gases. *International Journal of Coal Geology* 32, 191–215.
- Widodo, S., Bechtel, A., Anggayana, K., Püttmann, W., 2009. Reconstruction of floral changes during deposition of the Miocene Embalut coal from Kutai Basin, Mahakam Delta, East Kalimantan, Indonesia by use of aromatic hydrocarbon composition and stable carbon isotope ratios of organic matter. *Organic Geochemistry* 40, 206–218.
- Willis, K.J., Kleczkowski, A., Briggs, K.M., Gilligan, C.A., 1999a. The role of sub-milankovitch climatic forcing in the initiation of the northern hemisphere glaciation. *Science (New York, N.Y.)* 285, 568–71.
- Willis, K.J., Kleczkowski, A., Crowhurst, S.J., 1999b. 124,000-year periodicity in terrestrial vegetation change during the late Pliocene epoch. *Nature* 397, 685–688.
- Winkler, E., 1986. Organic geochemical investigations of brown coal lithotypes. A contribution to facies analysis of seam banding in the Helmstedt deposit. *Organic Geochemistry* 10, 617–624.
- Wolff, G., Trendel, J., Albrecht, P., 1989. Novel monoaromatic triterpenoid hydrocarbons occurring in sediments. *Tetrahedron* 45, 6721–6728.
- Wolff, G.A., Rukin, N., Marshall, J.D., 1992. Geochemistry of an early diagenetic concretion from the Birchi Bed (L. Lias, W. Dorset, UK). *Organic Geochemistry* 19, 431–444.
- Wu, Z.Y., Zhu, Y.C., Jiang, H., 1987. *The vegetation of Yunnan*. Science Press, Beijing.
- Wüst, R., Bustin, R.M., Ross, J., 2008. Neo-mineral formation during artificial coalification of low-ash - mineral free-peat material from tropical Malaysia-potential explanation for low ash coals. *International Journal of Coal Geology* 74, 114–122.
- Wüst, R.A.J., Hawke, M.I., Marc Bustin, R., 2001. Comparing maceral ratios from tropical peatlands with assumptions from coal studies: do classic coal petrographic interpretation methods have to be discarded? *International Journal of Coal Geology* 48, 115–132.
- Xiao, X.Y., Shen, J., Wang, S.M., Xiao, H.F., Tong, G.B., 2010. The variation of the southwest monsoon from the high resolution pollen record in Heqing Basin, Yunnan Province, China for the last 2.78 Ma. *Palaeogeography, Palaeoclimatology, Palaeoecology* 287, 45–57.
- Xie, S., Sun, B., Wu, J., Lin, Z., Yan, D., Xiao, L., 2012. Palaeodimatic Estimates for the Late Pliocene Based on Leaf Physiognomy from Western Yunnan, China. *Turkish Journal of Earth Sciences* 21, 251–261.
- Xing, Y., Utescher, T., Jacques, F.M.B., Su, T., Liu, Y., Huang, Y., Zhou, Z., 2012. Paleoclimatic estimation reveals a weak winter monsoon in southwestern China during the late Miocene: Evidence from plant macrofossils. *Palaeogeography, Palaeoclimatology, Palaeoecology* 358–360, 19–26.
- Xu, J.X., Ferguson, D.K., Li, C. Sen, Wang, Y.F., 2008. Late Miocene vegetation and climate of the Lühe region in Yunnan, southwestern China. *Review of Palaeobotany and Palynology* 148, 36–59.
- Xu, J.X., Ferguson, D.K., Li, C. Sen, Wang, Y.F., Du, N.Q., 2004. Climatic and ecological implications of Late Pliocene Palynoflora from Longling, Yunnan, China. *Quaternary International* 117, 91–103.
- Yan, Z., Shao, L., Large, D., Wang, H., Spiro, B., 2019. Using geophysical logs to identify Milankovitch cycles and to calculate net primary productivity (NPP) of the Late Permian coals, western Guizhou, China. *Journal of Palaeogeography* 8, 2.
- Yang, Y., Zou, R., Shi, Z., Jiang, R., 1996. *Atlas for Coal Petrography of China*. China University of Mining and Technology Press, Beijing, China, 320pp. (in Chinese). ISBN: 7-81040-519-5.
- Yao, Y., Bruch, A.A., Cheng, Y., Mosbrugger, V., Wang, Y., Li, C., 2012. Monsoon versus Uplift in Southwestern China—Late Pliocene Climate in Yuanmou Basin, Yunnan. *PLoS ONE* 7, e37760.
- Yu, B., Zhang, J., Wang, D., 1997. The coal-forming characteristics and genesis of Baipao coal-from Tertiary Liaohu, Yunnan, Province. *Coal Geology of China* 9, 12–14.
- Yu, B., Zhang, J., Wang, S., Tang, j., 1996. The Pore Structure and Coal-Forming Plant of Tertiary Light Brown Coal in Yunnan. *Coal Geology of China* 8, 26–28.
- Yunnan BGMR (Yunnan Bureau Geological Mineral Resource), 1990. *Regional Geology of Yunnan Province*, Geology Publishing House, Beijing (1990), pp. 1-729.
- Zdravkov, A., Bechtel, A., Sachsenhofer, R.F., Kortenski, J., Gratzner, R., 2011. Vegetation differences and diagenetic changes between two Bulgarian lignite deposits - Insights from coal petrology and biomarker composition. *Organic Geochemistry* 42, 237–254.
- Zhang, Q.Q., Ferguson, D.K., Mosbrugger, V., Wang, Y.F., Li, C. Sen, 2012. Vegetation and climatic changes of SW China in response to the uplift of Tibetan Plateau. *Palaeogeography, Palaeoclimatology, Palaeoecology* 363–364, 23–36.
- Zhao, C., Liu, B., Ma, J., Liu, S., Blokhin, M.G., 2017. Occurrence of rubidium and cesium in Iqe coal, Qinghai-Tibet Plateau: Evidence from sequential chemical extraction experiment. *Energy Exploration and Exploitation* 35, 376–387.
- Zhu, H., Jacques, F.M.B., Wang, L., Xiao, X.H., Huang, Y.J., Zhou, Z.K., 2015. Fossil endocarps of *Aralia* (Araliaceae) from the upper Pliocene of Yunnan in southwest China, and their biogeographical implications. *Review of Palaeobotany and Palynology* 223, 94–103.

- Zhu, R.X., Potts, R., Pan, Y.X., Lü, L.Q., Yao, H.T., Deng, C.L., Qin, H.F., 2008. Paleomagnetism of the Yuanmou Basin near the southeastern margin of the Tibetan Plateau and its constraints on late Neogene sedimentation and tectonic rotation. *Earth and Planetary Science Letters* 272, 97–104.
- Zhu, Y., Shi, B., Fang, C., 2000. The isotopic compositions of molecular nitrogen: Implications on their origins in natural gas accumulations. *Chemical Geology* 164, 321–330.
- Životić, D., Bechtel, A., Sachsenhofer, R., Gratzner, R., Radić, D., Obradović, M., Stojanović, K., 2014. Petrological and organic geochemical properties of lignite from the Kolubara and Kostolac basins, Serbia: Implication on Grindability Index. *International Journal of Coal Geology* 131, 344-362.

## Appendix

**Table A1 Values of stable carbon isotopes ( $\delta^{13}\text{C}$ ) and stable nitrogen isotopes ( $\delta^{15}\text{N}$ ) of lignites and fossil woods from Jinsuo Basin, Yunnan Province.**

Sample	Lithotypes	$\delta^{13}\text{C}$	$\delta^{15}\text{N}$	TOC (wt%)	TN (wt%)	Sample	$\delta^{13}\text{C}$	$\delta^{15}\text{N}$
JS-39	dark	-25.57	0.83	51.3	1.32	W <sup>6</sup> -1	-25.71	-0.44
JS-38	dark	-26.03	0.09	55.2	1.22	W-5	-25.08	-0.08
JS-37	pale	-26.28	1.06	52.5	0.76	W-6	-26.68	-2.10
JS-36	dark	-25.36	0.61	55.8	1.26	W-9	-24.70	-0.60
JS-35	pale	-26.36	1.08	54.3	1.02	W-10	-24.46	-0.86
JS-34	dark	-25.74	0.84	55.2	1.09	W-12	-23.51	-0.35
JS-33	pale	-25.96	1.72	55.2	0.92	W-14	-23.92	-1.18
JS-32	dark	-25.54	2.09	55.8	1.09	W-28	-25.23	-0.06
JS-31	pale	-26.26	3.46	53.7	0.81	W-31	-24.43	-0.56
JS-30	dark	-25.65	n.a. <sup>7</sup>	47.7	1.11	W-36	-24.22	-0.06
JS-29	pale	-26.71	1.49	57.0	0.90	AV-W <sup>3</sup>	-24.79	-0.63
JS-28	dark	-25.77	2.08	52.8	1.07	AV-F <sup>4</sup>	-24.19	1.29
JS-27	pale	-27.38	1.67	53.4	0.78	AV-L <sup>5</sup>	-26.69	1.94
JS-26	dark	-26.82	2.01	48.6	1.01			
JS-25	pale	-28.38	2.43	62.4	0.68			
JS-24	dark	-26.35	2.46	54.6	1.28			
JS-23	pale	-28.05	2.35	54.6	1.07			
JS-22	dark	-27.07	2.32	46.2	1.36			
JS-21	pale	-27.82	3.18	52.2	0.73			
JS-20	dark	-26.65	1.74	51.0	1.16			
JS-19	pale	-26.41	1.95	55.8	1.27			
JS-18	dark	-26.66	2.59	49.2	1.35			
JS-17	pale	-26.23	2.24	43.8	0.94			
JS-16	dark	-26.30	2.09	51.6	1.16			
JS-15	pale	-26.35	n.a.	56.4	0.71			
JS-14	dark	-26.55	2.13	53.4	1.36			
JS-13	pale	-26.06	1.86	42.0	0.77			
JS-12	dark	-25.94	2.44	51.6	1.29			
JS-11	pale	-27.32	2.97	52.8	1.03			
JS-10	dark	-26.80	2.43	50.4	1.38			
JS-9	pale	-27.06	3.01	45.6	0.84			
JS-8	fusain	-23.38	1.37	55.8	n.a.			
JS-7	pale	-26.90	2.85	49.8	0.95			
JS-6	dark	-27.91	1.77	45.0	1.19			
JS-5	pale	-28.32	1.54	51.0	0.93			

<sup>1</sup> AV-P = average of pale lignites

<sup>2</sup> AV-D = average of dark lignites

JS-4	dark	-27.29	1.68	48.6	1.18	<sup>3</sup> AV-W = average of fossil woods
JS-3	fusain	-24.99	1.20	52.2	n.a.	
JS-2	pale	-28.02	1.97	52.2	0.87	<sup>4</sup> AV-F = average of fusain samples
JS-1	floor	-27.19	1.97	54.3	1.00	<sup>5</sup> AV-L = average of all lignite samples
AV-P <sup>1</sup>		-27.01	2.17	52.5	0.89	<sup>6</sup> W = fossil wood samples
AV-D <sup>2</sup>		-26.38	1.79	51.3	1.21	<sup>7</sup> n.a. = Not analyzed

**Table A2 Major-element oxides (%), Zr (ppm) and related parameters of the lignites from Jinsuo Basin, Yunnan Province, on a whole coal basis.**

Sample	SiO <sub>2</sub>	Al <sub>2</sub> O <sub>3</sub>	CaO	K <sub>2</sub> O	Na <sub>2</sub> O	Fe <sub>2</sub> O <sub>3</sub>	MnO	MgO	TiO <sub>2</sub>	P <sub>2</sub> O <sub>5</sub>	SiO <sub>2</sub> /Al <sub>2</sub> O <sub>3</sub>	Ash (wt%)	Zr
JS-39	3.33	2.71	1.47	0.14	bd <sup>1</sup>	1.60	0.0187	0.66	0.37	0.05	1.23	10.9	50.8
JS-38	0.32	1.05	1.39	0.01	bd	0.46	0.0063	0.53	0.04	0.02	0.31	4.6	8.65
JS-37	8.18	2.93	1.32	0.20	0.02	0.51	0.0063	0.62	0.39	0.07	2.79	14.3	91.4
JS-36	0.47	0.79	1.34	0.01	bd	0.59	0.0065	0.57	0.03	0.03	0.59	4.6	8.04
JS-35	5.11	1.64	1.16	0.08	0.01	0.42	0.0052	0.54	0.29	0.03	3.12	9.4	75.8
JS-34	0.10	0.74	1.48	0.00	bd	0.46	0.0066	0.62	0.01	0.02	0.14	4.0	3.23
JS-33	2.44	0.49	1.67	0.01	bd	0.60	0.0078	0.68	0.10	0.01	5.01	6.8	137.9
JS-32	0.88	0.44	1.74	0.01	bd	0.53	0.0090	0.65	0.09	0.01	2.00	5.1	17.8
JS-31	6.14	0.66	1.82	0.02	bd	0.55	0.0081	0.80	0.24	0.02	9.26	11.1	162.5
JS-30	2.29	2.41	1.68	0.13	bd	0.52	0.0067	0.82	0.11	0.09	0.95	9.6	22.4
JS-29	3.92	1.39	1.38	0.05	bd	0.51	0.0055	0.60	0.19	0.20	2.81	9.3	154.4
JS-28	0.12	0.79	1.67	0.01	bd	0.50	0.0074	0.64	0.01	0.02	0.15	4.9	0.33
JS-27	7.34	1.00	1.81	0.04	bd	0.69	0.0080	0.82	0.25	0.02	7.31	13.3	76.2
JS-26	0.06	0.62	1.29	0.00	bd	0.31	0.0051	0.54	0.02	0.01	0.10	3.6	4.91
JS-25	2.73	1.04	1.61	0.02	bd	0.50	0.0071	0.67	0.65	0.03	2.62	8.3	83.0
JS-24	0.30	0.85	1.89	0.01	bd	0.45	0.0080	0.70	0.06	0.02	0.36	5.2	10.4
JS-23	2.72	1.09	1.61	0.03	bd	0.98	0.0077	0.65	0.23	0.14	2.49	9.2	146.9
JS-22	5.44	4.27	1.69	0.28	bd	0.89	0.0116	0.86	0.38	0.03	1.28	15.2	68.7
JS-21	8.73	3.99	1.52	0.24	bd	1.08	0.0102	0.77	0.32	0.04	2.19	17.9	84.2
JS-20	3.21	2.74	1.69	0.21	bd	0.72	0.0104	0.77	0.14	0.06	1.17	11.0	32.1
JS-19	1.43	1.20	1.75	0.05	bd	0.40	0.0102	0.67	0.09	0.07	1.19	6.9	125.6
JS-18	6.79	5.53	1.73	0.17	bd	0.82	0.0191	0.79	0.30	0.07	1.23	17.7	182.0
JS-17	10.96	5.63	1.46	0.57	0.02	1.43	0.0108	0.82	0.75	0.05	1.95	22.2	139.0
JS-16	1.90	1.59	1.76	0.07	bd	0.34	0.0091	0.68	0.10	0.20	1.20	7.4	28.7
JS-15	3.38	2.21	1.09	0.16	0.01	0.28	0.0057	0.48	0.14	0.08	1.53	7.9	136.3



JS-14	1.10	1.24	1.31	0.06	bd	0.31	0.0064	0.51	0.06	0.14	0.88	5.2	16.1
JS-13	34.41	18.86	3.81	1.69	0.05	2.94	0.0252	2.37	2.02	0.22	1.82	67.0	119.0
JS-12	1.07	2.31	2.12	0.05	bd	0.41	0.0092	0.67	0.09	0.25	0.46	8.4	19.2
JS-11	5.80	3.73	1.55	0.30	0.01	0.53	0.0083	0.70	0.34	0.33	1.55	13.5	172.0
JS-10	6.22	4.39	1.16	0.43	0.00	0.72	0.0067	0.70	0.21	0.05	1.42	14.0	57.5
JS-09	8.05	4.23	1.10	0.48	0.02	0.43	0.0061	0.63	0.30	0.07	1.90	15.5	88.2
JS-08	3.34	2.46	2.00	0.15	0.00	0.56	0.0097	0.76	0.16	0.36	1.36	10.1	39.4
JS-07	5.70	3.41	1.50	0.26	0.04	0.88	0.0085	0.67	0.44	0.23	1.67	13.2	181.2
JS-06	3.33	2.93	1.10	0.16	0.01	1.18	0.0066	0.59	0.25	0.04	1.14	10.0	57.4
JS-05	6.46	2.48	0.94	0.12	0.02	0.61	0.0054	0.40	0.38	0.07	2.61	11.5	142.0
JS-04	4.39	3.78	1.02	0.27	bd	0.93	0.0061	0.54	0.40	0.05	1.16	11.6	87.5
JS-03	3.11	2.19	1.66	0.10	0.01	0.89	0.0087	0.59	0.19	0.06	1.42	9.18	55.1
JS-02	6.47	3.52	1.42	0.22	0.03	0.81	0.0080	0.56	0.44	0.05	1.84	13.6	108.0
JS-01	0.91	1.28	1.22	0.04	bd	0.63	0.0052	0.51	0.07	0.03	0.71	5.3	15.4
AV-P <sup>2</sup>	7.22	3.31	1.58	0.25	0.02	0.79	0.0086	0.75	0.42	0.10	2.82	15.1	123.5
AV-D <sup>3</sup>	2.30	2.16	1.56	0.11	0.01	0.59	0.0084	0.66	0.14	0.08	0.97	8.4	36.8

<sup>1</sup> bd = below detection limit.

<sup>2</sup> AV-P = average of pale lignites.

<sup>3</sup> AV-D = average of dark lignites

**Table A 3 Major-element oxides (%) and related parameters of the lignites from Jinsuo Basin, Yunnan Province, on ash basis.**

Sample	SiO <sub>2</sub>	Al <sub>2</sub> O <sub>3</sub>	CaO	K <sub>2</sub> O	Na <sub>2</sub> O	Fe <sub>2</sub> O <sub>3</sub>	SO <sub>3</sub>	MnO	MgO	TiO <sub>2</sub>	P <sub>2</sub> O <sub>5</sub>	DAI <sub>1</sub>
JS-39	30.60	24.91	13.49	1.27	bd <sup>2</sup>	14.71	4.57	0.172	6.10	3.40	0.422	1.55
JS-38	7.00	22.92	30.26	0.19	bd	10.13	11.72	0.137	11.64	0.79	0.510	0.48
JS-37	57.02	20.46	9.18	1.38	0.11	3.57	0.32	0.044	4.33	2.74	0.521	4.69
JS-36	10.14	17.21	29.10	0.11	bd	12.80	16.78	0.141	12.30	0.58	0.548	0.39
JS-35	54.50	17.49	12.40	0.81	0.14	4.46	0.70	0.055	5.73	3.07	0.346	3.26
JS-34	2.60	18.61	37.01	0.06	bd	11.47	13.39	0.165	15.60	0.33	0.430	0.28
JS-33	35.80	7.15	24.44	0.14	bd	8.83	11.66	0.115	9.94	1.47	0.133	0.81
JS-32	17.31	8.66	34.21	0.14	bd	10.32	14.39	0.177	12.65	1.67	0.159	0.39
JS-31	55.45	5.99	16.44	0.15	bd	4.98	7.10	0.073	7.20	2.19	0.150	1.79
JS-30	23.87	25.17	17.56	1.37	bd	5.42	15.45	0.070	8.61	1.20	0.935	1.10
JS-29	42.16	15.00	14.87	0.56	bd	5.47	10.76	0.059	6.48	2.07	2.100	1.59
JS-28	2.41	16.09	34.13	0.20	bd	10.28	22.58	0.152	13.17	0.30	0.394	0.24
JS-27	55.17	7.55	13.58	0.28	bd	5.16	9.79	0.060	6.14	1.86	0.177	1.87
JS-26	1.71	17.34	36.14	0.09	bd	8.67	19.44	0.141	15.13	0.67	0.352	0.25
JS-25	32.86	12.55	19.44	0.26	bd	6.08	12.03	0.086	8.03	7.78	0.419	1.17
JS-24	5.86	16.37	36.32	0.27	bd	8.63	16.86	0.154	13.48	1.21	0.456	0.31
JS-23	29.67	11.92	17.54	0.33	bd	10.63	18.28	0.084	7.08	2.50	1.490	0.83
JS-22	35.90	28.15	11.16	1.87	bd	5.88	8.17	0.076	5.69	2.53	0.220	2.22
JS-21	48.66	22.22	8.49	1.33	bd	6.03	6.61	0.057	4.28	1.78	0.233	2.91
JS-20	29.12	24.89	15.34	1.90	bd	6.52	12.89	0.095	6.96	1.30	0.590	1.37
JS-19	20.69	17.43	25.41	0.73	bd	5.82	17.31	0.148	9.72	1.28	0.978	0.69
JS-18	38.28	31.18	9.78	0.97	bd	4.64	1.02	0.108	4.47	1.67	0.396	3.62
JS-17	49.34	25.35	6.58	2.58	0.10	6.44	1.98	0.049	3.67	3.37	0.232	4.32
JS-16	25.62	21.38	23.71	0.90	bd	4.64	9.57	0.123	9.18	1.38	2.730	1.05
JS-15	42.93	28.05	13.77	2.04	0.08	3.49	0.36	0.073	6.06	1.74	1.020	3.16
JS-14	21.09	23.87	25.15	1.07	bd	6.01	8.28	0.124	9.88	1.20	2.670	0.96
JS-13	51.34	28.14	5.68	2.52	0.08	4.39	0.63	0.038	3.53	3.01	0.324	5.97

JS-12	12.7 4	27.57	25.3 1	0.6 6	bd	4.88	4.54	0.11 0	7.98	1.03	3.01 2	0.98
JS-11	42.9 9	27.65	11.5 2	2.2 2	0.06	3.90	0.73	0.06 2	5.18	2.52	2.48 0	3.53
JS-10	44.3 6	31.28	8.29	3.0 4	0.03	5.14	0.62	0.04 8	4.98	1.51	0.37 4	4.21
JS-09	52.0 3	27.37	7.12	3.1 1	0.12	2.80	0.67	0.03 9	4.05	1.95	0.43 9	5.77
JS-08	33.3 8	24.58	20.0 0	1.4 5	0.04	5.57	1.38	0.09 7	7.56	1.63	3.56 0	1.77
JS-07	43.0 3	25.72	11.2 9	1.9 8	0.30	6.66	0.27	0.06 4	5.06	3.32	1.76 0	3.18
JS-06	33.3 4	29.31	11.0 2	1.6 1	0.12	11.84	3.51	0.06 6	5.92	2.50	0.40 9	2.07
JS-05	55.9 9	21.49	8.15	1.0 5	0.20	5.32	0.12	0.04 7	3.45	3.25	0.59 0	4.80
JS-04	37.9 4	32.66	8.80	2.3 7	bd	8.07	1.22	0.05 3	4.65	3.44	0.43 2	3.36
JS-03	33.8 9	23.91	18.0 6	1.0 4	0.12	9.69	3.66	0.09 5	6.47	2.03	0.63 2	1.61
JS-02	47.6 0	25.90	10.4 4	1.6 3	0.22	5.98	0.11	0.05 9	4.12	3.23	0.38 0	3.79
JS-01	17.2 2	24.15	23.1 0	0.8 5	bd	11.99	10.9 6	0.09 8	9.55	1.23	0.48 9	0.78
AV-P <sup>3</sup>	45.4 0	19.30	13.1 3	1.2 8	0.14	5.56	5.53	0.07	5.78	2.73	0.77	3.01
AV-D <sup>4</sup>	20.9 0	23.25	22.6 3	1.0 0	0.07	8.53	10.3 1	0.12	9.37	1.47	0.82	1.35

<sup>1</sup> DAI = detrital/authigenic index =  $(\text{SiO}_2 + \text{Al}_2\text{O}_3 + \text{K}_2\text{O} + \text{Na}_2\text{O} + \text{TiO}_2)/(\text{Fe}_2\text{O}_3 + \text{CaO} + \text{MgO} + \text{SO}_3)$ , from Vassilev et al. (2009); <sup>2</sup> bd = below detection limit; <sup>3</sup> AV-P = average of pale lignites; <sup>4</sup> AV-D = average of dark lignites.

## Publications

- **Liu, B.**, Zhao, C., Ma, J., Sun, Y., Püttmann, W., 2018. The origin of pale and dark layers in Pliocene lignite deposits from Yunnan Province, Southwest China, based on coal petrological and organic geochemical analyses. *International Journal of Coal Geology* **195**, 172–188.
- **Liu, B.**, Vrabec, M., Markič, M., Püttmann, W., 2019. Reconstruction of paleobotanical and paleoenvironmental changes in the Pliocene Velenje Basin, Slovenia, by molecular and stable isotope analysis of lignites. *International Journal of Coal Geology* **206**, 31–45.
- **Liu, B.**, Zhao, C., Fiebig J., Bechtel, A., Sun, Y., Stable isotopic and elemental characteristics of pale and dark layers in an upper Pliocene lignite deposit basin in Yunnan Province, southwestern China: Implications for paleoenvironmental changes. *International Journal of Coal Geology*, submitted.

## Conference

- **Liu, B.**, Zhao, C., Ma, J., Sun, Y., & Püttmann, W. (2018). The influence of vegetation and paleoenvironmental changes on the formation of pale and dark layers in Pliocene lignite deposits from Yunnan Province, Southwest China: results from coal petrology and organic geochemistry. (TSOP 2018, Beijing, China). Oral presentation

# Curriculum Vitae

## Personal information

**Name:** Bangjun Liu  
**Sex:** Male  
**Date of birth:** 01, February, 1990  
**Nationality:** Chinese  
**Birth place:** Mianyang, Sichuan Province, China

## Education & research experience

- 06. 2016 –now**      **Doctoral Candidate**  
  
Goethe-University Frankfurt am Main, Germany  
Institute of Atmospheric and Environmental Sciences  
Department of Environmental Analytical Chemistry  
  
**Dissertation:** The origin of pale and dark layers in Pliocene  
Jinsuo lignite basin from Yunnan Province, Southwestern  
China  
  
Supervisor: Prof. Dr. Wilhelm Püttmann  
Second Supervisor: Prof. Dr. Jens Fiebig
- 09. 2013–01. 2016**      **M.S. in Geological Engineering**  
Hebei University of Engineering, China  
  
**Master thesis:** Enrichment mechanism of rare metal elements  
in the coal from Iqe Coalfield  
Supervisor: Prof. Dr. Yuzhuang Sun & Prof. Dr. Mingyue Lin
- 09. 2009–06. 2013**      **B.S. in Resources Exploration Engineering**  
Hebei University of Engineering, China